Green chemistry initiatives in Japan

In this issue, we feature an article in the news section from our colleagues in Japan who are leading the green chemistry initiatives there. The article describes the background in that country that led to the establishment of the *Green and Sustainable Chemistry Network* (GSCN). The article also highlights some of the activities of the GSCN, including their awards programme that has recently started. It is very pleasing to read about their excellent work after the discussions that we have had with them in the last few years about setting up the Network. The first international symposium on *Green and Sustainable Chemistry* will be held in Japan next year and we wish them every success. The symposium has attracted a number of distinguished speakers and will feature award-winning research and development, industrial case studies and an open session for the public. We look forward to reading more about the activities of the GSCN and about some of the papers at the symposium that we will feature in this journal. The open session for the public is, I believe, to be welcomed – green chemistry is an excellent opportunity for the chemistry community to demonstrate the ways that industry, scientists and educationalists are addressing fundamentally important issues of sustainability in the context of chemical processes and products.

In recent months I have heard a number of interesting presentations about areas of chemical technology that offer different ways of carrying out chemical processes than we are used to reading about in *Green Chemistry* and that are discussed in green chemistry symposia. One of these is electrochemical synthesis. These reactions can be considered to be 'green' especially when they provide methods for oxidising and reducing organic compounds without the use of often hazardous and ultimately polluting stoichiometric reagents. I hope that we can see more articles in *Green Chemistry* that describe electrochemical routes to important chemical products and intermediates. A more controversial technique is radiation processing. Can we consider chemical transformations and materials processing that involve radiation as 'green'? I believe that there are some interesting possibilities in this context that we should consider and I would like to consider appropriate articles for publication in *Green Chemistry* as well as inviting comments on the inherent safety and sustainability of the methods. We are keen to widen the scope of the articles in *Green Chemistry* to include new and emerging areas of chemical processing as well as considering older areas that can contribute to achieving the principles of green chemistry.

James Clark, York
November 2002

DOI: 10.1039/b211024p

Highlights

Duncan Macquarrie highlights some of the recent literature in green chemistry

Supercritical methanol

The use of supercritical methanol has been shown to affect dramatically the product selectivity in the methylation of hydroxyamines (*Angew. Chem., Int. Ed.*, 2002, **41**, 3476). Tomoharu Oku and Takao Ikariya of the Tokyo Institute of Technology, Japan, have shown that, while vapour-phase reactions of 2-aminoethanol over zeolites afforded predominantly intramolecular condensation reactions, the use of supercritical methanol caused a large swing towards N-methylation over intramolecular reactions. The use of mixed metal oxide catalysts with both weakly acidic and basic groups (*e.g.* Cs–P–Si) was also found to be ideal. Selectivity towards N-methylated products increased in the best cases from just over 50% to around 90%.

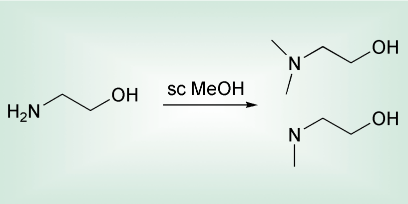

Metal-catalysed coupling reactions

Metal-catalysed coupling reactions are of great utility in synthetic chemistry, and their use is growing. Two examples of their application in the Pd catalysis of amination reactions are worth mentioning. The first, which is a nice example of a double coupling, avoiding isolation and purification of intermediates (which can be wasteful and inefficient) is provided by Robin Bedford and Catherine Cazin of the University of Exeter, UK (*Chem. Commun*, 2002, 2310). They show that 2-chloroanilines couple efficiently with bromoaromatics under Pd catalysis, with the first coupling being the formation of the diarylamine by catalytic amination. The second reaction is an *ortho–ortho* coupling which forms the carbazole product. Good-to-excellent yields were obtained for a range of substrates, and the avoidance of a separation stage is a real benefit.

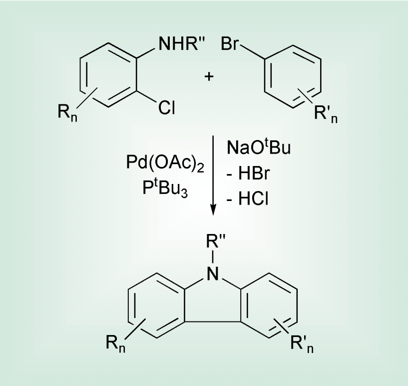

The second example is an extension of the catalytic amination to the formation of enamines, compounds of great synthetic importance which are often produced by acid-catalysed processes under relatively forcing conditions, leading to wasteful and functional-group-intolerant procedures. Jose Barluenga and colleagues from the University of Oviedo have now demonstrated that Pd-catalysed amination of alkenes is possible (*Chem. Commun.*, 2002, 2362) Thus a range of enamines can be formed in excellent yield under mild conditions. A relatively low number of different functional groups were involved in the transformations covered in the communication; it is, however, to be expected that the Pd catalytic system will have a wide applicability.

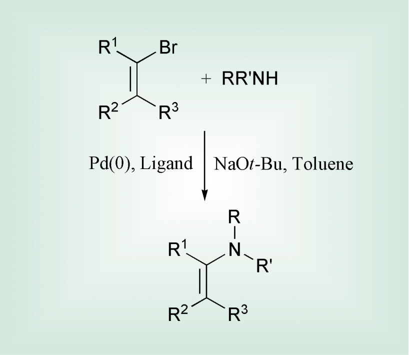

C–C bond formation

The Pd catalysed synthesis of ketones from boronic acids and carboxylic acids is another example of a selective and clean C–C bond forming process. Lukas Gooßen and Keya Ghosh of the Max-Planck Institut in Mülheim-an-der-Ruhr, Germany, have shown that pivalic anhydride is an excellent promotor for the reaction, and that high yields can be obtained under mild conditions using palladium acetate, a phosphine ligand and the anhydride as promotor. A large number of ketones were successfully formed (*Eur. J. Org. Chem.*, 2002, 3254).

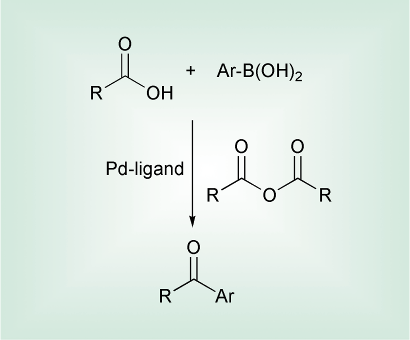

Hydroxyapatite

The use of hydroxyapatite and related solids is becoming popular (see below). The group led by Kiyotomi Kaneda has used this mineral support to form supported Pd complexes (*J. Am. Chem. Soc.*, 2002, **124**, 11572). The catalysts were tested in the catalytic aryl oxidation of phenethyl alcohol to acetophenone, where the turnover number was an exceptional 236000, 3 orders of magnitude higher than found for any catalyst operating under atmospheric pressure. They also report excellent results with a similar catalyst for both the Heck and Suzuki reactions (turnover numbers 40000-49000).

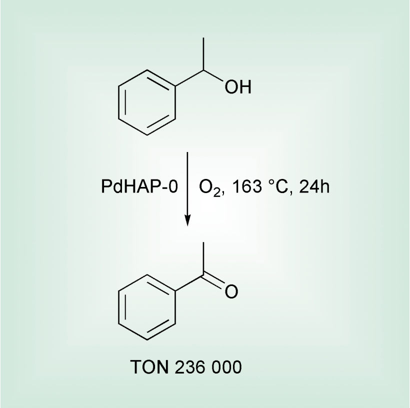

Hydrogenation of arenes

The hydrogenation of arenes is of significant interest in the production of

DOI: 10.1039/b210802j

low-aromatic diesel fuels, and conventional hydrogenation methods are under pressure to improve to meet this demand. Chien Wai and co-workers from the University of Idaho, USA, have now shown that supercritical carbon dioxide is a very good medium for carrying out such hydrogenation (*Chem. Commun.*, 2002, 2388). Their initial results show that a water-in-carbon dioxide microemulsion can be used to produce Rh nanoparticles by reduction in hydrogen, and that these nanoparticles are extremely active in the hydrogenation of arenes. The lifetime of the catalyst is currently relatively low, thought to be due to aggregation, but work is in progress to address this issue.

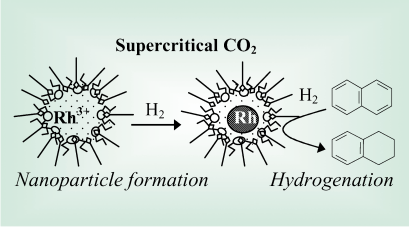

Epoxidations

The development of truly heterogeneous solid catalysts for liquid-phase systems continues, with the publication of a novel MCM-supported Mo catalysts (*Chem. Commun.*, 2002, 2392). Mingjun Jia and Werner Thiel of the University of Chemnitz have developed an immobilised oxomolybdenum catalyst which is stable in the epoxidation of alkenes using *t*-BuOOH. Their initial catalyst displayed very good activity in the epoxidation of cyclooctene (and excellent selectivity – cyclooctene does not undergo the normally competitive allylic oxidation), but filtration of the catalyst and continuation of the run indicated a reduction in activity, which may be due to a degree of leaching. Silylation of the catalyst reduced this homogeneous component to zero, and the catalyst could be reused after reactivation. Less active alkenes such as 1-octene were also efficiently epoxidised.

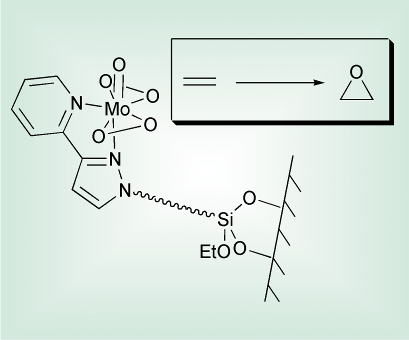

A metal-free epoxidation system has been proposed by Danièle Bonnet-Delpon and colleagues from the Laboratoire BioCIS associated to the CNRS in Châtenay-Malabry, France, (*Eur. J. Org. Chem.*, 2002, 3290). They have shown that the combination of urea–hydrogen peroxide and hexafluoroisopropanol is an effective system for the epoxidation of alkenes. Reactive alkenes were epoxidised directly, but less active double bonds required the presence of perfluorinated ketones as catalysts to allow the reaction to proceed efficiently. Excellent yields were obtained in a range of cases.

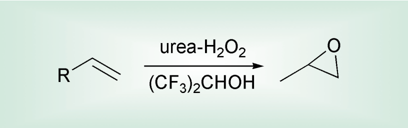

The epoxidation of electron-deficient alkenes can be carried out by a combination of basic catalysts and hydrogen peroxide. Jorge Palomeque, Joseph Lopez and François Figueras of the Institut de Recherches sur la Catalyse at Villeurbaine, France, have shown that mixed metal oxide catalysts are particularly good at this tricky rection (*J. Catal.*, 2002, **211**, 150). They prepared MgLa mixed oxides, KF–alumina, and MgAl hydrotalcite catalysts, and after appropriate activation, showed that they were capable of epoxidising 2-cyclohexenone and isophorone in high yields. The non-productive decomposition of hydrogen peroxide appears to be absent in the best cases.

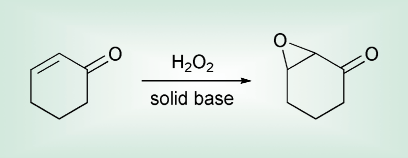

A further epoxidation system has been published by the groups led by Junko Ichihara at Osaka University and Yoh Sasaki at Kinki University in Osaka (*Tetrahedron Lett.*, 2002, **43**, 8231). They have supported heteropolyacids on fluoroapatite and used these to catalyse the epoxidation of a range of alkenes using ureahydrogen peroxide in a solvent free system. Yields are high with both phosphomolybdates and considerably lower with phopshotungstates. Yields are excellent with cyclic alkenes, but are lower with linear alkenes, where diol formation is a common problem. Sulfides can be oxidised to sulfoxides with reasonable selectivity and also, more slowly, to sulfones.

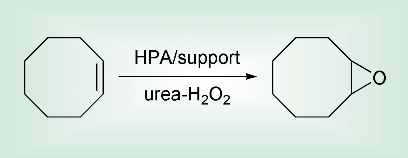

Oxidation of alcohols

The efficient oxidation of alcohols to carbonyl compounds using air as oxidant has been the subject of many efforts. Kiyotomi Kaneda's group at Osaka University, Japan, have now shown that this transformation can be very easily done using only air and a mixed metal oxide catalyst at room temperature (*Catal. Commun.*, 2002, **3**, 511). Their catalyst is a mixed Mn–Fe–Cu–Ru oxide, where coordinatively unsaturated Ru=O sites are tentatively suggested as the active centres. This catalyst converts secondary alcohols to ketones very readily at room temperature. More impressively, primary alcohols (alkyl, benzylic and allylic) are converted to the aldehyde in excellent yields and outstanding selectivities. Reaction times are typically in the range of an hour to several hours.

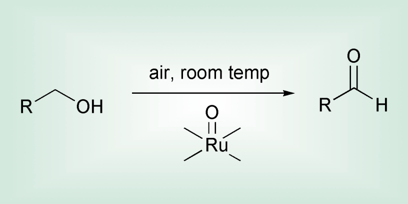

Reviews

The September edition of *Accounts of Chemical Research* (*Acc. Chem. Res.*, 2002, 685–816) contains a series of reviews of many key areas of green chemistry, with an introduction by Istvàn Horvath. The October edition of *Chemical Reviews* is devoted to the theme of recoverable catalysts and reagents, and covers a wide range of techniques and startegies for the effective recovery of both catalysts and reagents (*Chem. Rev.*, 2002, 3217–3892).

Green analytical strategies for sunscreen control

A. Salvador,† M. C. Pascual-Martí, A. Chisvert and M. D. de la Ossa of the Departamento de Química Analítica, in Valencia, Spain, explain how green chemical technologies can be used for environmentally benign analysis of cosmetics including sunscreens

Cosmetic products do not pose as many health implications as pharmaceuticals or food. However, if careful quality control is not conducted, their repeated daily use may be even more hazardous. This control must guarantee that the composition of the final product not only is that desired by the manufacter, but that it is conforms to current safety legislation. The cosmetic industry requires simple, accurate and green analytical methods that can be routinely and safety used without ambiental contamination in their own quality control laboratories.

The use of sunscreens has been advocated by many health care practitioners as a means of reducing skin damage produced by the UV radiation from sunlight.[1] The concentration of the UV-filters in cosmetic formulations must be monitored to ensure the labelled Sun Protection Factor in the commercial preparations but without exceeding the maximum authorized legislative levels, because induced allergic, photoallergic reactions and other dermatological side effects have been found in a few people using some organic UV-filters, such as benzophenones, butyl methoxy dibenzoylmethane and octyl methoxycinnamate[2] or *p*-aminobenzoic acid.[3]

Therefore, analytical methods for sunscreen control are required (Fig. 1) and, since there are no official analytical methods for sunscreen analysis, proposals that allow an easy and adequate control should be made. Several analytical strategies could be followed to obtain a green analytical control of sunscreens for the cosmetic industry:

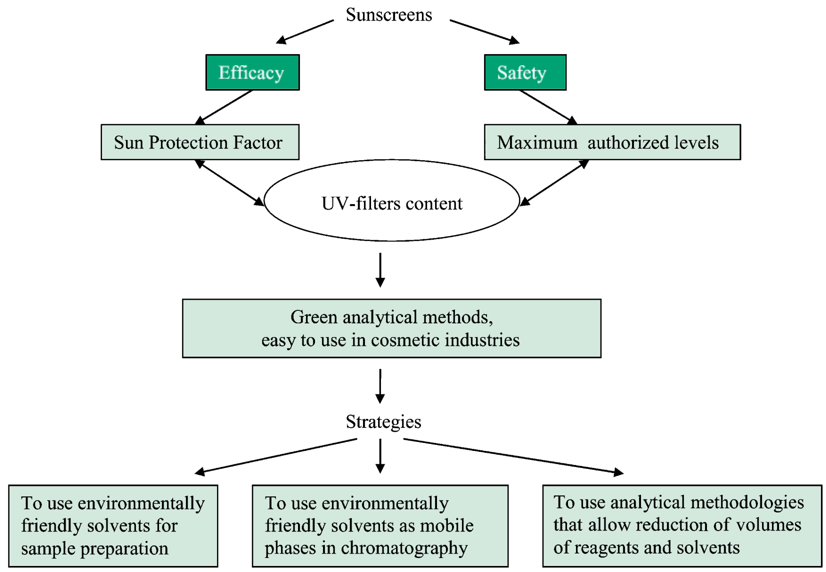

Fig. 1 Green analytical methods for sunscreen control.

The replacement of solvents habitually used in sample preparation by environmentally friendly solvents

Analytical methods for cosmetic samples with high liposoluble contents, such as sunscreens (including creams, oils, lipsticks, facial make-up formulations, *etc*.), usually require the use of organic solvents. Liquid–liquid extraction, direct dissolution with solvent mixtures and other classical procedures are the most commonly used procedures for sample preparation.

The replacement of hazardous organic solvents by more environmentally friendly solvents (for instance, ethanol–water mixtures) can sometimes be achieved either directly[4,5] or by the use of adequate methodologies such as sonication or microwave irradiation,[6] both of which facilitate the complete dissolution or the leaching of sunscreen samples. Supercritical carbon dioxide extraction can also be a good alternative to the use of highly toxic organic solvents in the sample treatment processes.[7] Supercritical fluid extraction allows a rapid leaching of UV-filters from sunscreen samples. A few articles have been recently published on the supercritical fluid extraction of some UV-filters[8–10] from cosmetics followed by liquid chromatography determination.

Replacement of solvents habitually used as mobile phases in chromatography by environmentally friendly solvents

Chromatography is undoubtably the most efficient technique for the simultaneous determination of several components in complex matrices such as cosmetics. The majority of published chromatographic methods for sunscreen analysis require the use of methanol,[9–15] THF,[9,10,12–14] acetonitrile[9–13,15] and other hazardous organic solvents as mobile phases. New liquid chromatographic methods for sunscreen analysis, based on the use of environmental friendly solvents as mobile phases, have been recently developed.[4,5,8] Fig. 2 shows that a good chromatographic separation of six worldwide authorized UV-filters can be performed in 24 min by

---

† Departamento de Química Analítica, Facultad de Química,Universitat de Valencia, Doctor Moliner St. 50, 46100-Burjassot, Valencia, Spain; Tel: 34-963983175; Fax: 34-963864436; E-mail: Amparo.Salvador@uv.es

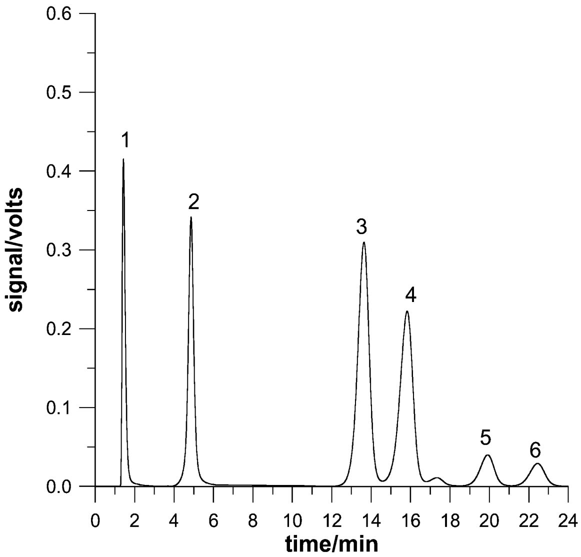

Fig. 2 Chromatogram obtained from 20 μl of a mixture of six UV-filters using a 100 LiChrospher® C_{18} (12.5 cm × 4 mm i.d., 5 μm particle size) column and ethanol–acetic acid: water (70:29.5:0.5) as mobile phase. UV–VIS detection carried out at 313 nm. Peaks: (1) benzophenone-4, (2) benzophenone-3, (3) octyl dimethyl PABA, (4) octyl methoxycinnamate, (5) octyl salicylate and (6) homosalate.

using an ethanol–water mixture as mobile phase.

The use of methodologies that allow a reduction in the volume of reagent and solvents used in spectrometric methods, such as flow analysis strategies

These techniques allow the on-line realization of some or all the steps of the analytical procedures: sample pretreatment, dilution, preconcentration, reaction of the analyte with the appropiate reactive, measurement of the analytical signal, *etc*. These systems accelerate the analytical process and allow, as described by Rocha and colleagues,[16] a considerable decrease in the toxicity of the procedure and the generated residues because they reduce the volume of reagents used in the analysis. Some analytical methods have recently been developed to determine UV-filters in sunscreens by flow injection analysis[17–19] or sequential injection analysis.[6,19–21]

Besides these and other possible green analytical chemistry strategies, other initiatives devoted to the search for green cosmetic active ingredients (for instance, compounds whose efficacy as UV-filters could be similar to those organic molecules used today, compounds that could replace some toxic organic dyes used in hair cosmetics, green solvents that could be used in nail cosmetics, *etc*.), and solvent-free technologies to extract cosmetic active ingredients from natural products, synthetize and/or purify them (such as microwave treatment, supercritical extraction), would improve both the safety and environmental characteristics of the cosmetic products.

References

1 F. P. Gasparro, M. Mitchnick and J. F. Nash, *Photochem. Photobiol.*, 2001, **68**, 243–256.

2 N. Cook and S. Freeman, *Australas. J. Dermatol*,, 2001, **42**, 257–259.

3 B. S. Mackie and L. E. Mackie, *Australas. J. Dermatol*.,, 1999, **40**, 51–53.

4 A. Chisvert, M. C. Pascual-Martí and A. Salvador, *Fresenius J. Anal. Chem.*, 2001, **369**, 638–641.

5 A. Chisvert, M. C. Pascual-Martí and A. Salvador, *J. Chromatogr. A*, 2001, **921**, 207–215.

6 A. Salvador, A. Chisvert, A. Camarasa, M. C. Pascual-Martí and J. G. March, *Analyst*, 2001, **126**, 1462–1465.

7 D. L. Hjeresen, *Crit. Rev. Anal. Chem.*, 1999, **28**, 9–12.

8 A. Salvador, I. Gadea, A. Chisvert and M. C. Pascual-Marti, *Chromatographia*, 2001, **54**, 795–797.

9 S. P. Wang and W. J. Chen, *Anal. Chim. Acta*, 2000, **416**, 157–167.

10 S. Scalia, *J. Chromatogr., A*, 2000, **870**, 199–205.

11 L. H. Wang, *Chromatographia*, 1999, **50**, 565–570.

12 S. C. Rastogi and G. H. Jensen, *J. Chromatogr. A*, 1998, **828**, 311–316.

13 J. E. DiNunzio and R. R. Gadde, *J. Chromatogr.*, 1990, **519**, 117–124.

14 K. Ikeda, S. Suzuki and Y. Watanabe, *J. Chromatogr*, 1989, **482**, 240–245.

15 L. Gagliardi, G. Cavazzutti, L. Montanarella and D. Tonelli, *J. Chromatogr.*, 1989, **464**, 428–433.

16 F. R. P Rocha, J. A. Nobrega and O. Fatibello, *Green Chem.*, 2001, **3**, 216–220.

17 A. Chisvert, A. Salvador and M. C. Pascual-Martí, *Anal. Chim. Acta*, 2001, **428**, 183–190.

18 A. Townshend, R. A. Wheatley, A. Chisvert and A. Salvador, *Anal. Chim. Acta*, 2002, **462**, 209–215.

19 A. Chisvert, A. Salvador, M. C. Pascual-Martí and J. G. March, *Fresenius J. Anal. Chem.*, 2001, **369**, 684–689.

20 A. Chisvert, M. T. Vidal and A. Salvador, *Anal. Chim. Acta*, 2002, **464**, 295–301.

21 A. Chisvert, J. V. Izquierdo and A. Salvador, *Anal. Bioanal. Chem.*, accepted July 2002, in press.

Green and sustainable Chemistry (GSC) in Japan

Masao Kitajima and Yasushi Yamamoto describe the Green and Sustainable Chemistry (GSC) activities in Japan, and the establishment and activities of the GSC Network.

Introduction

While enormous numbers of chemical products supported by various scientific inventions and innovative technologies have made our lives easier and improved our well-being in the last century, problems associated with chemicals became ever more serious in 1970s and early 1980s in industrialized countries, including Japan. It was inevitable that chemical industry would need to make efforts to develop cleaner and more environmentally friendly technologies to cope with such problems as pollution of air, water and land, endocrine disruptors *etc*. In the early stages, each problem was viewed as independent and unrelated, but it was later realized that many environmental problems are closely related and should be solved holistically and globally. A concept for developing new technologies based on a global perspective, 'Sustainable Development', was adopted by the United Nations Conference on Environment and Development (UNCED) in 1992, and this was followed by 'Green Chemistry' as a principal stance.[1]

A series of unpleasant experiences and problems associated with chemicals and their remediation follow-up in recent decades meant that Japan became one of the forerunners of those recognizing the importance and need to develop environmentally benign chemical technologies. Not only chemical industry, but academic societies, industrial associations and government, made extensive efforts to improve the environment and human health and safety. In response to these movements, the *Green and Sustainable Chemistry Network* (GSCN) was born in March 2000.

In this article we describe the background to the formation of the GSCN and its activities in the past and present.

Activities before GSCN

Activity by government

Society's concerns over environmental problems have been quite strong in Japan, especially after the tragic experiences with mercury, Minamata disease, and PCBs. Such experiences prompted government and industry to support research relating to the environment. National projects, aimed at improving the global environment, product performances, production processes in relation to energy and material consumption, emission, pollution and safety, also started in the 1980s. The Ministry of International Trade and Industry (MITI)—now known as the Ministry of Economy, Trade and Industry (METI)—started the first large project of this kind, named as *Sunshine Project*, in 1974. Then *Moonlight Project* followed in 1978. These projects consisted of a wide range of energy-related research on conservation, generation, storage, transportation, storage and efficient use of energy including sunlight, wind, fossil fuels, biomass and wastes, geothermal, hydrogen and fuel cells, as well as superconductors. Another project called *Research and Development of Global Environment Industrial Technology* was launched in 1989, aimed at the development of technologies relating to environmentally friendly manufacturing processes, pollution reduction, CO_2-fixation and utilization, waste management and recycling, and environmental remediation. Then a large project, *New Sunshine Project*, merging and reorganising the above three projects, was launched in 1993. A typical GSC-related national project, *Next-generation Chemical Process Technology Program*, nicknamed as *Simple Chemistry* was launched, in 1995, as a 10-year program as a part of *New Sunshine Project*. The purpose of this program was '*maximization of energy*

Table 1 GSC related activities by academic societies and industrial associations

Societies	Committee/study groups and their activities
The Chemical Society of Japan (CSJ)	Study Group on Green Chemistry Holding Symposia (twice a year)
The Society of Polymer Science, Japan (SPSJ)	Study Group on Plastic-recycling Study Group on Eco-materials Study Group on Polymer Degradation and Stabilization
The Society of Chemical Engineers, Japan (SCEJ)	Committee on Environment Subcommittee on Global Environment Subcommittee on Water Environment Subcommittee on Recycling Engineering
National Institute of Advanced Industrial Science and Technology (AIST)	Research Institute for Green Chemistry Promotion of national projects related to GSC
Japan Bioindustry Association (JBA)	Green Biotechnology Forum
Japan Chemical Industry Association (JCIA)	Japan Responsible Care Council Correspondence to LRI and OECD Risk Communication
Chemical Evaluation and Research Institute, Japan (CERI)	Total Evaluation of Chemical Substances Promotion of PRTR
Japan Chemical Innovation Institute (JCII)	Subcommittee on GSC Survey Study Group on GSC Management of Directory Database on GSC Promotion of National Projects related to GSC Promotion of Activities and Secretariat of GSCN

and resource savings and minimization of the emission of chemicals by simplifying industrial chemical process', which is exactly what GSC pursues. The reports from those projects and review papers have been published elsewhere.[2]

Activity by academic societies and industry associations

Academic societies and industrial associations have been working on environmental issues for decades in Japan. For example, the Society of Synthetic Organic Chemistry, Japan (SSOCJ) started *Awards to Chemistry for Environment* as early as in 1974. In industry, a committee for *Responsible Care (RC)* was formed within the Japan Chemical Industry Association (JCIA) and the *Responsible Care Association, Japan* was launched officially in 1995. In addition to these, new activities on GSC have started in many organizations in the last 5 years. Major standing subcommittees or study groups and their activities are summarized in Table 1. It should be noted that these activities are carried out independent of the GSC Network.

Green and Sustainable Chemistry Network (GSCN)

Establishment of GSCN

In February 1998, a study group on Sustainable Chemistry (SC) was formed by a proposal from the USA at the Joint Meeting of Chemical Group of OECD. Japan joined the steering group, together with Italy, Germany and The Netherlands. The MITI, representing Japanese government, asked the Japan Chemical Innovation Institute (JCII) to assist and work with them in this OECD SC activity.

In accordance with this movement, JCII proposed that chemical societies and associations of various sectors should form a consolidated organization to promote green chemistry activity in Japan. Eight organizations from academia, industry and national institutions agreed to join. After one year of preparative work, a workshop was held in November 1999, with more than 70 participants representing 10 organizations listed in Table 2. At this workshop it was agreed to form a new organization. The official name of the new organization, concept, definition, key-factors and guidelines were discussed and adopted. Thus the *Green and Sustainable Chemistry Network* (GSCN) was officially launched in March 2000. It should be noted that MITI/METI and New Energy and Industrial Technology Development Organization (NEDO) have been involved in these activities from the beginning as observers.

Table 2 Member organizations of GSC Network

The Chemical Society of Japan (CSJ)
The Society of Chemical Engineers, Japan (SCEJ)
The Society of Polymer Science, Japan (SPSJ)
National Institute of Advanced Industrial Science and Technology (AIST)
Japan Chemical Industry Association (JCIA)
Japan Bioindustry Association (JBA)
Association for the Progress of New Chemistry (ASPRONC)
Chemical Evaluation and Research Institute, Japan (CERIJ)
Japan Association for International Chemical Information (JAICI)
Japan Chemical Innovation Institute (JCII)

Vision, structure and activities of GSCN

Vision and structure

The GSCN adopted *Green and Sustainable Chemistry* as the official name for its activity. It views R&D and implementation by academia and industry as its main focus. At the general meeting for launching GSCN, definition, key factors and guidelines for GSC were also adopted as shown in Table 3. The organizational structure of GSCN was also adopted. It consists of a Steering Committee and seven task groups (Group and Work Group): Research Promotion, Research Support, Information, Education and International Cooperation, Research Area and Evaluation, as shown in Fig. 1.[3]

Activities and achievements

The GSCN has been working actively for the last two years. It opened a home page at http://gscn.net in English as well as Japanese and published a newsletter quarterly. Major activities and achievements by the task groups are summarized in Table 4. Some of these, for example those on GSC Award program and a proposal to the government and society, *Initiative GSC 21* should interest readers of *Green Chemistry*. Reports are being prepared on these major activities.

The GSCN held symposia in 2000 and 2001. These consisted of invited lectures and over 70 good-quality poster presentations.[4] As a follow-up of the annual GSC symposium, *The First International Conference on GSC* will be held in Tokyo on March 13–15, 2003. Detailed information on this conference is provided at http://gscn.net.

Table 3 Definition, key factors and guidelines for the GSC

Definition of GSC	Chemical technologies to realize human and environmental health and safety, for minimization of energy and resource consumption and others, through innovations and improvements in product and design, selection of feedstocks, formulations and applications and resource recycling
Key factors	• Technologies for pollution prevention based on holistic environment impact • Innovation technologies with wide and practical applicability • Global and international contribution • Conditions surrounding Japanese society, such as environment, resources and demographic change • Planning and actions with long term strategies and dynamic responses to changing society and global situations
Guidelines	• Pursuance of highly effective and economical product and process design and technologies in consideration of holistic life cycle assessment and the environment and human health and safety. • Development of products and technologies which contribute to minimize by-products, emissive chemicals, residues and wastes, recycling of materials to resources and cleaning and remediation of the environment. • Development of combined multiple technological and operational systems for reduction of energy and resources and cyclic utilization of materials and chemicals. • Reduction in dependency on non-renewable feedstock by promoting utilization of renewable feedstock and renewing technologies. • Promotion of collaboration and joint works among industry, academia and national institutions, other industries and various disciplines, both domestically and internationally. • Promotion of information exchange, dissemination and communication to enhance reliability of chemistry in society. • Promotion of education and enlightening in regards to Green & Sustainable Chemistry to achieve its ultimate goal, *i.e.* realization of sustainable society.

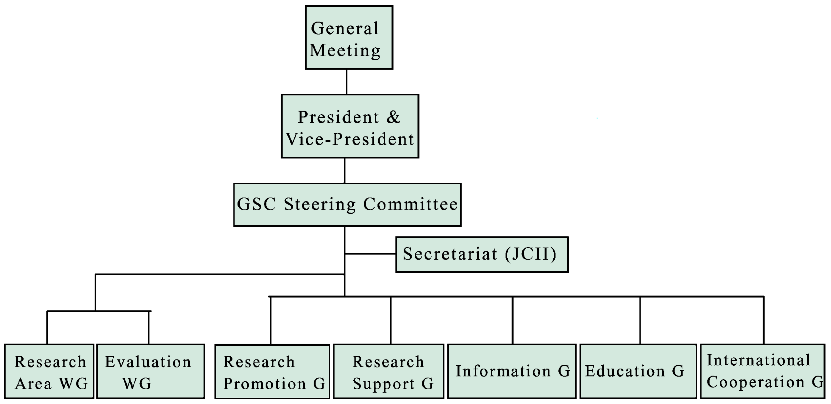

Fig. 1 Organization of the Green and Sustainable Network.

Table 4 Major achievements by task groups of the GSC Network

Group	Achievements in the first three years
Research Promotion Group	• Development of Awards on GSC. Launched in 2001, first awarded in April 2002 • Development of Proposal to Government, *Initiative GSC-21*, published in September 2002
Research Support Group	• Planning and holding of GSC Symposia (Annual). I in October 2000/Tokyo, II in November 2001/Yokohama • GSC New Letter, First publication: July 2001 (Quarterly)
Information Group	• Opening of GSC home page • Development and operation of GSC directory data base
Education Group	• Publication of text book on GSC *Environment and Chemistry–Green Chemistry*.
International Cooperation Group	• Assisting METI in relation to OECD SC Activity OECD Workshop in October 2000/Tokyo OECD Sustainable Chemistry Issue Team Meetings • Collaboration with international green chemistry activities
Research Area Working Group	• Proposals of focus research area on GSC
Evaluation Working Group	• Development of Metrics for GSC for evaluating GSC Award candidates

Conclusions

The mission of GSCN is not limited to work by chemists and chemical engineers. We, chemists, have to work together with society and government. The GSCN have placed the fundamental priority of its activity on *Environment and Human Health and Safety through Innovation of Chemical Technology*, in pursuit of the contribution to Sustainable Development. In this context, the GSC Network published a proposal to government and society, *'Initiative GSC 21– Challenge of Chemical Technology—'* in September 2002.[5] The aim of this proposal was to show how GSC is important and that chemists are working hard and collaboratively along the concept of GSC.

It was emphasized during the discussion that development of an evaluation tool, or metric, for GSC, is one of the most important subjects for the GSCN, in order to help researchers and managers in academia and industry, as well as government and society, to share common ideas and directions for GSC activity.

We believe that *The First International Conference on Green & Sustainable Chemistry* will lever our efforts to the next higher stage, especially in strengthening the collaborations between various sectors, regions and societies by global cooperation, toward Sustainable Development.

Acknowledgement

The authors thank Professor Makoto Misono of Kogakuin University and Mr. Akiyoshi Somemiya of JCII for their valuable advice in the preparation of this article.

References

1 (*a*) P. Anastas and J. Warner, *Green Chemistry: Theory and Practice*, Oxford University, Oxford, 1992; (*b*) M. Poliakoff and P. Anastas, *Nature*, 2001, **413**, 257.
2 *Annual Reports on NEDO National Projects*, 1993–2001, NEDO.
3 *Green & Sustainable Chemistry Network—Vision and Concept*, 2000, GSCN.
4 (*a*) Extended Abstracts, with English Summary, 1st Symposium on GSC, Tokyo, 2000, GSCN; (*b*) Extended Abstracts, with English Summary, 2nd Symposium on GSC, Yokohama, 2001, GSCN; (*c*) M. Kitajima, *Catalysis Surveys from Japan*, 2002, **6**, 2002.
5 *Initiative GSC-21—Challenge of Chemical Technology*, 2002, GSCN (http://www.gscn.net/).

Process intensification receives backing of Government and industry

Industry, both in the UK and overseas, has joined with Government in supporting the Process Intensification Network (PIN), based at Newcastle University. PIN was established in 1999 with support from the UK Research Council EPSRC as a network which would bring together industry and academe to further the technology of process intensification (PI). PI, conceived by Professor Colin Ramshaw when at ICI, may be defined as: '*Any chemical engineering development that leads to a substantially smaller, cleaner, safer and more energy efficient technology*.' Now PI is not limited to the chemical industry, and the concept is important in a range of sectors stretching from aerospace to micro-electronics and metals processing (*Green Chemistry*, 2000, G13)

PIN, which has regular meetings, a newsletter and a web site (http://www.ncl.ac.uk/pin/) — aims to stimulate technology transfer in PI and to encourage collaboration between industry, research laboratories, and universities in developing new PI technologies, such as micro-reactors and highly compact heat transfer systems. The sponsors, three of which comment below on the importance of PI, guide the PIN activity as well as funding the secretariat.

The Health & Safety Executive in the UK believes that PI can contribute to increased plant safety, in particular due to lower hazardous inventories. For many years now BP has been using PI offshore with, for example, hydrocyclones for oil/water separation and compact heat exchangers both of which substantially reduce topside loadings and as a sponsor BP is actively considering the benefits of implementing PI technologies within the Chemicals and Refining Businesses. Norsk Hydro, a major Norwegian oil and gas exploration and production company, is actively pursuing radical PI concepts, *e.g.* pipeline separation (*i.e.* subsea and downhole), and multipurpose inlet cyclones in separators.

For a modest registration fee, those attending the half-yearly PIN meetings receive up-to-date reports on industrial uses of PI, information on opportunities for collaborative projects and funding information, a visit to the laboratory, and a chance to 'float your idea' in five minutes!

Membership of PIN is currently free, and a form can be downloaded from the above web site. Additionally, the MINIPIN Expression of Interest for taking PIN fully into Europe may be seen on http://eoi/cordis.lu/dsp_results.cfm

For more information, contact: Professor D. A. Reay, David Reay & Associates, PO Box 25, Whitley Bay, Tyne & Wear UK NE26 1QT (email: DAReay@aol.com)

Metrics to ‘green’ chemistry—which are the best?

David J. C. Constable,[a] Alan D. Curzons[b] and Virginia L. Cunningham[a]

[a] *GlaxoSmithKline Pharmaceuticals, 2200 Renaissance Boulevard, King of Prussia, PA 19406, USA. E-mail: david.c.constable@gsk.com*
[b] *GlaxoSmithKline Pharmaceuticals, Southdownview Way, Worthing, West Sussex, UK BN14 8NQ*

Received 26th June 2002
First published as an Advance Article on the web 17th October 2002

A considerable amount has been written about the use of metrics to drive business, government and communities towards more sustainable practices. A number of metrics have also been proposed over the past 5–10 years to make chemists aware of the need to change the methods used for chemical syntheses and chemical processes. This paper explores several metrics commonly used by chemists and compares and contrasts these metrics with a new metric known as reaction mass efficiency. The paper also uses an economic analysis of four commercial pharmaceutical processes to understand the relationship between metrics and the most important cost drivers in these processes.

Selected metrics used in the past

A considerable number of publications have been written about the use of metrics to drive business, government and communities towards more sustainable practices. The reader is referred elsewhere for a discussion of what metrics have been proposed. There has also been much written about the characteristics of metrics, or what constitutes a good metric.[1–4] It is generally agreed that metrics must be clearly defined, simple, measurable, objective rather than subjective, and must ultimately drive the desired behaviour.[5] Over the past 5–10 years, a number of metrics have been proposed to make chemist’s aware of the need to change the practice of chemical syntheses so they are less wasteful. A few of these metrics will be reviewed.

Effective mass yield

Hudlicky *et al.*[6] proposed a metric known as effective mass yield that is defined ‘as the percentage of the mass of desired product relative to the mass of all non-benign materials used in its synthesis.’ Or, stated mathematically:

$$\text{Effective mass yield (\%)} = \frac{\text{Mass of products} \times 100}{\text{Mass of non-benign reagents}}$$

This metric attempts to define yield in terms of that proportion of the final mass, *i.e.*, the mass of the product, that is made from non-toxic materials. The introduction of reagent and reactant toxicity is an extremely important consideration that is frequently absent from discussions about yield. While Hudlicky’s metric makes an attempt to define benign (*i.e.*, ‘those by-products, reagents or solvents that have no known environmental risk associated with them for example, water, low-concentration saline, dilute ethanol, autoclaved cell mass, *etc.*’), the explanation suffers from a lack of definitional clarity. Defining ‘non-benign’ is difficult in practice when working with complex reagents and reactants that have limited environmental or occupational toxicity information.

Unless and until human toxicity and ecotoxicity information is routinely available for all chemicals, it would be difficult to use this metric for most synthetic chemical operations. In addition, depending on the situation, even saline, ethanol and autoclaved cell mass have some environmental impacts of one kind or another that would need to be evaluated and addressed.

E-factor

A second and earlier metric, E-factor, was proposed by Roger Sheldon[7] and is defined as follows:

$$\text{E Factor} = \frac{\text{Total waste (kg)}}{\text{kg product}}$$

This metric is relatively simple and easy to understand, and draws attention to the quantity of waste that is produced for a given mass of product. It also exposes the relative wastefulness of different parts of the chemical processing industries that includes industries as diverse as petrochemicals, specialities and pharmaceuticals. This metric may certainly be used by industry and can, if used properly, spur innovation that results in a reduction of waste.

It may, however, be difficult for an industry such as the Pharmaceutical Industry to routinely use this metric in its operations. This is because there may be a lack of clarity

Green Context

It is now widely accepted that the quantification of sustainable practices such as measuring the ″greenness″ of different chemical processes is essential if we are to make real progress. How else can we aim to compare the often numerous green chemistry approaches to reducing the environmental impact of an important chemical process? Here one of the worlds leading industrial groups studying process metrics critically compare and analyse some of the quantification methods available to the process chemist. Much interesting data resulting from applying these methods to important chemical transformations is presented.

JHC

DOI: 10.1039/b206169b

depending on how ‘total waste’ is ultimately defined and accounted for, and where the boundaries of the process are drawn. One may draw a boundary around the immediate process, around the facility or within the broader geographic region of the facility.

Some examples of this lack of clarity in defining waste might include: is waste that passes over the fence line the only waste considered? Is waste that is produced as a result of emissions treatment (*e.g.*, acid gas scrubbing, pH adjustment in wastewater treatment plants, *etc*.) included? Is waste that is produced as a result of energy use (heating or cooling reactions, abatement technology, *etc*) included? Finally, is waste solvent passed on to a waste handler to be burned in a cement kiln included?

From an operational perspective, these kinds of questions complicate the routine use of this metric for individuals whose primary concern is to get new products on to the market in as short a period of time as possible.

It may also be argued that drawing attention to waste does not always drive chemists to think about what might be done to avoid producing wastes. Instead, the tendency may be to ignore waste generated in a chemical reaction or process and let others focus on waste treatment at a later date.

Atom economy

When developing chemical processes, chemists for obvious reasons focus mainly on maximising selectivity and yield. In recent years, another variable some chemists have been considering is atom economy.[8] This term, first introduced by Barry Trost, was an attempt to prompt synthetic organic chemists to pursue ‘greener chemistry’. Simply stated, atom economy is a calculation of how much of the reactants remain in the final product. Final product in this context applies to a single chemical transformation, a series of chemical transformations in a single stage of a multistage synthetic route, or to the entire route to a final product.

The method for calculating atom economy is kept deliberately simple by making certain key assumptions, ignoring reaction yield and molar excesses of reactants. It also does not account for solvents and reagents.

Assumptions regarding atom economy

Reactants

A reactant is a substance of which some part is incorporated into a reaction product although not necessarily into the final product. The process of calculating atom economy may be simplified by only considering key reactants. For example, ‘catalysts’ used in stoichiometric quantities, or the acid or base used for hydrolysis, are considered to be reactants. These examples are in contrast to common inorganic reagents, even when used in stoichiometric quantities (*e.g.*, potassium carbonate in a Williamson ether formation), which have been ignored. Inorganic reagents and/or other materials are not included in the calculations as long as at least two other reacting substances are identified.

Reactants also include those materials incorporated into a reaction *intermediate*. Even if no part of a reactant is present in the final product itself (*e.g.*, in the case of addition and removal of a protecting group) it was part of an intermediate and is therefore included in the calculation. A good example of this would be the *in situ* formation of an acid chloride during an N-acylation reaction as shown in reaction scheme (1). The chlorinating agent, in this case the chemical complex formed from the reaction between DMF and oxaloyl chloride, would be included in the calculation, even if the chlorination is not a distinct step in the process.

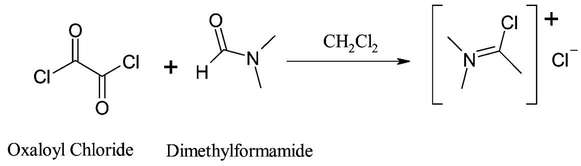

(1)

Stoichiometry

An excess of either or both reactants to maximise reaction yield/selectivity is not included in the calculation of atom economy. Reaction stoichiometry, on the other hand, has been taken into account. Thus, when two molecules of one substance combine with a single molecule of another to form a new molecule (either a reaction or process intermediate), the relevant ratio has been used.

Resolution and optical purity

In calculating atom economy for syntheses that employ a resolution step, the reaction stoichiometry needs to be adjusted to account for the fact that some portion of the mass will be discarded as the unwanted enantiomer. This includes those cases where the resolving agent is in a 1 : 1 or 2 : 1 ratio with respect to the desired enantiomer, or 1 : 2 as in the case where the desired enantiomer is difunctional.

How atom economy is calculated

For a generic reaction:

$$A + B \rightarrow C$$

$$\text{Atom economy} = \left(\frac{\text{m.w. of product C}}{\text{m.w. of A} + \text{m.w. of B}} \right) \times 100$$

The calculation considers only the reactants used and ignores the intermediates that are made in one stage and consumed in the next. *Because of this it is not possible to multiply the atom economy of each stage to give an overall process atom economy*. Process atom economy must be calculated as follows:

For a generic linear synthetic process:

$$(1)\ A + B \rightarrow C$$

$$(2)\ C + D \rightarrow E$$

$$(3)\ E + F \rightarrow G$$

Atom economy

$$= \left(\frac{\text{m.w. of product G}}{\text{m.w. of A} + \text{m.w. of B} + \text{m.w. of D} + \text{m.w. of F}} \right) \times 100$$

Processes with two or more separate branches are treated in an analogous way by taking into account all of the reactants but none of the intermediates in the calculation. Thus, for the

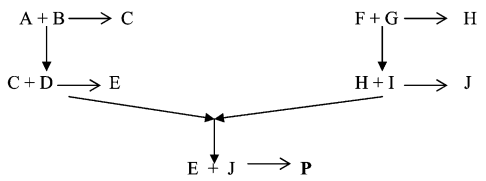

branched synthetic process where C, E, H and J are intermediates and E and J are coupled in the final step, atom economy is calculated as follows:

$$\text{Atom economy (\%)}=\frac{\text{mw P}}{\Sigma\,(\text{mw A, B, D, F, G, I})}\times 100$$

Mass intensity

A fourth metric discussed elsewhere[4] is mass intensity. Mass intensity is defined as follows:

$$\text{Mass intensity (MI)} = \frac{\text{Total mass used in a process or process step (kg)}}{\text{Mass of product (kg)}}$$

Mass intensity takes into account the yield, stoichiometry, the solvent, and the reagent used in the reaction mixture, and expresses this on a weight/weight basis rather than a percentage. In the ideal situation, MI would approach 1. Total mass includes everything that is used in a process or process step with the exception of water; *i.e.*, reactants, reagents, solvents, catalysts, *etc*. Total mass also includes all mass used in acid, base, salt and organic solvent washes, and organic solvents used for extractions, crystalisations, or for solvent switching. Water has been excluded from mass calculations since it skews mass data in many processes. Water *per se* also does not, in most instances, constitute a significant environmental impact.

It may also be useful to compare MI with E-Factor where:

$$\text{E Factor} = \text{MI} - 1$$

By expressing mass intensity as its reciprocal and making it a percentage, it is in a form similar to effective mass yield and atom economy. This metric will be called mass productivity.

$$\text{Mass productivity}=\frac{1}{\text{MI}}\times 100 = \frac{\text{Mass of product}}{\text{Total mass in process or process step}}\times 100$$

Other metrics that have been explored

Several other metrics related to atom economy have been developed and explored at GlaxoSmithKline. These are known as carbon efficiency (CE) and reaction mass efficiency (RME).[4] CE takes into account the yield and the amount of carbon in the reactants that is incorporated into the final product. RME takes into account yield, the actual molar quantities of reactants, and atom economy.

Carbon efficiency

When calculating carbon efficiency, yield and stoichiometry of reactants and products are included. CE is defined as the percentage of carbon in the reactants that remain in the final product.

For a generic reaction A + B → C

$$\%\ \text{Carbon efficiency}=\frac{\text{Amount of carbon in product}\times 100}{\text{Total carbon present in reactants}}$$

Thus, where the reaction is A + B = Product + co-product

$$\text{Carbon efficiency} = \frac{\text{no. of moles of product}\times\text{no. of carbons in product}\times 100}{(\text{moles of A}\times\text{carbons in A})+(\text{moles of B}\times\text{carbons in B})}$$

Reaction mass efficiency (RME)

When calculating reaction mass efficiency, atom economy (AE), yield and the stoichiometry of reactants are included. RME is the percentage of the mass of the reactants that remain in the product. There are two ways to calculate RME.

For a generic reaction A + B → C

$$\text{Reaction mass efficiency} = \left(\frac{\text{m.w. of product C}}{\text{m.w. of A}+(\text{m.w. of B}\times\text{molar ratio B/A}}\right)\times\text{yield}$$

or more simply:

$$\text{Reaction mass efficiency}=\left(\frac{\text{mass of product C}}{\text{mass of A}+\text{mass of B}}\right)\times 100$$

An example of how atom economy, carbon efficiency, reaction mass efficiency, mass intensity and mass productivity are computed follows: benzyl alcohol (10.81g, 0.10 mol, FW 108.1) is reacted with *p*-toluenesulfonyl chloride (21.9 g, 0.115 mol, FW 190.65) in toluene (500 g) and triethylamine (15 g) to give the sulfonate ester (FW 262.29) isolated in 90% yield (0.09 mol, 23.6 g).

$$\text{Atom economy}=\frac{262.29}{(108.1+190.65)}\times 100 = 87.8\%$$

$$\text{Carbon efficiency} = \frac{(0.09\times 14)}{(0.1\times 7)+(0.115\times 7)}\times 100 = 83.7\%$$

$$\text{Reaction mass efficiency}=\frac{23.6}{(10.81+21.9)}\times 100 = 70.9\%$$

$$\text{Mass intensity} = \frac{(10.81+21.9+500+15)}{23.6} = 23.2\ \text{g/g} = 23.2\ \text{kg/kg}$$

$$\text{Mass productivity}\ \frac{1}{\text{Mass intensity}}\times 100 = 4.3\%$$

The atom economy is less than 100% due to the formation of HCl as a by-product. The carbon efficiency accounts for the excess stoichiometry and the less than 100% yield of the product in terms of the number of carbons in the final molecule. The reaction mass efficiency also takes into account the 90% yield and the need for a 15% molar excess of *p*-toluenesulfonyl chloride.

To show how these metrics compare, the stoichiometry, yield, atom economy, carbon efficiency, reaction mass efficiency, mass intensity and mass productivity for 28 different chemistries are shown in Table 1. The values in Table 1 are averages of at least three examples for a given type of chemistry.

Detailed analysis of these data has revealed a number of things

1. Carbon efficiency, while an interesting attempt at an alternate metric, exhibits the same trends as RME, and offers

no additional insights on how one might improve chemistry or process conditions.

2. There are several chemistries that appear to be outliers in the data set; *e.g.*, resolutions and N-dealkylation reactions are significantly different in relation to the other chemistries.
3. These data indicate that most reactions are run at significant stoichiometric excesses which is not accounted for in atom economy.
4. Another observation is that reaction yield, a metric used almost universally by synthetic chemists, does not account for poor reaction mass efficiencies and a correspondingly significant waste of resource (mass or energy). While this may be an obvious statement, it should be noted that wasted resource may be expensive from both a direct materials cost and a more comprehensive life cycle costing perspective.
5. Data for mass intensity, yield, atom economy and stoichiometry do not correlate with each other in any meaningful way. These appear to be discretely different types of metrics, and following one metric in isolation of the others may not drive the best behaviour for 'greening' reactions.
6. Because reaction mass efficiency accounts for all reactant mass (*i.e.*, actual stoichiometric quantities used) and includes yield, and atom economy, the combined metric is probably the most helpful metric for chemists to focus attention on how far from 'green' current processes are being operated.
7. Mass productivity may be a useful metric for businesses since it highlights resource utilisation. This is illustrated in Table 2 where the average atom economy is compared with the average mass productivity for 38 drug-manufacturing processes.

As can be seen from Table 2, the average atom economy of 43% for a multi-step synthesis would not appear to be unreasonable to most chemists for a seven stage synthesis of a complex drug. However, the average mass productivity for these synthetic processes is only 1.5%. This means that 98.5% of the total mass used to make a drug is being wasted. Even if the atom economy for individual steps of the process were raised above 95%, this may not necessarily increase the overall average mass intensity of the process to a significant extent. Since a majority of the mass in a given process is not accounted for by atom economy or even reaction mass efficiency, it may be argued that atom economy may not be the most robust measure or the best measure of sustainability for industrial use.

Table 2 Comparing atom economy and mass productivity for 38 processes (average number of stages = 7)

	Overall process average (%)	Range (%)
Atom economy	43	21–86
Mass productivity	1.5	0.1–7.7

Cost implications

It would be a mistake to leave a discussion of metrics at the point of only considering mass implications. Clearly, wasted resources may have significant cost implications. Using the atom economy metric as an example, it is readily seen that reactions possessing low atom economy will affect the cost of synthesising a new chemical entity because:

(a) not all portions of each reactant molecule are incorporated into the molecule; *i.e.*, materials (and energy) are not used efficiently;
(b) the synthetic strategies will affect the length and complexity of the route;
  (i) portions of the molecule may be in the wrong oxidation state;
  (ii) protection/deprotection may be required;
  (iii) chiral resolutions may be required;

Table 1 Comparison of metrics for different chemistries

	Stoichiometry of B mol (%)	Yield (%)	Atom economy (%)	Carbon efficiency(%)	Reaction mass efficiency (%)	Mass intensity excluding water (kg/kg)	Mass productivity (%)
Acid salt	135	83	100	83	83	16.0	6.3
Base salt	273	90	100	89	80	20.4	4.9
Hydrogenation	192	89	84	74	74	18.6	5.4
Sulfonation	142	89	89	85	69	16.3	6.1
Decarboxylation	131	85	77	74	68	19.9	5.0
Esterification	247	90	91	68	67	11.4	8.8
Knoevenagel	179	91	89	75	66	6.1	16.4
Cyanation	122	88	77	83	65	13.1	7.6
Bromination	214	90	84	87	63	13.9	7.2
N-Acylation	257	86	86	67	62	18.8	5.3
S-Alkylation	231	85	84	78	61	10.0	10.0
C-Alkylation	151	79	88	68	61	14.0	7.1
N-Alkylation	120	87	73	76	60	19.5	5.1
O-Arylation	223	84	85	69	58	11.5	8.7
Epoxidation	142	78	83	74	58	17.0	5.9
Borohydride	211	88	75	70	58	17.8	5.6
Iodination	223	96	89	96	56	6.5	15.4
Cyclisation	157	79	77	70	56	21.0	4.8
Amination	430	82	87	71	54	11.2	8.9
Lithal	231	79	76	76	52	21.5	4.7
Base hydrolysis	878[a]	88	81	77	52	26.3	3.8
C-Acylation	375	86	81	60	51	15.1	6.6
Acid hydrolysis	478	92	76	76	50	10.7	9.3
Chlorination	314	86	74	83	46	10.5	9.5
Elimination	279	81	72	58	45	33.8	3.0
Grignard	180	71	76	55	42	30.0	3.3
Resolution	139	36	99	32	31	40.1	2.5
N-Dealkylation	2650[a]	92	64	43	27	10.1	9.9

[a] Inflated by use of solvent as reactant.

(c) purifications and separations may be required to remove by-products, reactants, reagents, solvents, *etc.*;
(d) there are environmental, safety and health costs associated with the management of materials and treatment of waste products.

The relationship between atom economy and cost

To illustrate the relationship between atom economy and cost, we employed a traditional costing approach to evaluate the cost of materials used to synthesize four different drugs. Seven different economic models were used and the results are shown in Table 3 and Fig. 1. These cost models are:

Minimum cost for minimum process stoichiometry + standard yield, reactant stoichiometry and solvent

This is the cost when process chemicals are not used in stoichiometric excess; *i.e.*, no more than 1 mol is used. All other costs are based on using standard amounts; *i.e.*, what is actually used and obtained in plant.

Minimum cost at 100% atom economy + standard yield, solvent and process stoichiometry

Reactant costs may be used to assign a cost to the proportion of each material that is incorporated into the product. From this, it is possible to calculate the cost if the AE were 100%. All other costs are based on using standard amounts; *i.e.*, what is actually used and obtained in plant.

Minimum cost at 100% yield + standard solvent and process stoichiometry

This is the cost for using standard quantities of reactants, process chemicals and solvent, but the yield is 100%.

Minimum cost at 100% solvent recovery and standard yield and process stoichiometry

This is the cost if 100% of all solvents are recovered and reused (assumes zero recovery cost). All other costs are based on using standard amounts; *i.e.*, what is actually used and obtained in plant.

Table 3 Comparison of cost models for four different drugs

	% Total cost[a]			
Cost model	Drug 1	Drug 2	Drug 3	Drug 4
Minimum cost for minimum process stoichiometry + standard yield, reactant stoichiometry and solvent	86	99	92	97
Minimum cost at 100% atom economy + standard yield, solvent and process stoichiometry	87	40	84	69
Minimum cost at 100% yield + standard solvent and process stoichiometry	71	32	56	57
Minimum cost at 100% solvent recovery and standard yield and process stoichiometry	63	84	64	55
Minimum cost at 100% atom economy, process stoichiometry and solvent recovery	36	22	40	21
Minimum cost at 100% yield, solvent recovery and standard process stoichiometry	34	16	20	11
Minimum cost at 100% yield, solvent recovery and reactant and process stoichiometry	20	15	12	8

[a] Total cost = cost of all materials actually used in the process. The table was constructed by calculating the theoretical cost associated with each cost model (column 1) and dividing by the total cost.

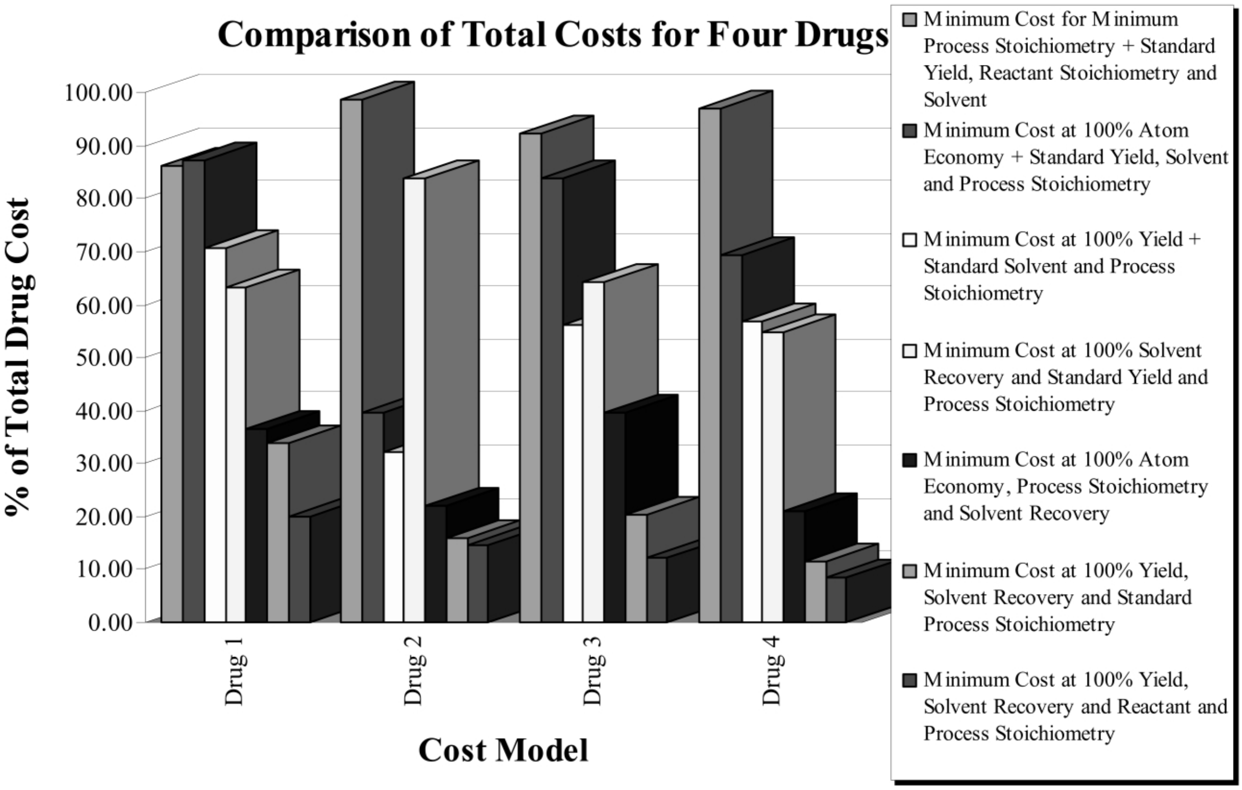

Fig. 1 A comparison of cost models for four different drugs.

Minimum cost at 100% atom economy, process stoichiometry and solvent recovery

Reactant costs may be used to assign a cost to the proportion of each material that is incorporated into the product. From this, it is possible to calculate the cost if the AE were 100%. Additional costs include the cost when process chemicals are not used in stoichiometric excess; *i.e.*, no more than 1 mol is used, and the cost if 100% of all solvents are recovered and reused (assumes zero recovery cost).

Minimum cost at 100% yield, solvent recovery and standard process stoichiometry

This is the cost when the yield is 100%, all solvents are recovered and reused (assumes zero recovery cost), and all other costs are based on using standard amounts; *i.e.*, what is actually used and obtained in plant.

Minimum cost at 100% yield, solvent recovery and reactant and process stoichiometry

A theoretical minimum cost may be derived assuming no stoichiometric excess, 100% solvent recovery, and a 100% overall yield.

As can be seen from Fig. 1 and Table 3, the pursuit of atom economy may be less of an economic driver than may be thought. This analysis suggests that progress towards higher yield reactions, a reduction in stoichiometric excesses of reactants, and elimination or complete solvent recycle and reuse may be more economically effective, at least in the short term.

A more detailed analysis of the costs associated with three of the four drugs evaluated is illustrated in Table 4 for drug 3 and in Figs. 2 and 3 for drug 1 and 2.

Our analysis of the materials costs for these drugs also indicates that more than 75% of the total costs are for either those portions of reactants that do not remain in the final product or reagents (column 4, Table 4) and this high percentage is attributable to about four materials. A review of costs in this fashion will help to identify those portions of the synthetic process that might be changed to afford the greatest economic and environmental benefit (*e.g.*, recovery and reuse). The data in Table 4 also illustrates the typical cost structure that might be expected when a chiral resolution is used. Replacing this synthesis and resolution by a chiral synthesis would, rather obviously, be a more beneficial economic and atom economical strategy.

A further comparison of the four drugs is shown in Table 5 and reveals that for three of the four compounds, the cost of poor

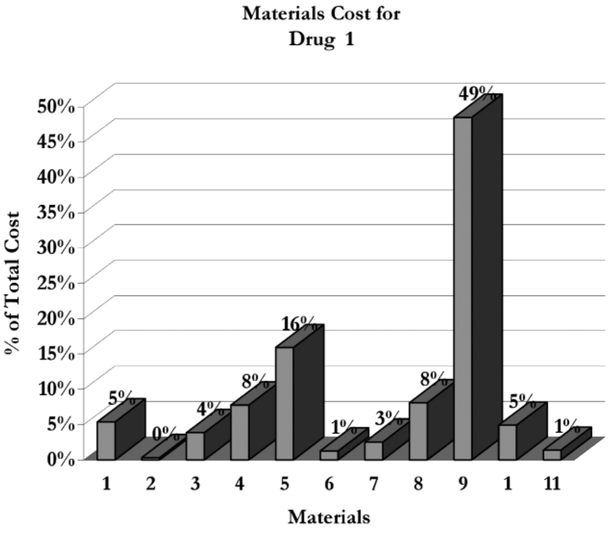

Fig. 2 Materials cost for drug 1.

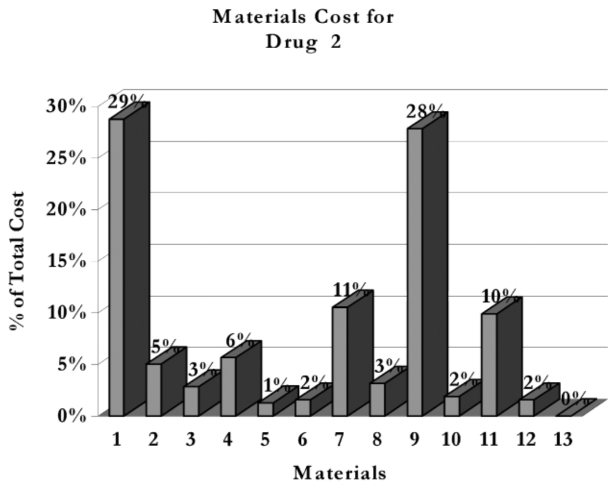

Fig. 3 Materials cost for drug 2.

Table 4 Comparison of costs for drug substance 3

Reactants	Molar equivalents used	% Of molecule in final drug[a]	% Contribution to overall cost of drug 3	% Of total cost for non-incorporated reactants[b]
Intermediate 1	2	43	12.8	12
Reducing agent	4.6	5	30.4	49
Resolving agent	2.2	0	16.0	26
Intermediate 2	2	27	4.5	6
Intermediate 3	1	0	0.6	1
Intermediate 4	1	0	0.7	1
Material 1	3	0	1.2	2
Material 2	1	0	0.1	
Material 3	1	100	10.4	
Material 4	6	0	0.5	1
Material 5	1.2	0	0.5	1
Material 6	1	100	0.0	
Material 7	10	14.5	0.3	
Material 8	2	0	0.3	
Solvents			21.7	
All other materials			0.1	

[a] This is the proportion of the molecule that remains in the final product molecule and can be calculated by the process chemist. [b] This is the wasted cost (in terms of percentage) for each material due to inefficient incorporation into product

Table 5 Comparison of solvent and poor atom economy costs for drug substances

	Solvent cost as % of total	Cost for non-incorporated reactants as % of total
Drug 1	45	32
Drug 2	36	21
Drug 3	22	61
Drug 4	14	10

atom economy is less than the solvent cost. In addition, yield and stoichiometry are the most significant cost drivers and exert significantly more influence on cost than poor atom economy.

Another point of interest is noted for drug 4 where the opportunity to reduce cost through atom economy does not appear to be significant. In this instance, a catalyst used for the synthesis is relatively costly. In the isolated case of using the catalyst within the gates of the company, a 10% loss of catalyst to effluent represents 16% of the total materials costs paid by the company for this drug. It should be noted that 16% of the total materials cost is not a small number! This cost does not include the life cycle total cost perspective, *i.e.*, the cost of raw materials extraction, catalyst production, use, recovery and loss to effluent, all of which may have significant costs in addition to environmental impacts. While this is not an argument against using catalysts, it is certainly true that the type of catalyst, its potential for re-use, and its recoverability are important features of good process design and environmental and economic performance.

It is recognised that this economic evaluation only considers costs for several existing industrial processes that represent the current state of affairs for drug manufacture. This evaluation also does not consider the total cost of drug synthesis; *i.e.*, those costs beyond simple materials costs. While it has been shown that the EHS costs in a total cost assessment for many industries can be quite significant, our studies have shown that the EHS costs for high value added materials are generally less than traditional materials costs, unless total life cycle costs are included. Until society forces markets to focus greater attention on, and build standardised, accepted economic models for life cycle costs, it will remain difficult to assess these costs and make acceptable business decisions based upon these costs.

This analysis also ignores the potential benefits from alternative more atom economical routes where it may be possible to have only two reactants producing a single easily isolated product in a completely recyclable reaction medium at room temperature and pressure. A second alternative would be a synthesis without solvent, but this may increase the energy or capital requirements. Thus, it must be understood that the point of striving for more atom economic reactions in the future is the hope that they use less resources (materials and energy) and have higher overall process efficiencies.

Effect of technology

While new chemistries will assist in delivering higher atom economies they are likely to require the use of different technologies. In the short to medium term, it is clear that the integration of technology and chemistry may deliver significant benefits when using current less atom economical chemistries.

Questions to be addressed:

Questions and considerations for further research currently being explored include.

(a) Is there a correlation between any of these metrics and the molecular complexity of the drug substance?
(b) Can a model for molecular complexity correlated with reaction mass efficiency be developed?
(c) Can realistic targets be set for reaction mass efficiency based on this complexity model?
(d) How does a pursuit of reaction mass efficient reactions influence energy intensity?

Conclusions

Exploration of a variety of metrics has revealed the following:

- Pursuing a metric such as yield, a ubiquitous metric chemist's utilise to evaluate reaction efficiency, will not by itself drive business towards sustainable practices. However, from an economic standpoint, yield remains a very good metric, especially for high value added materials such as pharmaceuticals;
- Atom economy may be useful as an organising concept or in combination with other metrics, but at this time it is not considered to be useful as a stand-alone metric;
- Reaction mass efficiency combines key elements of chemistry and process and represents a simple, objective, easily derived and understood metric for use by chemists, process chemists or chemical engineers;
- Mass intensity may be usefully expressed as mass productivity, and as such, seems to be more broadly understood by business managers;
- Reaction mass efficiency appears to be a useful metric for focusing attention away from waste towards the use of materials. As such, it is more likely to drive chemical and technology innovations that will lead to more sustainable business practices.

As current chemistries and the processes associated with these chemistries are reviewed, it appears that chemistry, in isolation of process, will not ‘green’ the chemical process industries, especially as represented by the pharmaceutical industry. It also appears that chemical process technology must change with changes in chemistry if industry is to move towards more sustainable business practices. The importance of this connection between ‘green chemistry’ and ‘green technology’ is being highlighted elsewhere.

References

1 *Sustainable Measures*, ed. M. Bennett and P. James, Greenleaf Publishing, Ltd., Sheffield, 1999.
2 *Industrial Environmental Performance Metrics, Challenges and Opportunities*, Committee on Industrial Environmental Performance Metrics, National Academy of Engineering, National Research Council, National Academy Press, 2101 Constitution Avenue, N.W., Washington, D.C., 20418, 1999.
3 *Corporate Environmental Performance 2000, Vol 1*, Strategic Analysis, Haymarket Business Publications, Ltd., Haymarket Business Publications, 174 Hammersmith Road, London, W6 7JP, 1999.
4 A. D. Curzons, D. J. C. Constable, D. N. Mortimer and V. L. Cunningham, *Green Chem.*, 2001, **3**, 1–6.
5 D. J. C. Constable, A. D. Curzons, L. M. Freitas dos Santos, G. R. Geen, R. E. Hannah, J. D. Hayler, J. Kitteringham, M. A. McGuire, J. E. Richardson, P. Smith, R. L. Webb and M. Yu, *Green Chem.*, 2001, **3**, 7–9.
6 T. Hudlicky, D. A. Frey, L. Koroniak, C. D. Claeboe and L. E. Brammer, *Green Chem.*, 1999, 57–59.
7 R. A. Sheldon, *Chem. Ind. (London)*, 1992, 903–906; R. A. Sheldon, *Chem. Ind. (London)*, 1997, 12–15.
8 B. M. Trost, *Science*, 1991, **254**, 1471.

Development of a green process for poly-α-olefin based lubricants

Ganapati D. Yadav* and Nirav S. Doshi

Department of Chemical Engineering, University Institute of Chemical Technology (UICT),
University of Mumbai, Matunga, Mumbai 400 019, India. E-mail: gdyadav@yahoo.com;
Tel: 91-22-410-2121; Fax: 91-22-414-5614

Received 24th June 2002
First published as an Advance Article on the web 4th October 2002

Poly-α-olefin (PAO) based lubricants have a large share of the synlubes market and these are produced in two stages—oligomerisation of **α**-olefins and hydrogenation. The current industrial processes use $AlCl_3$ and BF_3 as catalysts for oligomerisation, which are polluting, hazardous and give a very wide molecular weight distribution. This study reports a green synthesis of a PAO synlube by using 1-decene as the starting material with a variety of solid acidic catalysts, mainly based on clays. The activities for oligomerisation were found to be in the following order: K10 montmorillonite clay > 20% w/w $ZnCl_2$/K10 > 5% w/w (dodecatungstophosphoric acid, DTP)/K10 > 20% DTP/K10 > 10% $AlCl_3$ + 10% $FeCl_3$/K10 > S–ZrO_2 > Al-pillared clay > DTP > 20% DTP/carbon. K10 clay gave a conversion of 1-decene of 73% but the selectivities towards the dimer and trimer were 88 and 12%, respectively. 20% $ZnCl_2$/K10 led to a conversion of 68% with 100% dimer formation. The kinetics of reaction were established by using both K-10 and 20% $ZnCl_2$/K10. Oligomerisation is controlled by intrinsic kinetics. The catalysts are reusable. Other olefins such as 1-octene and 1-dodecene were also oligomerized in the presence of 20% $ZnCl_2$/K10. 1-Decene dimer was isolated and then in the next step hydrogenated by employing 20% w/w Ni/SiO_2, 20% w/w Ni–Cu (50:50)/SiO_2 and a clay anchored bipyridine–montmorillonite–$PdCl_2$ complex as catalysts. Amongst these 20% w/w Ni/SiO_2 was found to be the most active catalyst at 50 atm and 150 °C, whereas the anchored catalyst BM–Pd(II) was active at atmospheric pressure and 30 °C. Effects of various parameters were studied to arrive at a kinetic model with both the catalysts. The reactions are intrinsically kinetically controlled showing zero order in dimer concentration and first order in hydrogen partial pressure. 1-Decene based PAO with a viscosity of about 2 cSt has great many applications The hydrogenated product had a viscosity of 2.22 cSt which was found to be comparable with commercially available sample. High-speed spindle oil used in textile industry was also prepared and its performance tested.

1. Introduction

1.1 Synlube market and processes

Majority of the present-day lubricants are petroleum-derived mineral oils which are formulated into several grades to suit their automotive and industrial applications. Mineral oil lubricants contain hundreds of chemicals of different molecular weights owing to their origin in several refinery operations such as catcracking, distillation, hydrogenation and isomerisation.[1] These oils must be replaced frequently due to their performance failure leading to damage to the mobile parts and thus they generate a lot of waste. In spite of upgrades, mineral oils do not meet the specifications prescribed for lubricants in several areas of modern technology such as gas turbine engines in civilian aircraft, the associated high temperature at subsonic as well as supersonic speeds, military requirements in missile and weapon development, radiation hazards, high-profile assignments on big rigs, nuclear reactors and outer space.[1–3] These stringent requirements have been met by synthetic lubricants, or synlubes, which are used either as produced or as blends with the mineral oil base stocks. Synlubes possess unique performance properties such as excellent thermal and oxidative stability, low temperature fluidity, low volatility, high viscosity index, fire resistance, low corrosivity, hydrolytic stability, water insolubility, minimal decomposition-product deposits, and radiation resistance.[1] Thus frequent wastage is avoided and performance of equipment is assured under severe conditions.

Poly-α-olefins (PAOs) are the most widely used synlubes in the US and Europe.[2] The current methods of PAOs production involve use of highly corrosive and hazardous homogeneous acid catalysts such as $AlCl_3$, BF_3, HF, *etc*. In addition, these catalysts produce a wide range of products containing several oligomers for which costly separation technologies have to be used before they are processed further to make the synlubes. The use of acid catalysts is very extensive in chemical and allied industry, and those technologies employing highly corrosive, hazardous and polluting liquid acids are being replaced with solid acids; for instance, acid treated clays, zeolites, ion exchange resins, and a variety of metal oxides. Thus, there is a tremendous scope to devise green processes replacing the corrosive and polluting acids and also to synthesise tailor-made synlubes with controlled molecular weight, which automatically lead to enhanced life during operation and cheaper processing. The current paper is an attempt in that direction.

It is worthwhile to briefly review this area and bring into perspective the significance of our work. Synlubes have an

Green Context

Lubricants represent a group of chemicals which are used in enormous quantities worldwide. Improved methods for their production are sought which avoid the use of homogeneous acid catalysts. Here, a method is described which utilises a relatively cheap and easily handled solid acid, which has the additional benefit of improving selectiivty in the process. For a comprehensive review on green lubricants, see *Green Chem.*, 2002, 4, 293. ***DJM***

DOI: 10.1039/b206081g

estimated business of over \$2.5 billion in the United States alone, which is estimated to rise to 1.1 million metric tons per annum (MMTA) in 2003 and to 1.78 MMTA in 2008 with values of US \$3.96, and 7.32 billion, respectively.[2] Commercially valuable synlubes are (a) poly-α-olefins (PAO), (b) dibasic acid esters, (c) neopolyol esters, (d) polyalkylene glycols, (e) phosphate esters, (f) dialkylbenzenes, (g) polybutenes and (h) other small volume speciality products such as silicate esters, silicones and fluorosilicones, polyphenyl ethers, chlorotrifluoroethylene (CTFE), oligomers and perfluoropolyphenyl ethers (PFPE).

1.2 Poly-α-olefins (PAOs)

Unlike the mineral oils, PAOs are all-hydrocarbon structures, without any sulfur, phosphorus or metals. PAOs have good thermal stability, but they require suitable antioxidant additives to resist oxidation. They are generally manufactured in two steps from α-olefins and most of the PAO technologies are patented and owned by refiners (Scheme 1). The desired α-olefin is itself manufactured by polymerisation of ethylene. In the first step of PAO synthesis, the olefin is oligomerised, by using a variety of acidic catalysts, to give oligomers of different molecular weights. The second step involves the hydrogenation of unsaturated oligomers to make them chemically inert and more stable as PAO.

1.2.1 Oligomerisation processes. Currently the synlubes industry produces low viscosity grade oligomers from 2 cSt to 10 cSt, by using a BF_3–alcohol catalytic system whereas for the production of higher viscosity grade oligomers (40–100 cSt), $AlCl_3$ is used as catalyst. The use of linear α-olefin to synthesize a PAO has been reported using a variety of catalysts which include $AlCl_3$,[3] a free radical initiator,[4] and ethyl aluminium sesquichloride/titanium tetrachloride.[5] The use of BF_3 as catalyst with a protic co-catalyst like water, alcohol or carboxylic acid was made to produce oligomers of uniform quality.[6–9] Oligomers useful as heat transfer fluids were produced from 1-decene oligomerisation with BF_3 and an ethoxylated alcohol at 45 °C for 2 h to give a product containing monomer (23%), dimer (48%), trimer (20%) and tetramer (9%).[7] Other oligomers from straight chain C_6–C_{20} α-olefins were produced with BF_3 as catalyst and when *n*-butanol was used as protic co-catalyst in conjunction with BF_3, oligomerisation of 1-decene gave a product with the highest selectivity of the trimer (53%).[10] Oligomers of 1-decene were prepared by using alkyl aluminum chloride as catalyst and *tert*-butyl chloride as co-catalyst at 0–25 °C for 2 h.[11] A high quality synthetic lubricant was prepared from C_8–C_{14} straight chain α-olefins by using reduced chromium catalyst supported on silica.[12] The oligomerisation of 1-decene was studied over different kinds of solid acidic catalysts, among which boron phosphate showed highest oligomerisation activity than SiO_2–Al_2O_3 and sulfated zirconia.[13]

1.2.2 Hydrogenation process. There is no open literature on hydrogenation of oligomers of synlubes type.[14–20] There is a scope for investigating monometallic and bimetallic catalysts in the hydrogenation of poly-α-olefins as well as clay based complexes. The swelling type of silicates such as montmorillonite and hectorite are known to be good supports for the transition metal complexes in their interlayers which can be used as effective catalysts for hydrogenations and hydroformylations.[21] Anchored catalysts such as poly(styryl) bipyridine palladium complexes, montmorillonite palladium chloride and bipyridine montmorillonite palladium acetate complexes are used to conduct hydrogenation of various alkenes and alkynes of low molecular weight[22–24] at ambient temperature. Apparently no work has been reported for the use of such anchored catalysts for hydrogenation of PAO oligomers.

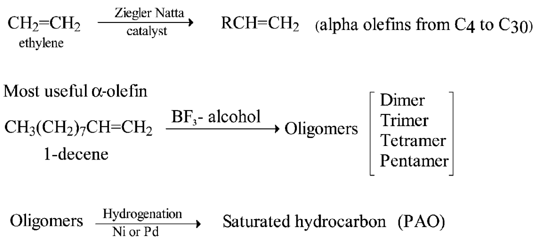

Scheme 1 Typical poly-α-olefin (PAO) manufacturing process.

1.3 Scope

The foregoing suggests that there is a tremendous scope to develop green processes for synlubes. The choice of the starting α-olefin, catalyst and its reusability are very critical aspect of the overall product development. The product distribution in the oligomers should be limited to a single oligomers only so that the final product could be used for specific applications. 1-Decene based PAO products have the widest range of operational temperature and most application performance testing have been done with 1-decene derived PAO.[1] In particular, the 2-cSt product has great many applications and it is mainly C_{20} alkane. This study was therefore undertaken to produce poly-α-olefins based synthetic lubricants of viscosity 2 cSt by using 1-decene as the starting material for which only the dimer should be produced. The synthesis has two clear-cut aspects, namely, oligomerisation and hydrogenation. We believed that modified clays should be better catalysts if their acidities could be properly controlled to produce the desired synlube. They could be used as supports for both oligomerisation and hydrogenation .The acidity of clays can be modified by impregnating them with a variety of inorganic acids leading to better activity and selectivity.[25–42] Among others, the nature of acidity in supported clays *vis-à-vis* the parent clay, has been studied by different researchers: the so-called clayzic by Clark's group[25–28] and Brown *et al.*,[29,30] heteropolyacids (HPA) supported on K10 firstly reported by us[33,34] and exploited in a number of reactions,[35–42] pillared clays by Pinnaivia's group.[31] The overall objective of the current work was to develop a green process for PAO based lubricants starting from an olefin including kinetics of individual reactions.

2. Experimental

2.1 Chemicals and materials

All chemicals were analytical grade and procured from firms of repute: 1-decene, 1-octene and 1-dodecene (Albemarle Corporation, USA), nickel nitrate, copper nitrate, bipyridine, *n*-butyllithium (1.6 M in hexane) (E. Merck), palladium chloride (Loba Chemicals, Mumbai), K10 montmorillonite clay (Fluka), Filtrol-24 (Engelhard, France), Aerosil-200 silica support (surface area 200 $m^2\ g^{-1}$, Degussa, Germany). All other chemicals were obtained from M/s s.d. Fine Chemicals Pvt Ltd., Mumbai, and used as obtained.

2.2 Acid catalysts

The following catalysts were prepared by well-developed procedures and characterised in the laboratory: 5–20% w/w DTP/K-10,[35–37] $AlCl_3 + FeCl_3$ (10% w/w each)/K-10,[35] 20% w/w DTP/carbon,[42] Al pillared clay,[35–37] 20% w/w $ZnCl_2$/K10 (clayzic)[35,37] and sulfated zirconia (S-ZrO_2)[43,44]

2.3 Silica supported metal catalysts

20% w/w Ni/SiO_2 and 20% w/w Ni–Cu (50 : 50)/SiO_2 were prepared by the incipient wetness technique using Aerosol-200 silica as the support and the corresponding metal nitrate solution equivalent to their pore volume as described in our earlier work.[45,46] The catalysts were dried and then reduced under H_2 flow at 450 °C for 6 h and then cooled to room temperature. The catalysts were fully characterised as discussed elsewhere.[46]

2.4 Anchored bipyridine montmorillonite palladium chloride complex catalyst

Wyoming montmorillonite, Swy-2, (surface area 232 $m^2 g^{-1}$) was the source of H^+montmorillonite and the preparation of catalyst. Swy-2 was suspended as slurry and allowed to sediment for 24 h to remove denser impurities like quartz and calcite. Na^+-montmorillonite was prepared by treating Swy-2 with saturated aqueous NaCl solution for 36 h. It was centrifuged, washed thoroughly with deionised water and air-dried. H^+-montmorillonite was obtained by treating Na^+-montmorillonite with 200 ml 0.1 M HCl solution. Then it was centrifuged, washed thoroughly with deionised water until free from chloride (confirmed with silver nitrate rest) and vacuum dried at 80 °C for 6 h. To remove any traces of water, the clay was further washed with dry ethanol. H^+-montmorillonite thus obtained was treated with excess $SOCl_2$ in dry benzene for 24 h to synthesize chloro-montmorillonite. Chloro-montmorillonite was suspended in dry THF and cooled to −74 °C using dry-ice and excess *n*-butyllithium (6.5 mM, 1.6 mol in hexane) was added to the stirred suspension. The solution was stirred at 0 °C for 4 h and allowed to warm at room temperature. Bipyridine (1 g, 6.3 mol) was added to it at room temperature and the solution was refluxed for 5 h. The resulting montmorillonite bipyridine was thoroughly washed with dry THF, ethyl acetate and benzene in repeated cycles to remove any adhered bipyridine.

1 g montmorillonite bipyridine and 0.2 g palladium chloride in phenylacetonitrile were taken in 50 ml of dry benzene and stirred at room temperature for 6 h. It was thoroughly washed with THF and dry benzene in repeated cycles, filtered and dried in an oven at 120 °C for 4 h. These catalysts were fully characterized. XRD of bipyridine montmorillonite and its complex (not shown here) with palladium chloride exhibited an interlamellar d_{001} spacing in the region between 14 and 15 Å (assigned to the anchored ligand and its complex) whereas d_{001} spacings of bipyridine montmorillonite and its complex were 14.07 and 14.54 Å, respectively. This increase in interlamellar spacing clearly indicated functionalisation of montmorillonite lattice and complexation with metal in the interlamellars. The peaks in the region 9–10 Å were due to unreacted montmorillonite layers.

2.5 Apparatus and procedure

2.5.1 Oligomerisation. All experiments were carried out in a 100 mL stainless steel Parr autoclave. A four-bladed-pitched turbine impeller was used for agitation. The temperature was maintained at ±1 °C of the desired value. Predetermined quantities of 1-decene, the catalyst and an internal standard (*n*-dodecane) were charged into the autoclave and the temperature raised to the desired value. Agitation was then commenced and an initial sample withdrawn. Further samples were taken out at periodic intervals up to 4 h.

2.5.2 Hydrogenation. Dimer of 1-decene was prepared by using 20% $ZnCl_2$/K10 catalyst as discussed in this work and separated from the monomer by vacuum distillation. A GC-MS of the dimer was also measured and it showed 100% purity. Its iodine value was found as 129 as given in literature,[47] which also confirmed its authenticity. A standard 100 ml S.S Parr autoclave, with a magnetically-driven pitched-blade turbine impeller, was used to carry out the hydrogenation reaction. The autoclave was externally heated by a heating mantle, which was connected to a programmer. The temperature could be controlled within ±1 °C.

Three different catalysts were used for hydrogenation. In the case of Ni/SiO_2 and Ni–Cu/SiO_2 catalysts, the following procedure was adopted. A predetermined quantity of 1-decene dimer was dissolved in dry THF and a known amount of catalyst immersed in the same solvent were charged into the autoclave. The THF volume was 35 mL. It was purged with hydrogen for 5 min and then heated to 150 °C. When the desired temperature was reached, the autoclave was charged with hydrogen to the required pressure (usually 50 atm). A zero time sample was taken immediately, and the stirring was started. Samples were withdrawn periodically and analysed by GC. The hydrogen pressure was kept constant by intermittent pressurizing of the autoclave.

The clay supported catalyst, bipyridine montmorillonite palladium chloride was employed to conduct the hydrogenation of 1-decene dimer at atmospheric pressure and ambient temperature in the same reactor.

2.6 Analysis

Analysis was done by using gas chromatography (Perkin-Elmer 8500 model) with a flame ionisation detector by using a stainless steel column (2 m long × 3.0 mm i.d.) packed with 10% OV 17 supported on chromosorb WHP in both the processes. Products were separated by vacuum distillation and identification was made through GC–MS as well as comparison with authentic material. Synthetic mixtures of pure components were used for qualitative and quantitative analysis. The same analytical methods were used for both the systems. The iodine value of the reaction was also determined to estimate the double bond saturation in the case of oligomerisation. Both analyses matched very well.

3 Results and discussion

3.1 Oligomerisation of 1-decene

The mechanism involves formation of a carbocation on the catalyst site which can undergo isomerisation. It then combines with 1-decene to yield the dimer and so on (Scheme 2).

3.1.1 Efficacies of various catalysts. The efficacy of several K10 montmorillonite clay based catalysts, pillared clay and sulfated zirconia was evaluated at 190 °C and 1000 rpm for 4 h in the absence of any external or internal diffusion, limitation which will be explained later. The product distribution indicated that some catalysts formed the dimer selectively whereas others led to the dimer with some trimer. No higher oligomers were formed in any case (Table 1). The activities are in the following order:

K10 montmorillonite clay > 20% w/w $ZnCl_2$ /K10 > 5% DTP w/w /K10 > 20% DTP/K10 > 10% $AlCl_3$ + 10% $FeCl_3$/K10 > S–ZrO_2 > Al-pillared clay > DTP > 20% DTP/carbon

K10 clay was the most active with 73% conversion but with selectivities of 88% dimer and 12% trimer. 20% $ZnCl_2$/K10 gave 68% conversion and 100% selectivity of the dimer. Both 5% DTP/K10 and 20% DTP/K10 gave 100% selectivity to dimer but the conversion was much lower at 48 and 46%, respectively. Others were less active. To limit the product distribution to the dimer or trimer of 1-decene would require materials having large porosity in the mesoporous range. Clays and modified clay catalysts were thus thought to be attractive. Acid treated clays such as montmorillonite K10 are in fact mesoporous[31] with a broad distribution of pore sizes but with a majority in the range of 60–100 Å. Thus, K10 was found to be an ideal catalyst as well as support. K10 possesses mainly Brönsted acidity and thus by impregnating it with other Brönsted acids and Lewis acids also gave an idea of the effect of nature of acidity and pore size on oligomerisation. Sulfated zirconia has a wide pore size distribution and is superacidic in nature, with both Brönsted and Lewis acid sites.[44]

Analysis of surface area could be used to correlate the catalyst activity. Higher loadings of the active species are possible when the support has a larger surface area and thereby activity of the catalyst per unit weight increases. The surface areas of the catalysts were analysed by BET method using the N_2 adsorption technique on a Micromeritics ASAP 2010 instrument.

In the case of K-10 montmorillonite clay, which was dried at 150 °C before use, the surface area was 228 $m^2\ g^{-1}$ and the pore volume was 0.352 $cm^3\ g^{-1}$ with the pore sizes ranging in 45–150 Å. These values are consistent with those reported by others.[25] The wider distribution indicates the easy accessibility of the pore networks to 1-dodecene molecules. K-10 comprises mainly Brönsted acidity. DTP/K10 and clayzic were tested to find whether the type of acidity mattered in oligomerisation. 5% DTP/K10 and 20% DTP/K10 gave almost identical conversions with 100% selectivity to the dimer of 1-decene. This might be due to the decrease in the surface area of the catalyst when DTP was supported on K10 and the trimer being a bulky molecule its formation might be difficult, hence selectivity towards dimer had increased to 100%. Both these catalysts contain Brönsted acidic sites mainly with little Lewis acids. Characterization of the catalyst is reported earlier by us.[35,36,40] The surface areas of these catalysts had reduced to 178 $m^2\ g^{-1}$ (5% DTP/K10) and 107 (20% DTP/K10) $m^2\ g^{-1}$ from 228 $m^2\ g^{-1}$ of the K-10 clay support. This would suggest that all pores were not accessible to the bulkier 1-decene molecules and the total available acid strength of DTP/K10 was less than clayzic. The XRD studies of DTP/K10 had indicated that in the impregnation process, the clay had lost some of its crystallinity compared to K10. In the case of DTP/K10 there are lot of dispersed particles on the surface of the support K10 as revealed by SEM photomicrographs. FTIR of K10 showed that there were Si–O and Si–O–Al linkages and the OH groups are bonded to the Al atoms, whereas DTP/K10 indicated the presence of H_3O^+ (Brönsted acidity) and the linkage of phosphorus.[35,36]

In the case of the clayzic which is 20% $ZnCl_2$/K10, the surface area was found to be 145 $m^2\ g^{-1}$ which was closer to the one reported by Clark *et al.*[25] The pore size distribution of clayzic was much narrower and almost unimodal with an average size of 68 Å. Thus, there is a considerable reduction in surface area and pore size. This suggests that apart from the surfaces of bigger pores, $ZnCl_2$ is deposited at smaller junctions cutting off a few pore networks which are not accessible to N_2 molecule during the BET surface area measurement and of course to the much bigger reactant molecules. $ZnCl_2$ imparts the Lewis acidity to the catalyst and these sites are much stronger than the remaining Brönsted sites available in the clay.[29,30] A loading of 40% $ZnCl_2$ on K10 was found to decrease the conversions substantially to a meagre 21% which was a result of blocking off a lot of pore networks. This is not surprising since it has been reported that clayzic typically has the best activity around 2 mmol $ZnCl_2\ g^{-1}$ clay. (20% $ZnCl_2$/K10 is 1.83 mmol g^{-1} K10.)

Sulfated zirconia has a much wider pore size distribution (p.s.d.) but the pores in the mesoporous region are not many and thus the accessibility to the reactant molecules is limited and therefore a lower conversion was obtained. Formation of trimer is due to pore sizes in the range of 100–200 Å in the case of this catalyst. The acidity of Al pillared clay (Al-PILC) is less than clayzic but has wider p.s.d. with many pores in the mesopore region. The p.s.d. of Al-PILC, which was calcined at 500 °C, showed an average pore size of 40 Å with a surface area of 270 $m^2\ g^{-1}$ in the meso region and 40 $m^2\ g^{-1}$ in the micro-region. Obviously this catalyst has less acidity and the micro-porosity is not available for catalysis. Therefore at a lower conversion of 16%, there was still a 10% trimer formation. In the case of 10%$AlCl_3$ + 10%$FeCl_3$/K10 there was a surface area reduction (139 $m^2\ g^{-1}$) and obviously the acidity was lower than for clayzic.[34] DTP alone perhaps behaves as a heterogeneous catalyst with very limited solubility and surface area and therefore was ineffective. 20% DTP/carbon was also ineffective since the carbon pores are slit-like with narrow range of pore sizes and the active Brönsted sites are not freely available.

The screening of the catalysts suggested that both clayzic and K10 clay could be used for getting a 2 cSt PAO and were used in all further experiments. Both Lewis and Brönsted acids catalyse the reaction. Thus total acid strength and pore size distribution would matter in overall activity and selectivity.

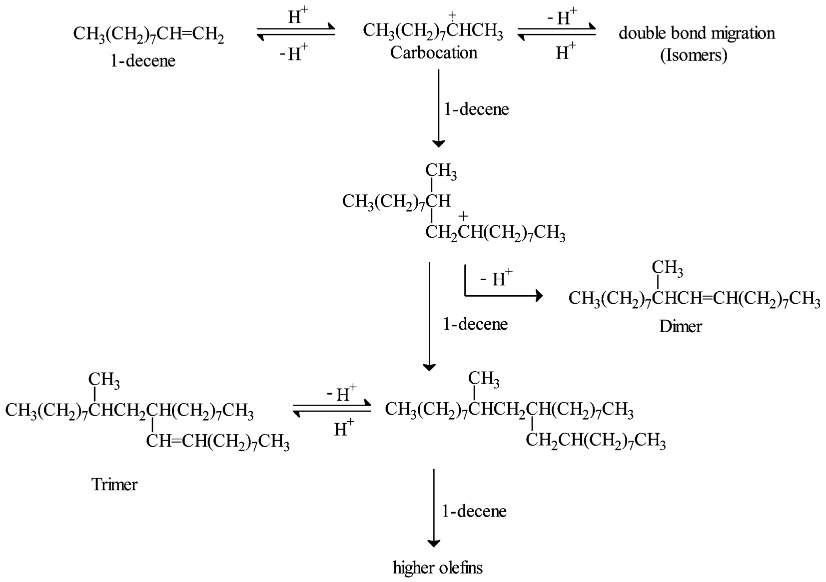

Scheme 2 Mechanism for oligomerisation of 1-decene.

3.1.2 Effect of speed of agitation. To study the influence of external mass transfer on the reaction rate, the speed of agitation was varied from 400 to 1000 rpm at five different values in the presence of 20% $ZnCl_2$/K10 and K10. It was found that the conversion and selectivity remained practically unchanged at all speeds of agitation beyond 500 rpm with both the catalysts. Thus, the external resistance to mass transfer was absent beyond 500 rpm. However, to be on safer side, further experiments were conducted at 1000 rpm. A theoretical analysis, as discussed in some of our work reported earlier,[38–41] was also done to make sure that it was indeed the case.

With pure monomer and a little quantity of the internal standard at the beginning there would be no external resistance to mass transfer. However, as the product(s) are formed and there is a counter diffusion, then mass transfer effect could become important. Thus typical calculations are done to show that at the highest conversion there was no mass transfer effect involving the transfer of the monomer 1-dodecene (M) or the dimer (D). In the case of the monomer it is transferred from the bulk liquid phase to the catalyst wherein external mass transfer of reactants to the surface of the catalyst particle, followed by intra-particle diffusion, adsorption, surface reactions and desorption take place. The influence of external solid–liquid mass transfer resistance must be ascertained before a true kinetic model could be developed. As the oligomers are formed, 1-decene has to diffuse through a mixture containing the monomer and dimer. Thus, a typical calculation was done for a mixture containing 32% 1-monomer and 68% dimer (corresponding to entry 1 in Table 1) for clayzic to find that there was an absence of resistance due to the solid–liquid external mass transfer for 1-decene the highest concentration and the rate may be either surface reaction controlled or intra-particle diffusion controlled. Therefore, the effects of catalyst loading at a fixed particle size and temperature were studied to ascertain the influence of intra-particle resistance. A theoretical calculation was also done based on the Wiesz–Prater criterion[48] to assess the influence of intra-particle diffusion resistance to find that the reaction was intrinsically kinetically controlled. However, in a separate experiment, the particles of clayzic were crushed and sieved and used for the reaction. At the same loading of catalyst, for average particle size of 125 μm, practically the same conversion and selectivity was obtained. This also supported the theoretical calculations. A further proof of the absence of the intra-particle diffusion resistance was obtained through the study of the effect of temperature and it will be discussed later.

3.1.3 Effect of catalyst loading. The effect of catalyst loading was studied between 0.01 and 0.08 g cm^{-3} by using both clayzic and K10 clay as the catalysts (Fig. 1). With an increase in loading, the rate of oligomerisation increases in both cases. Since the effect of different catalysts showed that the type of acidity did not matter catalysing the reaction, the rate would be proportional to total site concentration. At low catalyst loading (0.01 g cm^{-3}), the rate of reaction is very low with conversion of 1-decene being only 23% for K10. However, at high loading, although the conversion increases, the selectivity towards dimer decreases (Table 2). This is due to the fact that more active sites are available for the reaction when loading increases and thus more trimer was formed. Higher oligomers are also formed on the outer surface. In the presence of clayzic as catalyst, the rate of oligomerisation was higher with high catalyst loading and 100% selectivity towards dimer was obtained in all these cases.

Table 1 Efficacies of various catalysts in the oligomerisation of 1-decene

Catalyst	Conversion of C_{10} (%)	Selectivity (%)	
		Dimer	Trimer
20% w/w $ZnCl_2$/K10	68	100	—
K10 montmorillonite clay	73	88	12
5% DTP w/w/K10	48	100	—
20% DTP/K10	46	100	—
10%$AlCl_3$ + 10%$FeCl_3$/K10	23	100	—
S–ZrO_2	23	95	5
Al pillared clay	16	90	10
DTP	8	100	—
20%HPA/carbon	5	100	—
Filtrol-24	3	100	—

Conditions: 1-Decene = 0.25 mol, *n*-dodecane = 10% w/w of C_{10}, catalyst loading = 0.05 g cm^{-3}, temperature = 190 °C, speed = 1000 rpm, reaction time = 4 h.

3.1.4 Effect of temperature. It was found that oligomerisation of 1-decene is a highly temperature dependent reaction for both the catalysts (Fig. 2). At 180 °C, in the presence of K10 the conversion of 1-decene was 60% with 93% selectivity of dimer. When the temperature was maintained at 190 and 200 °C, the conversion of 1-decene increased to 73 and 80%, respectively. It was seen that the selectivity of trimer had increased with an increase in the temperature (Table 3) With 20% $ZnCl_2$/K10 as a catalyst, the oligomerisation reaction was studied in the range of 170–200 °C. At 170 °C, the conversion of 1-decene was only 40% whereas at 200 °C conversion increased to 79, and 100% selectivity of dimer was obtained in all cases.

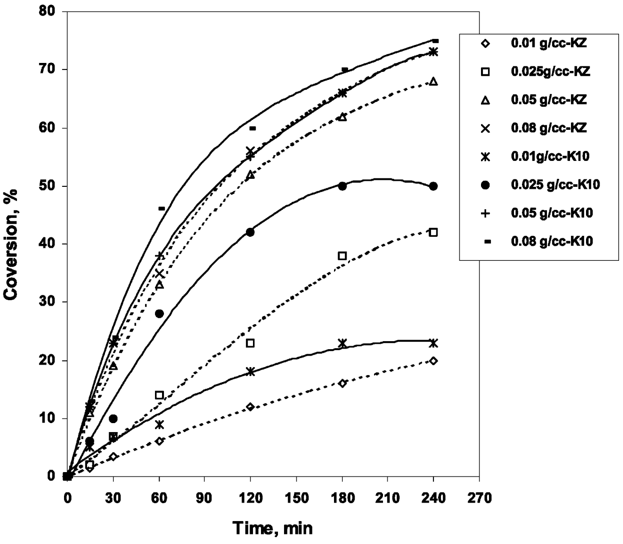

Fig. 1 Effect of catalyst and its loading on oligomerisation of 1-decene. Solid line: K10, dotted line: $ZnCl_2$/K10. 1-Decene = 0.25 mol, temperature = 190 °C, speed = 1000 rpm, *n*-dodecane 10% w/w of substrate.

Table 2 Effect of catalyst loading on oligomerisation of 1-decene

Catalyst loading/g cm^{-3}	Conversion of C_{10} (%)	Selectivity (%)		
		Dimer	Trimer	Higher oligomers
0.01	23	100	—	—
0.025	50	100	—	—
0.050	73	88	12	—
0.080	75	74	19	7
0.05*	68	100	—	—

Conditions: 1-decene = 0.25 mol, *n*-dodecane = 10% w/w of C_{10}, catalyst K10 montmorillonite, temperature = 190 °C, speed = 1000 rpm, reaction time = 4 h. *20% $ZnCl_2$/K10.

3.1.5 Effect of $ZnCl_2$ loading on K10 montmorillonite support. The loading of $ZnCl_2$ on K10 was varied between 5 and 40% and the reaction was monitored (Fig. 3). At low $ZnCl_2$ loading (5 and 10%), conversion of 1-decene was 57 and 61%, respectively. These experiments also confirmed that the nature of acid sites was immaterial for oligomerisation. The maximum conversion (68%) of 1-decene was obtained at 20% w/w of $ZnCl_2$ on K10 which is 1.83 mmol g^{-1} K10 clay. Clark *et al.*[25] have mentioned that the maximum activity is attained at about 2 mmol g^{-1}-K10 for clayzic. The conversion only marginally increased from 15 to 20% loading. As stated earlier loading of 40% $ZnCl_2$ on K10 was found to decrease the conversions substantially to a meagre 21% which was a result of blocking off a lot of pore networks.

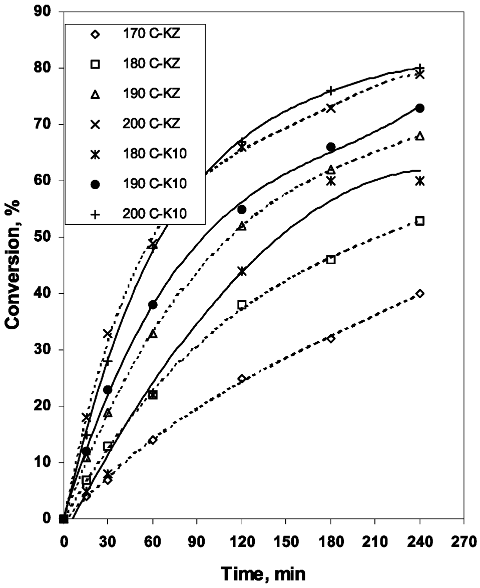

Fig. 2 Effect of temperature of using K-10 and $ZnCl_2$/K10 (KZ) on conversion of 1-decene. Solid line: K10; dotted line: $ZnCl_2$/K10 (KZ). 1-Decene = 0.25 mol, cat. loading = 0.05 g cm^{-3}, temperature = 190 °C, speed = 1000 rpm, *n*-dodecane 10% w/w of substrate.

Table 3 Effect of temperature on oligomerisation of 1-decene

		Selectivity (%)		
Temperature/°C	Conversion of C_{10} (%)	Dimer	Trimer	Higher oligomers
180	60	93	7	—
190	73	88	12	—
200	80	60	34	6
210	84	60	40	—

Conditions: 1-decene = 0.25 mol, *n*-dodecane = 10% w/w of C_{10}, catalyst K10 montmorillonite = 0.05 g cm^{-3}, speed = 1000 rpm, reaction time = 4 h.

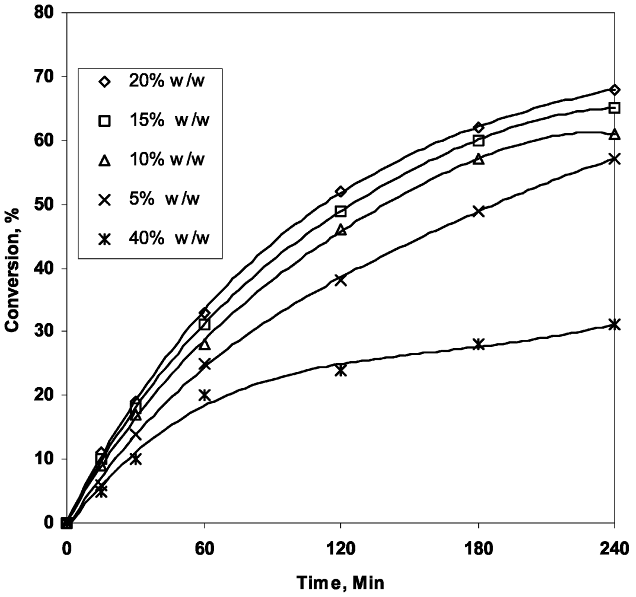

Fig. 3 Effect of $ZnCl_2$ loading on K10 clay. C_{10} = 0.25 mol, cat. loading = 0.05 g cm^{-3}, temperature = 190 °C, 1-decene = 0.25 mol, speed = 1000 rpm, *n*-dodecane = 10% w/w of substrate.

3.1.6 Reusability of K10 montmorillonite and $ZnCl_2$/K10. To study the reusability of catalyst, K10 and $ZnCl_2$/K10 were reused three and five times, respectively. After each run, the catalyst was washed with hexane and dried in an oven at 120 °C for 2 h (Fig. 4). Both the conversion of 1-decene and selectivity of trimer decreased after each run in the presence of K10 montmorillonite. During the first run, the conversion of 1-decene was 73%. However, after the third run the conversion had drastically reduced to 27% with no formation of trimer, as shown in Table 4.The trimer formed in K10 is not totally washed out of the clay and in the next run, it gets converted to higher oligomers thereby cutting of some pore networks. However, in the presence of 20% $ZnCl_2$/K10, very close conversions were obtained after the first and the second runs and there was very minimal loss in activity of the catalyst up to five runs. The reason for this is that the dimer is not retained inside the pore matrix. In all runs, the selectivity to the dimer

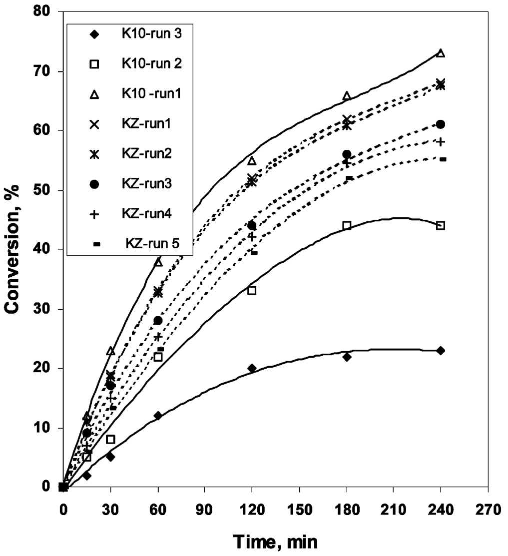

Fig. 4 Effect of reusability of K10 and $ZnCl_2$/K10 (KZ) for oligomerisation of 1-decene. Solid line: K10, dotted line: KZ. 1-decene = 0.25 mol, cat. loading = 0.05 g cm^{-3}, temperature = 190 °C, speed = 1000 rpm, *n*-dodecane = 10% w/w of substrate.

Table 4 Reusability of K10 montmorillonite on oligomerisation of 1-decene

		Selectivity (%)		
Run	Conversion of C_{10} (%)	Dimer	Trimer	Higher oligomers
1	73	88	12	—
2	44	94	6	—
3	23	100	—	—

Conditions: 1-decene = 0.25 mol, *n*-dodecane = 10% w/w of C_{10}, catalyst loading = 0.05 g cm^{-3}, speed = 1000 rpm, temperature = 190 °C, reaction time = 4 h.

was 100%. At the end of the fifth run the conversion was 55% and this can be considered as reasonable since no fresh catalyst was added to make up for any loss during filtration. The catalyst is thus reusable.

3.1.7 Oligomerisation of other olefins. Other olefins such as 1-octene and 1-dodecene were also oligomerized in the presence of 20% $ZnCl_2$/K10 under otherwise similar conditions. The rate of oligomerisation of 1-octene was higher (with 78% conversion to its dimer) than that of 1-decene and 1-dodecene (Fig. 5). With increasing chain length, the rate of oligomerisation decreased and only 40% of 1-dodecene was converted to its dimeric form. It was found that the rate of oligomerisation was inversely proportional to the chain length of α-olefin. The accessibility of some of the pores in clayzic to 1-octene and its C_{16} dimer was much greater than to 1-decene and its C_{20} dimer. Many pores are not accessed by 1-dodecene and its C24 dimer.

3.1.8 Oligomerisation of mixture of olefins. Oligomerisation reaction was also studied by using a mixture of α-olefins such as 1-octene and 1-decene. In a typical experiment, equimolar quantities of 1-octene and 1-decene were charged into the autoclave using 20% $ZnCl_2$/K10 as a catalyst. It was observed that for 1-decene, a bulky molecule, the rate of oligomerisation was lower than that of 1-octene. Conversion of 1-octene and 1-decene was 69 and 52% and 100% selectivity of the dimer was obtained for both the olefins. There was apparently no cross-alkylation leading to the octadecene molecule. It can be inferred that the monomers get adsorbed on the catalyst surface and do not react with the adjacent molecules by the dual site mechanism but by the Eley–Rideal mechanism.

3.1.9 Kinetics of oligomerisation. Since the nature of acid sites did not matter in oligomerisation, it was postulated that the oligomerisation of 1-alkene (M) on a solid acid followed the Eley–Rideal type of mechanism.[48] Because only one monomer needs to form a chemisorbed complex on the site, it was the first choice in the analysis of the rate data. The second molecule sits on the top of the adsorbed molecule and the reaction proceeds.

Adsorption of M

$$\mathrm{M} + \mathrm{S} \overset{K_\mathrm{M}}{\rightleftarrows} \mathrm{MS} \qquad (1)$$

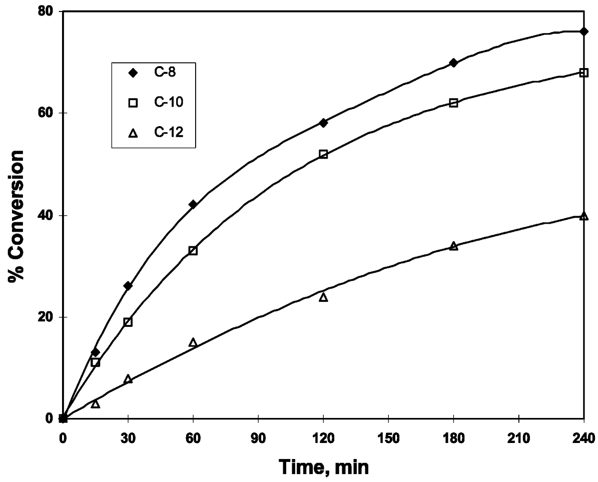

Fig. 5 Oligomerisation of different olefins. Olefin = 0.25 mol, 20%$ZnCl_2$/K10, 0.05 g cm^{-3}, speed = 1000 rpm, temperature = 190 °C, *n*-dodecane 10% w/w of olefin.

Surface reaction of adsorbed M with M from liquid according to the Eley–Rideal mechanism

$$\mathrm{M} + \mathrm{MS} \overset{K_\mathrm{SR1}}{\rightleftarrows} \mathrm{DS} \qquad (2)$$

$$\mathrm{M} + \mathrm{DS} \overset{k_\mathrm{SR2}}{\rightleftarrows} \mathrm{TS} \qquad (3)$$

Desorption of products

$$\mathrm{DS} \overset{1/K_\mathrm{D}}{\rightleftarrows} \mathrm{D} + \mathrm{S} \qquad (4)$$

$$\mathrm{TS} \overset{1/K_\mathrm{T}}{\rightleftarrows} \mathrm{T+S} \qquad (5)$$

(All constants are defined separately at the end.)

Since the type of sites do not matter, the total site balance is,

$$C_\mathrm{tot} = C_\mathrm{MS} + C_\mathrm{DS} + C_\mathrm{TS} + C_\mathrm{S} \qquad (6)$$

or,

$$C_\mathrm{S} = \frac{C_\mathrm{tot}}{(1+K_\mathrm{M}C_\mathrm{M} + K_\mathrm{D}C_\mathrm{D} + K_\mathrm{T}C_\mathrm{T})} \qquad (7)$$

If the rate of dimerisation, r_M, is controlling, then the following results:

$$r_\mathrm{M} = \frac{-\mathrm{d}C_\mathrm{M}}{\mathrm{d}t} = k_\mathrm{SR1}C_\mathrm{M}C_\mathrm{MS} = k_\mathrm{SR1}K_\mathrm{M}C_\mathrm{M}C_\mathrm{S}C_\mathrm{M}$$
$$= \frac{k_\mathrm{SR1}K_\mathrm{M}C_\mathrm{tot}C_\mathrm{M}^2}{\left(1+\sum K_iC_i\right)} \qquad (8)$$

In the above equation C_MS is substituted in terms of C_tot and C_M by using eqn. (7) and

$$C_\mathrm{MS} = K_\mathrm{M}C_\mathrm{M}C_\mathrm{S}$$

If the adsorption terms are insignificant, then

$$r_\mathrm{M} = -\mathrm{d}C_\mathrm{M}/\mathrm{d}t = k_\mathrm{SR}K_\mathrm{M}\, wC_\mathrm{M}^2 \qquad (9)$$

where w is substituted for C_tot without loss of generality since C_tot , the total number of sites is proportional to the catalyst loading w/g cm^{-3} . The proportionality constant is merged with the rate constant, k_SR. In terms of fractional conversion the above equation leads to the following:[48]

$$-\frac{\mathrm{d}C_\mathrm{M}}{\mathrm{d}t} = C_{\mathrm{M}_0}\frac{\mathrm{d}X_\mathrm{M}}{\mathrm{d}t}$$
$$\frac{\mathrm{d}X_\mathrm{M}}{\mathrm{d}t} = (k_\mathrm{SR}K_\mathrm{M}w)C_{\mathrm{M}_0}(1-X_\mathrm{M})^2 \qquad (10)$$

This equation can be integrated easily with the limits @ $t = 0$, $X_\mathrm{M} = 0$ and $t = t$, $X_\mathrm{M} = X_\mathrm{M}$ which upon integration gives,

$$\left(\frac{X_\mathrm{M}}{1-X_\mathrm{M}}\right) = k_\mathrm{SR}K_\mathrm{M}wC_{\mathrm{M}_0}t$$
$$= k_\mathrm{r}C_{\mathrm{M}_0}wt = k_0t \qquad (11)$$

where

$$k_\mathrm{r} = k_\mathrm{SR}K_\mathrm{M}, \text{ and } k_0 = k_\mathrm{r}C_{\mathrm{M}_0}w \qquad (12)$$

In order to validate the above theory, plots of $[X_\mathrm{M}/(1 - X_\mathrm{M})]$ *vs.* t were made as shown in Fig. 6 with catalyst loading as the parameter, the slope of which is equal to k_0. A plot of k_0 *vs.* w, the catalyst loading was made (Fig. 7) to get the slope equal to $k_\mathrm{r}C_{\mathrm{M}_0}$. Thus, for instance, the rate constant k_r was as calculated 6.67 cm^6 mol^{-1} g-cat^{-1} s^{-1} at 190 °C.

The conversion *vs.* time data at different temperature were used for the same C_{M_0} and w, to plot $(X_\mathrm{M}/1 - X_\mathrm{M})$ *vs.* t (Fig. 8. The slopes of these plots (k_0) could be directly used to make the Arrhenius plot (not shown). Thus, the energy of activation was calculated as 17.36 kcal mol^{-1} for 20%$ZnCl_2$/K10. This value also indicates that the dimerisation of 1-decene was intrinsically kinetically controlled.

3.2 Hydrogenation of 1-decene dimer

3.2.1 Efficacies of different catalysts. The activities of 20% w/w Ni/SiO_2, 20% w/w Ni–Cu/SiO_2 and bipyridine–montmorillonite–$PdCl_2$ complex [BM–Pd(II)] were evaluated and the conversion profiles recorded for 4 h at a speed of 1000 rpm (Fig. 9). Table 5 gives the conversions in each case at the end of 4 and 8 h. 20% w/w Ni/SiO_2 was the most active metallic catalyst giving a conversion of 89.4% in 8 h. By reducing the amount of Ni by 50% and substituting it with Cu resulted in a conversion of 78.4%. However, a pressure of 50 atm and 150 °C were necessary for the mono-metallic and bimetallic catalysts to get appreciable conversions whereas atmospheric pressure and 30 °C were sufficient for the anchored catalyst BM–Pd(II) which led to 57.4% conversion in 8 h. We have discussed the effect of second metal content on hydrogenation activity for Ni–Cu/SiO_2 at varying compositions for carbonyl and nitrile reductions wherein 20%Ni–Cu (50 : 50)/SiO_2 was found to be the most active.[45,46] For olefins the activity is less but within 11%. It was thus thought desirable to conduct further experiments with both 20% w/w Ni/SiO_2 and BM–Pd(II) and also to deduce a kinetic model for the reaction.

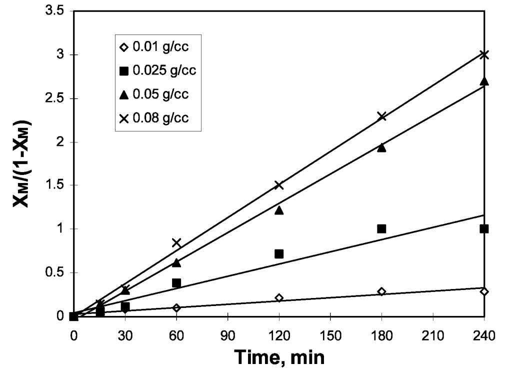

Fig. 6 Plot of $X_M/(1 - X_M)$ *vs.* time at different catalyst loadings. 1-Decene = 0.25 mol, catalyst 20%$ZnCl_2$/K10, temperature = 190 °C, *n*-dodecane = 10% w/w of 1-decene.

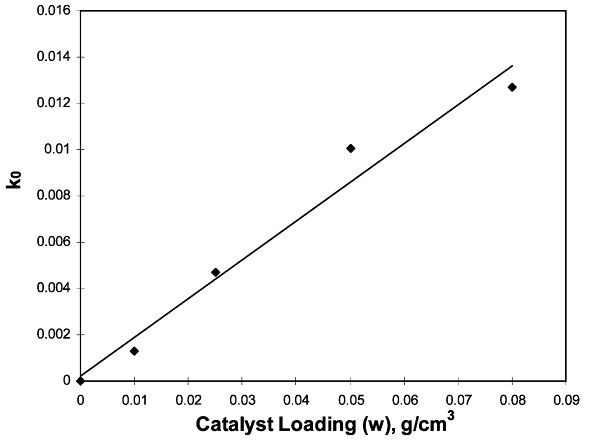

Fig. 7 Plot of K_0 *vs.* catalyst loading (*w*). 1-Decene = 0.25 mol, catalyst 20%$ZnCl_2$/K10, temperature = 190 °C, *n*-dodecane = 10% w/w of 1-decene.

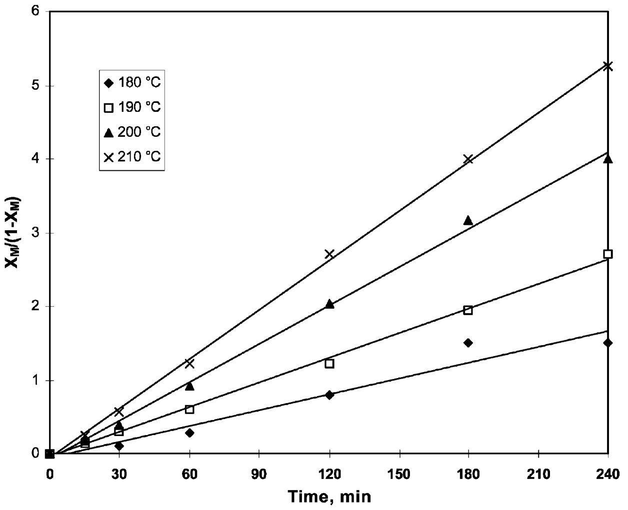

Fig. 8 Plot of $X_M/(1 - X_M)$ *vs.* time at different temperatures. 1-Decene = 0.25 mol, 20% $ZnCl_2$/K10 = 0.05 g cm^{-3}, *n*-dodecane = 10% w/w of 1-decene.

3.2.2 Effect of speed of agitation. The effect of external mass transfer on the rate of hydrogenation was studied with 20% w/w Ni/SiO_2, the most active catalyst. It was found that at 800 rpm, the conversion was 44% as compared to 47% at 1000 and 1200 rpm. The conversion profiles at 1000 and 1200 were almost identical within experimental error and that at 800 rpm the conversions were marginally lower. The rate of hydrogenation was also independent of the speed of agitation. The inspection of the data suggested that the conversions were linear with time showing a zero order kinetics. Theoretical calculations were also done by using the same approach given for oligomerisation to find that there was no mass transfer effect beyond 1000 rpm for 20% Ni/SiO_2. Hence further experiments were carried out at 1000 rpm. Typical experiments were also done with BM–Pd(II) catalyst to establish that there was no effect of speed of agitation at any speed in the range of 500–1200 rpm for that catalyst as well.

3.2.3 Effect of catalyst loading. Five different catalyst loadings were employed under otherwise similar conditions.

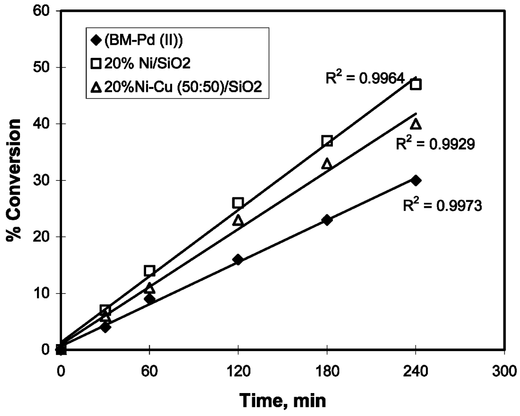

Fig. 9 Effect of different catalysts on hydrogenation of 1-decene dimer. Dimer = 0.028 mol, cat. loading = 0.035 g cm^{-3}, speed = 1000 rpm, solvent = THF.

Table 5 Hydrogenation of PAO dimer using different catalysts

Catalyst	Temperature/ °C	H_2 Pressure/ atm	Conversion (%) 4 h	8 h
BM–Pd(II)	30	1	30.1	57.3
20% Ni/SiO_2	150	50	47.2	89.4
20% (Ni–Cu : 1 : 1)/SiO_2	150	50	78.7	

Conditions: 1-decene dimer = 0.028 mol, catalyst loading = 0.035 g cm^{-3}, speed = 1000 rpm, solvent = THF.

With an increase in the catalyst loading from 0.005 to 0.045 g cm^{-3}, the rate of hydrogenation also increased for both catalysts (Fig. 10). The conversions were linear with time at all loadings for both the catalysts suggesting that the number of active sites were proportional to the catalyst amount and that there was no onset of mass transfer effects.

3.2.4 Effect of substrate concentration. Fig. 11 shows the effect of 1-decene dimer concentration on conversion in the presence of 20% w/w Ni/SiO_2. The conversion increases as the substrate concentration is increased and there was marginal loss in conversion as the concentration was increased from 6.44×10^{-4} to 8.33×10^{-4} mol cm^{-3}. The conversions were linear in time. Similar observation was also made for BM–Pd(II). To avoid repetition, these plots are not shown here. However, these data for BM–Pd(II) are used later to interpret the model development and validation. This would suggest that the rate of reaction was independent of the concentration beyond a certain value which could be explained on the basis of a Langmuir–Hinshelwood–Hougen–Watson model where the adsorption terms become very dominant as will be explained in section 3.2.8.

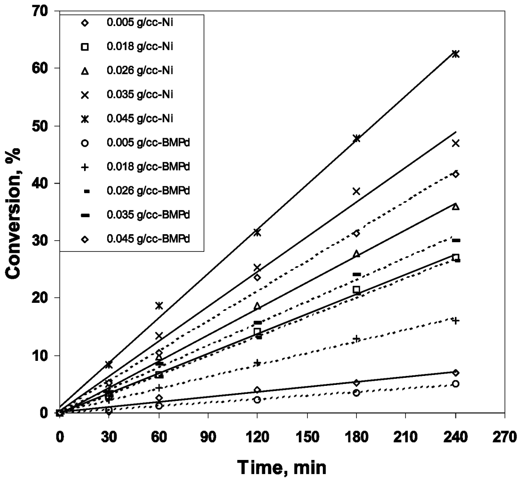

Fig. 10 Effect of catalyst loading on conversion of 1-decene dimer with Ni/SiO_2 and BM–PD(II) catalysts. Dimer = 0.028 mol, speed = 1000 rpm, solvent THF. Solid line: Ni/SiO_2, H_2 pressure = 50 atm, temperature = 150 °C. Dotted line: BM–Pd(II), H_2 pressure = 1 atm, temperature = 30 °C.

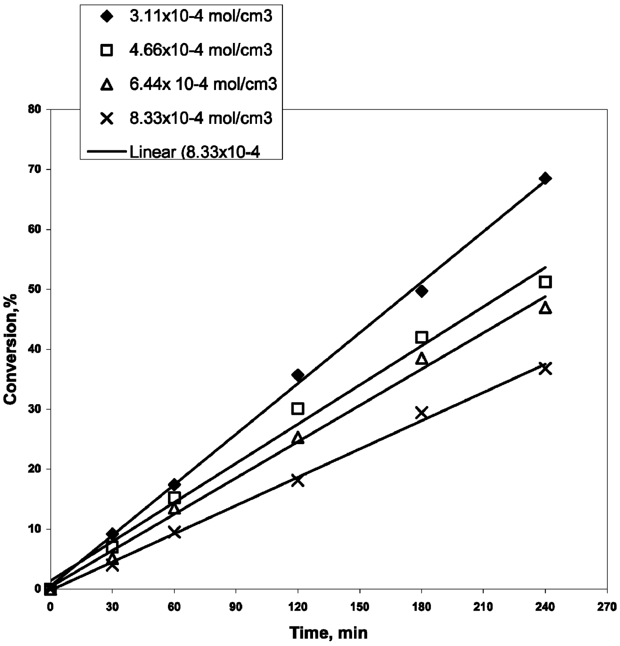

Fig. 11 Effect of dimer concentration on its conversion. Catalyst 20%Ni/SiO_2, 0.035 g cm^{-3}, temperature = 150 °C, speed = 1000 rpm, solvent THF, H_2 pressure = 50 atm.

3.2.5 Effect of temperature. It was observed that the rate of reaction linearly increased with an increase in the operating temperature (Fig. 12) with both the catalysts. At 130 °C, hydrogenation of unsaturated dimer over Ni/SiO_2 was only 18%, but at 150 and 170 °C the conversion was 47 and 62%, respectively, after 4 h. The effect of temperature was also studied with BM–Pd(II) at 30, 40 and 50 °C. The conversion of the dimer increases with an increase in the temperature but the increase is not substantial with BM–Pd(II). These observations also show that the reaction is zero order in substrate concentration at a fixed catalyst loading and hydrogen partial pressure.

3.2.6 Effect of hydrogen pressure. The rate of hydrogenation was studied at different pressures of hydrogen with 20% w/w Ni/SiO_2. Initially three pressures of 10, 20 and 50 atm were chosen and the conversion profiles were recorded for 4 h (Fig. 13). It suggested a linear dependence of rate of hydrogenation on hydrogen partial pressure and thus the initial rates were measured at 30, 40 and 60 atm. Fig. 14 shows a linear dependence on pressure because the solubility of H_2 increases with pressure.

3.2.7 Reusability of catalysts. The reusability of Ni/SiO_2 was tested five times. There was practically no loss of activity. Similar experiments were performed with BM–Pd(II) catalyst. After each run, the catalyst was filtered and thoroughly washed with hexane and THF. After this step, it was dried in an oven at 120 °C for 4 h. During the first and the second run, the conversion of the hydrogenated product was 30 and 28%, respectively after 4 h, which showed no loss in catalyst activity up to second run. During the third run, the conversion was reduced to 21%. There could be some loss of catalyst during filtration due to attrition.

3.2.8 Kinetics of hydrogenation. The inspection of conversion *vs.* time profiles for hydrogenation over both Ni/SiO_2 and BM–Pd(II) shows that the reaction follows zero-order kinetics since these are straight lines for both the catalysts. This behaviour is possible only if strong adsorption of 1-decene dimer takes place. The rate is independent of dimer concentration, above a certain minimum value. The mechanism for olefin hydrogenation is well known over metal catalysts and for the BM–Pd(II) which is a complex formed over the clay, it is given in Scheme 3.

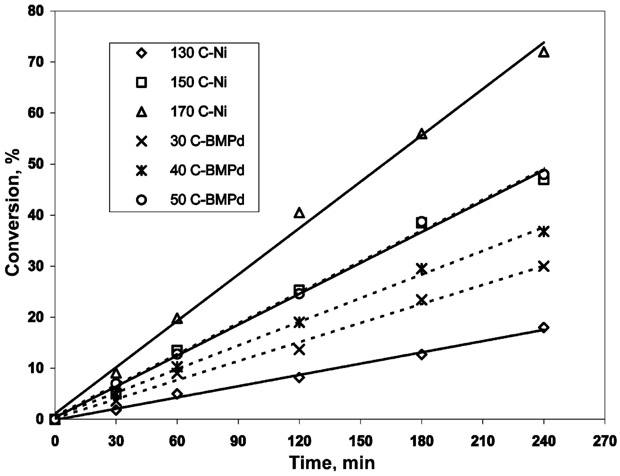

Fig. 12 Effect of temperature on hydrogenation of 1-decene dimer. Solid line: Ni/SiO_2, pressure H_2 = 50 atm, dotted line: BM–Pd(II), H_2 pressure = 1 atm.

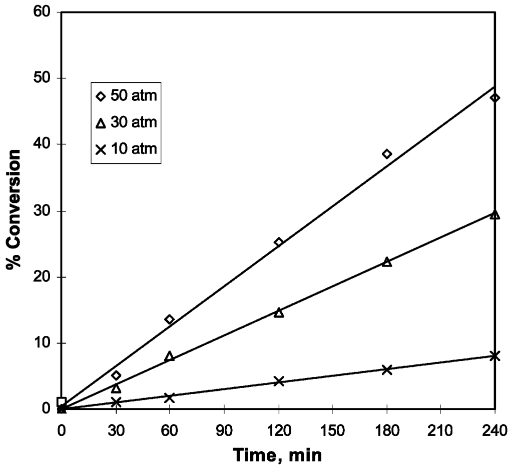

Fig. 13 Effect of hydrogen pressure on conversion. Dimer = 0.028 mol, Catalyst 20% w/w Ni/SiO$_2$, 0.035 g/cm^3, temperature = 150 °C, speed = 1000 rpm, solvent THF.

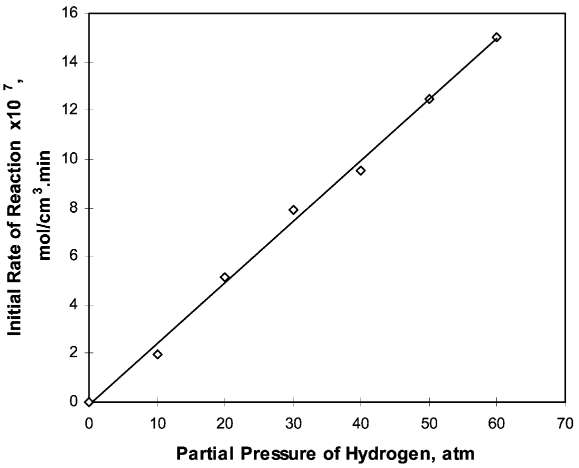

Fig. 14 Plot of initial reaction rate *vs.* partial pressure of hydrogen (20% Ni/SiO$_2$).

The Langmuir–Hinshelwood–Hougen–Watson model was used in both the cases assuming the adsorption of the substrate is not influenced by hydrogen adsoprtion. The details of derivation are omitted since these are covered in detail in a recent publication by us.[49]

The rate of hydrogenation is given by the following equation:

$$r_{H_2} = \frac{-dC_D}{dt} = \frac{kK_D K_{H_2} C_D P_{H_2} w}{(1+K_D C_D + K_P C_P)(1+K_{H_2} P_{H_2})} \qquad (10)$$

when adsorption of H$_2$ is weak ($K_{H_2}P_{H_2} \ll 1$), then the following equation results,

$$r_{H_2} = \frac{-dC_D}{dt} = \frac{kK_D K_{H_2} C_D P_{H_2} w}{(1+K_D C_D + K_P C_P)} \qquad (12)$$

When the product adsorption is also weak ($K_P C_P \ll 1$), then

$$r_{H_2} = \frac{-dC_D}{dt} = \frac{kK_D K_{H_2} C_D P_{H_2} w}{(1+K_D C_D)} \qquad (13)$$

when the dimer is strongly adsorbed ($K_D C_D \gg 1$), then the following results.

$$r_{H_2} = \frac{-dC_D}{dt} = kK_{H_2} P_{H_2} w \qquad (14)$$

This is in fact a kinetics with zero order in dimer concentration and first order in hydrogen partial pressure. The constant $k_{01} = kK_{H_2}$ is used to get the following and the rate is written in terms of fractional conversion (X_D) of the dimer.

$$r_{H_2} = \frac{-dC_D}{dt} = k_{01} P_{H_2} w \qquad (15)$$

$$= C_{D_0} \frac{dX_D}{dt} = k_{01} P_{H_2} w \qquad (16)$$

Thus the rate of hydrogenation is constant at a constant pressure and catalyst loading and zero order in dimer concentration.

Integration of the above equation gives the following in terms of the fractional conversion:

$$X_D = \frac{k_{01} P_{H_2} w t}{C_{D_0}} \qquad (17)$$

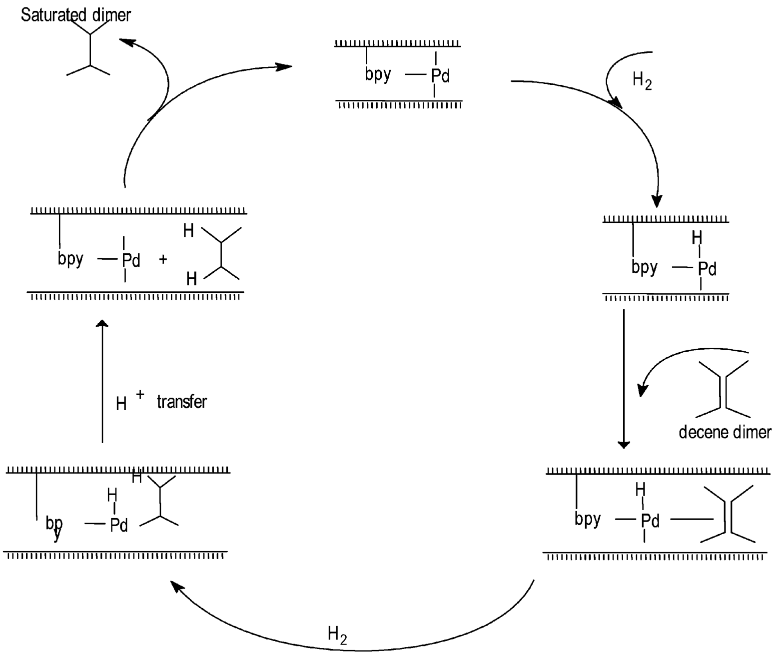

Scheme 3 Mechanism of hydrogenation with BM–Pd(II) catalyst.

The inspection of Fig. 11 again shows that eqn. (17) indeed fits the data since the slopes are $k_{01}P_{H_2}w/C_{D_0}$. Another validation of the model could be done as follows.

By reorganizing equation (17),

$$X_D C_{D_0} = k_{01} P_{H_2} wt \qquad (18)$$

Following eqn. (18), plots were made of $X_D C_{D_0}$, the amount of dimer consumed, against time for BM–Pd(II) at different initial concentrations to get a straight line as shown in Fig. 15. This validates the model very well. Indeed similar plots were also made for Ni/SiO$_2$ catalysts to bolster the model.

A further proof advanced by plotting the initial rate of hydrogenation (r_0) at a constant pressure against catalyst loading *w* (Fig. 16) shows a linear relationship in consonance with eqn. (2) and the slope is $k_0P_{H_2}$. Thus, from the knowledge of the slope and operating pressure the k_{01} values were obtained. The Arrhenius plot were made from the collected data at different temperature to get the energy of activation as 12.60 kcal mol^{-1} for 20% w/w Ni/SiO$_2$ catalyst. This high value suggests that the hydrogenation of the 1-decene dimer is intrinsically kinetically controlled and zero order in the dimer and first order in hydrogen partial pressure. The Arrhenius plot for the BM–Pd(II) was also made from which the activation energy was calculated as 4.76 kcal mol^{-1}. This catalyst is highly active. A comment is in order for this value of activation energy which is a sort of norm for mass transfer controlled reaction for many reactions. However, with hydrogen as a species, this low value of activation energy is still considered as acceptable for a kinetically controlled reaction. There are literature reports which state that for values as low as 3 kcal mol^{-1} have been obtained for a few hydrogenation reactions.[16–19]

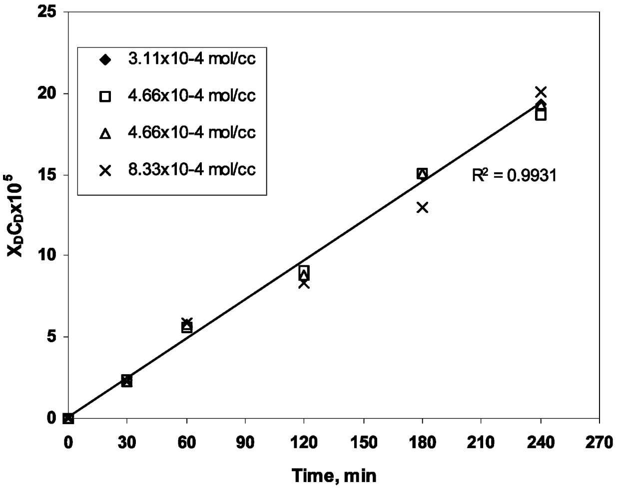

Fig. 15 Plots of X_DC_{D0} (amount of dimer hydrogenated) *vs.* time to verify the validity of model with the BM–Pd(II) complex catalyst. Catalyst BM–Pd(II), 0.035 g cm^{-3}, speed = 1000 rpm, solvent THF.

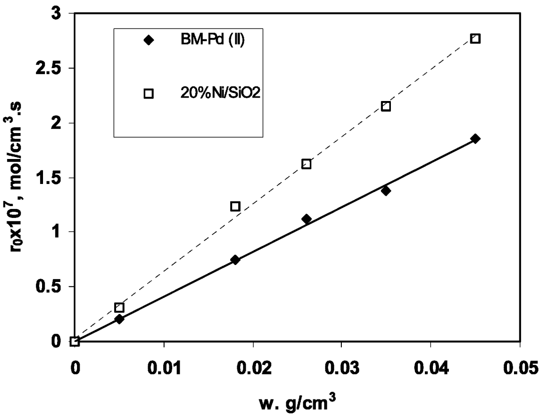

Fig. 16 Effect of catalyst loading on initial rate of hydrogenation. Dimer = 0.028 mol, speed = 1000 rpm, solvent THF, H$_2$ pressure = 1 atm for BM–Pd(II) and 50 atm for 20%w/w Ni/SiO$_2$.

3.2.9 Physical properties of saturated dimer of 1-decene. After the hydrogenation of 1-decene dimer, the product was separated and its physical properties were evaluated and compared with authentic material. Generally an oil is identified by its viscosity. In the present work, the viscosity of the prepared lubricant was measured at four different temperatures and it was found that it was comparable with the commercial material (Table 6).

3.2.10 Preparation of high speed spindle oil. A large quantity of spindle oil is utilized in the textile industry. Generally it is manufactured from conventional mineral oil of viscosity 2 cSt. Specific quantities of *n*-butyl stearate and dibutyl *p*-cresol is normally mixed with the mineral oil to enhance its physical properties such as pour point and flash point. In the current study, synthetic high speed spindle oil was prepared by mixing 0.1 g of butyl stearate (1% w/w of dimer) and 0.01 g of dibutyl *p*-cresol (0.1% w/w of dimer) with the hydrogenated dimer of 1-decene using 20% w/w Ni/SiO$_2$. Physical properties of the prepared lubricant were evaluated and compared with a mineral oil based lubricant (Table 7). It is obvious that the specification of prepared lubricant is comparable with standard mineral oil based lubricant.

3.2.11 Conclusion. Poly-α-olefins (PAO) are a very important class of synlubes and there is a great scope to develop

Table 6 Physical properties of PAO (hydrogenated 1-decene dimer) prepared in this work

Physical property	Prepared PAO	Durasyn 162[a]	Test method
C_{10} monomer left in product (%)	0.5	0.5	GC
Molecular weight	280	287	GC–MS
Viscosity @ 100 °C/cSt	2.22	1.80	ASTM D 445
Viscosity @ 40 °C/cSt	6.0	5.54	ASTM D 445
Viscosity @ −18 °C/cSt	60	62	ASTM D 445
Viscosity @ −40 °C/cSt	305	310	ASTM D 445
Pour Point	−60 °C	−65 °C	ASTM D 97

[a] Durasyn 162 is authentic material obtained from Amoco Corporation, USA

Table 7 Specification of high speed spindle oil for the textile industry

	Kinematic viscosity		Viscosity index	Flash pt/°C	Pour pt/°C, max	TAN/mg KOH g^{-1}	Rust test[a]
	40 °C	100 °C					
Mineral oil based	20–22	4.1	90	160	−3	0.1	Pass
PAO based (current method)	22	4.8	90	165	−5	0.1	Pass

[a] ASTM D 665.

green processes. Particularly 1-decene based PAO with a viscosity range of 2 cSt has the widest range of applications. Thus the current paper addressed the development of a green process for which both oligomerisation and hydrogenation were systematically studied. The oligomerisation of 1-decene was conducted by using a variety of solid acidic catalysts, in particular acid treated clays and their modified versions, to limit the product distribution to mostly to the dimer so that the final product could be used for the specific application. The activities were found as:

K10 montmorillonite clay > 20% w/w $ZnCl_2$/K10 > 5% DTP w/w /K10 > 20% DTP/K10 > 10%$AlCl_3$ + 10%$FeCl_3$/K10 > S–ZrO_2 > Al-pillared clay > DTP > 20% DTP/carbon.

K10 clay was the most active with conversion of 1-decene of 73% but the selectivities towards the dimer and trimer were 88 and 12%, respectively, whereas 20% $ZnCl_2$/K10 led to a conversion of 68% with 100% selectivity of the dimer. Selectivity to the dimer would reduce the separation cost considerably. Other olefins such as 1-octene and 1-dodecene were also oligomerised in the presence of 20% $ZnCl_2$/K10 under otherwise similar conditions. It was found that the rate of oligomerisation was inversely proportional to the chain length of the α-olefin. The kinetics of the reaction was established on the basis of the Eley–Rideal mechanism. The reaction is intrinsically kinetically controlled. The catalysts are reusable.

In next step, the hydrogenation of the 1-decene dimer was studied systematically over 20% w/w Ni/SiO_2, 20% w/w Ni–Cu (50 : 50)/SiO_2 and a clay anchored catalyst, bipyridine–montmorillonite–$PdCl_2$ complex. 20% w/w Ni/SiO_2 was found to be the most active catalyst giving a conversion of 89.4% in 8 h. By reducing the amount of Ni by 50% and substituting it with Cu resulted into a conversion of 78.4%. However, a pressure of 50 atm and 150 °C were necessary for the mono-metallic and bimetallic catalysts to get appreciable conversions whereas atmospheric pressure and 30 °C were sufficient for the anchored catalyst BM–Pd(II) giving 57.4% conversion in 8 h. A kinetic model was developed with both 20% w/w Ni/SiO_2 and bipyridine–montmorillonite–$PdCl_2$ complex as catalysts. The reactions are intrinsically kinetically controlled and the rate is zero order in dimer concentration and first order in hydrogen partial pressure. The values of energy of activation are established measured as 12.60 kcal mol^{-1} for 20% w/w Ni/SiO_2 and 4.76 kcal mol^{-1} for bipyridine-montmorillonite-$PdCl_2$ complex. The hydrogenated product had a viscosity of 2.22 cSt which was found to be comparable with commercially available sample. High speed spindle oil used in textile industry was also prepared and tested to get a satisfactory performance on par with the commercial sample.

Abbreviations and nomenclature

C_D	concentration of dimer of 1-decene/mol cm^{-3}
C_{D_0}	initial concentration of dimer of 1-decene/mol cm^{-3}
C_{DS}	concentration of adsorbed dimer of 1-decene/ mol g^{-1}-cat
C_{MS}	concentration of adsorbed 1-decene/mol g^{-1}-cat
C_S	concentration of vacant sites/mol g^{-1}-cat
C_{tot}	concentration of total sites/mol g^{-1}-cat
C_{TS}	concentration of adsorbed trimer of 1-decene/ mol g^{-1}-cat
D	dimer of 1-decene
DS	adsorption of dimer of 1-decene
DTP	dodecatungstophoshoric acid
HPA	heteropoly acid
k	rate constant/mol g-cat^{-1} s^{-1} [eqn. (1)]
K_D	adsorption constant for dimer D/cm^3 mol^{-1}
K_{H_2}	adsorption of constant for hydrogen/atm^{-1}
K_M	adsorption constant for monomer M/cm^3 mol^{-1}
k_0	pseudo-first order constant/s^{-1} [eqn. (12)]
k_{01}	rate constant for the hydrogenation reaction/mol s^{-1} atm^{-1} g-cat^{-1} [eqn. (15)]
k_r	second order rate constant based on catalyst loading/ cm^6 mol^{-1} g-cat^{-1} s^{-1}, given by [eqn. (12)]
k_{SR}	surface reaction constant/cm^3 g-cat^{-1} s^{-1} [eqn. (11)]
k_{SR1}	surface reaction rate constant for dimerisation reaction (2)/s^{-1} mol^{-1} g-cat
k_{SR2}	surface reaction rate constant for trimerisation reaction (3)/$s^{-1}$$mol^{-1}$ g-cat
K_T	adsorption constant for trimer T/cm^3 mol^{-1}
KZ	clayzic or 20% $ZnCl_2$/K10
M	monomer 1-decene
MS	adsorbed species M (1-decene)
P	hydrogenated 1-decene dimer
P_{H_2}	partial pressure of hydrogen/atm
PS	adsorbed hydrogenated 1-decene dimer
r_{H_2}	rate of hydrogenation based on liquid volume/ mol cm^{-3} s^{-1}
r_0	initial rate of hydrogenation based on liquid volume/ mol cm^{-3} s^{-1}
S	catalytic site
t	time/s
T	trimer of 1-decene
T	temperature/K
w	catalyst loading in liquid phase/g cm^{-3}
X_D	fractional conversion of dimer of 1-decene (D) during hydrogenation
X_M	fractional conversion of 1-decene (M) during oligomerisation
XRD	X-ray diffraction

Acknowledgement

Research funding was received from A.I.C.T.E. and Darbari Seth Professorship Endowment. G. D. Y. is grateful to the Michigan State University for providing excellent facilities for creative pursuits as the Johansen Crosby Visiting Professor of Chemical Engineering during 2001–2002.

References

1 R. L. Shubkin, *Synthetic Lubricant and High Performance Functional Fluids*, Marcel Dekker, New York, 1992.
2 *Global Information Inc., Market Research Report, Synthetic Lubricants: Potential Applications and Markets in Western Europe, North America, and Asia-Pacific, Technical Insights*, John Wiley & Sons, New York, 1999.
3 C. W. Montgomery, W. I. Gilbert and R. E. Kline, *US Pat.*, 2,559,984, 1955 (to Gulf Oil Co.).
4 W. E. Garwood, *US Pat.*, 2,937,129, 1960 (to Socony Mobil).
5 D. Southern, C. B. Milne and T. G. Evans, *Br. Pat.*, 873,064, 1961 (to Shell Research).
6 J. A. Brennan, *US Pat.*, 3,382,291, 1968 (to Mobil Oil).
7 R. L. Shubkin, *US Pat.*, 3,763,244, 1973 (to Ethyl Corp.).
8 R. L. Shubkin, *US Pat.*, 3,780,128, 1973 (to Ethyl Corp.).
9 R. L. Shubkin, *Eur Pat.*, 467345, 1990 (to Ethyl Corp.).
10 K. J. Theriot, *US Pat.*, 5,068,487, 1991.
11 H. Mach, P. Hans and H. Watter, *Ger. Offen DE*, 3,641,237, 1988) (to BASF-AG).
12 M. M. Wu, *US Pat.*, 4827 073, 1989 (to Mobil Oil).
13 T. Akio and H. Suzuka, *Chem. Lett.*, 1987, **2**, 423.
14 R. L. Augustine, *Catalytic Hydrogenation; Techniques and Applications in Organic Synthesis*, Marcel Dekker, New York, 1965.
15 M. Freifelder, *Practical Catalytic Hydrogenation; Techniques and Applications*, Wiley-Interscience, New York, 1971.
16 P. N. Rylander, *Catalytic Hydrogenation in Organic Syntheses*, Academic Press, New York, 1979.
17 G. C. Bond and R. Burch, in *Catalysis*, ed. G. C. Bond and G. Webb, The Royal Society of Chemistry, London, p. 6, 1983.

18 P. N. Rylander, H. Greenfield and R. L. Augustine, *Catalysis of Organic Reactions*, M. Dekker, New York, 1988.
19 *Stud Surf Sci. Catal Vol. 78, Heterogeneous Catalysis and Fine Chemicals III*, ed. M. Guisnet, Elsevier, Amsterdam, 1993.
20 R. L. Augustine, *Catal. Today*, 1997, **37**(4), 419.
21 T. J. Pinnavaiva and F. Farzaneh, *Inorg. Chem.*, 1983, **22**, 2216.
22 D. C. Neckers, R. J. Card and C. E. Liesner, *J. Org. Chem.*, 1979, **44**, 1095.
23 B. M. Choudary, K. Ravikumar, Z. Jamil and G. Thyagarajan, *J. Chem. Soc., Chem. Commun.*, 1985, 31.
24 K. Ravikumar, B. M. Choudary, Z. Jafar and G. Thyagarajan, *J. Chem. Soc., Chem. Commun.*, 1986, 130.
25 J. H. Clark, S. R. Cullen, S. J. Barlow and T. W. Bastock, *J. Chem. Soc., Perkin Trans. 2*, 1994, 1117.
26 J. H. Clark, A. P. Kybett, D. J. Macquarrie, S. J. Barlow and P. J. Landon, *J. Chem. Soc., Chem. Commun.*, 1989, 1353.
27 S. J. Barlow J. H. Clark, M. R. Darby, A. P. Kybett, P. Landon and K. Martin, *J. Chem. Res. (S)*, 1991, 74.
28 J. H. Clark, A. P. Kybett and D. J. Macquarrie, *Supported Reagents; Preparation, Analysis and Applications*, VCH, New York, 1992.
29 D. R. Brown and J. Massam, *Catal. Lett.*, 1995, **35**, 335.
30 D. R. Brown, J. Massam and H. M. G. Edwards, *J. Chem. Soc., Faraday Trans.*, 1996, **92**, 1029.
31 J. P. Butrille and T. J. Pinnavaia, *Catal. Today*, 1992, **14**, 141.
32 Y. Izumi, K. Urabe and M. Onaka, *Zeolites, Clays and Heteropoly Acids*, VCH Publishers Inc., London, 1992.
33 G. D. Yadav and N. J. Kirthivasan, *Chem. Commun.*, 1995, 203.
34 G. D. Yadav and N. Kirthivasan, *Indian Pat.*, 95-D1785, 2001 (CSIR).
35 G. D. Yadav and N. Kirthivasan, *Appl. Catal. A: Gen.*, 1997, **154**, 29.
36 G. D. Yadav and V. V. Bokade, *Appl. Catal. A: Gen.*, 1996, **147**, 299.
37 G. D. Yadav and N. Kirthivasan, in *“Fundamental and Applied Aspects of Chemically Modified Surfaces*, ed. J. P. Blitz and C. B. Little, Royal Society of Chemistry, UK, London, 1999, pp. 254–269.
38 G. D. Yadav, A. A. Pujari and A. V. Joshi, *Green Chem.*, 1999, **1**(6), 269.
39 G. D. Yadav and N. S. Doshi, *Catal. Today*, 2000, **60**, 263.
40 G. D. Yadav and N. S. Doshi, *Appl. Catal. A: Gen.*, 2002, in press.
41 G. D. Yadav and N. S. Doshi, *J. Mol. Catal. A: Chem.*, 2002, in press.
42 G. D. Yadav and D. V. Satoskar, *J. Chem. Technol. Biotechnol.*, 1997, **69**, 438.
43 P. S. Kumbhar and G. D. Yadav, *Chem. Eng. Sci.*, 1989, **44**, 2535.
44 G. D. Yadav and J. J. Nair, *Microporous Mesoporous Mater.*, 1999, **33**, 1.
45 P. S. Kumbhar, M. N. Kharkar, G. D. Yadav and R. A. Rajadhyaksha, *J. Chem. Soc., Chem. Commun.*, 1992, 584.
46 G. D. Yadav and M. N. Kharkar, *Appl. Catal. A: Gen.*, 1995, **126**(1), 115–23.
47 C. S. James, *Analytical Chemistry of Foods, C.H.I.P.S.*, New York, 1998.
48 H. S. Fogler, *Elements of Chemical Reaction Engineering*, Prentice-Hall, New Delhi, 1995.
49 G. D. Yadav and P. K. Goel, *J. Mol. Catal. A: Chem.*, 2002, **184**(1–2), 281.

Studies on the conversion of 1,1,1-trichlorotrifluoroethane, chloro-2,2,2-trifluoroethane, and 1,1,1-trifluoroethane by catalytic oxidation, hydrolysis and ammonolysis

Stephan Rüdiger, Udo Gross, S. Chandra Shekar,† V. Venkat Rao,† M. Sateesh† and Erhard Kemnitz*†

Department of Chemistry, Humboldt-University, Brook-Taylor-Str. 2, 12489 Berlin, Germany.
E-mail: erhard.kemnitz@rz.hu-berlin.de

Received 24th June 2002
First published as an Advance Article on the web 8th October 2002

Catalytic hydrolysis and ammonolysis of CF_3CCl_3 (CFC-113a) and CF_3CH_2Cl (HCFC-133a) and oxidation of CF_3CH_3 (HFC-143a) were studied as possible routes to produce trifluoroacetic acid (TFA), trifluoroethanol (TFE) or trifluoroethylamine (TFEA), respectively. Catalysts employed in this study included oxides/halides of Fe, Pd, Cs, Cu, Sn, supported on carbon, Al_2O_3, ZrO_2, TiO_2, sulfated zirconia and fluoride supports like β-AlF_3, and MgF_2, as well as modified lanthanum phosphates. The reaction temperatures were varied from 100 to 450 °C, under these conditions CF_3CCl_3 and CF_3CH_2Cl could be hydrolysed giving trifluoroacetic acid or trifluoroethanol, respectively, in moderate yields, however all other reactions yielded predominantly CF_2CHCl. Optimum conditions were identified for obtaining TFA over Fe/C catalyst by hydrolysis of CFC-113a, and for TFE by hydrolysis of HCFC-133a over alkaline modified lanthanum phosphate.

Introduction

Chlorofluorocarbons are found to be major culprits for stratospheric ozone depletion. Much pressure has been put on the industrialised world to ban production and use of these compounds.[1] Several research groups have tried to identify technologies, concerned to safe disposal of these compounds or their transformation to useful products. In this respect dismutation,[2] isomerisation[3] and hydrodechlorination[4] were studied to produce fluorine-rich compounds and hydrofluorocarbons, respectively, and some of these processes were met with outstanding success. However, all these processes do not result in fluorocompounds having a functional group. On the other hand, C_2 fluorocarbon compounds containing both CF_3 and an active functional group, such as trifluoroacetic acid (TFA), trifluoroethanol (TFE) or trifluoroethylamine (TFEA), are of importance in synthetic chemistry, *e.g.* in pharmacy and agricultural chemistry. In principle, TFA or TFE can be obtained by hydrolysis of CFC-113a or HCFC-133a, respectively. However, these reactions have to be carried out discontinuously either in an autoclave (HCFC-133a), or using fuming sulfuric acid (CFC-113a) or under otherwise difficult to handle conditions.[5] In contrast, the present work was intended to explore the potential of various catalysts for producing such valuable compounds by vapour phase catalytic hydrolysis, ammonolysis, or oxidation, and preliminary experimental results are reported.

Experimental

Preparation of the catalysts

Impregnation methods. Carbon supported Fe, Cu, Zn, Sn, MoFe, and Pd catalysts were prepared by impregnation of acid washed (conc. HCl, H_2O) carbon (extrudate with a granule size from 1 to 3 mm; Norit) in aqueous media with the respective metal precursor at room temperature. The appropriate amount of the respective metal precursor (Table 1) was dissolved in water, the carbon was added to the solution, and the mixture stirred for 6 h, followed by evaporation to remove the water, and finally dried at 120 °C for 12 h. Further, these catalysts were calcined at 300/400 °C for 3 h under nitrogen. Iron loading was varied in between 5 and 30 wt%. MoFe and PdBi bimetallic catalysts were prepared by co-impregnation of two metal salt solutions in aqueous media according to a procedure described elsewhere.[6] Oxide supported catalysts were calcined in air at 450 °C for 3 h. To prepare Sn/C, and CsF/MgF_2 acetonitrile and ethanol were used as solvents, respectively.

K10-clay (K10-montmorillonite, Fluka) and Fe-pillared clay catalysts were also prepared according to literature procedures[7] by impregnation. The supports β-AlF_3 and sulfated zirconia were prepared according to earlier reports.[8,9]

Alkali metal doped phosphate catalysts were prepared[10] by mixing equimolar amounts of hot 0.05 M solutions of $(NH_4)_2HPO_4$ and either $La(NO_3)_3$ or $Al(NO_3)_3$, or $Fe(NO_3)_3$, filtrating the mixture after cooling to room temperature and washing the precipitate several times with distilled water until it was free of nitrate. After drying at 110 °C the phosphate was doped with the appropriate amount of alkali metal hydroxide solution, dried again, and calcined in atmospheric air at 500 °C.

Green Context

The presence of large amounts of CFCs and HCFCs presents a major challenge in terms of safe disposal. However, if they are looked at as raw materials for various useful chemicals, then opportunities exist for their use. In this paper, potential routes to their utilisation as raw materials for various trifluoromethyl-containing compounds are given. ***DJM***

---

† On leave from Indian Institute of Chemical Technology, Hyderabad, India

DOI: 10.1039/b206098c

Table 1 Catalyst codes, precursors, supports and method of preparation

No.	Catalyst	Support	Metal (wt%)	Metal precursor	BET/m² g⁻¹	XRD
1	10%Fe/Al_2O_3	Alumina	10	$FeCl_3$	173.1	Amorph.
2	Fe/K10	K10-clay	10	$FeCl_3$	n.d.	n.d.
3	Fe/PILC	Clay	10	$FeCl_3$	255.1	Clay
4	10%Cu/C	Active carbon	10	$Cu(NO_3)_2$	n.d.	n.d.
5	Sulf. ZrO_2	Zirconia	—		122	Zirconia
6	β-AlF_3	β-Aluminium fluoride	—	$FeCl_3$	40.4	β-AlF_3
7	Fe/β-AlF_3	β-Aluminium fluoride	10	$FeCl_3$	27.7	β-AlF_3
8	20%Fe/C	Active carbon	20	$FeCl_3$	n.d.	n.d.
9	10%Zn/C	Active carbon	10	$ZnCl_2$	n.d.	n.d.
10	10%Sn/C	Active carbon	10	$SnCl_2$	n.d.	n.d.
11	Carbon	Active carbon	—		870	
12	Carbon-AW	Active carbon	—		863	
13	10% Fe/ZrO_2	Zirconia	10	$FeCl_3$	n.d.	n.d.
14	V_2O_5-K4	V_2O_5	—		n.d.	n.d.
15	Pd/C	Active carbon	4	$PdCl_2$	586	α-Pd
16	MoFe/C	Active carbon	5, 10		n.d.	n.d.
17	VMoPO4				n.d.	n.d.
18	CsF/MgF_2	Magnesum fluoride	10	CsF	n.d.	CsF, MgF_2
19	ZLF-412[a]				n.d.	n.d.
20	ZLFPO4-412[a]				n.d.	n.d.
21	8% Pd/Al_2O_3	Alumina	8	$PdCl_2$	181	α-Pd
22	4% PdBi/C	Active carbon		$PdCl_2$, $Bi(NO)_3$	160	Bi_3Pd
23	Pd-ZrO_2/C	Active carbon		$PdCl_2$	n.d.	n.d.
24	Cs/$LaPO_4$ 0.07	$LaPO_4$	4	CsOH	75.7	$LaPO_4$
25	Cs/$LaPO_4$ 0.14	$LaPO_4$	8	CsOH	70.2	$LaPO_4$, Cs_3PO_4
26	Cs/$LaPO_4$ 0.21	$LaPO_4$	12	CsOH	n.d.	n.d.
27	Na/$LaPO_4$ 0.1	$LaPO_4$	1	NaOH	n.d.	n.d.
28	K/$LaPO_4$ 0.1	$LaPO_4$	1.7	KOH	n.d.	n.d.
29	Cs/$AlPO_4$ 0.07	$AlPO_4$	7.6	CsOH	n.d.	n.d.
30	Cs/$AlPO_4$ 0.14	$AlPO_4$	15	CsOH	n.d.	n.d.
31	$FePO_4$	$FePO_4$			n.d.	n.d.

n.d. = Not determined.[a] Catalysts prepared by coprecipitation method.

Coprecipitation method. Coprecipitated catalysts were prepared with an atomic ratio of Zr to La to Fe of 4 : 1 : 2, and $FeCl_3$, $LaCl_3$ and $ZrOCl_2$ were used as precursors. The respective amounts of the metal precursor were dissolved in 500 ml of deionised water and the solution was precipitated with 2% ammonia solution under continuous mechanical stirring. It was continued until the pH of the mixture reached 9.2. After complete precipitation, the solution was vacuum-filtered and the slurry was washed several times with deionised water to completely remove the chloride ions. Then, the obtained material was dried for 12 h at 120 °C. To prepare phosphated catalyst, 1 ml of 85% H_3PO_4 was added to 2 g of an oven-dried sample, the mixture was stirred for 1 h and dried again. The dried mixed hydroxides and phosphate-modified samples were calcined at 450 °C for 4 h in air and denoted as ZLF-412 and ZLFPO4-412.

V_2O_5/K-4 was prepared according to the procedure described elsewhere.[11]

Catalyst details are displayed in Table 1 along with their method of preparation.

Procedures

Catalytic hydrolysis activities of the catalysts were evaluated in an on-line microreactor interfaced with a FID equipped GC (Shimadzu-17a). Experiments were performed under atmospheric pressure using a fixed bed nickel tubular reactor. 0.5 g of catalyst was plugged in the reactor with silver wool, and *in situ* activation was performed in the range 350–450 °C for 1 h under nitrogen. After attainment of the chosen reaction temperature, the reactant was fed into the reactor. CFC-113a and water were fed with infusion pumps (Injectomat-2000). Before entering into the reactor, the reactant mixture was passed through a preheater to vaporise the reactants. The HCFC-133a, HFC-143a and N_2 gas flows were maintained by MKS mass flow controllers.

The effluent (CF_3COOH, CF_3CH_2OH, and fluoro-olefins, along with unconverted reactant and by-products such as HF and HCl) was passed through an alkali (KOH-solution) trap to neutralise the acids produced in course of the reaction. The acid-free, gaseous effluent was analysed on-line by GC (60–190 °C, rate of heating 10 °C min^{-1}, Innowax column 0.32 mm i.d. and 25 m length), and in addition by GC/MS (SHIMADZU; PONA capillary 50 m, 0.2 mm i.d.). The total reaction products trapped in alkali solution were analysed by ^{19}F NMR. The amount of acids (CF_3COOH, HCl, HF) formed was determined by titration of unconverted alkali solution with 0.5 M H_2SO_4. The F^- ion concentration was determined by a potentiometric method with a fluoride specific electrode. The specific surface areas of the catalysts were determined by a standard BET method of nitrogen adsorption using an ASAP 2000 system (MICROMETRICS, maximal experimental error ±1%). Powder XRD was performed using a XRD 7 Seiffert-FPM (Ni filtered Cu-Kα radiation).

Results

Hydrolysis of 1,1,1-trichlorotrifluoroethane (CFC-113a). The expected and aimed summary reaction is given by eqn. (1)

$$CF_3CCl_3 + 2H_2O \rightarrow CF_3COOH + 3HCl \qquad (1)$$

A series of Lewis acidic catalysts was tested for hydrolysis of CFC-113a under conditions, which had proved optimum for Fe/C catalysts. The results are displayed in Table 2. Most of these metal modified solid acid catalysts were active for selective hydrolysis reactions. However, catalyst stability has always been a problem of great concern, especially with catalytic research involving CFCs. From Table 2, Fe/Al_2O_3 showed good initial hydrolysis activity of CFC-113a. However, the catalyst deactivation rate became increasingly faster over a period of 3 h, obviously due to formation of HF in course of the reaction.[12,13] The highly acidic metal ion exchanged clay catalyst was also found to be effective at the initial stage. However, the catalyst was also deactivated rapidly during the hydrolysis reaction. This can be attributed to a collapse of the clay structure due to the formation of HF and HCl in the reaction.[14] The hydrolysis reaction with sulfated zirconia catalyst was good only for destruction of CFC-113a, consonant with earlier reports,[15] but no TFA could be detected. Therefore, these catalysts were not suitable for trifluoroacetic acid production. On the other hand, β-AlF_3 catalyst showed stable activity (Table 2), and good selectivity towards TFA but the conversion was low. Moreover, the gaseous products obtained from the reaction included also dismutation and isomerisation products of CFC-113a as would be expected.[2,3] Subsequently, Fe/β-AlF_3 was also tested for hydrolysis reaction of CFC-113a and found to be an active catalyst. However, the conversion and selectivity to TFA were lower than those of the Fe/C catalyst (Table 2). In view of these results, our efforts were concentrated on hydrolysis reaction of CFC-113a on carbon supported transition metal catalysts only, which were found to have good tolerance towards fluorinating species.

Therefore, further experiments were carried out with Fe/C catalysts varying parameters to improve conversion and selectivity to TFA. Feed ratios, reaction temperature and Fe loading on carbon-supported catalyst were thus varied.

The influence of water on the hydrolysis reaction is illustrated in Fig. 1(1). The H_2O : CFC-113a ratio was varied from 5 to 20. The conversion increased with the water excess and the selectivity to TFA was highest when the reaction was conducted with 10–20 moles of water per mole of TFA. Although an excess of water is suitable for this reaction, even higher ratios are not preferable as leaching of the catalyst was noticed at higher water content. On the other hand, the excess water may reduce or suppress the fluorination of the catalyst surface.

The effect of reaction temperature in the range from 200 to 400 °C is shown in Fig. 1(2). The conversion of 113a goes through a maximum at 350 °C, whereas selectivity towards TFA was found to be maximum at 300 °C. Beyond 350 °C there was a decrease in activity due to the deactivation of the catalyst which may be attributed either to coke formation or catalyst fluorination, or both.

The effect of Fe loading on Fe/C catalyst on hydrolysis activity of CFC-113a is displayed in Fig. 1(3) for Fe loadings from 5 to 30%. The activity increased with Fe loading, but this effect is only marked between 10 and 20% of Fe. The selectivity towards TFA was found to be almost independent of Fe content. Under optimum conditions, *i.e.*, at 300 °C and 20-fold excess of water, hydrolysis of CFC-113a over 20% Fe/C catalyst gave TFA with 59.5% conversion and 87.2% selectivity.

It is remarkable that several other metal oxides/chlorides supported on carbon catalysts were able to stimulate the hydrolysis of CFC 113a, also yielding TFA. The activity of these catalysts under conditions found to be optimum for Fe/C are shown in Table 3. With Zn/C, the selectivity is highest, but the conversion is lower compared to Fe/C catalyst. On the other hand, Sn/C catalyst gave 57% conversion with lower selectivity to TFA, and in the case of Cu/C catalyst both conversion and selectivity were low (Table 3). Therefore, Fe/C catalyst was the best catalyst among the tested transition metal salts impregnated on carbon.

In addition, the catalytic activity of the purified carbon support towards CFC-113a hydrolysis was also investigated (Table 2). No TFA formation but only destruction products such as CO and CO_2 were observed. Obviously, the formation of TFA depends on the presence of metal salts and their inherent Lewis acidity.

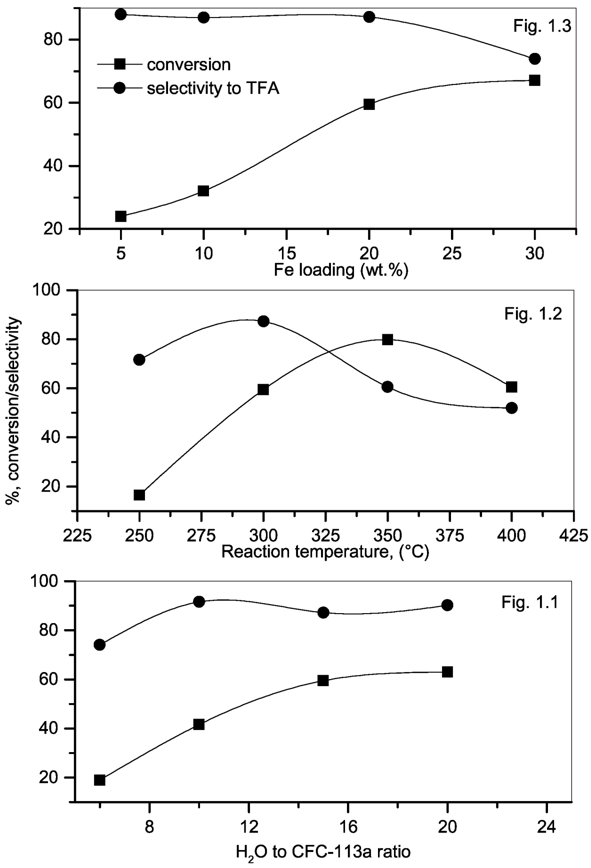

Fig. 1 (1) Effect of feed composition on conversion rate of CFC-113a over 20 wt% Fe/C at a reaction temperature of 300 °C (2) Hydrolysis of CFC-113a in the presence of iron impregnated carbon catalyst (Fe/C 20 wt%) at different temperatures. (3) Effect of Fe content on conversion rate of CFC-113a at a reaction temperature of 300 °C.

Table 2 Hydrolysis of CFC-113a on different catalysts

No.	Catalyst	Contact time/s	Temp./°C	Conv. of CFC 113a (%)	Selectivity towards TFA (%)
1	10 wt% Fe/γ-Al_2O_3	1.2	350	43.2	38
2	Fe/K10	1.0	300	33.0	68.0
3	Fe/PILC	1.2	300	28.5	54.5
4	10 wt% Cu/C	1.3	300	28.5	53.8
5	Sulf. ZrO_2	1.1	350	53.5	Trace
6	β-AlF_3	1.1	300	21.0	68.0
7	Fe-β-AlF_3	1.2	320	27.0	80.0
8	20 wt% Fe/C	1.2	300	59.5	87.2
9	10 wt% Zn/C	1.3	300	34.2	90.2
10	10 wt% Sn/C	1.3	300	57.0	64.5
11	10 wt% Cu/C	1.3	300	28.5	53.8
12	Carbon	1.9	300	24.0	5.0
13	Carbon (HCl washed)	1.9	300	19.0	—

Table 3 Hydrolysis of HCFC-133a on different catalysts at various temperatures

	Conversion of HCFC-133a/ CF_2CHCl (%) in the effluent			
Catalyst	200 °C	250 °C	300 °C	350 °C
Pd/C	20/40	38/63	43/72	17/21
Fe/C	20/n.d.	34/n.d.	27/n.d.	38/n.d.
MoFe/C	Trace	Trace	8/n.d.	3/n.d.
$VMoPO_4$	Nil	2/—	5/trace	7/40
CsF/MgF_2	9/—	24/59	39/43	52/39
ZLF-412	18/45	24/52	27/39	39/33
ZLFPO4-412	27/56	49/44	59/33	76/29

Hydrolysis of HCFC-133a. While the dehydrochlorination of CF_3CH_2Cl to the corresponding olefin is an unwanted side reaction in the HCFC-134a manufacture, little is known about its gas phase hydrolytic reaction to yield trifluoroethanol as given by eqn. (2):

$$CF_3CH_2Cl + H_2O \rightarrow CF_3CH_2OH + HCl \qquad (2)$$

Using Lewis acidic catalysts, no TFE could be detected with any of the catalysts, but in some cases CF_2CHCl was obtained with HCFC-133a conversion rates up to 70% (Table 3).

The experiments with basic catalysts showed quite different results (Table 4). Using alkali metal doped lanthanum phosphate, hydrolysis of HCFC-133a gave TFE in small yields in accordance with the literature,[10] with caesium being the best dopant. In contrast, $LaPO_4$ as well as $AlPO_4$ without dopant showed no catalytic activity (not shown in Table 4), whereas $FePO_4$ directed the reaction towards olefin formation. With the most active catalyst, *i.e.* $Cs/LaPO_4$ ratio 0.07, at 503 °C reaction temperature, the influence of the water to HCFC-133a ratio on TFE yield was tested in the range from 0.44 to 4.4. With increasing amount of water the conversion rate increased from 6.5 to 13.2%, and the selectivity towards TFE from 56.9 to 69.1%; higher amounts of water did not further improve the outcome for TFE.

Ammonolysis of HCFC-133a. Ammonolysis experiments with HCFC-133a were carried out aiming at the formation of trifluoroethylamine, as given in summary in eqn. (3):

$$CF_3CH_2Cl + 2NH_3 \rightarrow CF_3CH_2NH_2 + NH_4Cl \qquad (3)$$

However, with the catalysts tested, Pd/C, PdBi/C, and PdZr/C, no trifluoroethylamine but CF_2CHCl only could be obtained (Table 5).

Oxidation of HFC-143a. The oxidation of HFC-143a aimed at formation of TFA, as given by eqn. (4):

$$CF_3CH_3 + 1\tfrac{1}{2}\,O_2 \rightarrow CF_3COOH + H_2O \qquad (4)$$

Oxidation reactions of HFC-143a were conducted in the temperature range 200–450 °C with an O_2 to HFC-143a ratio of 2.5 (air was used as the molecular oxygen source) using Pd/Al_2O_3, Fe/ZrO_2, ZLF-412 and V_2O_5-K4 catalysts (Table 6). Although conversion reached up to 72% no TFA could be detected. Besides carbon oxides and HF some CF_2CH_2 was formed only at lower reaction temperature.

Table 4 Hydrolysis of HCFC-133a on phosphate based catalysts at 500 °C

Catalyst	Conversion of HCFC 133a (%)	Olefin (%) in the effluent	TFE (%) in the effluent
$Cs/LaPO_4$ 0.07	12	25	69
$Cs/LaPO_4$ 0.14	18.3	46.7	24.4
$Cs/LaPO_4$ 0.21	9.2	36	40
$Na/LaPO_4$ 0.1	0.8	—	—
$K/LaPO_4$ 0.1	11.8	20.3	25.4
$Cs/AlPO_4$ 0.07	< 0.5	—	—
$Cs/LaPO_4$ 0.14	< 0.5	—	—
$FePO_4$	6.0	88.0	4.1

Table 5 Ammonolysis of HCFC-133a on carbon supported Pd based catalysts at various reaction temperatures

	Conversion of HCFC/ Olefin (%) in the effluent at various temperatures			
Catalyst	200 °C	250 °C	300 °C	350 °C
Pd/C	29/78	37/61	46/53	12/47
PdBi/C	20/83	31/72	38/57	53/42
$Pd-ZrO_2/C$	38/70	47/58	61/41	80/38

Table 6 Oxidation of HFC-143a on different catalysts at various temperatures

	Conversion of HFC 143a (%) at varioustemperatures/ amount of CF_2CH_2 (%) in the effluent			
Catalyst	200 °C	300 °C	400 °C	450 °C
8% Pd/Al_2O_3		33/90	47/62	
Fe/ZrO_2	[a]	[a]	6/70	[a]
ZLF-412	[a]	32/55	27/43	[a]
V_2O_5-K4	6.5/88	24/52	31/28	72/17

[a] < 5% conversion.

Discussion

The molecules which are subject of this paper can be represented by the common formula CF_3CXYZ, with X = Y = Z = Cl for CFC-113a, X = Y = H and Z = Cl for HCFC-133a, and X = Y = Z = H for HFC-143a (Scheme 1).

The properties of these compounds and hence their possible reaction pathways are predominantly determined by the CF_3 group.

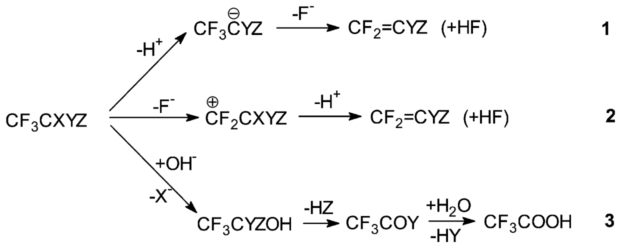

Scheme 1 Reaction pathways of solvolytic/oxidative reactions.

Hydrolysis of HCFC-133a. Due to the strong electron withdrawing power of a CF_3 group, which is nearly equivalent to that of fluorine, hydrogen atoms bound to an adjacent carbon atom become to a certain extent acidic. A geminal chlorine atom as in HCFC-133a further increases the acidity. Therefore, abstraction of a proton can take place comparatively easily as exemplified in Scheme 1, pathway 1,[16] and in the following specified equation for HCFC-133a [*viz.* eqn. (5a)]:

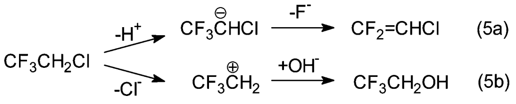

Energetically, this dehydrofluorination is driven by the high enthalpy of formation of HF. Therefore; olefin formation takes place even with the weak base water, but much better with the stronger base ammonia. However, in the case of HCFC-133a, there exists a second competitive reaction route yielding TFE under, *e.g.*, autoclave conditions [eqn. (5b)].[17] Suitable catalysts for directing heterogeneously catalysed hydrolysis reaction towards TFE formation are not to predict easily because excess water will influence the catalysts' activity to a certain but unpredictable extent. Therefore, a broad spectrum of catalysts ranging from very acidic to moderate alkaline have been prepared and tested. Whereas with none of the acidic catalysts TFE could be obtained but olefin only, with alkali metal doped lanthanum phosphate some TFE was obtained *via* hydrolysis, with higher water to HCFC-133a ratios favouring TFE formation. Obviously, with a specific catalyst system the C–Cl bond can be split successfully forming a carbonium ion [*viz.* eqn. (5b)], which reacts with water to give TFE. In addition, olefin formation also took place.

Oxidation of HFC-143a. Regarding the catalytic oxidation reactions with HFC-143a, two competitive routes have to be considered [*viz.* eqn. (6a) and (6b)], which might depend on the type of catalyst used.

$$CF_3CH_3 \xrightarrow{+2O_2} [CF_3C(O)H] \longrightarrow 2CO_2 + 3HF \qquad (6a)$$

$$CF_3CH_3 \xrightarrow{-F^-} [CF_2CH_3]^+ \xrightarrow{-H^+} CF_2{=}CH_2 \qquad (6b)$$

$$CF_2{=}CH_2 \xrightarrow{+2O_2} 2CO_2 + 2HF \qquad (6c)$$

There was no formation of the respective fluorinated alcohols, aldehydes or acids; instead, carbon oxides and HF were detected, according to eqn. (6a). Evidently, C–H bond activation is difficult in this molecule, in accordance with the well-known chemical stability of the so-called R_FR_H compounds. However, once the oxidation reaction started, it will result in total oxidation, as the highly polarised C–C bond is not stronger than the C–H bonds. HFC-143a is reported to react over acidic catalysts to give the olefin CF_2CH_2 (Scheme 1, pathway 2, and eqn. (6b)).[18] On MgP_2O_7 catalyst olefin formation proceeds through a C–F bond cleavage promoted by interaction with the acidic sites of the catalyst to produce a $(CF_2CH_3)^+$ carbonium ion. Obviously, the hydrogen atoms in CF_3CH_3 are, in contrast to CF_3CH_2Cl, not sufficiently acidic to become split off as protons.[16] Some olefin was also detected, however, it is likely that most of the olefin formed reacts primarily further with oxygen [eqn. (6c)].

Hydrolysis of CFC-113a. CFC-113a yields the expected product, *i.e.* trifluoroacetic acid, upon catalytic hydrolysis [eqn. (7)].

$$CF_3CCl_3 \xrightarrow{-Cl^-} [CF_3CCl_2]^+ \xrightarrow{+OH^-} [CF_3CCl_2OH] \xrightarrow{-HCl} CF_3C(O)Cl \xrightarrow[-HCl]{+H_2O} CF_3COOH \qquad (7)$$

Because of the absence of (acidic) hydrogen, there is no possibility for splitting off hydrogen fluoride to form an olefin. On the other hand, interactions between the active acidic sites of the catalyst and a chlorine atom of the molecule results in a partially positive charge at the carbon and a weakening of the C–Cl bond. The carbon is thus susceptible to a nucleophilic attack of a hydroxyl ion displacing chlorine, resulting in a CCl_2OH group, which in term readily splits off HCl to form the carboxylic acid derivative, CF_3COCl, and this is immediately transformed into trifluoroacetic acid under the reaction conditions employed (Scheme 1, pathway 3; eqn. (7)).

Conclusion

CFC-113a (CF_3CCl_3) and HCFC-133a (CF_3CH_2Cl) but not HFC-143a (CF_3CH_3), can be used as sources of valuable fluorine containing building blocks for organic syntheses by heterogeneously catalysed gas phase reactions. In the case of HCFC-133a, the comparably highly acidic hydrogen tends to direct hydrolytic and especially ammonolytic reactions towards HF elimination, *i.e.* olefin formation, although under certain conditions trifluoroethanol is the major product, albeit at relatively low conversions. In contrast, CFC-113a, having no hydrogen in the molecule, is rather susceptible to hydrolysis, *i.e.* to nucleophilic replacement of chlorine by hydroxyl, yielding trifluoroacetic acid, as expected. Oxidation of HFC-143a proceeds more irregularly, resulting predominantly in complete destruction of the molecule, and small amounts of CF_2CH_2.

Acknowledgements

The authors are thankful to DLR, Bonn, for providing financial assistance inside the bilateral CSIR–DLR project INI-007-99.

References

1 (*a*) M. J. Molina and F. S. Rowland, *Nature*, 1974, **249**, 810; (*b*) J. E. Lovelock, *Nature*, 1971, **230**, 379; (*c*) C. Holden, *Science*, 1992, **255**, 155; (*d*) United Nations Environment Programme, Ozone Secretariat, *Handbook for the Montreal protocol on substances that deplete the ozone layer*, 12th edn, October 1991; (*e*) *Chem. Ind.*, 18 November, 1991, 820; (*f*) W. Brune, *Nature*, 1996, **379**, 486; (*g*) L. E. Manger and V. N. M. Rao, *Adv. Catal.*, 1993, **39**, 329.
2 (*a*) A. Hess and E. Kemnitz, *J. Fluorine Chem.*, 1995, **74**, 27; (*b*) H. Quan, Z. Li, Z. Zhao, H. Yang, J. Lu, J. Ren, S. Chen, H. Li and H. Li, *Appl. Catal. B*, 1996, **8**, 209.
3 (*a*) L. Rowley, J. Thamson, G. Webb and J. M. Winfield, *Appl. Catal. A: General*, 1991, **79**, 89; (*b*) R. Ohinishi, W. Wang and M. Ichikawa, *Appl. Catal. A*, 1994, **113**, 29.
4 R. M. Rioux, C. D. Thamson, N. Chen and F. H. Ribero, *Catal. Today*, 2000, **62**, 269.
5 (*a*) C. Doussain, M. Gubelmann and P. Tirel, *US Pat.*, 4 950 811, 1989; (*b*) Y. Lin, S. Zhao, Y. Wu, Y. Zhou and W. Cheng, *Chinese Pat.*, 1 190 092, 1998; (*c*) E. V. Kashutina and A. N. Lavent'ev, *Russ. J. Gen. Chem.*, 1999, **69**, 801; (*d*) J. A. Elliott and W. G. Astrologes, *US Pat.*, 4 618 718, 1989; (*e*) M. Gubelmann-Bonneau, C. Poix-Davaine and H. Ponceblanc, *World Pat.*, WO 9906338, 1998; (*f*) S. Morikawa, M. Yoshitake and S. Tatematsu, *Jpn. Pat.*, 01 319 441, 1989.
6 G. Krishna Reddy and P. Kanta Rao, *Catal. Lett.*, 1997, **45**, 93.
7 (*a*) E. G. Rightor, M. Tzou and T. J. Pinnavaia, *J. Catal.*, 1991, **130**, 29; (*b*) J. H. Clark, A. P. Kybett, D. J. Macquarrie, S. J. Barlow and P. Landon, *J. Chem. Soc., Chem. Commun.*, 1989, 1353.
8 A. Hess, E. Kemnitz, A. Lippitz, W. E. S. Unger and D.-H. Menz, *J. Catal.*, 1994, **148**, 270.
9 V. Quaschning, J. Deutsch, P. Druska, H.-J. Niclas and E. Kemnitz, *J. Catal.*, 1998, **177**, 164.
10 C. Doussain, L. Gilbert, M. Gubelmann and H. Pernot, *US Pat.*, 5 118 651, 1991.
11 A. Martin, U. Bentrup and G.-U. Wolf, *Appl. Catal. A*, 2002, **227**, 131.
12 H. Bozorgzadeh, E. Kemnitz, M. Nickkho-Amiry, T. Skapin and J. M. Winfield, *J. Fluorine Chem.*, 2001, **112**, 225.
13 B. Coq, J. Cognion, F. Figueras and D. Tournigant, *J. Catal.*, 1993, **141**, 21.
14 B. Coq, F. Figueras, S. Hub and D. Tournigant, *J. Phys. Chem.*, 1995, **99**, 11159.
15 K.-U. Niedersen, E. Lieske and E. Kemnitz, *Green Chem.*, 1999, **1**, 225.
16 J. Burdon, P. L. Coe, I. B. Haslock and R. L. Powell, *J. Fluorine Chem.*, 1999, **99**, 127.
17 K. Wu and Q. Y. Chen, *J. Fluorine Chem.*, 2002, **113**, 79.
18 G.-L. Li, H. Nishiguchi, T. Ishihara, Y. Moro-oka and Y. Takita, *Appl. Catal. B: Environmental*, 1998, **16**, 309.

Sustainable development: efficiency and recycling in chemicals manufacturing†

Jean-Paul Lange

Shell Research & Technology Centre, Amsterdam, Badhuisweg 3 1031 CM, Amsterdam, The Netherlands. E-mail: jean-paul.lange@shell.com; Fax: +31(20)630.3010

Received 1st August 2002
First published as an Advance Article on the web 8th October 2002

Since the Rio Earth Summit in 1992, Sustainable Development has been increasingly accepted as a way to run businesses by balancing economic, environmental and societal responsibilities. Important aspects of environmental responsibility are the utilisation of natural resources and the disposal of wastes. These are addressed here. Manufacturing processes and integrated manufacturing chains applied in the petrochemical industry are analysed in terms of feed, energy and chemicals that are consumed. Several chemical intermediates and polymers with large consumption of energy and/or chemicals are readily identified. These may be prime candidates for process improvement efforts. Two indices are proposed for the preliminary evaluation of the recycle options of major polymers. They allow discrimination between materials that need to be reused, those that can also be depolymerised and those for which pyrolysis/gasification or incineration with energy recovery are also responsible options.

1. Introduction

10 years after the Earth Summit of Rio, the importance of Sustainable Development has been recognised by the energy and chemical industries.[1,2] Accordingly, business options are evaluated on their triple bottom line of economic, environmental and societal responsibilities. Within the industry, we call it the strategy of the 3P's, those of Profit, Planet and People. With the 'Profit' dimension, we recognise that businesses need to make a robust profit while allowing their customers to make profits as well. The 'Planet' responsibility calls for efficient management of the available resources and protection of the environment from waste disposal. Finally, the 'People' dimension requires respect of the people and the communities the businesses are in contact with.

The various aspects of the 'Profit' dimension have been discussed in some length in an earlier paper.[3] Hence, I have devoted the present publication to the second dimension, namely the 'Planet' and, more specifically, certain aspects of basic resource use.

We will consider ~50 large chemicals processes and analyse their efficiency in utilising energy and raw materials. This will help us to identify the processes that are prime candidates for improvement. We will then focus on some major polymers and integrate the process efficiencies throughout the whole manufacturing chain. This will highlight important differences in manufacturing efficiency. Finally, we will consider the recycle options of these polymers. We will develop two indices that can guide us in identifying recycle options that are theoretically preferred for the various polymers.

2. Resource efficiency

2.1 Methodology

Data for nearly 50 chemical processes have been obtained from the Process Economic Program of SRI consulting.[4] Similar data are available in the open literature.[5] These data, which are based on open literature data rather than on manufacturing experience, present a fairly approximated description of fully integrated plants. They should therefore be used with a significant uncertainty margin.

The efficiency in organic raw materials has been expressed as carbon lost per carbon built into the product. The efficiency in inorganic raw materials has been expressed as ton of inorganics formed per ton of carbon in the product. It usually consists of acid or base co-reactants or of N- or Cl-compounds that are formed. The energy efficiency has also been expressed as carbon lost per carbon in the product, after converting the consumption of fuel, power and steam to methane equivalent. Details on the methodology, the assumptions and the calculated wastes are published as electronic supplementary information (ESI†).

This approach complements the pioneering analysis of *E*-factor[6] by including the energy utilisation. The conversion of energy consumption to methane equivalent allows us to reduce the number of parameters by combining it with the feed efficiency into an overall C-loss parameter.

2.2 Chemical intermediate manufacturing

This analysis reveals that the majority of processes waste <0.5 C and <0.1 ton of inorganic material per C and ton of C in the product, respectively (see Fig. 1). The C-waste corresponds to a C-efficiency of >67 %. These processes are considered to be

Green Context

Appropriate production/recycling data and methods for dealing with it are still scarce. Here, the production of some large volume products (polymers and their monomers) is treated from the points of view of both production and recycling/reuse. The approach highlights some key products as being particularly difficult environmentally; these products are often associated with the incorporation of functionality required for high performance. ***DJM***

---

† Electronic supplementary information (ESI) available: appendix A: calculation of carbon and inorganic waste production; appendix B: production of carbon and inorganic wastes from petrochemical processes. See http://www.rsc.org/suppdata/gc/b2/b207546f/

DOI: 10.1039/b207546f

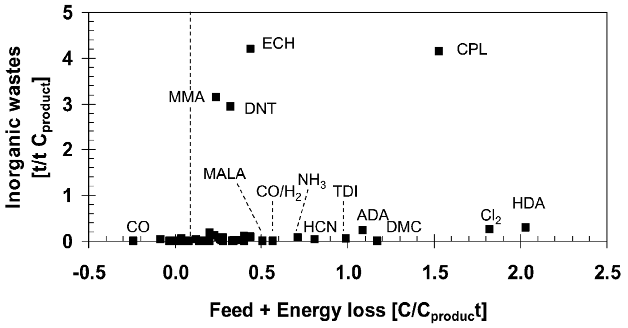

Fig. 1 Resource utilisation of chemical manufacturing processes, expressed as wastes of inorganics and total carbon.

fairly efficient with their resources. However, a few other processes produce more wastes than desired product.

Conspicuous C-consuming processes are converting methane to HCN and NH_3 (wastes defined per N or ton N), dinitrotoluene to toluene diisocyanate (TDI), CO + methanol to dimethyl carbonate (DMC), cyclohexane to caprolactam (CPL), butadiene to 1,6-hexyldiamine (HDA), benzene to adipic acid (ADA) and NaCl to Cl_2 (waste defined per Cl or ton Cl).

Conspicuous inorganic waste producing processes are the conventional processes for the conversion of toluene to dinitrotoluene (DNT), acetone to methyl methacrylate (MMA), cyclohexane to caprolactam (CPL) and propene to epichlorohydrin (ECH). In fact, all these processes utilise inorganic chemicals based on H_2SO_4, NH_3 or Cl_2 as stoichiometric co-reactants.

The stoichiometric reactions involved in these resource-demanding processes are reported in Table 1.

This analysis can be improved upon integrating the production line of these intermediates from the basic raw materials, which are typically naphtha and/or methane. The integration results in significant shifts towards higher carbon losses and/or higher inorganic waste production (Fig. 2). It confirms the high resource utilisation of the nylon intermediates (in particular of caprolactam and hexyldiamine), as well as of toluene diisocyanates, methyl methacrylate and epichlorohydrin. It also unravels vinyl chloride (VCM) and phosgene (Cl_2CO) as energy demanding intermediates.

Table 1 Stoichiometric equations of selected resource-demanding processes

Adipic acid (ADA), hexyldiamine (HDA) and caprolactam (CPL)
$C_6H_6 + 3\ H_2 + 5/2\ HNO_3 \rightarrow HOOCC_4H_8COOH + 5/4\ N_2O + 9/4\ H_2O$
$C_4H_6 + 2\ HCN + 4\ H_2 \rightarrow H_2NC_6H_{12}NH_2$
$\text{cyclo-}C_6H_{12} + 3\ NH_3 + 3\ O_2 + 3\ H_2 + H_2SO_4 \rightarrow C_6H_{11}ON + 5\ H_2O + (NH_4)_2SO_4$

Dinitrotoluene (DNT) and toluene diisocyanate (TDI)
$MeC_6H_5 + 2\ HNO_3 \rightarrow MeC_6H_3(NO_2)_2 + 2\ H_2O$
$MeC_6H_3(NO_2)_2 + 6\ H_2 + 2\ Cl_2CO \rightarrow MeC_6H_3(NCO)_2 + 4\ H_2O + 4\ HCl$

Epichlorohydrin (ECH)
$C_3H_6 + 2\ Cl_2 + 1/2\ Ca(OH)_2 \rightarrow ClCH_2C_2H_3O + 2\ HCl + 1/2\ CaCl_2$
Methyl methacrylate (MMA)
$CH_3COCH_3 + HCN + H_2SO_4 + CH_3OH \rightarrow CH_2{=}C(CH_3)COOCH_3 + NH_4HSO_4$

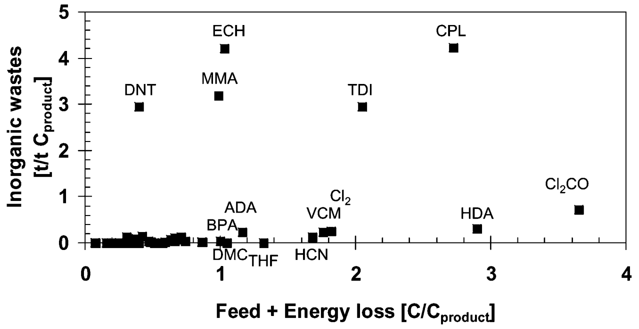

Fig. 2 Resource utilisation of chemical intermediates, expressed as wastes of inorganics and total carbon integrated over the whole manufacturing chain.

This analysis easily justifies the research activities on alternative routes to caprolactam,[5,7,8] adipic acid,[5,8] methyl methacrylate[5,9] and vinyl chloride.[5,10] Similarly, the substitution of phosgene by *e.g.* diphenyl carbonate[11,12] is also the subject of much research for improving the manufacture of diisocyanate and polycarbonates. By comparison, there appears to be less effort to improve the manufacture of epichlorohydrin or dinitrotoluene, which also would provide improvement opportunities.

2.3 Polymer manufacturing

Beyond the intermediates, the manufacturing lines can be integrated up to the final polymers in an attempt to highlight their respective demands on primary resources. According to Fig. 3, the integrated manufacture of polyolefins and polystyrene proceeds fairly efficiently with integral waste productions of < 0.5 C/C and $< 0.1\ t_{inorganic}/t_C$. This is expected to hold for most of the commodity hydrocarbon polymers used *e.g.* in packaging. Other integral production chains appear much less efficient, however. The production of PVC and Nylons are striking examples of energy-consuming routes. Comparatively large amounts of inorganic wastes are produced during the manufacture of many higher-performance polymers such as Nylon-6, poly(methyl methacrylate) (PMMA), epoxy resins, polyurethane (PU) and polycarbonate (PC) (Fig. 3).

Fig. 3 seems to suggest a relationship between the performance of a polymer and the efficiency of its integrated production chain. High performance is frequently achieved by using sophisticated monomers that provide polarity, H-bonding and/or cross-linking and that usually require additional resource inputs at some point in the value chain. Consequently, one can identify a clear research driver aimed at achieving these performance attributes through other, less resource-intensive means.

For example the properties of polyolefins and polystyrene can be significantly improved by changing the tacticity, microstructure and/or incorporating simple apolar and polar comonomers.[13–16] The deep hydrogenation of polystyrene to polycyclohexylethylene provides a glassy polymer with performance that can compete with polycarbonate or poly(methyl methacrylate) in certain applications.[13,17]

Some properties of polyamides are now duplicated by a new polyester, poly(trimethylene terephthalate) (PTT), which is based on monomers—1,3-propane diol and terephthalic acid—

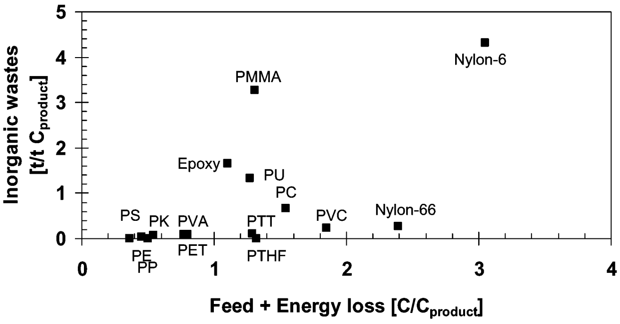

Fig. 3 Resource utilisation of polymers, expressed as wastes of inorganics and total carbon integrated over the whole manufacturing chain.

that consume much less resources than those of polyamides (Fig. 3). The resource consumption of PTT is expected to decrease further in the future when operational experience allow for further optimisation.

Engineering-type performance has been achieved by co-polymerising the simplest monomers, *i.e.* alkenes and CO, into regular polyketones.[13,18] This polymer is characterised by very low integral wastes of ~0.5 C/C and ~0.02 $t_{inorganic}/t_C$ (Fig. 3).

Finally, polar monomers might be more efficiently obtained from natural resources such as carbohydrates. Several companies are indeed commercialising aliphatic polyesters based on natural hydroxy alkanoates.[13,19,20] Preliminary (and often complex) analysis of the integral production chain, from crop to polymer, frequently indicates however that such routes tend to consume more (fossil-based) energy than do their oil-based alternatives.[21]

New polymers offer new possibilities for producing materials with minimal waste production. They do, however, represent true business adventures, for the development of new polymers can take 10 years and cost several hundreds of millions to a billion of dollars development without guarantee of market acceptance.[13] One should therefore not stop the research efforts for continuous process and product improvement on existing polymers, which frequently offer a higher chance of implementation.

3. Polymer recycling

A true sustainability analysis should not be limited to the production chain. It should also cover the utilisation and disposal of the material. For spent polymers (post-consumer waste), the options (Fig. 4) vary between

- reuse after simple cleaning or after cleaning and reprocessing to equal or lower grade material,
- depolymerisation back to the monomer(s),
- conversion to a general feedstock such as naphtha—*via* pyrolysis—or synthesis gas—*via* gasification,
- incineration to use the energy content to produce electricity, and
- landfill disposal.

The first three options represent true recycling back to a polymer. Incineration and landfill do not. We will however see that they can still be appropriate disposal options. Political pressure for 'true recycling' can be very strong. For example, targets for recycling *via* reuse and/or depolymerisation of 20% for packaging plastics[22] and 80% for end-of-life vehicles[23] have been proposed for 2006 within the European Union. The optimal recycling option depends on many factors, some technical, some economical and some societal.[24,25] Such a life-cycle analysis is clearly outside the scope of the present conceptual analysis. We nevertheless see some utility in offering a simple conceptual framework that helps to discriminate between theoretically preferred options.

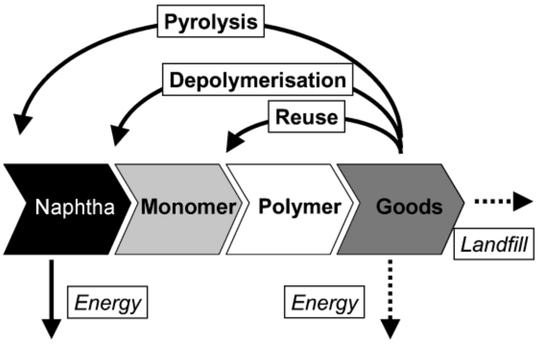

Fig. 4 Options for disposing of spent polymers.

We propose here two indices for polymer disposal. The first index is the integral waste production of polymer manufacture that we have developed above. The second index is the enthalpy of depolymerisation.‡ The lower the enthalpy requirement, the easier the depolymerisation. This implies low energy consumption and, most likely, also low consumption of stoichiometric reagents. Obviously, it ignores the chemistry of depolymerisation, *e.g.* by ignoring the difficulty to selectively depolymerise PE to ethylene, as well as potential waste production during recycling. It also neglects the energy consumed for cleaning the spent polymer or purifying the depolymerised mono- or oligomers from solvents and additives.

The combination of these two indices leads us to Fig. 5, which clearly shows the contrasting characteristics of the condensation and addition polymers. The former are characterised by high waste production and easy depolymerisation, whereas the latter are characterised by low waste production but demanding depolymerisation.

In fact, Fig. 5 can be further divided into four quadrants, according to the disposal options that are theoretically preferred:

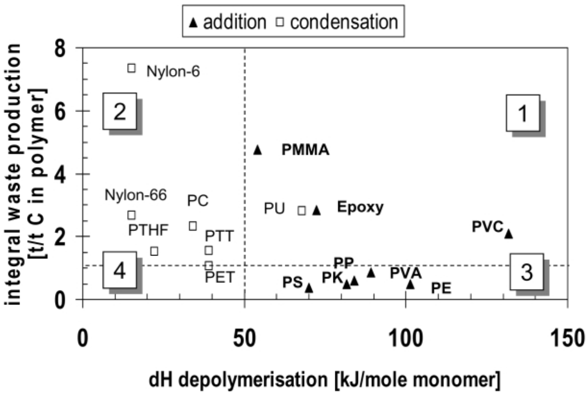

Fig. 5 Environmental friendliness of polymers, expressed as the ease of depolymerisation and the C- and inorganic-wastes produced during virgin manufacture. The four quadrants represent theoretically preferred options for the disposal of spent polymers, namely (1) reuse, (2) reuse or depolymerisation, (3) reuse or gasification/pyrolysis and (4) all of the above + landfill.

Reuse. The polymers in quadrant 1 (*e.g.* PVC, epoxy resins and polyurethane) regroup the polymers that unfavourably combine high waste production during virgin manufacture with difficult depolymerisation. These polymers are the least attractive from the environmental point of view. They should be reused as much as possible, as performed commercially by Dow for polyurethane[17] and by Solvay for PVC.[26] While these polymers add substantial value in many applications, development of more efficient manufacturing routes could enhance their versatility further.

Reuse or depolymerise. Conversely, polymers in quadrant 2 (*e.g.* nylon-6 and -66 as well as polycarbonate) are characterised by high emissions during virgin manufacture but easy depolymerisation. Hence depolymerisation is also an option besides reuse. This is consistent with the depolymerisation of nylon carpets that is presently operated at the commercial scale,[27] even though the plant(s) might be presently shut down for

---

‡ The heat of depolymerisation was taken as the negative of the heat of polymerisation reported in the literature for most of the polymers (K. J. Ivin, in *Polymer Handbook*, ed. J. Brandrup and E. H. Immergut, Interscience, New York, 1966, pp. 363–398) and calculated by molecular modelling for PC, PU and epoxy resins.

techno-economic reasons, and the depolymerisation of PC, PMMA and PU that are/have been under development.[24]

Reuse, pyrolyse or incinerate. Polymers located in quadrant 3 (*e.g.* polyolefins, polystyrene and polyketone) are characterised by low emissions during virgin manufacture but difficult depolymerisation. These polymers can be viewed as 'crude oil' equivalent and thus processed analogously. When reuse is not convenient, they could be pyrolysed[28,29] or gasified[30] or efficiently incinerated to utilise their energy content. The chemical industry indeed strongly advocates incineration as an environmentally responsible option in these cases.[31,32] This philosophy is appropriate as long as fossil energy sources are being utilized, which can be anticipated for many decades.

Green polymers. Finally, quadrant 4 (*e.g.* PET) contains polymers that favourably combine low emission during virgin manufacture with easy depolymerisation. These are candidate for all recycle options. Even landfill could be a responsible option for those polymers that fall into this quadrant in cases where they are biodegradable under applicable conditions. This could be the case for poly(hydroxy alkanoates) and polylactates if their manufacture is accompanied by acceptably low inorganic waste production. Their energy consumption is expected to be higher than that of polyethylene but still moderate compared to high valued polymers.[21,33]

These four quadrants have arbitrary boundaries and do not account for all aspects of polymer disposal. Nevertheless, they seem to offer a reasonable framework for the purposes of mapping the appropriate disposal options adopted by responsible industries.

4. Life cycle analysis

The present analysis has been purposely extended to an integrated analysis over the whole production chain. This analysis is indeed more representative of the 'true' environmental burden of satisfying the desired need for packaging or construction materials. It can be extended in several ways.

It can be extended to non-polymeric materials that ensure a similar function. For example, a similar analysis that was limited to energy consumption of the manufacture of various packaging showed that the manufacture of polymeric packaging requires ~50% and 10–20% of the energy required for glass and metal manufacture, per volume of material.[24]

However, the analysis can also be extended to include the environmental cost/benefits of installing, using and disposing of the various materials. This approach would ideally compare the various material types in terms of unit 'utility' rather than mass or volume. Such a full life cycle analysis is at a level of specificity that is beyond the present scope.

5. Conclusions

We have seen that chemical intermediates are generally manufactured with efficient use of resources. They typically waste <30 w% of carbon and <10 w% of inorganics used. However, a few exceptions have been identified such as the manufacture of Cl_2, NH_3, HCN, phosgene, hexyldiamine and vinyl chloride, which are large energy consumers, and the manufacture of caprolactam, epichlorohydrin, methyl methacrylate and diisocyanates, which are large consumers of inorganics. Research efforts are already devoted to improving these processes.

Similarly, the major polymers exhibit significant differences in resource utilisation, when integrated over the whole manufacturing chain. The polyolefins and other pure hydrocarbon polymers are manufactured with low carbon and inorganic consumption. In contrast, polyamide, poly(methyl methacrylate), polycarbonate, polyurethane and epoxy resins are produced with relatively high inorganic waste. These observations suggest worthwhile targets for process and product improvement.

An efficient approach to reduce consumption of the resources and, at the same time, protect the environment consists of recycling the spent polymers. Based on two indices, namely the integral manufacturing efficiency and the heat of depolymerisation, one can easily classify the major polymers into four recycle categories: the polymers that need to be reused (*e.g.* PVC), the polymers to reuse or depolymerise (*e.g.* polyamide), the polymers to reuse, pyrolyse or incinerate (*e.g.* polyolefins) and the 'green' polymers that can be recycled by any means. Of course, this classification is only a crude first step of a more comprehensive life cycle analysis.

6. List of symbols

ADA	adipic acid
CPL	caprolactam
DMC	dimethylcarbonate
DNT	dinitrotoluene
ECH	epichlorohydrin
Epoxy	epoxy resins
HDA	1,6-hexyldiamine
MALA	maleic anhydride
MMA	methyl methacrylate
PC	polycarbonate
PDO	1,3-propanediol
PE	polyethylene
PET	poly(ethylene terephthalate)
PK	polyketone
PMMA	poly(methyl methacrylate)
PP	polypropylene
PS	polystyrene
PTHF	polytetrahydrofuran
PTT	poly(trimethylene terephthalate)
PU	polyurethane
PVA	poly(vinyl acetate)
PVC	poly(vinyl chloride)
TDI	toluene diisocyanate
VCM	vinyl chloride monomer

Acknowledgement

I wish to acknowledge SRI consulting for collecting and providing an excellent and extensive set of data. I wish also to acknowledge numerous colleagues for valuable discussions, in particular A. W. van der Made (who also provided some valuable thermodynamic data), E. Drent, G. Vaporciyan, J. Harmsen and K. Schram.

References

1 M. Eissen, J. O. Metzger, E. Schmidt and U. Schneidewind, *Angew. Chem., Int. Ed.*, 2002, **41**, 414.
2 K. S. Watkins, *Chem. Eng. News*, 2002, (April 22), 15.
3 J.-P. Lange, *CatTech*, 2001, **5**, 82.
4 *PEP Yearbook International*, ed. S.H. Wang, vol. 1E, United States, SRI consulting, Menlo Park/USA, 1997.
5 A. Chauvel and G. Lefebvre, *Petrochemical Processes: 1. Synthesis gas derivatives and major hydrocarbons*, Technip, Paris, 1989; A.

Chauvel and G. Lefebvre, *Petrochemical processes: 2. Major oxygenated, chlorinated and nitrated derivatives*, Technip, Paris, 1989.

6 R. A. Sheldon, *Chemtech*, 1994, (March), 38.

7 G. Dahlhoff, J. P. M. Niederer and W. F. Hoelderich, *Catal. Rev.*, 2001, **43**, 381.

8 G. Bellussi and C. Perego, *CatTech*, 2000, **4**, 4.

9 M. Morgan, *Eur. Chem. News*, 2002, (February 11), 20.

10 *Eur. Chem. News*, 1999, (October 18), 26.

11 Y. Ono, *Appl. Catal. A: Gen.*, 1997, **155**, 133.

12 J. Plotkin and E. Glatzer, *Eur. Chem. News*, 2002, (July 18), 32.

13 A. H. Tullo, *Chem. Eng. News*, 2002, (May 20), 13.

14 P. M. Morse, *Chem Eng. News*, 1998, (July 6), 11.

15 Ph. Dubois, *Chim. Nouv.*, 2001, **75**, 3297.

16 S. Mecking, *Angew. Chem., Int. Ed.*, 2001, **40**, 534.

17 M. Reisch, *Chem. Eng. News*, 2001, (September 17), 22; Modern Plastics International, 2000 (July 7), p. 17; www.dow.com.

18 E. Drent, J. A. M. van Broekhoven and P. H. M. Budzelaar, in *Applied homogeneous catalysis with organometallic compounds*, eds. B. Cornils and W. A. Hermann, VCH, New York, 1996, p. 333.

19 J. Baker, *Eur. Chem. News*, 2002, (February 18), 24.

20 A. BenBrahim, www.chemsoc.org/chembytes/ezine/2002/benbrahim_apr02.htm.

21 T. U. Gerngross and S. C. Slater, *Sci. Am.*, 2000, (August), 25.

22 *Eur. Chem. News*, 2002, (December 17), 24.

23 N. Elghamy, *Eur. Chem. News*, 2000, (November 6), 50.

24 W. Kaminsky, *Ullmann's Encyclopedia of Industrial Chemistry*, A21, VCH Publishers, Weinheim, 1992, p. 57.

25 J. K. Borchardt, *Kirk-Othmer Encyclopedia of Chemical Technology*, 4th edn., supplement volume, John Wiley & Sons, New York, 1998, p. 460.

26 A. Scott, *Chem. Week*, 2002, (March 6), 31; www.solvay.com/pvc/what/whatli03.htm.

27 A. H. Tullo, *Chem. Eng. News*, 2000, (January 24), 23.

28 L. J. Broadbelt, *Catalysis*, 1999, **14**, 110.

29 G. P. Huffman and N. Shah, *Chemtech*, 1998, **12**, 34.

30 *Eur. Chem. News*, 1994, (October 31), 23.

31 L. C. E. Struik, *Polytech. Tijdschr.*, 1992, **12**, 40.

32 A. Scott, *Chem. Week*, 2000, (February 16), 23.

33 S. K. Ritter, *Chem. Eng. News*, 2002, (July 1), 26.

A simple and green procedure for the synthesis of α-aminophosphonate by a one-pot three-component condensation of carbonyl compound, amine and diethyl phosphite without solvent and catalyst

Brindaban C. Ranu* and Alakananda Hajra

Department of Organic Chemistry, Indian Association for the Cultivation of Science,
Jadavpur, Calcutta-700 032, India. E-mail: ocbcr@mahendra.iacs.res.in;
Fax: 91-33-4732805

Received 13th June 2002
First published as an Advance Article on the web 3rd October 2002

A simple, general, efficient and greener method has been developed for the synthesis of **α**-aminophosphonates through a solvent-free and catalyst-free one-pot three-component condensation of carbonyl compound, amine and diethyl phosphite.

Introduction

α-Aminophosphonates, due to their structural analogy to α-amino acids, have been the subject of considerable current interest.[1] A number of synthetic methods have been developed during past two decades.[2] Of these methods, the nucleophilic addition of phosphites to imines catalyzed by a base or an acid, is the most convenient one. A variety of metal halides such as $TiCl_4$,[2b] $SnCl_4$,[2c] $ZnCl_2$,[2d] $MgBr_2$,[2d] $InCl_3$,[2e] $TaCl_5$–SiO_2[2f] and lanthanide triflates[2g,h] have been used as Lewis catalysts in methylene chloride or other organic solvents to promote this addition. However, organic solvents, particularly chlorinated hydrocarbons are high on the list of damaging chemicals because of their volatile nature, considerable toxicity and use in large quantities for a reaction. On the other hand, the metal halides employed as catalysts in these procedures are not all eco-friendly and often entail severe environment pollution during the process of waste disposal. To avoid these disadvantages a couple of modifications using montmorillonite clay[3a] and alumina[3b] in dry media under microwave irradiation have been reported recently. As a part of our green technology program we would also like to disclose here a more practical green alternative for the synthesis of α-aminophosphonates by a three-component condensation of carbonyl compounds (aldehydes and ketones), amines and diethyl phosphite at 75–80 °C in neat without any solvent and catalyst (Scheme 1).

Results and discussion

In a typical experimental procedure, a mixture of carbonyl compound, an amine and diethyl phosphite was heated (75–80 °C) in neat without any solvent and catalyst for few minutes (TLC). The liquid products were isolated by direct distillation from the reaction pot under reduced pressure and the solid ones were recrystallized from ethyl acetate.

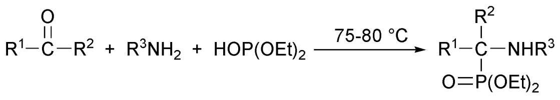

Scheme 1

A wide range of structurally varied aldehydes and ketones underwent reactions with aromatic and aliphatic amines to produce the corresponding α-aminophosphonates by this procedure. The results are summarized in Table 1. This procedure is equally effective for conversion of open-chain, cyclic, heterocyclic and aromatic aldehydes and ketones to the respective α-aminophosphonates. The presence of electron-withdrawing or electron-donating substituents on the aromatic ring does not make any difference to the course of reaction. Several sensitive functionalities such as OH, OMe, Cl, NO_2, CO_2Me, C=C bond, methylenedioxy are well tolerated under the present reaction conditions.

The reactions are, in general very fast, clean and atom-economic. No side product has been isolated in any reaction leading to a minimum waste. The products obtained after distillation or recrystallization are of high purity and do not require any chromatographic purification. This avoids use of large quantities of volatile organic solvents usually required for work-up and purification in many existing procedures. On the other hand, use of no catalyst in this process makes easier waste disposal.

When the reaction was carried out in a solvent like THF under similar reaction conditions the condensation proceeds to a marginal extent (10–15%) for aldehydes and does not occur at all for ketones. The reaction can be scaled up to the extent of a batch of 10g (not optimized) without any difficulty avoiding use of any organic solvent in any step.

Green Context

Minimisation of solvent usage and catalyst waste are key factors in any process. The synthesis of aminophosphonates is typically carried out using an imine and a phosphite, and reacting them together in an organic solvent using one of a wide range of catalysts. Remarkably, this paper indicates that neither is required. Simply heating the two reaction partners together neat is sufficient in many cases to give high yields of pure products. ***DJM***

DOI: 10.1039/b205747f

Conclusion

The present procedure for the synthesis of α-aminophosphonates by a solvent-free and catalyst-free one-pot reaction of carbonyl compounds, amines and diethyl phosphite provides a very simple, efficient, general, cost-effective and greener methodology. Most significantly, this protocol now throws a challenge to the existing procedures[2] using solvents and catalysts and in general, leads to a new technology of solvent-free, catalyst-free reaction.[4] Finally, we believe that this will present a better and more benign alternative to the existing methodologies[2,3] for the synthesis of α-aminophosphonates to cater the need of academia as well as industries.

Experimental

General

^{1}H NMR (300 MHz) and ^{13}C NMR (75 MHz) spectra were run in $CDCl_3$ solutions. Analyses were done on a Perkin Elmer 2400 autoanalyzer. The aldehydes, ketones, amines and diethyl phosphite are all commercial materials and were distilled before use.

General experimental procedure for the synthesis of α-aminophosphonates

Representative procedure for the aminophosphonate listed in entry 8. A mixture of 4-chlorobenzaldehyde (140.6 mg, 1 mmol), 4-chloroaniline (127.6 mg, 1 mmol) and diethyl phosphite (138 mg, 1 mmol) was stirred at 75–80 °C (oil bath) in neat without any solvent for 35 min (monitored by TLC). A solid appeared and was recrystallized from ethyl acetate–hexane (1 : 4) to furnish the corresponding α-aminophosphonate as a colorless solid (342 mg 88%), mp 117–118 °C; ν_{max} (KBr)/cm^{-1} 3292, 1598, 1490, 1230; δ_H 7.46–7.24 (m, 4H), 7.04 (d, J = 8.7 Hz, 2H), 6.50 (d, J = 8.8 Hz, 2H), 4.96 (br, 1H), 4.69 (d, J = 24.2 Hz, 1H), 4.22–3.73 (m, 4H), 1.38–1.08 (m, 6H); δ_C 145.2, 145.0, 134.6, 134.4, 129.7, 129.6, 129.5, 129.4, 123.6, 123.5, 115.3 (2C), 63.9, 63.7, 55.9 (d, J_{CP} = 150.3 Hz), 16.8,

Table 1 Synthesis of α-aminophosphonates

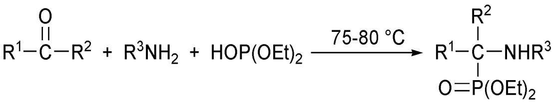

$$R^1\text{–}C(=O)\text{–}R^2 + R^3NH_2 + HOP(OEt)_2 \xrightarrow{75\text{-}80\ °C} R^1\text{–}C(R^2)(NHR^3)\text{–}P(=O)(OEt)_2$$

Entry	R¹	R²	R³	Time/min	Yield[a] (%)	Ref.
1	Ph	H	Ph	25	92	2*g*
2	Ph	H	*o*-$OTsC_6H_4$	30	86	
3	Ph	H	$PhCH_2$	25	93	2*g*
4	Ph	H	Cyclohexyl	30	88	2*e*
5	*p*-$OMeC_6H_4$	H	*p*-BrC_6H_4	30	85	
6	*m*-$OMeC_6H_4$	H	*p*-IC_6H_4	30	88	
7	*p*-ClC_6H_4	H	*o*-$OMeC_6H_4$	35	90	
8	*p*-ClC_6H_4	H	*p*-ClC_6H_4	35	88	
9	*p*-$NO_2C_6H_4$	H	*o*-$CO_2MeC_6H_4$	35	82	
10	*p*-$NMe_2C_6H_4$	H	Cyclohexyl	30	85	
11	*o*-OHC_6H_4	H	*m*-ClC_6H_4	30	85	
12	*p*-$OAllylC_6H_4$	H	*p*-MeC_6H_4	30	85	
13	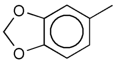	H	*p*-ClC_6H_4	30	94	
14	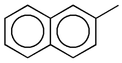	H	*o*-MeC_6H_4	30	90	
15	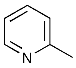	H	Ph	25	88	2*e*
16	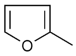	H	Ph	25	81[b]	2*g*
17	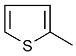	H	Cyclohexyl	25	85	
18	PhCH=CH(t)	H	Ph	25	80[b]	2*g*
19	n-Bu	H	Me_2CH	25	92	2*e*
20	Me_2CH	H	$PhCH_2$	25	88	2*e*
21	Me_2CH	H	*n*-Bu	25	88	
22	Citral	H	$PhCH_2$	25	80[b]	2*e*
23	Et	Et	$PhCH_2$	140	86	2*e*
24	Me_2CHCH_2	Me	$PhCH_2$	150	84	
25	Cyclopentanone		$PhCH_2$	45	90	
26	Cyclohexanone		$PhCH_2$	40	94	2*e*
27	Cyclohexanone		Ph	40	94	2*f*
28	Cycloheptanone		$PhCH_2$	50	88	
29	Cycloctanone		$PhCH_2$	50	88	
30	4-Methylcyclohexanone		n-Bu	45	89	
31	4-*tert*-Butylcyclohexanone		$PhCH_2$	45	88	2*e*
32	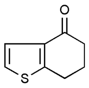		$PhCH_2$	180	80	

[a] The yields refer to pure products characterized by spectral and analytical data. [b] The reaction was started at −20 °C and then temperature was riased to 75 °C.

16.5. (Found: C, 52.51; H, 5.08; N, 3.53. $C_{17}H_{20}NO_3PCl_2$ requires C, 52.61; H, 5.15; N, 3.61%).

This procedure is followed for the synthesis of all the aminophosphonates listed in Table 1. The liquid products are distilled directly from the reaction vessel under reduced pressure. The products are characterized by their IR, ^{1}H NMR , ^{13}C NMR spectral data and elemental analysis.

Spectral and analytical data of the α-aminophosphonates , not reported earlier are presented below in order of their entries in Table 1.

Entry 2. ν_{max} (neat)/cm^{-1} 3442, 1610, 1456, 1232; δ_H 7.86 (d, J = 8.3 Hz, 2H), 7.33–7.23 (m, 7H), 6.95–6.87 (m, 2H), 6.55 (t, J = 7.9 Hz, 1H), 6.34 (d, J = 8.0 Hz, 1H), 5.31 (br, 1H), 4.68 (dd, J = 5.3, 23.9 Hz, 1H), 4.12–3.77 (m, 4H), 2.19 (s, 3H), 1.28–1.16 (m, 6H); δ_C 145.8, 139.7, 139.5, 137.5, 135.6, 135.5, 133.2, 130.3 (2C), 129.0 (2C), 128.9, 128.3, 128.1, 128.0, 122.8, 117.9, 113.6, 63.9, 63.6, 56.0 (d, J_{CP} = 149.1 Hz), 22.2, 16.9, 16.6. (Found: C, 58.78; H, 5.72; N, 2.81. $C_{24}H_{28}NO_6SP$ requires C, 58.89; H, 5.77; N, 2.86%).

Entry 5. Mp 108–109 °C; ν_{max} (KBr)/cm^{-1} 3456, 1615, 1452, 1226; δ_H 7.34 (d, J = 8.1 Hz, 2H), 7.15 (d, J = 7.8 Hz, 2H), 6.85 (d, J = 7.8 Hz, 2H), 6.46 (d, J = 8.1 Hz, 2H), 4.65 (m, 1H), 4.10–3.83 (m, 4H), 3.77 (s, 3H), 3.69 (m, 1H), 1.36–1.10 (m, 6H); δ_C 159.8, 145.7, 132.2 (2C), 129.3, 128.9, 126.8, 115.9 (2C), 114.5, 110.5, 63.8, 63.6, 55.8 (d, J_{CP} = 151.2 Hz), 55.6, 16.8, 16.6. (Found: C, 50.31; H, 5.37; N, 3.22. $C_{18}H_{23}NO_4PBr$ requires C, 50.48; H, 5.41; N, 3.27%).

Entry 6. Mp 112–114 °C; ν_{max}(KBr)/cm^{-1} 3429, 1624, 1457, 1231; δ_H 7.33 (d, J = 8.7 Hz, 2H), 7.25–6.77 (m, 4H), 6.37 (d, J = 8.7 Hz, 2H), 4.65 (d, J = 24.0 Hz), 4.14–3.78 (m, 4H), 3.75 (s, 3H), 3.68–3.65 (m, 1H), 1.27 (t, J = 7.1 Hz, 3H), 1.11 (t, J = 7.1 Hz, 3H); δ_C 160.3, 146.5, 138.1 (2C), 137.4, 130.1, 130.0, 120.5, 116.4 (2C), 113.8, 113.7, 63.9, 63.6, 56.3 (d, J_{CP} = 149.8 Hz), 55.6, 16.9, 16.6. (Found: C, 45.31; H, 4.77; N, 2.87. $C_{18}H_{23}NO_4PI$ requires C, 45.49; H, 4.88; N, 2.95%).

Entry 7. ν_{max}(neat)/cm^{-1} 3419, 1600, 1510, 1244; δ_H 7.42–7.23 (m, 4H), 6.76–6.64 (m, 3H), 6.34–6.31 (m, 1H), 5.28 (br, 1H), 4.72 (d, J = 24.1 Hz, 1H), 4.13-3.88 (m, 3H), 3.85 (s, 3H), 3.83-3.72 (m, 1H), 1.33 (t, J = 7.1 Hz, 3H), 1.12 (t, J = 7.1 Hz, 3H); δ_C 147.7, 136.4, 135.2, 134.0, 129.6, 129.5, 129.1, 129.0, 121.3, 118.3, 111.5, 110.0, 63.8, 63.5, 55.9, 55.8 (d, J_{CP} = 149.9 Hz), 16.8, 16.6. (Found: C, 56.21; H, 6.01; N, 3.55. $C_{18}H_{23}NO_4PCl$ requires C, 56.33; H, 6.04; N, 3.65 %).

Entry 9. Mp 82–84 °C; ν_{max}(KBr)/cm^{-1} 3317, 1685, 1519, 1232; δ_H 8.90–8.84 (m, 1H), 8.16 (d, J = 8.5 Hz, 2H), 7.89 (d, J = 7.9 Hz, 1H), 7.63 (dd, J = 2.2, 8.7 Hz, 2H), 7.14 (t, J = 7.3 Hz, 1H), 6.60 (t, J = 7.3 Hz, 1H), 6.32 (d, J = 8.5 Hz, 1H), 4.94 (dd, J = 7.1, 25.3 Hz, 1H), 4.15–3.89 (m, 4H), 3.89 (s, 3H), 1.24 (t, J = 7.1 Hz, 6H); δ_C 169.1, 149.4, 149.2, 148.0, 144.2, 134.9, 132.2, 129.0, 128.9, 124.5, 124.0, 117.0, 112.3, 64.2, 63.8, 55.6 (d, J_{CP} = 148.1 Hz), 52.2, 16.8 (2C). (Found: C, 53.93; H, 5.37; N, 6.56. $C_{19}H_{23}N_2O_7P$ requires C, 54.03; H, 5.49; N, 6.63%).

Entry 10. ν_{max}(neat)/cm^{-1} 3444, 1614, 1519, 1236; δ_H 7.20 (dd, J = 2.2, 8.8 Hz, 2H), 6.65 (d, J = 8.6 Hz, 2H), 4.11–4.01 (m, 5H), 2.92 (s, 6H), 2.35-1.03 (m, 18H); δ_C 150.4, 129.5 (2C), 124.2, 112.7 (2C), 63.3, 62.8, 57.1 (d, J_{CP} = 154.8 Hz), 53.5, 53.3, 40.9, 34.7, 32.3, 26.5, 25.3, 24.8, 16.9, 16.6. (Found: C, 53.90; H, 5.41; N, 6.52. $C_{19}H_{23}N_2O_7P$ requires C, 54.03; H, 5.49; N, 6.63%).

Entry 11. ν_{max}(neat)/cm^{-1} 3480, 2927, 1610, 1222; δ_H 9.16 (br, 1H), 7.36–6.54 (m, 8H), 5.27 (d, J = 23.7 Hz, 1H), 4.90 (br, 1H), 4.25–3.82 (m, 4H), 1.39–1.07 (m, 6H); δ_C 155.9, 148.1, 135.2, 130.6, 129.8, 129.1, 121.7, 120.6, 118.8, 117.2, 114.2, 112.5, 64.3, 64.1, 51.4 (d, J_{CP} = 154.5 Hz), 16.8, 16.5. (Found: C, 55.08; H, 5.59; N, 3.70. $C_{17}H_{21}NO_4PCl$ requires C, 55.22; H, 5.72; N, 3.79%).

Entry 12. ν_{max}(neat)/cm^{-1} 3432, 1609, 1460, 1238; δ_H 7.36–6.48 (m, 8H), 6.01–5.90 (m, 1H), 5.36–3.62 (m, 10H), 2.14 (s, 3H), 1.30 (t, J = 7.1 Hz, 3H), 1.07 (t, J = 7.1 Hz, 3H); δ_C 158.6, 144.6, 133.6, 129.6 (2C), 129.4, 129.3, 128.6, 128.5, 127.5, 115.2, 115.1, 114.4 (2C), 69.0, 63.4, 63.3, 56.01 (d, J_{CP} = 151.2 Hz), 20.7, 16.9, 14.5. (Found: C, 64.61; H, 7.19; N, 3.51. $C_{21}H_{28}NO_4P$ requires C, 64.77; H, 7.25; N, 3.60%).

Entry 13. mp 114–115 °C; ν_{max}(KBr)/cm^{-1} 3460, 1612, 1460, 1254; δ_H 7.02–6.50 (m, 7H), 5.87 (s, 2H), 4.84 (br, 1H), 4.60 (d, J = 23.9 Hz, 1H), 4.14–3.69 (m, 4H), 1.28 (t, J = 7.1 Hz, 3H), 1.13 (t, J = 7.1 Hz, 3H); δ_C 148.4, 147.8, 145.4, 129.6, 129.3 (2C), 123.3, 121.7, 115.4 (2C), 108.7, 108.4, 101.5, 63.8, 63.6, 56.2 (d, J_{CP} = 151.8 Hz), 16.8, 16.6. (Found: C, 54.22; H, 5.27; N, 3.41. $C_{18}H_{21}NO_5PCI$ requires C, 54.35; H, 5.32; N, 3.52%).

Entry 14. ν_{max}(neat)/cm^{-1} 3430, 1608, 1452, 1236; δ_H 7.91–6.39 (m, 11H), 4.99–4.75 (m, 2H), 4.13-3.58 (m, 4H), 2.31 (s, 3H), 1.25 (t, J = 7.1 Hz, 3H), 0.86 (t, J = 7.1 Hz, 3H); δ_C 144.9, 134.1, 130.7, 128.9, 128.4, 128.3, 128.2, 128.1, 127.5, 127.1, 126.6, 126.5, 125.4, 124.9, 118.7, 111.8, 63.7, 63.6, 56.9 (d, J_{CP} = 148.6 Hz), 18.1, 16.6, 14.6. (Found: C, 68.81; H, 6.75; N, 3.52. $C_{22}H_{26}NO_3P$ requires C, 68.92; H, 6.83; N, 3,65 %).

Entry 17. ν_{max}(neat)/cm^{-1} 3422, 1601, 1458, 1252; δ_H 7.13–6.85 (m, 3H), 4.32 (d, J = 22.0 Hz, 1H), 4.08–3.75 (m, 4H), 2.40–0.92 (m, 18H); δ_C 141.2, 127.1, 126.3, 125.2, 63.7, 63.1, 54.1, 53.5 (d, J_{CP} = 159.2 Hz), 34.5, 32.3, 26.3, 25.2, 24.7, 16.8, 16.5. (Found: C, 54.22; H, 7.85; N, 4.16. $C_{15}H_{26}NO_3SP$ requires C, 54.36; H, 7.91; N, 4.23%).

Entry 21. ν_{max}(neat)/cm^{-1} 3452, 1658, 1235; δ_H 4.04–3.92 (m, 4H), 2.70–2.63 (m, 1H), 2.51–2.44 (m, 2H), 1.98–1.96 (m, 1H), 1.34–0.74 (m, 20H); δ_C 61.8, 61.5, 61.1 (J_{CP} = 140.6 Hz), 49.9, 32.9, 29.3, 21.0, 20.8, 20.5, 18.2, 16.8, 14.2. Found: C, 54.21; H, 10.48; N, 5.17. $C_{12}H_{28}NO_3P$ requires C, 54.32; H, 10.54; N, 5.28%).

Entry 24. ν_{max}(neat)/cm^{-1} 3446, 1454, 1228; δ_H 7.39–7.20 (m, 5H), 4.20–3.89 (m, 7H), 2.04–0.96 (m, 18H); δ_C 141.5, 129.1 (2C), 128.5 (2C), 127.1, 62.3, 62.0, 57.6 (J_{CP} = 137.9 Hz), 48.1, 42.6, 25.7, 25.4, 23.4, 21.1, 17.0, 16.6. (Found: C, 62.24; H, 9.21; N, 4.22. $C_{17}H_{30}NO_3P$ requires C, 62.37; H, 9.24; N, 4.28%).

Entry 25. ν_{max}(neat)/cm^{-1} 3446, 1452, 1228; δ_H 7.31–7.16 (m, 5H), 4.18–3.87 (m, 6H), 1.99–1.22 (m, 15H); δ_C 141.7, 128.6 (2C), 128.4 (2C), 127.1, 64.2 (d, J_{CP} = 145.2 Hz), 62.2, 61.1, 48.7, 34.7, 34.6, 24.8, 24.7, 17.1, 17.0. (Found: C, 61.59; H, 8.29; N, 4.38. $C_{16}H_{26}NO_3P$ requires C, 61.72; H, 8.42; N, 4.50%).

Entry 28. ν_{max}(neat)/cm^{-1} 3446, 1456, 1234; δ_H 7.38–7.21 (m, 5H), 4.20–4.10 (m, 4H), 3.92–3.91 (m, 2H), 2.00–1.25 (m, 19H); δ_C 141.9, 128.6 (2C), 128.5 (2C), 127.1, 62.1, 62.0, 59.7 (d, J_{CP} = 135.0 Hz), 48.0, 34.2, 34.1, 30.4 (2C), 22.3, 22.2, 17.1, 17.0. (Found: C, 63.58; H, 8.79; N, 4.09. $C_{18}H_{30}NO_3P$ requires C, 63.70; H, 8.91; N, 4.13%).

Entry 29. ν_{max}(neat)/cm^{-1} 3442, 1450, 1230; δ_H 7.43–7.17 (m, 5H), 4.24–3.83 (m, 6H), 2.39–0.90 (m, 21H); δ_C 141.8, 128.8 (2C), 128.5 (2C), 127.1, 62.0, 61.9, 59.7 (d, J_{CP} = 134.8 Hz), 48.0, 30.0, 29.5 (2C), 28.5, 24.9, 21.4, 21.3, 17.1, 17.0. (Found: C, 60.01; H, 6.83; N, 3.61. $C_{19}H_{32}NO_3P$ requires C, 60.14; H, 6.91; N, 3.69 %).

Entry 30. ν_{max}(neat)/cm^{-1} 3444, 1455, 1234; δ_H 3.95–3.83 (m, 4H), 2.47–2.44 (m, 2H), 1.55-0.67 (m, 26H); δ_C 61.6, 61.5, 55.4 (d, J_{CP} = 141.0 Hz), 42.4, 33.5, 32.4, 29.9, 29.2, 28.7, 28.5, 22.8, 20.6, 16.9, 16.8, 14.3. (Found: C, 58.90; H, 10.51; N, 4.48. $C_{15}H_{32}NO_3P$ requires C, 58.99; H, 10.56; N, 4.59%).

Entry 32. ν_{max}(neat)/cm^{-1} 3442, 1452, 1236; δ_H 7.35–7.05 (m, 7H), 4.18–3.57 (m, 7H), 2.81–2.78 (m, 2H), 2.24–2.03 (m, 4H), 1.34 (t, J = 7.1 Hz, 3H), 1.12 (t, J = 7.1 Hz, 3H); δ_C 141.0, 140.8, 133.3, 128.7 (2C), 128.6 (2C), 127.9, 127.2, 122.0, 63.5, 62.8, 58.9 (d, J_{CP} = 153.0 Hz), 47.8, 29.7, 25.3, 21.0, 16.9, 16.7. (Found: C, 60.01; H, 6.82; N, 3.59. $C_{19}H_{26}NO_3PS$ requires C, 60.14; H, 6.91; N, 3.69%).

Acknowledgements

This investigation has enjoyed financial support from CSIR, New Delhi [Grant No. 01(1739)/02]. A.H. is also thankful to CSIR for his fellowship.

References

1 (*a*) S. C. Fields, *Tetrahedron*, 1999, **55**, 12237; (*b*) M. C. Allen, W. Fuhrer, B. Tuck, R. Wade and J. M. Wood, *J. Med. Chem.*, 1989, **32**, 1652; (*c*) E. K. Baylis, C. D. Campbell and J. G. Dingwall, *J. Chem. Soc., Perkin Trans. 1*, 1984, 2845; (*d*) F. R. Atherton, C. H. Hassal and R. W. Lambert, *J. Med. Chem.*, 1986, **29**, 29.

2 (*a*) V. P. Kukhar and V. A. Solodenko, *Russ. Chem. Rev. (Engl. Transl.)*, 1987, **56**, 859; (*b*) T. Yokomatsu, Y. Yoshida and S. Shibuya, *J. Org. Chem.*, 1994, **59**, 7930; (*c*) S. Laschat and H. Kunz, *Synthesis*, 1992, 90; (*d*) J. Zon, *Pol. J. Chem.*, 1981, **55**, 643; (*e*) B. C. Ranu, A. Hajra and U. Jana, *Org. Lett.*, 1999, **1**, 1141; (*f*) S. Chandrasekhar, S. J. Prakash, V. Jagadeshwar and Ch. Narsihmulu, *Tetrahedron Lett.*, 2001, **42**, 5561; (*g*) C. Qian and J. Huang, *J. Org. Chem.*, 1998, **63**, 4125; (*h*) S. Lee, J. H. Park, J. Kang and J. K. Lee, *Chem. Commun.*, 2001, 1698; (*i*) K. Manabe and S. Kobayashi, *Chem. Commun.*, 2000, 669.

3 (*a*) J. S. Yadav, B. V. S. Reddy and Ch. Madan, *Synlett*, 2001, 1131; (*b*) B. Kaboudin and R. Nazari, *Tetrahedron Lett.*, 2001, **42**, 8211.

4 Although there are a couple of isolated examples of solvent-free, catalyst-free reactions like preparation of hydrazone under microwave irradiation (see: M. Joselink, R. S. Varma, S. Palanc and M. Kocevar, *Chem. Commun*, 2001, 1716); this protocol has not been explored for multi-component condensation or any complex reaction to any great extent.

Preparation of chelating agents from sugarcane bagasse by microwave radiation as an alternative ecologically benign procedure

Ugo S. Orlando,* Aloysius U. Baes, Wataru Nishijima and Mitsumasa Okada

Laboratory of Greenchemistry, Department of Chemical Engineering, Graduate School of Engineering, Hiroshima University, 1-4-1 Kagamiyama, Higashi-Hiroshima 739-8527, Japan. E-mail: ugo@environ.hiroshima-u.ac.jp

Received 8th April 2002
First published as an Advance Article on the web 8th October 2002

Microwave radiation was utilized to produce neutral chelating agents (BCA) from sugarcane bagasse. BCA were prepared by reaction of urea with reactive sites present in bagasse such as hydroxyl and carboxylic groups. BCA prepared through microwave radiation had slightly lower yield (83%) compared to the conventional oven-drier process (87%). BCA demonstrated maximum chelating adsorption capacity ($Q_{\max}$) of 1.2 mmol g^{-1} for Cu(II) at pH of 5.5 and 1.4 mmol g^{-1} for Hg(II) at pH 6.0. These results could be comparable with the $Q_{\max}$ of 1.46 mmol g^{-1} for Cu(II) and 2.4 mmol g^{-1} for Hg(II) obtained from Duolite GT-73, a commercial chelating resin, macroreticular with tiol (S–H) functional groups.

Introduction

In recent years, due to the concern over the impact of industrial processes on the environment, many researches are trying to minimize the use of hazardous chemicals and develop green technology synthesis.[1,2]

Since the early 1970s, agricultural wastes have been a focus of investigation due to its high reactivity for grafting polymerization. Agricultural residues such as rice husk, sugarcane bagasse, sawdust of wood and wheat straw have been applied as efficient adsorbents for heavy metal removal. Apart the use of such agricultural residues as adsorbents, its use certainly will reduce hazardous materials in the environment and create new alternatives for the utilization of waste materials.

Conventionally, chelating agents are produced from cellulose, petroleum derivatives and agricultural residues by using of hazardous chemicals in multi-polymerization steps. In most cases, organic solvents, swelling agents for cellulose and some catalysts are used to increase the efficiency of the chemical process.[3,4]

Recently, a new method has been developed for the preparation of chelating agents based on amination of vinylbenzyl chloride–styrene–divinylbenzene copolymer bearing ethoxycarbonylethyl phosphonate, with ethylenediamine and diethylenetriamine.[5] Although this method can produce resins with a high capacity for the removal of Cu(II), Cd(II), Ni(II) and Zn(II), the use of hazardous chemicals such as KCN, dioxane, DMF and triethyl phosphite and the multi-step polymerization make this method expensive and significantly toxic.

Another widely used chemical strategy to introduce ion exchangeable groups into agricultural residues is based on the epoxidation of the hydroxyl groups.[6,7] The epoxide group is responsible for giving a suitable spacer between the carrier (agricultural residue) and the ion exchangeable groups.[8] All the preparation methods on the epoxidation of the copolymers are totally chlorine free (TCF) process, whereas the technique still requires the handling of hazardous substances.

Ahuja and Rai reported that guaran, derived from the seeds of the guaran plant (*Cyamoposis tetragonalobus*) could be converted into a neutral chelating agents after chemical modifications with epichlorohydrin, dioxane, HCl and other reagents in order to incorporate amino acid hydroxamate and fatty acid hydroxamate groups into the guaran matrix.[9]

The main goal of this work was to demonstrate a new procedure, which is a simple, efficient and environmentally acceptable method to prepare chelating agents from easily available agricultural residues. Experiments were conducted by using two preparation techniques, oven drying and microwave radiation. Bagasse chelating agents (BCA) were prepared by heating pure urea with granular bagasse. Based on the chemical composition of bagasse utilized on this study, the reaction took place probably throughout the most common reactive sites presents in lignin and holocellulose, hydroxyl and carboxylic groups (Table 2).

According to previous work, basically two donating atoms are responsible for chelation and adsorption, *i.e.* one oxygen and one nitrogen atom, for chelating resins with urea as a functional

Green Context

The sustainable use of chemicals by an increasingly demanding world population will require a substantial diversification in raw materials and product composition. Agricultural residues are a very attractive feedstock since they have little or no value and can consume resources on disposal. In tropical countries sugarcane bagasse is widely available as a waste product and through its functionality it can be converted into an ion exchange resin by chemical modification. We must be careful however, that we do not develop biomass utilisation methods that are resource intensive or involve hazardous procedures. Here we see a simple and environmentally benign process for converting the bagasse into effective chelating agents by reaction with urea under microwave irradiation, in the absence of solvent or other auxiliaries. The capacity of the new materials for Cu(II) and Hg(II) is comparable to commercial resins derived from traditional, polluting, processes but the raw materials do suffer from limited regenerative potential due to a limited pH stability range. ***JHC***

DOI: 10.1039/b203440a

group.[10] Thus resins with urea provide bidentate ligand sites. Urea was utilized in this process due to its classification as a non-toxic reactant, being a solid and stable at room temperature and not ranked by any system regulated by US-EPA as a hazardous chemical.[11,12]

Native sugarcane bagasse (referred to here as bagasse) was tested as a possible chelating agent. Bagasse can be considered one of the most widely available agricultural residues in tropical countries with a yearly global production of 234 million tons.[13] Bagasse is accumulated in large quantities as waste in sugarcane mills. In a previous work, it was demonstrated that bagasse could be converted into an ion exchanger resin after chemical modification.[14]

Maximum adsorption capacity (Q_{max}) of the bagasse chelating agents was evaluated for the removal of Cu(II) from aqueous solution at pH 5.5 and for Hg(II) at pH 6.0. The results were then compared with a commercial chelating resin, Duolite GT-73, macroreticular with tiol (S-H) functional groups.[15]

Experimental

Reagent grade urea was purchased from Wako Pure Chemical Industries, Ltd., Japan. Sugarcane was collected from the local plantations in the Amazon region of Brazil.

One gram of semi-dried bagasse (10–21% moisture content) with particle size around 250 μm was irradiated for 12 min with 2 g of urea in a 50 ml glass beaker using a microwave oven (Sharp REM20) emitting 2.450 MHz microwave frequency. The product was then washed with hot water (60 °C) and boiled for 30 min to remove residues and excess urea. The products were vacuum dried for 10 min and sieved to obtain particles of <250 μm, which were used in all chelating exchange experiments. The nitrogen content of the final product was determined using a Perker-Elmer Elemental analyzer CHNS/O (model 2400II).

Single chelating adsorption experiments were performed by agitating 0.5 g of BCA in mercury solutions with a concentration of 10 mg l^{-1} for 24 h at 30 °C. The pH was set at 6.0 by adding a small amount of 0.1 M NaOH. For the determination of the maximum chelating adsorption capacity, stock solutions with different concentrations of Hg(II) and Cu(II) (10–520 mg l^{-1}) were prepared in deionized water using the chloride and nitrate salts, respectively. In order to determine the Q_{max} of copper(II) and mercury(II), batch adsorption experiments were conducted agitating 0.1 g of the product or Duolite GT-73 in 25 ml solution containing different concentrations of copper and mercury for 24 h at 30 °C. The pH was set at 5.5 for copper and 6.0 for mercury solutions by adding 0.1 M NaOH. After filtration, the concentration of metals was determined using an Inductively Coupled Argon Plasma Atomic Emission Spectrophotometer (Nippon Jarrel-Ash Model 575II).

Results and discussion

The amount of nitrogen incorporated into bagasse after heating with urea was investigated to explain the relationship between nitrogen content and chelating adsorption capacity. A single adsorption study was performed by adding known amounts of BCA and native bagasse into a mercury solution with a known concentration. Native bagasse with low concentration of native nitrogen, 0.34%, demonstrated no chelating adsorption capacity (Table 1). On the other hand, BCA with the highest nitrogen content of 14.9% demonstrated the ability to remove 95% of the total amount of mercury ions from aqueous solution.

To compare the reaction efficiency achieved by the microwave radiation with the conventional heating process, production of bagasse chelating agents was conducted by using an oven-dryer at different reaction times and temperatures. The controlling of experiments were made through the analysis of some parameters such as yield, chelating adsorption capacity and nitrogen content obtained after incorporation of urea into bagasse at different reaction times and temperatures (Table 1). After 12 min of microwave radiation, approximately 14.8% of nitrogen-amide was incorporated into bagasse while nitrogen-amide incorporated into bagasse was 6.2% after 120 min of heating in a oven-dryer. On the other hand, based on the same experimental conditions and reagent concentrations, significantly shorter reaction times and higher nitrogen contents were achieved by using microwave radiation.[16]

Slightly higher yields were obtained for chelating agents prepared by an oven-dryer (87%). It is known that the microwave radiation reduces the crystallinity of some agricultural residues, resulting in lower yields (83%).[17–19] Usually a pre-treatment is required before reaction to improve the accessibility of the hydroxyl groups in the agricultural residues.[20] The modest yields obtained from both types of chelating agents may be due to the high extractive content in bagasse used

Table 2 Composition of native bagasse

α-Cellulose (%)	41
Hemicelluloses (%)	4
Lignin (%)	9
Ash (%)	1
Extractives (%)	45

Table 1 Characteristics of the bagasse chelating agents

Conditions	Sample	Temp./°C	Reaction time/min	Nitrogen (%)	Yield (%)	% Removal
Microwave radiation	BCA		3	0.9	81	3
			5	5	82	5
			10	10	81	60
			12	14.9	83	95
			15	12	83	74
			20	7.4	85	15
Oven-dryer process	BCA	80	40	3	74	2
		100	100	6.1	82	65
		120	120	6	81	75
		160	160	6.3	87	75
		160	180	6	75	74
		160	220	6	69	68
	Unmodified bagasse			0.34		0.5

% Removal experiment conditions: chelating resin dose 0.5 g, volume 50 ml, mercury concentration 10 mg l^{-1}, temperature 30 °C, agitating time 24 h, agitating speed 180 rpm.

in this process. The chemical composition of bagasse utilized in this study is shown in Table 2.

Based on the higher values of nitrogen content, the metal adsorption capacities were evaluated only for chelating agents prepared by microwave radiation. The equilibrium isotherms of Cu(II) and Hg(II) onto bagasse chelating agents and Duolite GT-73 at pH 5.5 and 6.0 are shown in Fig. 1 and 2, respectively. The Langmuir equation was utilized to determine the maximum adsorption capacity ($Q_{\max}$) as follows:

$$\frac{1}{q_{\mathrm{e}}} = \frac{1}{Q_{\max}} + \frac{1}{bQ_{\max}} \cdot \frac{1}{C_{\mathrm{e}}} \qquad (1)$$

where, $Q_{\max}$ and q_{e} are the maximum adsorption capacity and concentration of metals in the adsorbent (mmol g^{-1}), respectively; C_{e} is the equilibrium metal concentration in solution (mmol l^{-1}) and b is the energy of adsorption.

$Q_{\max}$ of Duolite GT-73 and bagasse chelating agents for Cu(II) were 1.5 and 1.2 mmol g^{-1} and for mercury were 2.3 and 1.4 mmol g^{-1}, respectively. Duolite GT-73 exhibited slightly higher $Q_{\max}$ than bagasse chelating agents.

The cost for the preparation of BCA was evaluated based on the current market price of urea in Brazil (40 US$/100 kg). Assuming that 0.83 kg of BCA is produced from 1 kg of bagasse and there is no cost for bagasse because it is treated as waste, the cost of BCA is about 0.96 US$/kg. Comparing this value with the cost of 85.00 US$/kg obtained for Duolite GT-37, it can be concluded that the present method for the production of chelating agents from bagasse is a viable alternative method for the economic treatment of wastewater containing mercury(II) and copper(II).

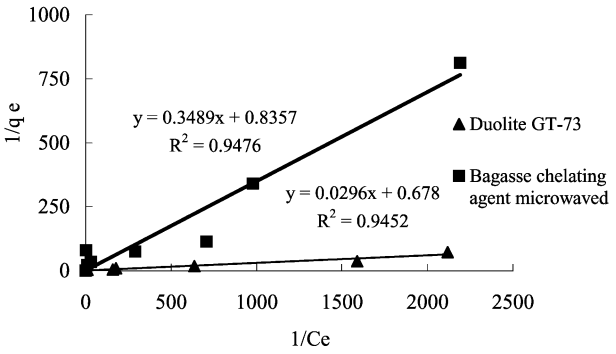

Fig. 1 Equilibrium isotherms of Cu(II) onto the Duolite GT-73 and bagasse chelating agents prepared by microwave radiation. Chelating resin dose is 0.1 g (dry wt) l^{-1}. The pH of the solution was adjusted to 5.5.

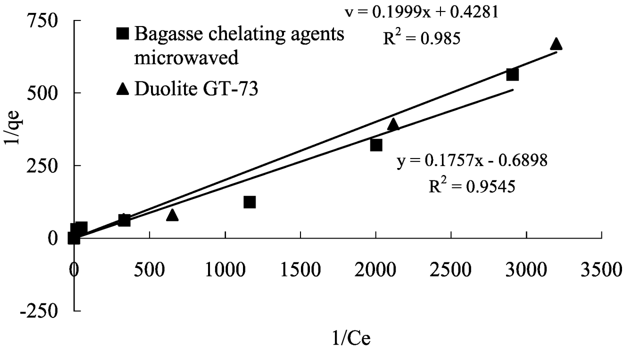

Fig. 2 Equilibrium isotherms of Hg(II) onto the Duolite GT-73 and bagasse chelating agents prepared by microwave radiation. Chelating resin dose is 0.1 g (dry wt) l^{-1}. The pH of the solution was adjusted to 6.0.

The disadvantage regarding this new procedure relative to Duolite GT-73 is based on its capacity of regeneration. BCA has a working range between pH 4.9 and 7.5, in contrast to Duolite GT-73 which operates in the range pH 1–14. Thus BCA can not be treated with alkaline and acidic solutions for regeneration. The high instability of the structure of BCA at low and high pH leads to solubilization of the chelating amide groups. It is proposed that after saturation due to its low preparation cost, the resin should be disposed of and burned or treated with acidic solutions to remove the metals and again treated with urea to regenerate new adsorption sites.

Conclusion

Bagasse chelating agents were successfully prepared by the reaction of urea with granular bagasse using microwaves or an oven-dryer. These results demonstrate that the present method is an efficient means of producing chelating agents with 14.8% of nitrogen-amide functional groups in 82% yield. Bagasse chelating resins showed almost an identical ability to remove Cu(II) and Hg(II) as the commercial resin Duolite GT-73. Based on the preparation cost and $Q_{\max}$, the present method for production of chelating agents from bagasse would be a viable alternative method for the economic treatment of wastewater containing Hg(II) and Cu(II). In addition to its proven efficacy, the method is a simple and ecologically benign process, utilizing only one polymerization step and using no hazardous chemicals.

References

1 T. Salmi, V. Serra-Holm, T.-K. Rantakylä, P. Mäki-Arvela and L. P. Lindfors, *Green Chem.*, 1999, **1**(6), 283.
2 H. M. Sampath Kumar, B. V. Subba Reddy, E. Jagan Reddy and J. S. Yadav, *Green Chem.*, 1999, **1**(3), 141.
3 R. R. Navarro, K. Sumi and M. Matsumura, *Water Res.*, 1999, **33**(9), 2037.
4 A. B. Burdukov, V. I. Ovcharenko, V. A. Reznikov, V. N. Ikorskii, Y. G. Shvedenkov and N. V. Pervukhina, *Cryst. Eng.*, 2000, **3**, 41.
5 A. W. Trochimczuc and J. Jezierska, *Polymer*, 2000, **41**, 3463.
6 R. R. Navarro, K. Sumi, N. Fujii and M. Matsumura, *Water Res.*, 1996, **30**(10), 2488.
7 I. Šimkovic, *Ind. Crops Prod.*, 1999, **10**, 167.
8 V. C. Malshe and M. S. Vaidya, *React. Funct. Polym.*, 1999, **39**, 83.
9 M. Ahuja and A. K. Rai, *Carbohydr. Polym.*, 1997, **33**, 57.
10 R. J. Brown, A. G. Pierce and L. M. Trenomas Jr., *Inorg. Chem.*, 1970, **11**, 1830.
11 EPA, Office of Solid Waste and Office of Pollution Prevention and Toxics, 1998, Waste Minimization Prioritization Tool, Spreadsheet Document for the RCRA Waste Minimization PBT. Chemical List Docket. #F-98-MMLP-FFFFF, EPA,Washington, DC. September.
12 EPA, Indiana Pollution Prevention and Safe Materials Institute, 1996. The Development of Pollution Prevention Progress Measurement Methods Project. Project No. NP995716-010, EPA Region V.
13 D. S. Chahal, *Availability of forest biomass*, Oxford and IBH, New Delhi, 1991, p. 15.
14 J. A. Lazslo, *Textile Chem. Color.*, 1996, **28**(5), 13.
15 S. Caddick, *Tetrahedron*, 1995, **51**, 10403.
16 S. Chiarle, M. Ratto and M. Rovatti, *Water Res.*, 2000, **34**(11), 2971.
17 G. Lewandowicz, J. Fornal, A. Walkowski, M. Maczynski, G. Urbaniak and G. Szymanska, *Ind. Crops Prod.*, 2000, **11**, 249.
18 G. Lewandowicz, T. Jankowski and J. Fornal, *Carbohydr. Polym.*, 2000, **42**, 193.
19 C. Gourson, R. Benhaddou, R. Granet, P. Krausz, L. Saulnier and J. Thibault, *Macromol. Chem., C. R. Acad. Sci. Paris, Ser. II*, 1999, 75.
20 G. Chauvelon, N. Gergaud, L. Saulnier, D. Lourdin, A. Buleon, J. Thibault and P. Krausz, *Carbohydr. Polym.*, 2000, **42**, 385–392.

Vapour phase methylation of pyridine with methanol over the $Zn_{1-x}Mn_xFe_2O_4$ ($x = 0, 0.25, 0.50, 0.75$ and 1) ferrite system

A. Radhe Shyam,[a] Reena Dwivedi,[a] V. S. Reddy,[a] K. V. R. Chary[b] and R. Prasad[a]

[a] *School of Chemical Sciences, Devi Ahilya University, Indore 452001, India*
[b] *Indian Institute of Chemical Technology, Hyderabad, India.*
E-mail: r_prasad99@yahoo.com;radhe007@yahoo.com

Received 29th July 2002
First published as an Advance Article on the web 22nd October 2002

Alkylation of pyridine by methanol to methylpyridines has been studied in the vapour phase in a fixed bed reactor, in the temperature range 473–723 K over the $Zn_{1-x}Mn_xFe_2O_4$ ($x = 0, 0.25, 0.50, 0.75$ and 1) ferrospinel system. 2-Picoline and 3-picoline were found to be major products. It was observed that, systems possessing high x values are highly selective for 2-picoline. Reaction parameters were optimized over $MnFe_2O_4$. A maximum yield of 67.6% of 2-methylpyridine, with a selectivity of 79.5%, and 17.5% of 3-methylpyridine with a selectivity of 20.5%, was obtained over $MnFe_2O_4$ at a temperature of 673 K, using a methanol to pyridine molar ratio of 5 and weight hour space velocity of 0.2 h^{-1}. Catalyst characterization has been made by XRD, infrared spectroscopy and ammonia desorption methods. A tentative mechanism for production of 2-picoline and 3-picoline, involving dihydropyridine as the intermediate has been proposed.

1. Introduction

Recently, there has been an upsurge on the alkylation of organic compounds by alkylating agents over ferrospinel catalysts,[1–3] having general formula $M^{2+}[Fe^{3+}{}_2]O_4$, formed due to close packing of oxygen anions having tetrahedral and octahedral interstitial sites filled by M^{2+} and Fe^{3+} ions, respectively. Metal ions in square brackets are in octahedral sites. Depending upon the position of metals in the tetrahedral and octahedral sites, ferrospinel can be normal $M^{2+}[Fe^{3+}{}_2]O_4$, inverse $Fe^{3+}[M^{2+}\text{-}Fe^{3+}]O_4$, or mixed spinel in which the divalent cations are distributed between both sites. This type of cation distribution significantly affects acido–basic[3] and surface properties of ferrospinels.[4,5]

Methylpyridines and their derivatives are industrially valuable compounds, as fine chemicals, bulk drugs, insecticides, fungicides and herbicides.[6,7] Increasing demands for the production of methylpyridines and their derivatives exceeds that traditionally obtained from coal tar distillation. Attempts have therefore been made to develop synthetic processes for these chemicals.[8–10] Vapour phase catalytic processes seem to be the preferred technology as this does not produce any solid waste and is environmentally friendly.

Although, there are many reports on the synthesis of pyridine bases using different raw materials and catalysts,[6–12] there seems to be no detailed report on synthesis of pyridine bases by alkylation of pyridine with methanol over ferrite catalysts, except one by Sreekumar *et al.*[3] The present study of the alkylation of pyridine was therefore undertaken with a view to (i) search for a suitable ferrite catalyst, (ii) to optimize the composition of catalyst and to (iii) optimize the process for maximum yield to methylpyridines. Additionally, catalysts have been characterized using XRD, IR, surface area and ammonia desorption methods with a view to understand the structure, nature of bonding and acido-basic properties of the catalysts.

2. Results and discussion

2.1 Acidity, surface area and performance of various catalysts in the alkylation of pyridine

The acidity and surface area data of various ferrite catalysts $ZnFe_2O_4$ (ZF), $Zn_{0.75}Mn_{0.25}Fe_2O_4$ (ZMF-1), $Zn_{0.5}Mn_{0.5}Fe_2O_4$ (ZMF-2), $Zn_{0.25}Mn_{0.75}Fe_2O_4$ (ZMF-3) and $MnFe_2O_4$ (MF) are listed in Table 1. Performance of various ferrite catalysts in the alkylation of pyridine is presented in Table 2. The order of catalytic activity of ferrospinels toward overall conversion was found to be MF > ZMF-3 > ZMF-2 > ZMF-1 > ZF. An examination of Table 1 reveals that the acidity as well as surface area increases with increasing x value and better performance of the MF catalyst can be ascribed to its higher acidity and surface area, compared to Zn ferrite. Further process development work was therefore undertaken over the MF catalyst.

2.2 Effect of temperature on alkylation of pyridine

The effect of temperature on alkylation of pyridine over MF, at constant methanol/pyridine molar ratio, was investigated in the

Green Context

Methylpyridines have diverse uses including insecticides, fungicides and various fine chemicals. Their ideal synthesis is from pyridine plus methanol in the absence of solvent so that water is the only obvious by-product. Here, such a reaction is demonstrated, using for the first time ferrite catalysts. Particularly impressive is the selectivity observed for 2-alkylation so that *ca.* 80% selectivity to 2-picoline can be achieved. The effects of varying the Zn : Mn ratio in the catalyst have been studied in some detail. *JHC*

DOI: 10.1039/b207410a

Table 1 Acidity and surface area of ferrite catalysts

No	Catalyst	Acidity (NH_3 uptake/mmol g^{-1}) 423–523 K	523–623 K	623–723 K	Total	Surface area/m^2 g^{-1}
1	ZF	0.36	0.33	0.34	1.03	32.21
2	ZMF-1	0.38	0.32	0.36	1.06	32.96
3	ZMF-2	0.40	0.28	0.41	1.09	39.72
4	ZMF-3	0.41	0.34	0.40	1.15	42.45
5	MF	0.43	0.37	0.42	1.22	43.27

Table 2 Performance of various catalysts in the alkylation of pyridine. Methanol/pyridine molar ratio = 5, temperature = 673 K, WHSV = 0.2 h^{-1}

Catalyst	Pyridine conversion (%)	Product distribution (%) Pyridine	2-Picoline	3-Picoline
ZF	24.0	76.0	22.7	1.3
ZMF-1	29.4	70.6	25.2	4.2
ZMF-2	36.8	63.2	29.6	7.3
ZMF-3	52.2	47.8	39.3	12.8
MF	85.1	14.9	67.7	17.5

temperature range 473–723 K and results are presented in Table 3. Negligible conversion was obtained below 473 K while conversion occurs effectively in the temperature range 673–698 K. Lower temperatures were favorable for 3-picoline formation. The best performance by the catalyst was shown at 673 K with conversion of 67.6 and 17.5% for 2-picoline and 3-picoline, respectively, and selectivity of 79.5 and 20.5% for 2-picoline and 3-picoline, respectively. At temperatures higher than 673 K, conversions decreased due to charring and deposition of carbon on the catalyst surface.

Table 3 Effect of temperature on alkylation of pyridine. Methanol/pyridine molar ratio = 5, WHSV = 0.2 h^{-1}

Temperature/K	Pyridine conversion (%)	Product distribution (%) Pyridine	2-Picoline	3-Picoline	Others
473	2.0	98.0	Nil	Nil	2.0
573	41.8	58.2	16.2	20.5	5.2
673	85.2	14.8	67.6	17.5	Nil
723	51.2	43.8	45.9	5.3	Nil

2.3 Effect of methanol/pyridine molar ratios on alkylation of pyridine

The effect of methanol/pyridine molar ratios on alkylation of pyridine over MF catalyst at 673 K is represented graphically in (Fig. 1). With increase in methanol/pyridine molar ratio, conversion of pyridine increases, reaches a maximum and then decreases. While conversion to 2-picoline increases at lower molar ratio and ultimately became almost constant at higher molar ratio, conversion to 3-picoline decreased with increase in molar ratio. An almost linear increase in the conversion of pyridine at lower molar ratio, reaching a maximum and then decreasing at higher molar ratio suggests a Langmuir–Hinselwood type of bimolecular reaction. A maximum yield of 67.6 and 17.5%, respectively, for 2-picoline and 3-picoline was obtained at a methanol/pyridine molar ratio of 5. The selectivity for 2-picoline and 3-picoline was 79.5 and 20.5%, respectively, at this molar ratio of 5.

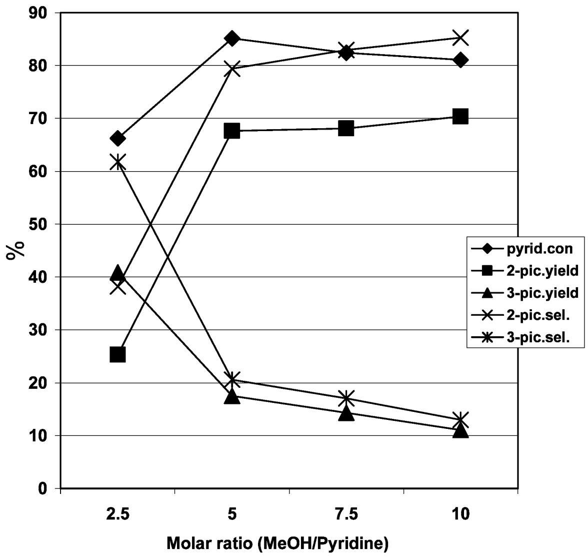

Fig. 1 Effect of molar ratio of methanol to pyridine on conversion, selectivity and yield over $MnFe_2O_4$ catalyst. WHSV = 0.2 h^{-1}; reaction temperature = 673 K.

2.4 Effect of weight hour space velocity on alkylation of pyridine

The effect of weight hour space velocity on alkylation of pyridine over MF catalyst at 673 K and constant methanol/pyridine molar ratio, was investigated in the weight hour space velocity range 0.1–0.8 h^{-1} and results are represented graphically in (Fig. 2). Conversion of pyridine and the yield of 2-picoline first increased and reached a maximum at WHSV = 0.2 h^{-1} and thereafter decreased, perhaps due to decrease in contact time.

2.5 Mechanism

On passing vapour of methanol alone over the catalyst at a temperature of 673 K, we obtained formaldehyde. Passing 2-picoline over the catalyst at this temperature did not produce 3-picoline which rules out the formation of 3-picoline due to isomerization of 2-picoline over this catalyst. Conversion to 2-picoline increased with increasing methanol/pyridine molar ratio and temperature. It seems initially that methanol is dehydrogenated over the acidic solid surface to formaldehyde. Pyridine abstracts the hydrogen atoms produced due to dehydrogenation of methanol and is converted to dihydropyridine. Formaldehyde attacks dihydropyridine at the 3-position as an electrophile leading to 3-picoline (Scheme 1(a)). Mixing formaldehyde with methanol in the feed suppressed formation

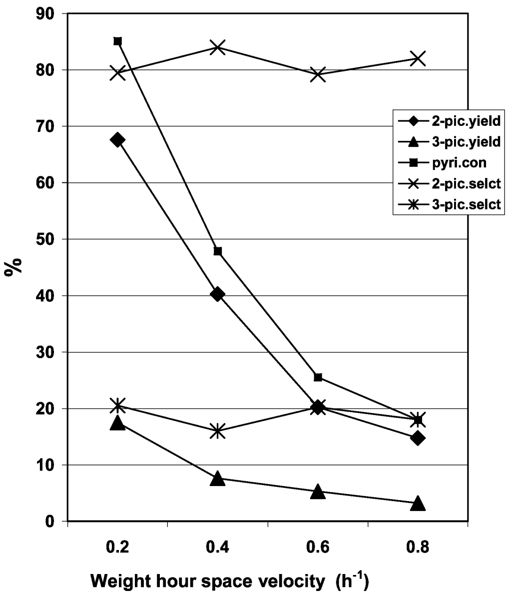

Fig. 2 Effect of weight hour space velocity on alkylation of pyridine over $MnFe_2O_4$ catalyst. Reaction temperature = 673 K; molar ratio of methanol to pyridine = 5.

of picolines appreciably. This rules out direct reaction of formaldehyde with pyridine. When pyridine and formaldehyde (in equimolar ratio) were passed over the bed along with hydrogen gas, all of the formaldehyde was converted to 3-picoline. This experiment further confirmed formation of dihydropyridine as the intermediate. Passing hydrogen peroxide with the feed also suppressed the formation of picolines, which rules out the possibility of formation of free radicals. Direct attack of formaldehyde at the 2-position is not possible due to the electron deficient nature of ring and formation of 2-picoline seems to proceed through interaction of formaldehyde with the lone pair of electrons of the nitrogen of the pyridine ring producing the *N*-methylpyridinium ion, which above 573 K rearranges to 2-picoline (Scheme 1(b)). Higher availability of HCHO molecules with increasing methanol/pyridine molar ratio and temperature supports this mechanism. The mechanism is represented in Scheme 1(a) and (b).

2.6 Conclusions

1. $Zn_{1-x}Mn_xFe_2O_4$ (x = 0, 0.25, 0.50, 0.75 and 1) ferrite spinal systems were studied for alkylation of pyridine using methanol as the alkylating agent. It was found that these systems can effectively alkylate pyridine to give 2-picoline selectively. 79.5% selectivity towards 2-picoline was obtained under optimized reaction conditions. Activity increases as the x value increases. Highest activity was observed for MF, whereas ZF was only mildly active. As x increases, the acidity and surface area of the systems also increases.
2. Substitution of Zn by Mn leads to higher acidity and surface area of the ferrite catalysts as is supported by the present surface area and ammonia desorption measurements. Similar trends have also been reported by others.[1–3]
3 A tentative mechanism for production of 2-picoline and 3-picoline, involving dihydropyridine as the intermediate has been proposed.

3. Experimental

3.1 Preparation of $ZnFe_2O_4$ (ZF)

A solution of 1.2 mol of NaOH in 150 cm^3 of H_2O was allowed to react with a solution of 0.075 mol of $ZnCl_2$ in 50 cm^3 of water. The resulting $Na[Zn(OH)_3]$ solution was added to a 5 dm^3 beaker containing 0.15 mol of $FeCl_3{\cdot}6H_2O$ in 2.5 dm^3 of 0.6 M HCl and stirrered for 2 h. The resulting mixture was further heated for 0.5 h at 333 K. The mixture was allowed to settle and reacted with 2 M NaOH until a permanent red phenolphthalein colour was obtained. The product was washed by repeated decantation with 2.5 dm^3 portions of water until the supernatant was free of Cl^- (about 15 washings were required), filtered through a sintered glass filter, dried in an oven at 393 K and calcined at 773 K for 5 h. Finally the product was sieved through a 6/10 mesh size.

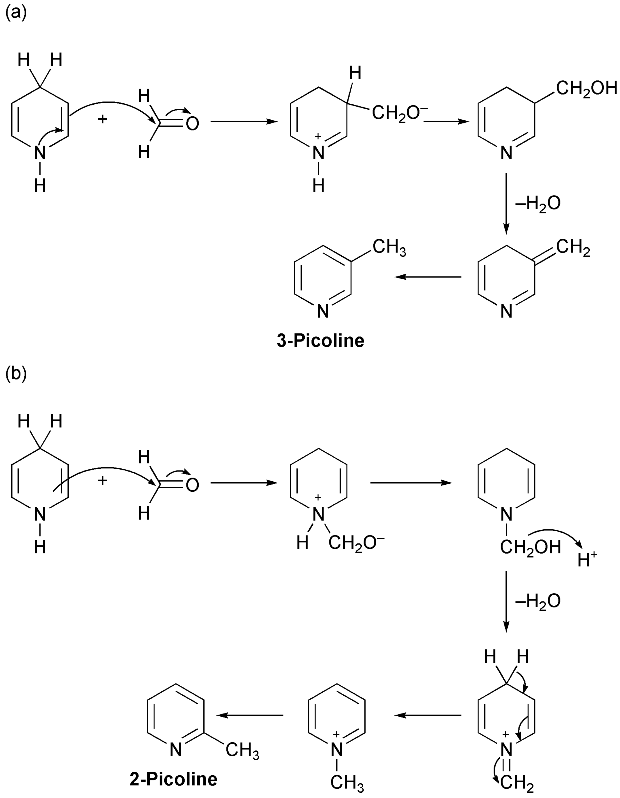

Scheme 1 Mechanism of alkylation of pyridine with methanol.

The preparation of $MnFe_2O_4$ (MF) was similar to that of $ZnFe_2O_4$ described above except that now 0.075 mol of $MnCl_2{\cdot}4H_2O$ were used in place of $ZnCl_2$. Similarly, $Zn_{0.75}Mn_{0.25}Fe_2O_4$ (ZMF-1), $Zn_{0.5}Mn_{0.5}Fe_2O_4$ (ZMF-2) and $Zn_{0.25}Mn_{0.75}Fe_2O_4$ (ZMF-3) were prepared by taking 0.0562, 0.0375 and 0.0187 mol of $ZnCl_2$ and 0.0187, 0.0375 and 0.0562 mol of Mn salt.

3.2 Catalyst characterization, surface area and acidity measurements

The XRD diffractogram of ZF, ZMF-2 and MF were recorded on a Rigaku diffractometer with Cu-Kα radiation and are reproduced in (Fig. 3). All peaks in the pattern match well with the characteristic reflections of corresponding ferrites reported (JCPDS 22-1012, 10-319) and confirm the phase purity of the samples. The FTIR spectra of these ferrite catalysts were recorded on a Perkin Elmer Series 1600 FTIR spectrometer and are reproduced in Fig. 4. Two broad bands appearing at 700 and 500 cm^{-1} can be assigned to metal–oxygen stretching frequencies. Since tetrahedral M–O bonds (T_d M–O) are associated with higher force constants and lower bond lengths,[13] this stretching frequency is expected to appear at higher frequency compared to the M–O stretching frequency of octahedral (O_h M–O) sites. In view of this, the band appearing at 700 cm^{-1} is assigned to the M–O stretching mode of the tetrahedral group and that at 500 cm^{-1} is assigned to the M–O stretching mode of the octahedral group.

Ammonia desorption experiments were carried out to measure the acidity of the catalyst using ammonia as an adsorbate. 5 g of catalyst was packed in a Pyrex tube down flow reactor and heated to 673 K under a nitrogen gas flow rate of 0.5 $cm^3\ s^{-1}$ for 3 h. The reactor was then cooled to 298 K and adsorption conducted at this temperature by exposing the sample to ammonia for 2 h. Physically adsorbed ammonia was removed by purging the sample with a nitrogen gas flow rate of 0.5 $cm^3\ s^{-1}$ at 353 K for 1 h. The acid strength distribution was obtained by raising the catalyst temperature from 353–773 K in a flow of nitrogen gas of 0.5 $cm^3\ s^{-1}$ and absorbing the ammonia evolved in double distilled water containing phenolphthalein as indicator. Quantitative estimation was made by titrating the water solution with standard 0.1 M HCl solution in different temperature ranges. The results are presented in Table 1. Surface area measurements were made using the BET method and results are shown in Table 1.

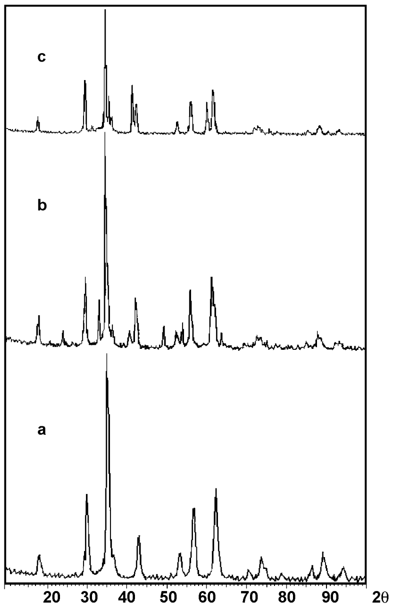

Fig. 3 XRD diffractogram of (a) ZF, (b) ZMF-2 and (c) MF.

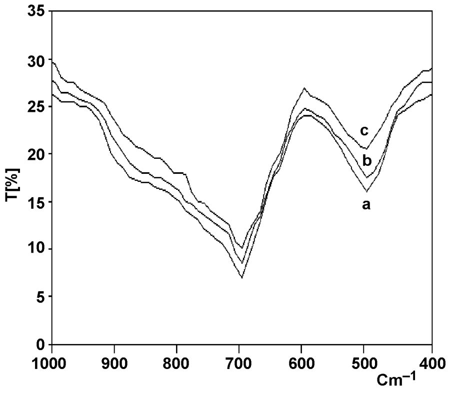

Fig. 4 IR spectra of (a) ZF, (b) ZMF-2 and (c) MF.

3.3 Apparatus and procedure

The reaction was carried out in a fixed bed down-flow Pyrex glass tubular reactor (0.45 m in length and 0.025 m i.d.) at atmospheric pressure. The upper half worked as the preheater and the lower half worked as the reactor, where the catalyst was packed between two plugs of Pyrex glass wool. The catalyst was activated at 773 K by passing of air and then brought down to the desired temperatures by cooling in a current of nitrogen. The mixture of pyridine and methanol was fed by a 10 cm^3 pressure-equalizing funnel. The liquid products were condensed with the help of a cold-water condenser and cold trap and were analyzed with a Shimadzu 14B Gas Chromatograph using SE-30 column and FID detector.

Acknowledgements

The authors wish to express their appreciation to Inter University Consortium, Devi Ahilya University, Indore for recording XRD spectra.

References

1 K. Sreekumar, T. Raja, B. P. Kiran, S. Sugunan and B. S. Rao, *Appl. Catal., A*, 1999, **182**, 327.
2 K. Sreekumar, T. M. Jyothi, T. Mathew, M. B. Talawar, S. Sugunan and B. S. Rao, *J. Mol. Catal.*, 2000, **159**, 327.
3 K. Sreekumar, T. Mathew, B. M. Devassy, R. Rajgopal, R. Vetrivel and B. S. Rao, *Appl. Catal., A*, 2001, **205**(1–2), 11.
4 J. P Jacobs, A. Maltha, J. C. H. Reintjes, J. Drimal, V. Ponec and H. H. Brogersma, *J. Catal.*, 1994, **147**, 194.
5 J. A. Toledo, M. A. Valenzuela, P. Bosch, H. Armendariz, A. Montoya, N. Nova and A. Vazquez, *Appl. Catal., A*, 2001, **218**(1–2), 39.
6 H. Kashiwagi, Y. Fujiki and S. Enomoto, *Chem. Pharm. Bull.*, 1982, **30**, 2575.
7 H. Kashiwagi and S. Enomoto, *Chem. Pharm. Bull*, 1982, **30**(2), 404.
8 C. D. Chang and P. D. Perkins, *US Pat.*, 4388461, 1983.
9 C. D. McAteer, C. D. Brown and R. D. Davis, *US Pat.*, 5780635, 1998.
10 C. D. Chang and W. H. Lang, *US Pat.*, 4220783, 1980.
11 C. D. Chang and P. D. Perkins, *US Pat.*, 4395554, 1983.
12 H. Beschke and H. Friedrich, *US Pat.*, 4149002, 1979.
13 B. P. Ladgaonkar, C. B. Kolekar and A. S. Vaingankar, *Bull. Mater. Sci.*, 2002, **25**(4), 351.

Silica modified sulfuric acid/NaNO$_2$ as a novel heterogeneous system for the oxidation of 1,4-dihydropyridines under mild conditions

Mohammad Ali Zolfigol,*[a] Farhad Shirini,[b] Arash Ghorbani Choghamarani[a] and Iraj Mohammadpoor-Baltork[c]

[a] *Chemistry Department, College of Science, Bu-Ali Sina University, Hamadan Zip Code 65174Post Box No. 4135, I. R. Iran. E-mail: Zolfi@basu.ac.ir; Fax: (+98) 81 8272404*
[b] *Chemistry Department, College of Science, Gilan University, Rasht, Iran*
[c] *Chemistry Department, College of Science, Isfahan University, Isfahan, I. R. Iran*

Received 27th August 2002
First published as an Advance Article on the web 8th October 2002

A combination of silica modified sulfuric acid and sodium nitrite in the presence of wet SiO$_2$ were used as an effective oxidizing agent for the oxidation of dihydropyridines to their corresponding pyridine derivatives under mild and heterogeneous conditions in moderate to excellent yields.

4-Substituted Hantzsch dihydropyridines (**1**) are analogues of NADH coenzymes and an important class of drugs.[1] For example, Amlodepine besylate, Nifedepine and related dihydropyridines are Ca^{2+} channel blockers, and are rapidly emerging as one of the most important classes of drugs for the treatment of cardiovascular diseases including hypertension. In the human body, it has been observed that these compounds undergo oxidation to form pyridine derivatives. These oxidized compounds are largely devoid of the pharmacological activity of the parent compounds. Additionally, dihydropyridines are often produced in a synthetic sequence, and have to be oxidized to pyridines.[2] Numerous reagents and procedures have been recommended for this purpose, such as ferric or cupric nitrates on a solid support (clayfen or claycop),[3] ceric ammonium nitrate,[4] clay-supported cupric nitrate accompanied by ultrasound promotion,[5] manganese dioxide or 2,3-dichloro-5,6-dicyano-1,4-benzoquinone (DDQ),[6] nitric oxide,[7] bismuth nitrate pentahydrate,[8] pyridinium chlorochromate (PCC),[9] tetrakis-(pyridine) cobalt(II) dichromate (TPCD),[10] nicotinium dichromate,[11] S-nitrosoglutathion,[12] N$_2$O$_4$ complex of 18-crown-6,[13] diphenylpicrylhydrazyl and benzoyl peroxide as free radical oxidizing agents,[14] KMnO$_4$,[15] CrO$_3$,[16] HNO$_3$,[17] HNO$_2$,[18] *tert*-butylhydroperoxide,[19] silica gel supported ferric nitrate (silfen),[20] N$_2$O$_3$,[21] photochemical oxidation,[22] inorganic acidic salts and sodium nitrite or nitrate.[23–26]

Recently, Ohsawa *et al.* reported an excellent procedure for this transformation. They have demonstrated the remarkably practical use of NO gas as a clean and efficient oxidant for this purpose.[2]

Although a variety of reagents are capable of effecting these oxidations,[1–26] this transformation is not so easy and is a tricky step because these compounds (they have different functional groups within the molecule) are very sensitive to the oxidizing agents and reaction conditions. Most of the reported reagents produce by-products which are difficult to remove from the desired products. Another major drawback to the older procedures is their use of reagents which are either highly toxic or present serious disposal problems (or both). For example, we know that the NO gas is corrosive and highly toxic and must be used under Ar atmosphere and in an effective fume-hood with caution.[2] Therefore, we decided to choose a new reagent or reagent systems to overcome the above limitations. In addition, for our purpose both clean and easy work-up were also important.

On the other hand, any reduction in the amount of sulfuric acid needed and/or any simplification in handling procedures is required for risk reduction, economic advantage and environment protection.[27] In addition, there is current research and general interest in heterogeneous systems because of the importance such systems have in industry and in developing technologies.[28] In continuation of our studies on the application of inorganic acidic salts[29] we found that silica gel reacts with chlorosulfonic acid to give silica modified sulfuric acid (**I**). It is interesting to note that the reaction is easy and clean without any work-up procedure because HCl gas is evolved from the reaction vessel immediately (Scheme 1).[30]

We hoped that the silica modified sulfuric acid (**I**) would be a superior proton source to all of the reported acidic solid supports or acidic resins such as polystyrene sulfonic acid and Nafion-H[31] for running reactions under heterogeneous conditions. Therefore, we were interested in using this inorganic acidic resin (**I**) as a new sulfuric acid function immobilized on

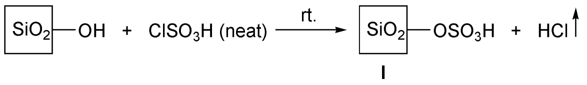

Scheme 1

Green Context

A very large number of methods have been reported for the important oxidation of 1,4-dihydropyridines. However, these are largely unacceptable in these environmentally-conscious days, since they involve toxic and/or hazardous reagent systems. In particular a reduction in the amount of acid used in such reactions would be welcome. Here a silica–sulfuric acid is used in combination with NaNO$_2$ to effect the oxidation under mild conditions. There are aspects of the reaction that could be further improved. (*e.g.* replacement of an halogenated solvent) but it already represents significant improvements. ***JHC***

DOI: 10.1039/b208328k

the surface of silica gel *via* covalent bonding for the *in-situ* generation of HNO_2 (as an efficient oxidizing agent) when used in conjunction with $NaNO_2$ and wet SiO_2. We report here a simple, cheap and chemoselective method for the effective oxidation of 1,4-dihydropyridines (**1**) to their corresponding pyridine derivatives (**2** or **3**) under mild and heterogeneous conditions *via in-situ* generation of NOCl (Table 1).

Different types of dihydropyridines (**1**) were subjected to the oxidation reaction in the presence of silica modified sulfuric acid (**I**), $NaNO_2$ (**II**) and wet SiO_2 (50% *w*/*w*) in dichloromethane (Table 1). The oxidation reactions were performed under mild and completely heterogeneous conditions at room temperature and take place with moderate to excellent yields (Table 2).

It was also observed that the oxidation of 1,4-dihydropyridines (entry 13) bearing an alkyl substituent (alkyl moieties may be responsible for generating stable carbocations) at the 4-position gives only the dealkylated pyridine derivative (**2**). This is in agreement with the observation made by others employing different oxidative conditions.[2,19,23–26] However,

Table 1 1,4-Dihydropyridines (**1**) and their corresponding pyridine derivatives (**2** or **3**)

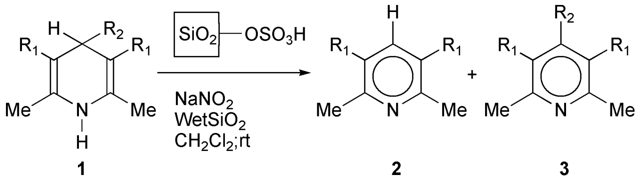

1, **2**, **3**	R_1	R_2	**1**, **2**, **3**	R_1	R_2
a	COOEt	H	**m**	COOEt	CH_3CHCH_3
b	COOEt	Me	**n**	COOEt	2-Py
c	COOEt	Et	**o**	COOEt	4-Py
d	COOEt	Ph	**p**	$COCH_3$	H
e	COOEt	2-Thienyl	**q**	$COCH_3$	Me
f	COOEt	$2-NO_2-C_6H_4-$	**r**	$COCH_3$	Ph
g	COOEt	$3-NO_2-C_6H_4-$	**s**	$COCH_3$	$4-CH_3O-C_6H_4-$
h	COOEt	$2-CH_3O-C_6H_4-$	**t**	$COCH_3$	$2-CH_3O-C_6H_4-$
i	COOEt	$2,5-(CH_3O)_2-C_6H_3-$	**u**	$COCH_3$	$2,5-(CH_3O)_2-C_6H_3-$
j	COOEt	$4-Br-C_6H_4-$	**v**	$COCH_3$	2-Thienyl
k	COOEt	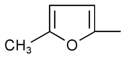 CH3 O	**w**	$COCH_3$	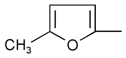 CH3 O
l	COOEt	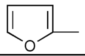 O	**x**	$COCH_3$	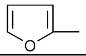 O

Table 2 Oxidation of 1,4-dihydropyridines (**1**) to their corresponding pyridine derivatives (**2** or **3**) with a combination of silica modified sulfuric acid (**I**), $NaNO_2$ (**II**) and wet SiO_2 (50% *w*/*w*) in dichloromethane at room temperature

			Reagent–substrate/mmol[a]			
Entry	Substrate	Product	**I**	**II**	Time/min	Yield (%)
1	**1a**	**2**	0.15	1.5	30	98
2	**1b**	**3b**[b]	0.3	3	30	97
3	**1c**	**3c**	0.3	3	30	96
4	**1d**	**3d**	0.412	4.125	15	93
5	**1e**	**3e**	0.45	4.5	20	98
6	**1f**	**3f**	0.55	5.5	25	93
7	**1g**	**3g**	0.55	5.5	25	92
8	**1h**	**3h**[b]	0.3	3	20	99
9	**1i**	**3i**[b]	0.225	2.25	15	98
10	**1j**	**3j**[b]	0.375	3.75	50	93
11	**1k**	**3k**[b]	0.45	4.5	35	98
12	**1l**	**3l**	0.45	4.5	20	98
13	**1m**	**2**[b]	0.2	2	20	97
14	**1n**	**3n**	0.8	8	120	95
15	**1o**	**3o**	0.8	8	165	94
16	**1p**	**3p**	0.15	1.5	40	90
17	**1q**	**3q**	0.35	3.5	30	97
18	**1r**	**3r**	0.412	4.125	45	90
19	**1s**	**3s**	0.3	3	15	90
20	**1t**	**3t**	0.3	3	15	91
21	**1u**	**3u**	0.3	3	15	92
22	**1v**	**3v**	0.45	4.5	15	90
23	**1w**	**3w**	0.45	4.5	30	91
24	**1x**	**3x**	0.45	4.5	15	92

[a] Wet SiO_2 : substrate (0.2 g : 1 mmol), **I** and **II** refer to mmol of the silica modified sulfuric acid and $NaNO_2$. [b] Selected MS data of some products are as follows: **3b**: Found (M^+) 279, Calc. (MW) 279, **3h**: Found (M^+) 357, Calc. (MW) 357, **3i**: Found (M^+) 388, Calc. (MW) 388, **3j**: Found (M^+) 406, Calc. (MW) 406, peak of M + 2 was also observed, **3k**: Found (M^+) 331, Calc. (MW) 331, the oxidation product of the substrate **1m** gives only **2**: Found (M^+) 265, Calc. (MW) 265.

aryl substituted 1,4-dihydropyridines (entries 4–12, 14, 15 and 18–24) furnished the corresponding pyridine derivatives (Table 2).

This present oxidation reaction can be readily carried out by placing silica modified sulfuric acid (**I**), $NaNO_2$ (**II**), 1,4-dihydropyridine (**1**), wet SiO_2 (50% *w*/*w*) and CH_2Cl_2 as the solvent in a reaction vessel and efficiently stirring the resulting heterogeneous mixture at room temperature. The pyridine derivatives (**2** or **3**) can be obtained simply by filtration and evaporation of the solvent. The results and reaction conditions are given in Table 2.

The oxidation reaction did not occur in the absence of wet SiO_2. This observation suggests that the water molecule is essential for such processes. The presence of wet SiO_2 thus provides an effective heterogeneous surface area for *in-situ* generation of HNO_2. It also eases the reaction work-up.

1,4-Dihydropyridines (entries 5, 8–9 and 19–22) bearing very electron rich aryl or thienyl substituents (these compounds are also very susceptible to electrophilic aromatic substitution) at the 4-position give only the corresponding pyridine derivative (**3**) confirming that these compounds have not been nitrosated or nitrated (or both) during the oxidation reaction. Therefore, this system behaves chemoselectively and NO^+ attacks only the nitrogen site of the secondary amines in 1,4-dihydropyridines.[24]

In conclusion, the cheapness and the availability of the reagents, easy and clean work-up, and high yields make this an attractive methodology. This simple procedure is highly selective and contamination by nitration side-products is avoided. We believe that the present methodology could be an important addition to existing methodologies.

Experimental

General

Chemicals were purchased from Fluka, Merck, Riedel-de Haen AG and Aldrich chemical companies. Yields refer to isolated products. Silica modified sulfuric acid was synthesised according to our previously reported prosedure.[30] The oxidation products were characterized by comparison of their spectral (IR, ^{1}H-NMR) data with the reported physical data in the literature. All Hantzsch 1,4-dihydropyridines were synthesized by the reported procedures.[18]

Oxidation of dihydropyridine (1h) to substituted pyridine (2h). A typical procedure

A suspension of compound **1h** (0.358 g, 1 mmol), silica modified sulfuric acid (0.3 g), wet SiO_2 (50% *w*/*w*, 0.2 g) and $NaNO_2$ (0.207 g, 3 mmol) in CH_2Cl_2 (6 mL) was stirred at room temperature for 20 min (the progress of the reaction was monitored by TLC) and then filtered. The residue was washed with CH_2Cl_2 (20 mL). Anhydrous Na_2SO_4 (5 g) was added to the filtrate and filtered after off 20 min. Dichloromethane was removed. The yield was 0.352 g, (99%) of crystalline pale yellow solid (**2h**), mp 56–58 °C [Lit.[22] mp 57–58 °C]. ^{1}H-NMR (FT-90 MHz, $CDCl_3$/TMS): δ_{ppm} 0.89 (t, 6H), 2.63 (s, 6H), 3.72 (s, 3H) 4.03 (q, 4H), 6.93–7.34 (m, 4H), Mass spectrum (M^+) Found 357, Calc. (MW) 357.

Acknowledgement

Financial support for this work by the research affair, Bu-Ali Sina University, Hamadan, Iran, is gratefully acknowledged.

References

1 D. Mauzeral and F. H. Westheimer, *J. Am. Chem. Soc.*, 1955, **77**, 2261.
2 T. Itoh, K. Nagata, Y. Matsuya, M. Miyazaki and A. Ohsawa, *J. Org. Chem.*, 1997, **62**, 3582.
3 M. Balogh, I. Hermecz, Z. Meszaros and P. Laszlo, *Helv. Chim. Acta*, 1984, **67**, 2270.
4 J. R. Pfister, *Synthesis*, 1990, 689.
5 A. Maquestiau, A. Mayence and J. J. V. Eynde, *Tetrahedron Lett.*, 1991, **32**, 3839.
6 J. J. V. Eynde, F. Delfosse, A. Mayence and Y. Van Haverbeke, *Tetrahedron*, 1995, **51**, 6511.
7 T. Itoh, K. Nagata, M. Okada and A. Ohsawa, *Tetrahedron Lett.*, 1995, **36**, 2269.
8 S. H. Mashraqui and M. A. Karnik, *Synthesis*, 1998, 713.
9 J. J. V. Eynde, A. Mayence and A. Maquestiau, *Tetrahedron*, 1992, **48**, 463.
10 B. Wang, Y. Hu and H. Hu, *Synth. Commun.*, 1999, **29**, 4193.
11 M. M. Sadeghi, I. Mohammadpoor-Baltork, H. R. Memarian and S. Sobhani, *Synth. Commun.*, 2000, **30**, 1661.
12 Y. Z. Mao, M. Z. Jin, Z. L. Liu and L. M. Wu, *Org. Lett.*, 2000, **2**, 741.
13 M. A. Zolfigol, M. H. Zebarjadian, M. M. Sadeghi, I. Mohammadpoor-Baltork, H. R. Memarian and M. Shamsipur, *Synth. Commun.*, 2001, **31**, 929.
14 M. M. Sadeghi, H. R. Memarian and A. R. Momeni, *J. Sci. Islamic Repub. Iran*, 2001, **12**, 141.
15 J. J. V. Eynde, R. D. Orazio and Y. Van Haverbeke, *Tetrahedron*, 1994, **50**, 2479.
16 E. Grinsteins, B. Stankevice and G. Duburs, *Kim. Geterotsikl. Soedin*, 1976, 1118.
17 (*a*) B. Loev, M. M. Goodman, K. M. Snader, R. Tedeschi and E. Macko, *J. Med. Chem.*, 1986, **29**, 1596; (*b*) O. Garcia and F. Delgado, *Tetrahedron Lett.*, 1993, **34**, 623.
18 (*a*) B. Loev and K. M. Snader, *J. Org. Chem.*, 1965, **30**, 1914; (*b*) E. H. Huntress and E. N. Shaw, *J. Org. Chem.*, 1948, **13**, 674.
19 S. P. Chavan, S. W. Dantale, U. R. Kalkote, V. S. Jyothirmai and R. K. Kharul, *Synth. Commun.*, 1998, **28**, 2789.
20 B. Khadikar and S. Borkat, *Synth. Commun.*, 1998, **28**, 207.
21 A. Hantzsch, *Annalen*, 1982, 215.
22 H. R. Memarian, M. M. Sadeghi and H. Aliyan, *Indian J. Chem.*, 1998, **37B**, 219.
23 M. A. Zolfigol, M. Kiany-Borazjani, M. M. Sadeghi, I. Mohammadpoor-Baltork and H. R. Memarian, *Synth. Commun.*, 2000, **30**, 551.
24 M. A. Zolfigol, M. Kiany-Borazjani, M. M. Sadeghi, H. R. Memarian and I. Mohammadpoor-Baltork, *J. Chem. Res. (S)*, 2000, 167.
25 M. A. Zolfigol, M. Kiany-Borazjani, M. M. Sadeghi, H. R. Memarian and I. Mohammadpoor-Baltork, *Synth. Commun.*, 2000, **30**, 2945.
26 M. A. Zolfigol, M. Kiany-Borazjani, M. M. Sadeghi, I. Mohammadpoor-Baltork and H. R. Memarian, *Synth. Commun.*, 2000, **30**, 3919.
27 J. M. Riego, Z. Sedin. J. M. Zaldivar. N. C. Marziano and C. Tortato, *Tetrahedron Lett.*, 1996, **37**, 513.
28 N. J. Turro, *Tetrahedron*, 1987, **43**, 1589.
29 (*a*) M. A. Zolfigol, M. Torabi and S. E. Mallakpour, *Tetrahedron*, 2001, **57**, 8381 and references cited therein (*b*) F. Shirini, M. A. Zolfigol, B. Mallakpour, S. E. Mallakpour, A. R. Hajipour and I. M. Baltork, *Tetrahedron Lett.*, 2002, **43**, 1555.
30 (*a*) M. A. Zolfigol, *Tetrahedron*, 2001, **57**, 9509; (*b*) M. A. Zolfigol and A. Bamoniri, *Synlett*, 2002, 1621.
31 G. A. Olah, R. Molhotra and S. C. Narang, *J. Org. Chem.*, 1978, **43**, 4628.

Design of a solid catalyst for the synthesis of a molecule with blossom orange scent

M. J. Climent, A. Velty and A. Corma*

Instituto de Tecnologia Quimica, UPV-CSIC, Universidad Politécnica de Valencia, Avenida de los Naranjos s/n, 46022 Valencia, Spain. E-mail: acorma@itq.upv.es

Received 31st July 2002
First published as an Advance Article on the web 7th October 2002

The synthesis of 2-methyl-2-naphthyl-4-methyl-1,3-dioxolane, a compound with blossom orange scent, has been successfully carried out by acetalization reaction between methyl naphthyl ketone and propylene glycol using different acid solid catalysts. The size and polarity of reactants, intermediates and product determine the strong influence of the textural properties of the catalyst (crystal size, acidity and adsorption properties) with the large pore tridirectional zeolites (Y and Beta) being the most active. It has been found that the hydrophobicity of the catalyst can be more determinant than the number of active sites present in the catalyst. The results show an optimum in activity for Si/Al ratios in Y and Beta zeolites that correspond to 35 and 100, respectively.

Introduction

The acetalization reaction is sometimes a necessary requirement to protect carbonyl groups in the presence of other functional groups during the manipulation of multifunctional organic molecules.[1] Acetals are generally stable to bases, Grignard reagents, hydrogenation reagents, metal hydrides, oxidants, bromination and esterefication reagents. Besides the interest of acetals as protecting groups, many of them have found direct applications as fragrances, in cosmetics, food and beverage additives, pharmaceuticals, in detergents and in lacquer industries.[2] Sometimes, several acetals named as ‘potential fragrances’ (which exhibit little or no odour) are introduced together into the different formulations and, at the contact with the skin the products are hydrolysed and the odorous molecules are released.[3]

It is known that the conversion of a carbonyl compound to an acetal, profoundly changes its vapour pressure, solubility, aroma characteristics and generally attenuates or alters its flavour impact. For example propylene glycol of vanillin is used as vanilla flavours because it causes flavour attenuation.[4]

The most general method for the synthesis of acetals is to react carbonyl compounds with an alcohol or an orthoester in the presence of acid catalysts. A number of acetalization procedures include the use of protic acids, Lewis acids (zinc chloride)[5] alumina,[6] montmorillonite,[7] zeolites[8] and mesoporous aluminosilicates.[9] Acetalization of aldehydes can be performed in the presence of weak acids, while ketones generally need stronger ones like sulfuric, hydrochloric or *p*-toluenesulfonic acid and larger amounts of catalyst than aldehydes. However, many of the methods mentioned above present limitations derived from the use of expensive reagents, tedious work-up procedure, and necessity of neutralisation of the strongly acidic media, with the production of undesired wastes. In this sense, synthetic zeolites appear as promising catalysts with the obvious advantages over conventional Brönsted or Lewis acids, such as easy separation from the reaction mixture, shape selectivity, reusability, and overall the possibility to control the population, strength and distribution of acid sites.

The propylene glycol acetal of methyl naphthyl ketone[3] is a flavouring material with blossom orange, which involves the acetalization of the methyl naphthyl ketone with propylene glycol. The commercial process is catalysed by strong acids such as *p*-toluenesulfonic acid.

In continuation of our ongoing efforts to develop environmental friendly active catalysts for the production of fine chemicals[8–10] we have studied the possibilities of zeolite catalysts for the formation of a cyclic acetal from an aromatic ketone that presents industrial interest and which is now produced by using liquid acid catalyst. Thus, we have carried out the synthesis of the propylene glycol acetal of methyl naphthyl ketone (**1**) with different zeolites. It will be shown that the process is diffusion controlled when working with large pore zeolites, and their activity can be increased by a factor of four by decreasing the crystallite size. It is interesting that for the reaction studied which involved products with different polarity, the adsorption properties, *i.e.*, the hydrophobicity properties of the catalyst becomes more determinant than the number of active sites. It will be shown that by tailoring the catalyst variable it is possible to obtain very highly active and selective solid catalyst for the synthesis of the Blossom orange fragrancy product.

Experimental

Catalysts

Beta-1 zeolite was supplied by PQ corporation, in the acidic form. Zeolite Beta samples (Beta-2, Beta-3, Beta-4 and Beta-5

Green Context

The synthesis of acetals is used widely in organic synthesis as a way of protecting carbonyl compounds. It is also of interest as a way of masking or modifying odours, and as such finds use in the flavour and fragrance sector. This paper discusses a solid acid-catalysed route to such a compound. It is shown to be possible to replace the homogeneous acid with a solid acid, and also, importantly, that the controlling factor for catalytic efficiency is not the acidity of the catalyst, but rather the adsorption/desorption characteristics of the system. *DJM*

DOI: 10.1039/b207506g

and Beta-6) were synthesised in our laboratory according to the procedure presented in ref. 11.

The acid form of Mordenite (MOR) was obtained by calcination, followed by an acid treatment to extract the portion of the extraframework Al of a commercial Conteka sample.

The USY samples were obtained from PQ Zeolites B.V., and they were NH_4^+ exchanged followed by calcination at 773 K during 3 h.

One sample of MCM-41 (pore diameter 3.5 nm and framework Si/Al = 50) was synthesised following the procedure given in ref. 12, using hexadecyltrimethylammonium (Aldrich) cation as template, and pseudobohemite (Capatal B, Vista) and Aerosil (Degussa) as the aluminium and silicon source, respectively. The sample was calcined in N_2 for 4 h and in air for 6 h at 813 K.

Acidity measurements were carried out by adsorption–desorption of pyridine monitored by IR spectroscopy. The infrared spectra were recorded on a Nicolet 710 FTIR using self-supported wafers of 10 mg cm^{-2}. The calcined samples were outgased overnight at 673 K and 10^{-3} Pa dynamic vacuum; then, pyridine was admitted into the cell at room temperature. After saturation, the samples were outgased at 523 K for 1 h under vacuum, cooled to room temperature and the spectra were recorded.

Methyl naphthyl ketone, propylene glycol and toluene (purity = 99%) were purchased from Aldrich and were used without further purification.

Reaction procedure

Activation of the catalyst (114 mg) was performed *in situ* by heating the solid under vacuum (1 Torr) for 2 h. After this time, the system was left at room temperature and then, a solution of methyl naphthyl ketone (8.8 mmol) propylene glycol (21 mmol) in toluene (40 ml) was poured onto the activated catalyst and a Dean–Stark instrument was adapted to remove the water formed. The resultant suspension was heated at 419 K in a silicone oil bath with an automatic temperature control system while magnetically stirring. Samples were taken at regular time periods and analysed by gas chromatography (GC). At the end of the reaction the catalyst was filtered off and washed with dichloromethane. The organic phase was washed with water in order to remove the excess of propylene glycol and dried over anhydrous sodium sulfate. The samples with solvent were previously distilled under reduced pressure. Finally, the product was characterised by ^1H NMR (400 MHz Varian VXR-400S). After reaction, the catalyst was submitted to continuous solid–liquid extractions with dichloromethane in a micro-Soxhlet extractor. After removal of the solvent the residue was also weighed and analysed by GC-MS and ^1H NMR spectroscopy. In all experiments the recovered material was $>95\%$ (wt/wt).

Results and discussion

Acetal formation is a reversible reaction which proceeds by a two-step mechanism. The first step (Scheme 1) is the formation of an hemiacetal, followed by the removal of a water molecule. Acetal or ketal formation is strongly affected by electronic and steric factors, but it is generally accepted that the rate-determining step of acetalization is the formation of a cation from the protonated hemiacetal. In order to compensate for the low rate of hemiacetal formation, the reaction media must be sufficiently acidic to promote effective protonation of any hemiacetal formed, and sufficiently polar to allow stabilisation of the cationic intermediate.

We have shown that zeolites are acidic enough to carry out selectively this type of reaction.[8] However, according to the reaction mechanism, acetalizations may involve relatively bulky intermediates, that can limit the activity and selectivity of zeolite molecular sieves. Here, we have studied the possibility of acid zeolites with different pore topologies and a mesoporous molecular sieve (MCM-41) for carrying out the synthesis of methyl naphthyl ketone propylene glycol acetal (2-methyl-2-naphthyl-4-methyl-1,3-dioxolane, **1**), a compound with blossom orange scent. In this case, the crystallite size, acidity and polarity of the catalyst should have an impact on the final results. In this way, the synthesis of **1** was carried out by reacting methyl naphthyl ketone with propylene glycol (Scheme 2) using as catalysts a series of molecular sieves with different pore topologies and dimensions: a 12 MR tridirectional zeolite with cavities (Y), a tridirectional 12 MR zeolites without cavities (Beta), a zeolite with 10 and 12 ring windows (SSZ-33), a 12 MR unidirectional zeolite (Mordenite) and a mesoporous material (MCM-41). In all cases only the corresponding 1,3-dioxolane was detected in the reaction mixture. Total conversion obtained on these catalysts after 3 h of reaction time are given in Table 1.

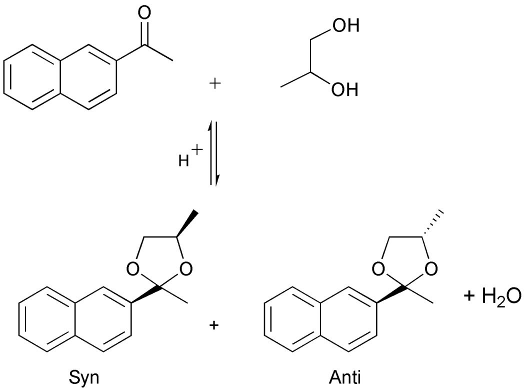

1

Scheme 2 Reaction scheme of the formation of 2-methyl-2-naphthyl-4-methyl-1,3-dioxolane, **1**.

Table 1 Results obtained in the acetalization of methyl naphthyl ketone and propylene glycol with different catalysts

Catalyst	Si/Al	Brönsted acidity[a] 523 K	623 K	Yield of **1**[b] (%)	r_0/n_B[c] (mmol h^{-1}/μmol Py)
USY-2	35	46	18	99[d]	0.62
Beta-4	50	19	8	92	0.35
MCM-41	50	2.4	1	48	0.73
SSZ-33	50	49	44	60	0.10
MOR	10	80	47	14	0.15

[a] μmol Py/g catalyst. [b] 3 h reaction time. [c] Initial rate per Bronsted acid site [d] 1 h reaction time. *Reaction conditions*: molar ratio methyl naphthyl ketone/propylene glycol = 1/2.4, 419 K, 7.4 wt/wt% catalyst relative to carbonyl compound, ratio toluene/carbonyl compound = 26.6.

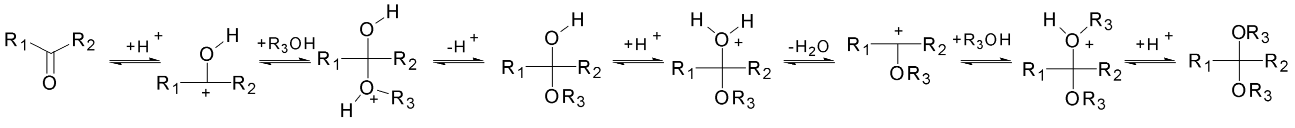

Scheme 1 General reaction mechanism for acetalization of aldehydes or ketones catalysed by acids.

It can be seen that USY-2 and Beta-4 zeolites present the best performance followed by SSZ-33, MCM-41 and finally MOR zeolite.

The very low activity of Mordenite is surprising despite its large pore diameter. This is probably due to diffusional limitations owing to the monodirectionality of the channels and the very strong acidity that interacts with reaction products and by-products of higher molecular weight that remain adsorbed and block the channels. The blocking occurs to a smaller degree in the case of the bidirectional SSZ-33 since reactants can diffuse not only through the 12 MR pores but they may also diffuse from one cavity (generated by the crossing of channels) to another through the 10 MR windows. Indeed when the acetalization reaction was carried out in the presence of SSZ-33, in spite of a strong deactivation being observed, this material gives higher conversion than Mordenite, achieving at 1 h of reaction time a maximum conversion of 60% which does not change with time (Fig. 1).

Taking into account the results obtained above one could expect that MCM-41, with a large accessible surface, would be an active catalyst for the synthesis of 2-methyl-2-naphthyl-4-methyl-1,3-dioxolane. However, the results (see Table 1) show a much lower performance for MCM-41 than for zeolites. The reason for this should be associated to the differences in the number and strength of the acid sites between mesoporous and microporous aluminosilicates. Indeed, the pyridine adsorption–desorption results show that when comparing with zeolite samples (Beta and SSZ-33) synthesised with the same Si/Al ratio, MCM-41 has lost a larger number of acid sites than zeolites during calcination. However if the initial rate of formation of 1,3-dioxolane per Brönsted acid site (measured by the pyridine remaining adsorbed at 523 K) is calculated, MCM-41 presents practically the same activity as USY zeolite (see Table 1).

The two tridirectional 12MR pore zeolites, *i.e.* USY and Beta samples, show high yield but if the activity per acid site is calculated, these two zeolites and specially the Beta zeolite gives a lower turnover frequency than USY, indicating that at least in this case there is still a limitation by diffusion. In order to see this and to improve the activity of Beta zeolite, the influence of the zeolite crystal size has been studied.

Influence of the crystal size

There are some precedents in the literature reporting that when bulky transition states and/or products with molecular dimensions close to the diameter of the pores of the zeolite are involved, the activity of the catalyst is controlled by diffusion. In our case, we thought that the lower activity of Beta with respect to the USY zeolite should be due to larger diffusional constraints for diffusion of 2-methyl-2-naphthyl-4-methyl-1,3-dioxolane, through the smaller pores of Beta zeolite. In a first step, molecular modelling calculations at a semi-empirical level[13] were performed and they showed that the smallest molecular axis of **1** is around 0.56 nm, which is close to the pore dimensions of Beta zeolite (0.75 × 0.57 and 0.65 × 0.56 nm). The experimental catalytic results obtained with zeolites of different crystallite size (Fig. 2) confirm that indeed the reaction is controlled by diffusion in the case of Beta zeolite. In fact in Fig. 2 one can see that when the average crystal size decreases from 0.33 to 0.02 μm, keeping constant the framework Si/Al ratio (≈13), the initial rate becomes four times higher. It appears then, that a Beta zeolite synthesised with a small enough crystallite size should be a very active and selective catalyst for carrying out the synthesis of 2-methyl-2-naphthyl-4-methyl-1,3-dioxolane.

Zeolite framework Si/Al ratio: the influence of hydrophobicity

The effect of the acidity on the acetalization reaction was examined by using samples of USY and Beta zeolites with different Si/Al ratios. It is known that for a given zeolite the concentration of Brönsted acid sites decreases when decreasing the Al content.[14] Taking this into account and the fact that acetalizations are not highly demanding reactions from the point of view of acid strength, we should expect a decrease of catalyst activity when the Si/Al ratio of the zeolite increases. However the results from Table 2 show that contrary to our expectations, a maximum in activity is found for a USY sample with Si/Al ratio of 35. Indeed, a maximum in activity when changing the framework Si/Al ratio is normally interpreted by assuming that the reaction requires strong acid sites. More specifically, in the case of USY zeolites, a maximum is found, for many acid catalysed reactions, in the range of Si/Al ratios between 8 and 12 for which maximum concentration of strong acid sites occurs. However, in our case, the maximum in activity is shifted towards a much higher framework Si/Al ratio and consequently an univocal correlation between activity and acidity can not be claimed. It should, however, be considered that the framework Si/Al ratio not only defines the number and strength of acid sites, but it also determines the adsorption–desorption properties of the zeolite. Zeolite adsorption can be of paramount

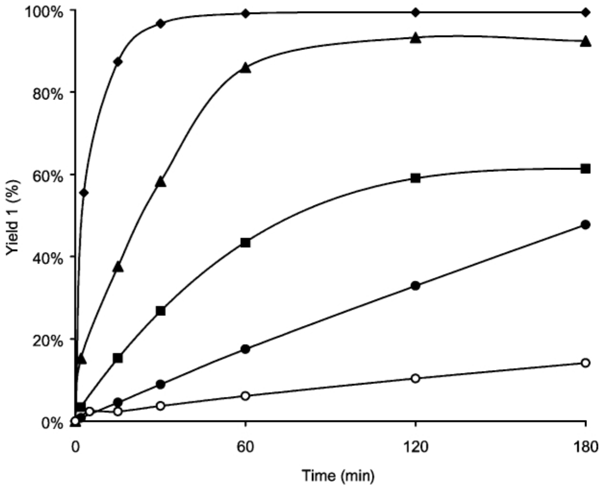

Fig. 1 Yield of methyl naphthyl ketone propylene glycol acetal **1** *vs.* the reaction time, when the acetalization reaction was carried out in the presence of: (◆) USY-2, (▲) Beta 4, (■) SSZ-33, (●) MCM-41 and (○) MOR.

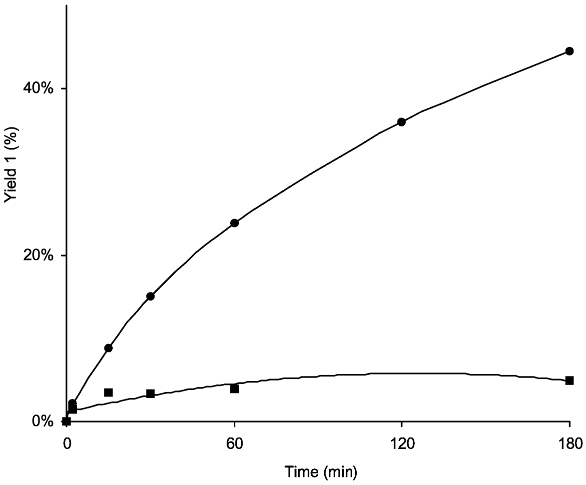

Fig. 2 Influence of the crystal size on the yield of methyl naphthyl ketone propylene glycol acetal in the presence of different Beta zeolites: (●) crystal size = 0.02 μm, and (■) crystal size = 0.33 μm.

Table 2 Results of acetalization between methyl naphthyl ketone and propylene glycol in the presence of USY and Beta samples with different Si/Al ratios

		Brönsted acidity[a]			Yield (%)	
Catalyst	Si/Al	523 K	623 K	r_0/mmol h^{-1}	0.5 h	3 h
USY-1	19	80	32	5.28	45	77
USY-2	35	46	18	30.62	97	99
USY-3	62	39	15	12.32	87	99
Beta-1	13	42	22	0.48	3	5
Beta-2	15	33	15	0.18	2	32
Beta-3	25	36	28	2.82	29	82
Beta-4	50	19	8	6.69	58	92
Beta-5	100	11	10	7.22	62	95
Beta-6	250	8	1	6.51	56	93
Silica-Beta	Pure Si	—	—	—	0	0

[a] μmol Py/g catalyst. *Reaction conditions*: molar ratio methyl naphthyl ketone/propylene glycol = 1/2.4, 419 K, 7.4 wt/wt% catalyst relative to carbonyl compound, ratio toluene/carbonyl compound = 26.6.

Table 3 Amount of water desorbed on Beta samples with different Si/Al ratios

Zeolite	Si/Al	Water desorption[a] (wt/wt%)
Beta-1	13	17.0
Beta-2	15	16.8
Beta-3	25	11.9
Beta-4	50	6.7
Beta-5	100	4.0
Beta-6	250	2.5

[a] Determined by thermogravimetric analysis (TG, Mettler Toledo Star[e] System).

importance for the synthesis of methyl naphthyl ketone propylene glycol acetal, since a highly hydrophilic reactant (propylene glycol) and a less hydrophilic reactant (methyl naphthyl ketone) have to diffuse through the pores and adsorb on the acid sites of the zeolite. Thus, in the case of hydrophilic zeolites (lower Si/Al ratio), the propylene glycol will be preferentially adsorbed and the reaction will become limited by diffusion and adsorption of methyl naphthyl ketone. In other words, it appears that, besides the concentration of the adequate Brönsted acid sites, the adsorption properties of the zeolite should play an important role in the catalyst activity.

Based on this, we decided to optimise the Beta zeolites from the point of view of the framework composition. To do this, a pure silica Beta and Beta samples with Si/Al ratios of 15, 25, 50, 100 and 250 were prepared in fluoride media. This synthesis procedure gives samples without internal defects (internal silanol groups) and consequently produces samples more hydrophobic than the conventional synthesis in OH$^-$ media, that results in samples with a large number of internal silanols. If the concentration of acid sites, *i.e.* the concentration of active sites was the main factor governing the activity of the catalyst, a maximum in activity should be found for a Beta zeolite with a Si/Al ratio of 10–15.[15] The results presented in Table 2, show however, that a maximum in activity is obtained at a Si/Al ratio of 100, that presents on the other hand a much lower concentration of acid sites than that of samples with lower Si/Al ratio (see Table 2). Therefore, adsorption effects should play an important role in this reaction, since both reactants present a different polarity. If this is so, then the hydrophobicity of the catalyst could be more determinant than the concentration of active sites. In order to check if there is a correlation between activity and hydrophobicity of the zeolite, the water adsorption–desorption of the different Beta samples was measured by thermogravimetric analysis. From the results given in Table 3 it can be seen that the water adsorption decreases when increasing the Si/Al ratio of the Beta catalyst, indicating that samples with lower Al content are more hydrophobic. Meanwhile the activity of the catalyst increases except for the last sample in where the concentration of active sites is sufficiently low to start to be the controlling factor. Therefore, we believe that zeolite catalyst adsorption properties, *i.e.* hydrophobicity, plays a determinant role during the synthesis of blossom orange scent.

Conclusions

For the synthesis of 2-methyl-2-naphthyl-4-methyl-1,3-dioxolane, a potential fragrance with blossom orange scent, we have found that tridirectional zeolites (Y and Beta) were the most active. The lower activity of Beta with respect to the Y zeolite could be due to diffusional constraints. In fact, the study of the influence of the crystal size of Beta zeolite on the catalytic activity showed that by decreasing this from 0.33 to 0.02 μm, the initial rate increased four times.

It has been found that a higher concentration of acid sites in the catalyst does not guarantee a better catalytic performance and the adsorption properties, such as hydrophobicity of the catalyst, can be more important than the number of the active sites.

The results showed an optimum in activity for samples with Si/Al ratios in Y and Beta zeolites that correspond to 35 and 100, respectively.

References

1 T. W. Green and P. G. M. Wuts, in *Protective Groups in Organic Synthesis*, Wiley, New York, 2nd edn., 1991, vol. 4, p. 212.

2 K. Bauer, D. Garbe and H. Surburg, *Common Fragrances and Flavors Materials*, VCH, New York, 2nd edn., 1990.

3 R. Suffis, L. B. Morton, K. Ishida, K. Sawano, A. G. Van Loveren, N. Tetsuo, C. B. Green, G. A. Reitz, R. K. L. Kang and T. Sato, *US Pat.*, 5626852, 1997.

4 G. A. Burdock, *Fenaroli's Hanbook of Flavor Ingredients*, CRC, New York, 1995, vol. II.

5 M. J. Ashton, C. Lawrence, J. A. Karlsson, K. A. J. Stuttle, C. G. Newton, B. Y. J. Vacher, S. Webber and M. J. Withnall, *J. Med. Chem.*, 1996, **39**, 4888.

6 V. Vu Thuy and P. Maitte, *Bull. Soc. Chim. Fr.*, 1975, **9**, 2558.

7 L. Tong-Shuang, L. Sheng-Hui, L. Ji-Tai and L. Hui-Zhang, *J. Chem. Res. (S)*, 1997, 26; M. Csiba, J. Cleophax, A. Loupy, J. Malthete and S. D. Gero, *Tetrahedron Lett.*, 1993, **34**, 1787.

8 A. Corma, M. J. Climent, H. García and J. Primo, *Appl. Catal.*, 1990, **59**, 333; R. Ballini, G. Bosica, B. Frullanti, R. Maggi, G. Sartori and F. Schroer, *Tetrahedron Lett.*, 1998, **39**, 1615; M. J. Climent, A. Corma, A. Velty and M. Susarte, *J. Catal.*, 2000, **196**, 345; A. Corma,

M. J. Climent, M. Susarte and A. Velty, *Spanish Pat.*, 9902439, 1999.

9 M. J. Climent, A. Corma, S. Iborra, M. C. Navarro and J. Primo, *J. Catal.*, 1996, **161**, 783; Y. Tanaka, N. Sawamura and M. Iwamoto, *Tetrahedron Lett.*, 1998, **39**, 9457.

10 M. J. Climent, A. Corma, A. Velty and M. Susarte, *J. Catal.*, 2000, **196**, 345; A. Corma, M. J. Climent, M. Susarte and A. Velty, *Spanish Pat.*, 9902439, 1999; I. Rodriguez, M. J. Climent, A. Corma, S. Iborra and V. Fornes, *J. Catal.*, 2000, **192**, 441.

11 M. A. Camblor, A. Corma, S. Iborra S. Miquel, J. Primo and S. Valencia, *J. Catal.*, 1997, **172**, 76.

12 J. S. Beck, C. Chu, J. D. Johnson, C. T. Kresge, M. E. Leonowicz, W. J. Roth and J. C. Vartulli, *World Pat.*, WO 9111390, 1992.

13 Molecular dimensions were calculated with a Cerius 2 Visualizer Program, Version 3.8, Molecular Simulations Inc. San Diego, CA, 1999.

14 A. Corma, *Chem. Rev.*, 1995, **95**, 559.

15 D. Barthomeuf, *Mater. Chem. Phys.*, 1987, **17**, 49.

Surfactant-free emulsion electrosynthesis *via* power ultrasound: electrocatalytic formation of carbon–carbon bonds

Trevor J. Davies,[a] Craig E. Banks,[a] Bharathi Nuthakki,[b] James F. Rusling,[b] Robert R. France,[c] Jay D. Wadhawan[a] and Richard G. Compton*[a]

[a] *Physical and Theoretical Chemistry Laboratory, Oxford University, South Parks Road, Oxford, UK OX1 3QZ. E-mail: compton@ermine.ox.ac.uk; Fax: +44 (0) 1865 275 410; Tel: +44 (0) 1865 275 413*
[b] *Department of Chemistry, Box U-60, University of Connecticut, Storrs, Connecticut 06269-3060, USA*
[c] *Dyson Perrins Laboratory, Oxford University, South Parks Road, Oxford, UK OX1 3QY*

Received 12th June 2002
First published as an Advance Article on the web 25th September 2002

Proof-of-concept of the mediated electrosynthesis of carbon–carbon bonds in totally 'green' surfactant-free emulsion media generated by application of power ultrasound to a biphasic water–organic mixture is illustrated by reference to three systems, some requiring further activation by light, and each catalysed by vitamin B_{12}. The voltammetry of aqueous vitamin B_{12} solutions at an electrode modified with microdroplets of the organic reactant is employed to gain an insight into the electrocatalytic pathway and readily permits the identification of optimum reaction parameters, such as starting material ratios and wavelength of light. The latter are employed in proof-of-concept emulsion electrosynthesis under conditions of triple activation (electron transfer, ultrasound and light).

1. Introduction

Over the last decade, the environment has become a major focus for electrochemists offering 'green' and socially responsible solutions in a plethora of areas notably the clean and efficient production of fine chemicals required for modern society with a minimisation or elimination of the resulting industrial waste.[1,2] Electrosynthetic processes conducted in emulsion media as opposed to conventional non-aqueous solvents are thus attractive, since the formation of an oil-in-water emulsion in which the reactant is solubilised, provides a significant 'greening' of an otherwise potentially environmentally unfriendly synthetic route; conventional non-aqueous solvents are problematic since they can be immiscible with water and can yield poisons on degradation. Furthermore, since the major component of the emulsion is water, the electrochemical reaction benefits from this near-ideal reaction environment; water has both a high conductivity and polarity. Additionally, product isolation by extraction or filtration is straight-forward.[1]

Following earlier work by Eberson and Helgee,[3–7] Rusling *et al.* have pioneered the use of microemulsions as viable and 'green' media in which to conduct electrosynthetic processes for the last fifteen years,[8–14] as they are less toxic and less expensive replacements for organic solvents. Product yield and selectivity in these optically clear and stable microheterogeneous mixtures of surfactants, oils and water has been shown to be, *inter alia*, a function of the type of emulsion used; bicontinuous microemulsions, in which both the oil and water phases are continuous, with surfactant residing at the extended oil–water interfaces, have been shown to be superior in terms of selectivity and reaction efficiency compared with continuous oil-in-water microemulsions (where the oil droplets are typically between 0.01 and 0.1 μm in diameter). By the early 1990s, efficient dehalogenation of toxic organics such as PCBs and DDT was shown, and has subsequently been extended to other organic pollutants.[8,9] Mediated electrosynthesis, in which electrons are delivered from the electrode to reactants by employing a chemical mediator, in emulsion media is additionally attractive as the exact composition of the emulsion can influence the reaction pathway.[9] For carbon–carbon bond formation with alkyl bromides (RX) as reactants, vitamin B_{12} has proved to be useful as a chemical mediator,[15,16] in which a Co(III) species is ligated to a tetraazamacrocyclic (corrin) ring.[15–17] For organic synthesis, the seemingly 'special' ability of vitamin B_{12} and its derivatives to form alkyl–cobalt bonds, together with the ease of their homolysis, producing alkyl radicals, has lead to their use as 'radical-in-a-bottle' reagents, with applications in the synthesis of, *inter alia*, prostaglandins, pheromones, and chiral alcohols.[15,18–22] The mediated electrosynthetic pathway involves the electrochemical generation of a 'supernucleophile' intermediate, which in the case of vitamin B_{12}, Co(III)L, is the Co(I)L complex:[9–13,15–17]

Green Context

Electrosynthesis has considerable potential for greener organic chemistry including the manufacture of speciality chemicals. Electrosynthetic processes conducted in emulsion media where the major component is water are particularly attractive. Here we see described the extension of this approach through the use of an acoustically-emulsified biphasic system. The total absence of surfactants further adds to its green credentials. This preliminary study suggests that the surfactant-free electrocatalytic synthesis of carbon–carbon bonds can be achieved in yields of at least 50%. This is believed to be the first paper dealing with electrosynthesis under triple activation conditions (light, ultrasound and electron-transfer) nicely illustrating how the combination of cleaner technologies is often required to achieve the greenest chemistry. *JHC*

DOI: 10.1039/b205706a

$$\mathrm{Co(III)L} + e^- \rightleftharpoons \mathrm{Co(II)L},\ \mathrm{Co(II)L} + e^- \rightleftharpoons \mathrm{Co(I)L},\ \text{or}\ \mathrm{Co(III)L} + 2e^- \rightleftharpoons \mathrm{Co(I)L} \qquad \text{(A)}$$

$$\mathrm{RX} + \mathrm{Co(I)L} \xrightarrow{k} \mathrm{R - Co(III)L} + \mathrm{X}^- \qquad \text{(B)}$$

$$\mathrm{R{-}Co(III)L} + (\mathrm{H}^+,e^-)\ \text{or}\ (\mathrm{H}^\cdot) + \mathrm{CH_2{=}CHZ} \rightarrow \mathrm{R{-}CH_2CH_2Z} + \mathrm{Co(II)L} \qquad \text{(C)}$$

where Z is an electron-withdrawing group located α to the carbon–carbon double bond.

The above pathway is catalytic since Co(II)L, where L is the macrocyclic ligand, is regenerated. It is believed that the rate determining step is the attack by Co(I)L on the alkyl halide.[13,23,24] The resulting carbon–cobalt bond can be cleaved by visible light, electrolysis, or by reducing agents to give carbon-centred radicals that can add onto activated carbon–carbon double bonds.[25]

Since the late 1990s some of us have pioneered the development of 'clean' and novel strategies for biphasic electrosynthesis, employing emulsions generated by the application of power ultrasound to a mixture of an aqueous electrolyte and an oily, water-insoluble, depolariser.[26–31] The work has been recently reviewed.[32] In these arrangements, cavitational processes induced by the rarefractive component of the longitudinal acoustic wave at the liquid/liquid interface, together with the directed turbulent flow of material in the bulk mixture imposed by the sound field, results in the formation of an *intra muros* emulsion *via* the continuing dispersion of droplets of one phase into the other.[26,32] The type and degree of emulsion produced, oil-in-water or *vice versa*, depends upon a range of parameters such as the ultrasonic power and chemical composition of the system.[26] Banks *et al.*[33,34] have previously shown that for typical volume ratios of oil and aqueous phases used in our work (up to 50 vol% heptane and 0.1 M aqueous perchloric acid and ultrasound (20 kHz, *ca.* 300 W cm^{-2}), the droplets are monodisperse, with average diameter of 3 μm and standard deviation of 1.8 μm;[33,34] other work employing different phases has shown that sub-micron particle sizes are achievable.[32] The emulsions produced in this manner are metastable; although ultrasonic irradiation provides a shear stress great enough to overcome the interfacial energy of the suspended microdroplets, removal of the acoustic field (by, for example, switching off the ultrasound transducer), permits the facile separation of the two phases, since an excess of the surface energy at the oil/water interface exists, and the interfacial area is greater in the emulsion than in the separated, biphasic system. For electrosynthetic purposes, there are numerous advantages by employing *in situ* sono-emulsions. First, the acoustic streaming process ensures that the rate of mass transport to the electrode is fast, reducing potentiostatic electrolysis times. Second, the separation of products from starting materials is easy, since the removal of the ultrasonic source causes the emulsion mixture to phase separate; the organic phase likely contains the products of the electrosynthetic transformation, which can then be extracted and analysed by conventional techniques. Furthermore, we have observed that the use of an emulsion generated *via* application of power ultrasound to a liquid carboxylic acid/aqueous alkaline mixture permitted Kolbe electrosynthesis with a novel reaction pathway by virtue of encapsulation of the reaction intermediates and/or products in the oil phase, leading to an enhanced selectivity of the desired product.[30,31] Third, the sono-emulsion process has been shown to produce a layer of organic material at the electrode surface.[26,30–32] In the case of electrocatalysis in emulsions formed using surfactants, it has been shown that both the surfactant and the catalyst can be co-adsorbed onto the electrode surface, thereby providing enhanced catalytic rates.[35] Fourth and most significantly, ultrasound energy may be used *in lieu* of surfactants to decrease the interfacial energy of the two phases to form the emulsion. It is this advantage that we wish to exploit in the 'proof-of-concept' work presented in this paper; electrosynthesis in acoustically emulsified media is inherently 'green'. Using surfactants to form emulsions may be avoided in situations where catalysts and reactants are stable in the presence of the ultrasound energy.

In this paper, we aim to illustrate how mediated electrosynthetic processes pioneered by Rusling *et al.*[9–11] in surfactant-based emulsion media can be achieved using an acoustically-emulsified biphasic system in the total absence of surfactants. We begin by exploring the voltammetry of vitamin B_{12} (cyanocobalamine) in sono-emulsion media, before examining mediated electrosynthetic processes under both dark and light-irradiated conditions. In particular, we show that the simultaneous employment of light and ultrasonic irradiation can be mimicked *via* the immobilisation of the oil phase onto an electrode which is then immersed into the aqueous phase and studied using conventional voltammetric methods.[36] This model is the exact inverse of that pioneered by Rusling using a derivatised vitamin B_{12} scaffold.[37]

2. Experimental

2:1 Chemical reagents

Chemical reagents used were KBr (Fisons UK), vitamin B_{12} (98% Lancaster), 1-bromobutane (Aldrich), *trans*-1,2-dibromocyclohexane (Aldrich, 99%) and 2-cyclohexen-1-one (Aldrich). All these reagents were of the highest grade commercially available and were used without any further purification. 2-(4-Bromobutyl)cyclohexen-1-one was synthesised following a literature recipe,[25] as outlined in previous work.[25] The synthesised material was observed by gas chromatographic analysis of the analyte in ether to be of sufficient purity; the observed retention time was 2.261 min, compared with that expected, 2.317 min. All aqueous solutions and subsequent dilutions were prepared using deionised water from an Elgastat (USF, High Wycombe, Bucks., UK) grade water system with a resistivity of not less than 18 MΩ cm. Solutions were prepared by dissolving the appropriate analyte in pH 2 Britton–Robinson (BR) buffer (compromising equimolar amounts, 0.04 M, of acetic, phosphoric and boric acids adjusted to the required pH with NaOH), in pH 7 phosphate buffer solution containing 0.1 M KCl, or in 0.1 M EDTA at pH 9.3. Non-aqueous solutions were prepared using DMF (HPLC grade, Aldrich) with 0.1 M tetrabutylammonium perchlorate (TBAP, puriss grade, Fluka) as supporting electrolyte.

2.2 Instrumentation

Electrochemical experiments were undertaken using a commercially available three-electrode potentiostat (Autolab PGSTAT20, Eco Chemie, Utrecht, The Netherlands), with a potential program generated under computer-control. A bright platinum wire wound into a spiral provided the counter electrode, while a saturated calomel reference electrode (SCE, Radiometer, Copenhagen) was used the reference electrode. The working electrode employed depended on the type of experiment being conducted; for silent homogeneous experiments, a 3 mm diameter glassy carbon disc electrode was employed, sonovoltammetric experiments were conducted using a 5 mm diameter glassy carbon working electrode. For synthetic experiments, a 12 mm diameter glassy carbon disc (Goodfellow, Cambridge, UK) electrode was used in the dark, in conjunction with a cell described in earlier sono-emulsion electrosynthetic work.[31] The glassy carbon disc electrodes were polished using alumina lapping compounds (British Drug House) of decreasing size (10 μm to 0.25 μm) on soft lapping pads immediately prior to experimentation. For synthetic experiments undertaken under triple activation by electricity, light and sound irradiation, the cell employed was modified based on a previous cell design,[38] and is illustrated in Fig. 1. In this case, the working electrode comprised a reticulated glassy carbon electrode (The Electrosynthesis Co., Inc., Lancaster NY, USA, generously provided by Dr F. Marken, Loughborough University), with surface area of 22.3 cm^2 (measured electrochemically). The reference electrode was placed in a side arm, but still in electrical contact with the solution. In all experiments, the solutions were thermostated *via* a steel cooling coil at 22 ± 2 °C. Post-electrosynthetic work-up typically involved extracting the organic phase with 2×10 mL ethyl acetate, followed by evaporation of the solvent on a rotary-evaporator, and product analysis *via* ^{1}H NMR (both one-dimensional and COSY) on a 400 MHz Varian spectrometer, and IR spectroscopy.

Ultrasound was introduced into the system using a 20 kHz ultrasound horn transducer system (VCX400 Sonics & Materials Inc, Danbury, CT, USA) fitted with a stepped 3 mm diameter titanium-alloy microtip. In all cases, the ultrasonic horn was located directly opposite the working electrode; the end of the microtip was positioned 8 ± 1 mm away from the electrode. The ultrasonic power was determined calorimetrically[39] to be 310 W cm^{-2} for an amplitude of '15%'. For irradiation of the emulsion with UV–visible light, a Wotan XBO 900 W/2 xenon arc lamp was used in conjunction with a Jarrell-Ash 82-410 grating monochromator (maximum incident power 2.0 mW cm^{-2}), to select the wavelength of the incident irradiation.

Immobilisation of microdroplets of an oil phase (*trans*-1,2-dibromocyclohexane, or a mixture of 1-bromobutane and 2-cyclohexen-1-one, or 2-(4-bromobutyl)cyclohexen-1-one) on to a basal plane pyrolytic graphite (bppg, Le Carbone, Ltd., Sussex, UK) electrode was achieved by solvent evaporation of an aliquot of 1 mM oil/acetonitrile stock solution. The electrode was thoroughly cleaned by rinsing with acetonitrile or acetone, and the surface renewed by polishing on carborundum paper (P1000 grade, medium grit size 18.3 μm, Acton and Borman, Stevenage, UK) immediately prior to experimentation. The bppg electrode employed for dark experiments was 4.9 mm in diameter, whereas that employed for interrogation under conditions of light irradiation was a 3×3 mm square electrode constructed in a PTFE channel flow cell, onto which a silica plate was cemented to as to permit irradiation of the electrode.

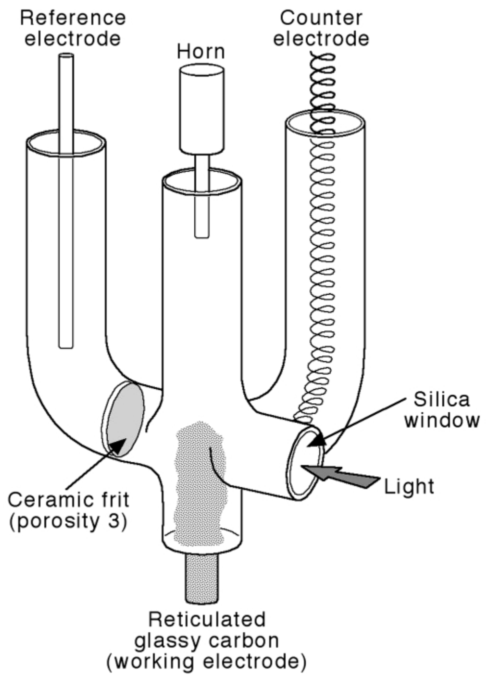

Fig. 1 Schematic illustration of the cell used for photosonoelectrosynthetic experiments.

The flow cell was connected to a gravity-fed flow system containing the aqueous electrolyte, so as to minimise any thermal effects due to light absorption. This particular system has been described previously by Marken and co-workers.[40]

In all experiments, solutions were thoroughly purged with oxygen-free nitrogen (BOC Gases, Guildford, Surrey, UK), so as to remove any oxygen from the solutions. Oxygen is known to interact with Co(II) and Co(I) species.[41,42]

3. Results and discussion

We first examine the effect of ultrasound on the electrochemical reduction of vitamin B_{12} in buffered, homogeneous aqueous solutions, prior to studying electrocatalysis in acoustically emulsified media.

3.1 Voltammetry of vitamin B_{12} in homogeneous aqueous solution

3.1.1 Quiescent voltammetry. Fig. 2 depicts a voltammogram corresponding to the electrochemical reduction of a 0.56 mM solution of vitamin B_{12} (cyanocobalamine) in a 0.1 M aqueous solution of EDTA at pH 9.3 at a 3 mm diameter glassy carbon electrode at a scan rate of 20 mV s^{-1}. The shape of the voltammogram is consistent with that reported elsewhere.[15,42–47] In the first scan, a single reductive wave is observed at a peak potential, $E_p^{Red} = -0.92$ V *vs.* SCE. This is a quasi-reversible (*vide infra*) two-electron reduction of vitamin B_{12}, with the oxidation state of the central cobalt species going from +3 to +1. Out of the three possible oxidation states of vitamin B_{12}, the Co species is hexa-coordinate in the +3 oxidation state, penta-coordinate in the +2 state, and tetra-coordinate when in the +1 oxidation state.[15,43] In the two-electron reduction of cyanocobalamine, the two, weaker axial coordinate bonds have to be broken (see Scheme 1). The two-electron reduction takes place since the strong axial coordination of Co(III) by CN$^-$ renders the transfer of a single electron slow, as CN$^-$ is a poor leaving group;[15,43] the reduction potential is thus shifted in a region where the Co(II)L species is itself reduced to Co(I)L.[43] Upon reversal of the potential sweep direction, three anodic waves are seen with $E_p^{Ox} = -0.85$, -0.39 and -0.06 V *vs.* SCE. The first re-oxidation at -0.85 V *vs* SCE, corresponds to re-oxidation of Co(I)L to Co(II)L, and that at -0.06 V *vs.* SCE corresponds to the re-oxidation of Co(II)L to Co(III)L.[42] The wave at -0.39 V *vs.* SCE is non-diffusional in shape, and its magnitude was observed to be linearly dependent on scan rate, suggesting that it is due to the re-oxidation of surface-bound (adsorbed) Co(II)L to Co(III)L. On the second reductive sweep, a new wave is observed in the

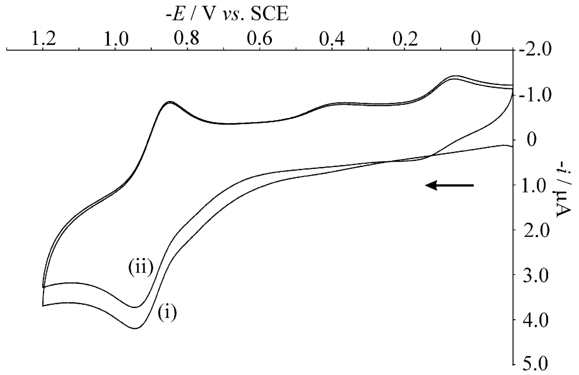

Fig. 2 Cyclic voltammogram (scan rate 20 mV s^{-1}) for the reduction of 0.56 mM vitamin B_{12} in 0.1 M aqueous EDTA solution at pH 9.3, at a 3 mm diameter glassy carbon electrode; (i) scan 1 and (ii) scan 2.

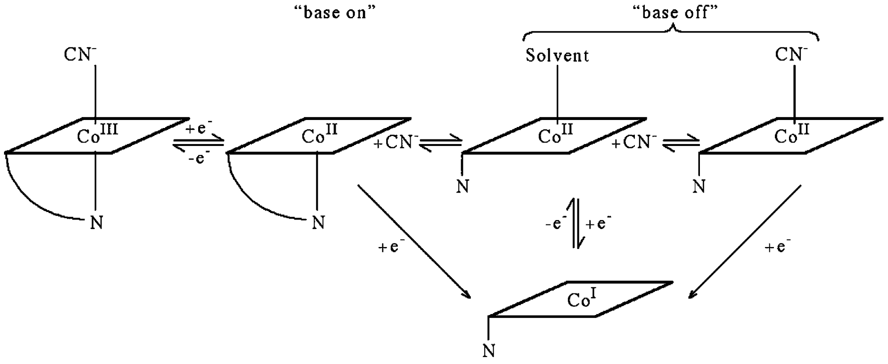

Scheme 1 (After references 17 and 43.)

region around −0.17 V *vs.* SCE, due to the reduction of Co(III)L to Co(II)L.[41] The reduction wave around −0.92 V *vs.* SCE observed in the first reductive scan is again observed, albeit with a reduced magnitude.

The voltammetry of cyanocobalamine at a glassy carbon electrode in DMF solutions containing 0.1 M TBAP as supporting electrolyte gave qualitatively similar results to those reported above and by Savéant and co-workers for DMSO solutions.[15,43]

The Co(II)L species that is electrochemically generated can exist in either the 'base on' or 'base off' forms (see Scheme 1), in which the latter have a protonated benzimidazole species. In aqueous media with pH below 2.9,[13] the 'base-off' form of Co(II)L predominates. Savéant[15] and Rusling[43] have both reported that electron transfer from an electrode to the 'base off' form is significantly faster than that to the 'base on' form. It is for this reason that subsequent experiments reported here were undertaken in aqueous media at pH 2.0.

3.1.2 Voltammetry of cyanocobalamine in the presence of power ultrasound. Fig. 3 illustrates the effect of insonation with simultaneous electrochemical reduction of a 0.85 mM solution of cyanocobalamine in 0.1 M aqueous KBr at pH 2.0 at a 5.0 mm diameter glassy carbon electrode. The 20 kHz power ultrasound was provided *via* an immersion horn located 8 ± 1 mm opposite the glassy carbon cathode. As has been reported earlier,[48] the introduction of ultrasound to homogeneous solution affects mass transport processes considerably,[49] due to macroscopic streaming[50] and due to microscopic interfacial cavitation events.[51] The augmentation in the mass transport regime can be regarded as a 'thinning' of the size of the diffusion layer;[52] resulting in sigmoidal voltammograms due to steady-state currents.[47] The observed limiting current may be described in terms of the average diffusion layer thickness, δ, which can be parameterised using a Nernstian model:[53]

$$i_{\text{lim}} = \frac{nFADc_{\text{bulk}}}{\delta} \tag{1}$$

In this expression, i_{lim} denotes the mass transport controlled limiting current, n, the number of electrons transferred per reacting molecule, F, A, D are the Faraday constant (96485 C mol^{-1}), the electrode area, and the diffusion coefficient of cyancobalamine respectively, and c_{bulk} denotes the the concentration of the redox reagent in the bulk solution. Based on the voltammograms shown in Fig. 3, and the diffusion coefficient of cyanocobalamine in aqueous perchloric acid solutions[13] 1.4 $\times$ 10^{-6} cm^2 s^{-1}, an average diffusion layer thickness of δ = 1.2 ± 0.2 μm is determined for conditions of 8 mm horn-to-electrode separation and 210 W cm^{-2} ultrasound intensity.

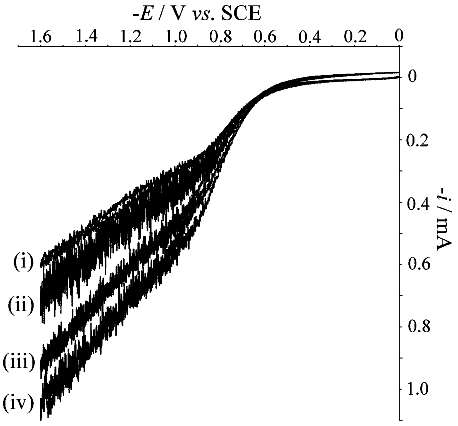

Fig. 3 Sonovoltammograms for the reduction of 0.85 mM aqueous vitamin B_{12} in 0.1 M KBr at pH 2.0, scan rate 50 mV s^{-1} at a 5.0 mm glassy carbon working electrode. Ultrasound intensities: (i) 105, (ii) 155, (iii) 210 and (iv) 250 W cm^{-2}.

3.2 Voltammetry of vitamin B_{12} in a sono-emulsified biphasic system

3.2.1 Effect of an inert organic phase. In previous work[26,34] we have examined the effect of adding an organic phase (up to as much as 50 vol%) to an aqueous solution. In the presence of 20 kHz ultrasound at intensities of *ca.* 300 W cm^{-2}, these two phases emulsify.[26–34] The nature of the emulsion is dependent on the relative amounts of aqueous and organic phases; at low ratios of organic : water phases, an oil-in-water emulsion is produced with relatively high conductivty.[31] In contrast, when the ratio of organic : aqueous phases increased above a threshold, the emulsion switches to a non-conducting water-in-oil emulsion.[26] Although in some systems,[26,31] the presence of an organic phase (up to as much as 40 vol%) has been shown to have little effect on the limiting current of an aqueous based electroactive species, suggesting that there is still sufficient electrode surface accessible for the redox process to proceed concomitant with no significant change in the magnitude of the mass transport towards the electrode, work on other systems has shown this not always to be the case:[34] there was a slight augmentation of the limiting current of the aqueous redox couple compared with that observed in a purely homogeneous system. These recently reported results suggest that the microdroplets of the electrochemically-inactive oil phase formed *via* the acoustic emulsification process penetrate into the thin diffusion layer at the electrode leading to an average thinning of the diffusion layer. Fig. 4 reveals that when 10 vol% heptane is emulsified with a 0.91 mM aqueous solution of cyanocobalamine at pH 2.0, whilst maintaining a constant total volume of solution, there is an augmentation in the limiting current due to the reduction of Co(III)L to Co(I)L. Further, as the amount of added heptane increases in the range 0–20 vol% heptane, the limiting current increases with added heptane, consistent with the above results, and with the formation of an oil-in-water sono-emulsion up to 20 vol% heptane.

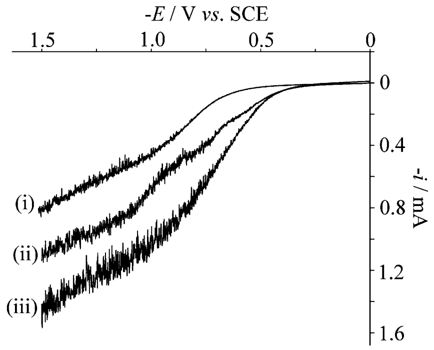

Fig. 4 Sonovoltammograms for the reduction of 0.91 mM vitamin B_{12} in 0.1 M aqueous KBr at pH 2.0, at a 5.0 mm glassy carbon working electrode (scan rate 50 mV s^{-1}), with (i) 0, (ii) 10 and (iii) 20 vol% heptane. In each case, the ultrasound intensity was 210 W cm^{-2}.

3.2.2 Effect of a reactive organic phase. The electrochemical reduction of vitamin B_{12} yields a nucleophilic moiety, Co(I)L. This species can react with bromoalkanes,[13,25] as outlined in the Introducton. Vicinal dibromides, in particular, *trans*-1,2-dibromocyclohexane (DBCH), react directly with Co(I)L in an inner-sphere electron transfer process between Co(I)L and the bromoalkane *via* a radical mechanism or by a concerted pathway,[11] to afford the corresponding alkene (such as cyclohexene) in high yield in surfactant-based emulsion media.[25] A plausible mechanism for this reaction is outlined in Scheme 2. Accordingly, increasing amounts of DBCH (in the range 3–13 vol%) were co-emulsified with an aqueous 0.91 mM cyanocobalamine solution at pH 2.0, at a constant total mixture volume. Due to the greater density of DBCH in comparison with water, the employment of ultrasound alone was not sufficient to initiate emulsification; successful emulsification was achieved by bubbling impurity-free nitrogen at a reasonably high rate close to the electrode under conditions of insonation. Once the small quantity of DBCH was successfully emulsified, ultrasound alone was required to maintain the emulsion. Fig. 5 illustrates a typical sono-voltammogram at a 5.0 mm diameter glassy carbon electrode in this medium. It can be seen that in contrast to Fig. 4, there is a very large increase in the electrochemical reduction process, consistent with a catalytic effect.[13,25] Furthermore, this signal increases both with time between successive scans, and with increasing the quantity of DBCH co-emulsified in the solution. In order to determine whether the reaction product was cyclohexene, constant potential electrosynthesis was undertaken in this medium using a 12 mm diameter glassy carbon disc electrode. After the passage of 2.5 F mol^{-1} of DBCH, the electrosynthesis was stopped, and the reaction mixture worked up and analysed *via* ^1H NMR and IR spectroscopies. The presence of cyclohexene was confirmed from an IR band at 1641.9 cm^{-1} (attributed to a C=C stretch), and further seen in the ^1H NMR spectra, from which an un-optimised reaction yield of 45 ± 4% was estimated.

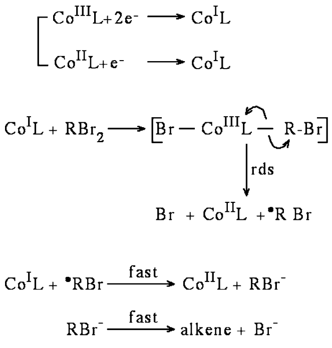

Scheme 2 (After reference 25.)

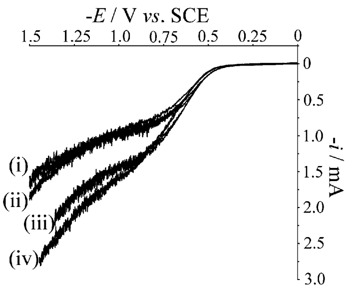

Fig. 5 Sonovoltammograms for the reduction of 0.91 mM vitamin B_{12} in aqueous 0.1 M KBr at pH 2.0 at a 5.0 mM glassy carbon electrode (scan rate 50 mV s^{-1}, ultrasound intensity 210 W cm^{-2}). The aqueous solution was co-emulsified with (i) 3, (ii) 6, (iii) 10 and (iv) 13 vol% *trans*-1,2-dibromohexane (DBCH).

The fact that only cyclohexene is produced in this reaction is consistent with the conventional pathway in surfactant-based emulsion media.[25]

3.3 Model for the electrocatalysis in biphasic media

Although the electrosynthesis of cyclohexene above takes place rapidly and easily, the same is not true for other reactions that require either further electrochemical activation or photolysis of the carbon–Co(III)L bond that is formed during the addition of Co(I)L to the alkyl bromide.[25] In order to establish reasonable conditions for sono-biphasic electrosysnthesis, we need to be able to mimic the system. Rusling and co-workers[37] have examined the voltammetry of vitamin B_{12} derivatives immobilised on the surface of an electrode in aqueous and microemulsion media. These modified electrodes appear to be amenable for electrosynthetic purposes in surfactant-based microemulsions.[37] Our previous work on emulsion electrosynthesis[26–31] has suggested that under insonation, since the oil microdroplets penetrate into the diffusion layer at the electrode, thereby acting as a local source of the depolariser, we may model these systems using microdroplets of the oil immobilised on an electrode surface and immersed into aqueous electrolyte.[36,40] In other work, we have seen that upon immobilisation of an electroactive oil as microdroplets, electrochemical processes may take place at the three phase boundary of electrode|oil|aqueous electrolyte.[40,54] Accordingly, microdroplets of DBCH were immobilised onto the surface of a basal plane pyrolytic graphite (bppg) electrode. This surface has been seen to be sufficiently rough so as to allow microdroplet formation;[54] highly polished surfaces tend to encourage the formation of large, globular deposits.[36] Fig. 6(a) depicts the current/voltage characteristics of an electrode modified with 8.3 nmol DBCH and immersed into a 9.6 mM aqueous solution of cyanocobalamine at pH 7.0. Whilst the voltammogram for the electrochemical reduction of cyanocobalamine at a naked bppg electrode (4.9 mm diameter) is qualitatively similar to those observed at a glassy carbon electrode, the presence of a small quantity of DBCH increases the magnitude of the reductive signals, as anticipated for a catalytic process. In contrast, modification of the electrode surface with microdroplets of an inert liquid dodecane *decreased* the size of the electrochemical reduction signal (not shown), due to the blocking of the overall electrode area. Increasing the amount of DBCH immobilised on the electrode surface first caused the electrochemical signal to increase, which then started to decrease (see Fig. 6(b)). The presence of this maximum in the electrochemical reduction occurs due to less available naked electrode area available for the voltammetric reduction process. These processes are schematically illustrated in Fig. 7. The presence of DBCH at the electrode modifies the voltammetric reduction of cyanocobalamine in two further ways. First, there is a signal around −0.5 V *vs.* SCE in the first reductive scan. This effect is likely due to the

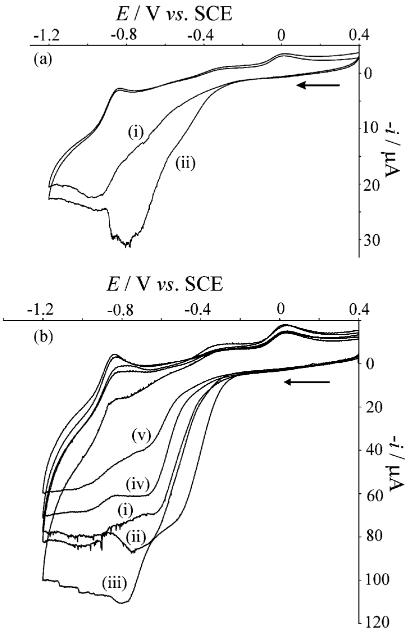

Fig. 6 (a) Cyclic voltammograms (scan rate 10 mV s^{-1}) for the reduction of 0.96 mM vitamin B_{12} in 0.1 M aqueous KBr (pH 2.0) at a 4.9 mm basal plane pyrolytic graphite electrode modified with (i) 0 and (ii) 8.3 nmol *trans*-1,2-dibromocyclohexane. (b) Cyclic voltammograms (scan rate 100 mV s^{-1}) for the reduction of 0.96 mM vitamin B_{12} in 0.1 M aqueous KBr (pH 2.0) at a 4.9 mm basal plane pyrolytic graphite electrode modified with (i) 3.3, (ii) 8.3, (iii) 16.5, (iv) 33.1 and (v) 66.1 nmol *trans*-1,2-dibromocyclohexane.

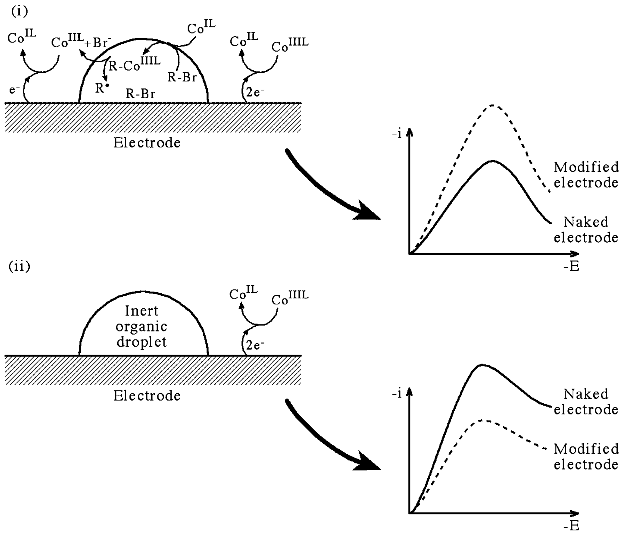

Fig. 7 Schematic diagram illustrating the catalytic (i) and the blocking (ii) responses of electrodes modified with organic, electrochemically-inactive microdroplets. For simplicity, a single microdroplet is shown.

electrocatalytic reduction of oxygen dissolved in the DBCH deposit by the Co(II)L species formed near the surface.[42] This effect was successfully minimised on outgassing the modified electrode prior to immersing in the aqueous electrolyte. The second new feature to the voltammetry is that there is a large amount of noise in the reduction signal. This might be attributed to surface tension effects at the oil microdroplet/aqueous electrolyte interface.[54]

Having established a voltammetric basis for the electrosynthetic process, *via* a 'reaction-on-a-drop' approach, we next use this approach to explore more complex photoelectrosynthetic processes in emulsions generated *in situ* using power ultrasound.

3.4 Biphasic photoelectrochemistry

The use of vitamin B_{12} and its derivatives for the formation of carbon–carbon bonds is of great synthetic use (*vide supra*).[9–11,15,16] In the simplest case, Rusling and co-workers[25] have shown that the radical produced from the reaction between an alkyl halide with vitamin B_{12} in the presence of light with wavelength above 480 nm[24] can react with an activated olefin. This process is illustrated in Scheme 3, and has been shown to work for both inter and intra-molecular systems.[25,55] Reduction of cyanocobalamine at the electrode surface yields Co(I)L which then oxidatively adds to the C–Br bond producing RCo(III)L. Photoactivated [RCo(III)L]*, going through a transition state [R··Co(II)L] leads to an alkyl radical (or alkene if Co(II)L leaves as a hydrido complex). The alkyl radical can rapidly add onto an activated alkene to form a new electrophilic radical. The latter can abstract a hydrogen atom from a component in the medium to yield the final product.[25] In particular, the ability to electrochemically and selectively synthesise *trans*-1-decalone in high yield from 2-(4-bromobutyl)-2-cyclohexen-1-one,[56] and to permit the synthesis of a fused five-membered ring from 2-3-bromopropyl)-2-cyclohexen-1-one,[55] under mild conditions, illustrates the scope of the previous work. The last reaction involves a 5-*endo-trig* cyclisation, a process that is generally considered unfavourable.

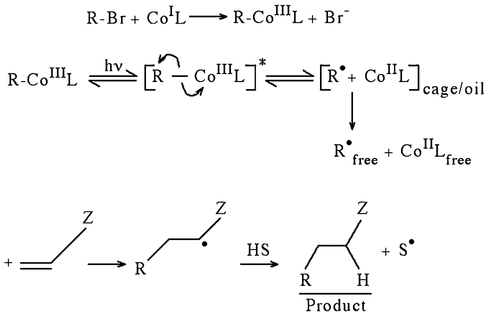

Scheme 3 (After reference 25.)

In this section we consider both types of synthetic process: the reaction between 1-bromobutane and 2-cyclohexen-1-one to afford 3-butyl-2-cyclohexen-1-one in a process that has been shown is mediated by vitamin B_{12},[25] and of the Baldwin-favoured intramolecular synthesis of 1-decalone from 2-(4-bromobutyl)-2-cyclohexen-1-one.[56] Both these mediated electrosyntheses have been shown to require activation by light.† In order to establish good reaction conditions (such as approximate quantity of oil required, and optimum wavelength required to cleave the carbon–cobalt bond) for the biphasic sonophotoelectrosynthesis, it was decided to first examine the photoelectrochemistry of the process in which the oil phase was immobilised on the electrode surface in the form of microdroplets (*vide supra*).

3.4.1 Photoelectrochemistry at immobilised microdroplets. In a previous paper,[40] microdroplets of a water-insoluble electroactive oil were immobilised on a bppg electrode, which was then placed into a channel flow cell constructed especially for this purpose. Solution was flowed over the surface of the electrode, and provided the flow rate was sufficiently slow (*ca.* 10^{-2} cm^3 s^{-1} or less), the oil droplets remained immobilised on the electrode surface. The silica cover plate of the flow cell was transparent, permitting the irradiation of the modified electrode with light of a wavelength selected using a monochromator.

---

† It has been shown that further electrochemical reduction can be employed to break the carbon–cobalt bond;[25] however, in this paper we wish to show that our approach can be useful under a variety of conditions.

First, a mixture of 1-bromobutane (BB) and 2-cyclohexen-1-one (CHO) was immobilised in this manner, and placed into the gravity-fed channel flow cell apparatus, into which a 0.45 mM aqueous solution of cyanocobalamine at pH 2.0 was flowed. The electrode potential was fixed at −0.87 V *vs.* SCE, to effect the two-electron transport-limited reduction of cyanocobalamine. The electrode was then irradiated with a beam of light of variable wavelengths, which was 'chopped' by the repeated insertion of a metal plate at intervals of 40 s. Reductive photocurrents were observed, due to a successful carbon–cobalt bond-cleavage, producing Co(II)L close to the electrode that is immediately reduced at the electrode surface. This chopping procedure permits a simple and effective way of alternating light and dark conditions at the electrode surface. The action spectrum of photocurrent versus wavelength for a ratio of BB : CHO of 1 : 40 (for a surface coverage of 200.5 nmol CHO) showed greatest photocurrents when the illumination wavelength was 470 or 630 nm, suggesting that at these wavelengths the fastest cleavage of the carbon–cobalt occurs. Increasing the BB : CHO molar ratio gave similar increases in photocurrent; decreasing the ratio, caused little or no photocurrents to be observed. This is consistent with the work undertaken by Rusling and co-workers in a bicontinuous microemulsion.[25]

The same experiment was repeated with microdroplets of 2-(4-bromobutyl)cyclohexen-1-one (BCHO) immobilised on the bppg electrode, and irradiated with light of a variable wavelength. Reductive photocurrents were again observed (not shown), with 450 and 650 nm wavelengths corresponding to maximum photocurrents.

These experiments employing a simplified 'mimic' not only show that the mediated electrosynthesis is possible, but also provide key information regarding the optimum irradiation wavelength and ratio of starting materials for which to undertake electrosynthesis.

3.4.2 Mediated photoelectrosynthesis in an acoustically-emulsified medium. Using the above results, the cyanocobalamine-mediated photoelectrochemical reaction between BB and CHO was scaled up, by undertaking photo-sonoelectrosynthesis with 0.5 mol vitamin B_{12} at pH 2.0 buffer solution in the cell illustrated in Fig. 1 at a wavelength of 630 nm, for ratios of BB : CHO of 1 : 40, 1 : 80 and 1 : 120, with, 2.0 F mol^{-1} of cycanocobalamine passed in each case. Analysis of the product by ^{1}H NMR showed that the major component was unreacted CHO, which is anticipated from the high ratio of CHO : BB. The IR analysis however, gave C=O absorption peaks at 1668.6 cm^{-1} (for pure CHO), and split peaks at 1668 and 1666 cm^{-1} for the 1 : 40, 1 : 80 and 1 : 120 ratios, with a 'bigger' split with increasing CHO : BB ratio. The peak around 1666 cm^{-1} can be attributed to an alkyl group in the 3-position, suggesting that the reaction in this medium proceeds.[25]

In the case of the scale up of the mediated intramolecular BCHO reaction, as only 60 mg of the BCHO precursor were synthesised, the reaction was undertaken in a biphasic sono-emulsion in which the BCHO starting material was dissolved in ethyl acetate ([BCHO] = 2.6 mM), using 0.51 mM vitamin B_{12} in pH 2.0 buffer solution. After the passage of 2.5 F mol^{-1} of vitamin B_{12}, the electrochemistry, ultrasound and light were switched off, and the products of the reaction analysed *via* ^{1}H NMR and IR spectroscopy. No C=C bond vibrations were observed in the IR spectrum, suggesting that the reaction went to completion. Further, the ^{1}H NMR spectrum gave results consistent with the formation of a decalone.[25]

4. Conclusions

In this paper, proof-of-concept has been demonstrated for mediated electrosynthesis in emulsion media in the total absence of surfactants. Although information regarding the reaction yield and selectivity would be desirable, the unoptimised results nevertheless indicate that reaction can occur in the biphasic sono-emulsion media with at least 50% reaction yield. To our best knowledge, this is the first paper dealing with electrosynthesis under *triple* activation (light, ultrasound and electron-transfer),[38] and we have illustrated a guide for reaction processes in acoustically-emulsified media *via* immobilisation of the organic component as microdroplets on the electrode surface.

5. Acknowledgements

We thank the EPSRC (C. E. B., R. R. F. and J. D. W.), and NSF, Grant No. CTS-9982854 (J. F. R. and B. N.) for financial support. We further thank Dr Frank Marken for providing the samples of reticulated glassy carbon used in this work.

References

1 *Electrochemistry in Colloids and Dispersions*, ed. R. A. Mackay and J. Texter, VCH, Weinheim, 1992.
2 H. Feess and H. Wendt, in *Techniques of Electro-organic Synthesis*, ed. N. L. Weinberg and B. V. Tilak, Wiley, New York, 1982, Part III, p. 81 ff.
3 L. Eberson and B. Helgee, *Acta Chem. Scand., Ser. B*, 1978, **32**, 313.
4 L. Eberson and B. Helgee, *Acta Chem. Scand., Ser. B*, 1978, **32**, 157.
5 L. Eberson and B. Helgee, *Acta Chem. Scand. Ser. B*, 1977, **31**, 813.
6 L. Eberson and B. Helgee, *Acta Chem. Scand., Ser. B*, 1975, **29**, 451.
7 L. Eberson and B. Helgee, *Chem. Scr.*, 1974, **5**, 47.
8 S. Schweizer, J. F. Rusling and Q. Huang, *Chemosphere*, 1994, **28**, 961.
9 See for example J. F. Rusling, *Pure Appl. Chem.*, 2001, **73**, 1895, and references therein.
10 J. F. Rusling and D.-L. Zhou, *J. Electroanal. Chem.*, 1997, **439**, 89.
11 J. F. Rusling, in *Electroanalytical Chemistry*, ed. A. J. Bard, Marcel Dekker, New York, **vol. 19**, 1994, p. 1 ff.
12 J. F. Rusling, T. F. Connors and A. Owlia, *Anal. Chem.*, 1987, **59**, 2123.
13 T. F. Connors, J. V. Arena and J. F. Rusling, *J. Phys. Chem.*, 1988, **92**, 2810.
14 J. F. Rusling in *Reactions and Synthesis in Surfactant Systems*, ed. J. Texter, Marcel Dekker, New York, 2001, p. 323 ff.
15 G. Pattenden, *Chem. Soc. Rev.*, 1988, **17**, 361.
16 G. N. Schrauzer, *Angew. Chem., Int. Ed. Engl.*, 1976, **15**, 417.
17 D. Lexa and J.-M. Savéant, *Acc. Chem. Res.*, 1983, **16**, 235.
18 R. Scheffold in *Modern Synthetic Methods*, ed. R. Scheffold, Wiley, New York, 1983, **vol. 3**, p. 355 ff.
19 R. Scheffold, S. Abrecht, R. Orlinski, H.-R. Ruf, P. Stamouli, O. Tinembart, L. Walder and C. Weymouth, *Pure Appl. Chem.*, 1987, **59**, 363.
20 R. Scheffold, *Chimia*, 1985, **39**, 203.
21 S. Torii, *Synthesis*, 1986, 873.
22 R. Scheffold, in *Electro-organic Synthesis*, ed. R. D. Little and N. L. Weinberg, Marcel Dekker, New York, 1991, p. 317 ff.
23 D.-L. Zhou, J. Gao and J. F. Rusling, *J. Am. Chem. Soc.*, 1995, **117**, 1127.
24 D.-L. Zhou, H. Carrero and J. F. Rusling, *Langmuir*, 1996, **12**, 3067.
25 J. Gao, J. F. Rusling and D.-L. Zhou, *J. Org. Chem.*, 1996, **61**, 5972.
26 See for example F. Marken and R. G. Compton, *Electrochim. Acta*, 1998, **43**, 2157, and references therein.
27 F. Marken, R. G. Compton, S. D. Bull and S. G. Davies, *Chem. Commun.*, 1997, 995.
28 R. P. Akkermans, S. L Roberts and R. G. Compton, *Chem. Commun.*, 1999, 1115.
29 R. P. Akkermans, S. L. Roberts, F. Marken, B. A. Coles, S. J. Wilkins, J. A. Cooper, K. E. Woodhouse and R. G. Compton, *J. Phys. Chem.*, 1999, **103**, 9987.

30 J. D. Wadhawan, F. Marken, R. G. Compton, S. D. Bull and S. G. Davies, *Chem. Commun.*, 2001, 87.
31 J. D. Wadhawan, F. J. Del Campo, R. G. Compton, J. S. Foord, F. Marken, S. D. Bull, S. G. Davies, D. J. Walton and S. Ryley, *J. Electroanal. Chem.*, 2001, **507**, 135.
32 J. D. Wadhawan, F. Marken and R. G. Compton, *Pure Appl. Chem.*, 2001, **73**, 1947.
33 C. E. Banks, N. V. Rees and R. G. Compton, *J. Phys. Chem. B*, 2002, **106**, 5810.
34 C. E. Banks, N. V. Rees and R. G. Compton, *J. Electroanal. Chem.*, in press.
35 G. N. Kamau, N. Hu and J. F. Rusling, *Langmuir*, 1992, **8**, 1042.
36 F. Marken, R. D. Webster, S. D. Bull and S. G. Davies, *J. Electroanal. Chem.*, 1997, **437**, 209.
37 See, for example: D.-L. Zhou, C. K. Njue and J. F. Rusling, *J .Am. Chem. Soc.*, 1999, **121**, 2909.
38 R. G. Compton, R. P. Akkermans, B. A. Coles and F. Marken, *Ultrason. Sonochem.*, 1997, **4**, 223.
39 M. A. Margulis and A. N. Mal'tsev, *Russ. J. Phys. Chem.*, 1969, **43**, 592.
40 J. D. Wadhawan, R. G. Compton, F. Marken, S. D. Bull and S. G. Davies, *J. Solid State Electrochem.*, 2001, **5**, 301.
41 G. Costa and C. Tavagnacco in *Molecular Electrochemistry of Inorganic, Bioinorganic and Organometallic Compounds*, ed. A. J. L. Pomberio and J. A. McCleverty, NATO ASI Series C, Kluwer, Netherlands, 1993, vol. 35, p. 391 ff.
42 J. H. Zagal, M. Páez and C. Páez, *J. Electroanal. Chem.*, 1987, **237**, 145.
43 D. Lexa, J.-M. Savéant and J. Zickler, *J. Am. Chem. Soc.*, 1980, **102**, 2654.
44 P. G. Swetik and D. G. Brown, *J. Electroanal. Chem.*, 1974, **51**, 433.
45 B. A. Abd-el-Nabey, *J. Electroanal. Chem.*, 1974, **53**, 317.
46 S. L. Tackett and J. W. Ide, *J. Electroanal. Chem.*, 1971, **30**, 510.
47 B. Jaselskis and H. Diehl, *J. Am. Chem. Soc.*, 1954, **76**, 4345.
48 D. J. Walton and S. S. Phull, *Adv. Sonochem.*, 1996, **4**, 205.
49 R. G. Compton, J. C. Eklund and F. Marken, *Electroanalysis*, 1997, **9**, 509.
50 F. Marken, R. P. Akkermans and R. G. Compton, *J. Electroanal. Chem.*, 1996, **415**, 55.
51 M. Atobe, T. Kaburagi and T. Nonaka, *Electrochemistry*, 1999, **67**, 1114.
52 R. G. Compton, J. C. Eklund, S. D. Page, T. J. Mason and D. J. Walton, *J. Appl. Electrochem.*, 1996, **26**, 775.
53 H. A. O. Hill, Y. Nakagawa, F. Marken and R. G. Compton, *J. Phys. Chem.*, 1996, **100**, 17395.
54 J. C. Ball, F. Marken, Q. Fulian, J. D. Wadhawan, A. N. Blythe, U. Schroeder, R. G. Compton, S. D. Bull and S. G. Davies, *Electroanalysis*, 2000, **12**, 1017.
55 J. Gao and J. F. Rusling, *J. Org. Chem.*, 1998, **63**, 218.
56 J. Gao, C. K. Njue, J. K. N. Mbindyo and J. F. Rusling, *J. Electroanal. Chem.*, 1999, **464**, 31.

Efficient Barbier reaction of carbonyl compounds improved by a phase transfer catalyst in water†

Zhenggen Zha,[a] Yusong Wang,[a] Guang Yang,[b] Li Zhang[b] and Zhiyong Wang*[a]

[a] *Department of Chemistry, University of Science and Technology of China, Hefei, Anhui, China 230026. E-mail: zwang3@ustc.edu.cn*
[b] *Department of Chemistry Suzhou Teacher College, Anhui, China*

Received 3rd July 2002
First published as an Advance Article on the web 7th October 2002

A phase transfer catalyst (PTC) is employed in allylation mediated by tin. This atom economical reaction was performed in water at room temperature without any assistance. In addition, the influence of PTC on diastereoselectivity of the allylation was studied.

More attention has been recently paid on both environmental protection and ecological balance. Green chemistry plays an important role in reducing and eventually eliminating the impacts from chemical industries on the environment. Organic reactions in aqueous media is a significant branch of green chemistry utilizing a variety of organometallic reagents to accomplish Grignard-type reactions in water. A typical example of such a reaction is allylation of aldehydes or ketones in water.

Up to now various metals have been employed as mediators during allylation in aqueous media under different conditions.[1–4] Generally, an acidic environment is necessary for promoting reactive activity of metals as well as increasing the solubility of insoluble carbonyl compounds in water.[5–8] However, a number of the functionalities on reactants can readily be hydrolyzed in the acidic environment. Furthermore, side reactions such as reduction and coupling may take place under this condition. Carrying out such a reaction in neutral water and realizing an atom economical reaction is still a desirable yet elusive goal. Previously, we used nano-tin to approach this goal and made progress in allylation in water.[9] In the present work, we have made an important improvement by using a phase transfer catalyst (PTC) to achieve this goal.

To start our study, metallic tin was employed as a mediator for the allylation of aldehydes and ketones. Then the reaction mixture was allowed to stir at ambient temperature for 2 h in order to obtain the allylation products. Generally, it takes 2–4 h to complete the allylations of aldehydes or ketones in the presence of a metal such as zinc in saturated ammonium chloride solution.[5,10] However, each reaction catalyzed by tin in distilled water (2–4 h) gave rise to the desired product only in trace amounts or not at all. Only on prolonging the reaction time to > 10 h, could the corresponding products be observed. After a series of trails, we decided to add PTC to the reaction mixture. As far as we know, PTC is widely used in chemical reactions since it offers high yield with reduced cycle time, reduced or no added solvent, mild reaction conditions, enhanced environmental performance and sometimes better selectivity. However, few studies were found concerning PTC employed in organic reactions in water. Here we wish to report results with PTC as additive to enhance reactive activity of metallic tin in water.

Allylations were mediated by tin in the presence of TPC in distilled water. The experiment results are listed in Table 1, clearly showing that the reaction was improved significantly. First, the reaction approached chemically green criteria. Previously the solvent used for allylations was a co-solvent of water and an organic solvent such as water mixed with DMF or THF under acidic or basic conditions.[11] Here the solvent is distilled water under neutral conditions, without either organic solvent or acidic environment. Moreover, the intricate protection and deprotection for those functionalities, which are sensitive to acidic or basic environment, were avoided. Secondly, the reaction is more atom economical. Since Trost put forward the atom efficient methodology as a critical first step in greening organic chemistry, chemists have been attempting to square the atomic accounts to form products and some achievement has been obtained.[12] The allylation here is another good example of an atom efficient reaction. In most of the reactions, the atoms in the reactants are totally reorganized into the corresponding products (Table 1, entries 5–9). Thirdly, PTC reduced the cycle time. The reactions were conducted under mild conditions without the assistance of microwaves, heat or sonication. From Table 1, the reaction time was shortened from 18–22 h to 1–2.5 h for entries 5–10. In particular, the reaction conditions were mild enough to allow the acid sensitive acetal group to survive the allylation reaction (Table 1, entry 6). Moreover, allylations of aliphatic aldehydes or ketones, which are traditionally thought to be unreactive,

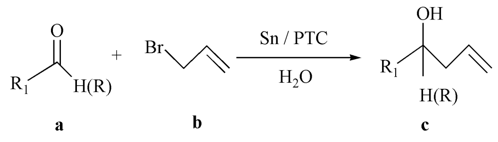

Scheme 1 R_1 = Phenyl, aryl or aliphatic group; R = CH_3

Green Context

Chemistry in water offers obvious advantages in a green chemistry context. Here we see an unusual example of an organic reaction in water that is significantly accelerated by phase transfer catalysts. The reactions under consideration are allylations of ketones and aldehydes. Points of interest and green relevance are that the reactions occur in distilled water with no added acid or co-solvent for example, and the reactions are very atom-efficient. Care will be needed however, to deal with any catalyst waste.

---

† Electronic supplementary information (ESI) available: experimental procedure for allylation and spectral data for the allylation products. See http://www.rsc.org./suppdata/gc/b2/b206452a/

Table 1 Allylation of carbonyl compounds improved by PTC in water

Entry	Carbonyl compound	PTC	Time/h	Yield (%)
1	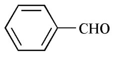 **1a**	—	16	72
		A	16	98
		B	16	97
		C	16	96
		D	16	72
2	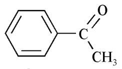 **2a**	—	16	43
		A	16	50
		B	16	50
		C	16	53
		D	16	54
3	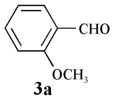 **3a**	—	16	71
		A	5	100
		B	6	99
		C	7	98
		D	6	92
4	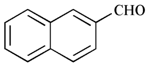 **4a**	—	3	0
		A	3	90
		B	3	95
		C	3	96
		D	3	95
5	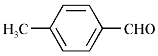 **5a**	—	2.5	0
		A	3	100
		B	2.5	100
		C	2.5	100
		D	12	87
6	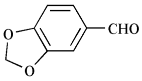 **6a**	—	2	0
		A	2	100
		B	2	100
		C	2	100
		D	2	100
7	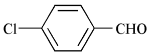 **7a**	—	2	0
		A	2	100
		B	2	100
		C	2	100
		D	2	100
8	n- $C_6H_{13}CHO$ **8a**	—	1	0
		A	1.5	100
		B	1	100
		C	1	100
		D	1	100
9	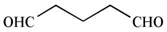 **9a**	—	2	0
		A	2	100
		B	2	100
		C	2	100
		D	2	100
10	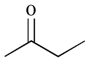 **10a**	—	7	40
		A	3	100
		B	3	98
		C	3	95
		D	3	95

A. Cetyltrimethammonium bromide; B. n-Bu_4NBr; C. polyethylene glycol; D. silica gel.

could also be greatly accelerated and quantitatively give the corresponding products (Table 1, entries 8–10). As for aromatic ketone **2a**, this shows more steric hindrance than that of aldehydes due to the bulk of both the phenyl ring and the methyl group; in the presence of PTC, however, it could be allylated and the yield of the allylation of **2a** reached 50–60%.

Finally, the diastereoselectivity was investigated in the presence of PTC. The allylations of benzaldehyde with ethyl-4-bromo-2-butenoate and 3-hydroxy-2-butanone with allyl bromide were studied as shown in Scheme 2. The results were summarized in Table 2. In comparison with the allylation catalyzed by tin without PTC, the diastereoselectivities for the allylation of 3-hydroxy-2-butanone with allyl bromide were a little different with the change of PTC as shown in entry 1 of Table 2. When the PTC was n-butyl ammonium bromide, allylation gave the best yield and the highest diatereoselectivity (Table 2. entry 1B) while the others gave good yields but lower diastereoselectivities. As for the allylation of benzaldehyde with ethyl-4-bromo-2-butenoate, the stereochemistry was greatly variable with the change of PTC as shown in entry 2 of Table 2. Without PTC, the ratio of *syn*:*anti* of **3γ** was 68:32 while the ratio was almost the same when mediated by either n-Bu_4NBr or silica gel. For silica gel, the diastereoselectivity decreased (*syn*:*anti* = 64:36). However, both polyethylene glycol and cetyltrimethylammonium bromide increased the diastereoselectivity greatly (*syn:anti* = 91:9 and 95:5, respectively). The allylation mediated by cetyltrimethylammonium bromide gave the best result, not only high diastereoselectivity but also good yield being obtained (Table 2, entry 2A).

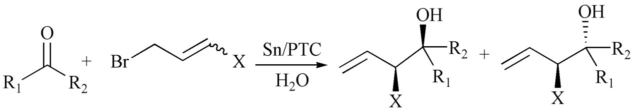

1 **2** **3γ**

Scheme 2

Table 2 Diastereoselectivity of allylation in the presence of PTC

Entry	R_1	R_2	X	PTC	3γ (*syn:anti*)[a]	Yield[b] (%)
1	MeCH(OH)	Me	H	—	(63:37)	72
				A	(60:40)	82
				B	(64:36)	88
				C	(61:39)	84
				D	(64:36)	81
2	Ph	H	COOEt	—	(68:32)	71
				A	(95:5)	81
				B	(70:30)	73
				C	(91:9)	71
				D	(64:36)	74

[a] The ratio of *syn* isomer to *anti* isomer was determined by ^{13}C NMR. [b] Isolated yield.

In conclusion, PTC has been employed in allylation of ketones and aldehydes in distilled water and satisfactory results were obtained. In the presence of PTC, the tin-mediated allylation of aldehydes proceed rapidly and the reactants were converted into the corresponding products efficiently under mild conditions. The introduction of PTC to the reactions in water has developed synthetic methodology and made progress in approaching greener chemistry. Additionally, the experiment results demonstrated a new way to access an atom economical reaction and to realize industrialization. The mechanism of PTC to promote the reactions is, as yet, uncertain, and investigation of the mechanism is in progress in our laboratory.

Acknowledgment

This research was supported by NSFC (No. 50073021), NSF of Anhui Province (No.01046301) and Basement of Green Chemistry at the University of Science & Technology of China.

Notes and references

1 C.-J. Li and T -H Chan, *Tetrahedron Lett.*, 1991, **32**, 7017.
2 M. Mada, H. Ohki and K. Akiba, *Bull. Chem. Soc. Jpn.*, 1990, **63**, 1738.
3 L.-H. Li and T.-H. Chan, *Tetrahedron Lett.*, 2000, **41**, 5009.
4 C.-J. Li, Y. Meng, X.-H Yi, J. Ma and T.-H. Chan, *J. Org. Chem.*, 1997, **62**, 8632.
5 S. R. Wilson and M. E. Guazzaroni, *J. Org. Chem.*, 1989, **54**, 3087.
6 K. Tanaka, S. Kishigami and F. Toda, *J. Org. Chem.*, 1991, **56**, 4333.

7 B. Abribat and Y. L. Bigot, *Tetrahedron*, 1997, **53**, 2119.

8 S. Venkatraman and C.-J. Li, *Tetrahedron Lett.*, 2000, **41**, 4831.

9 Z. Wang, Z. Zha and C. Zhou, *Org. Lett.*, 2002, **4**, 1683.

10 D. Marton, D. Stivanello and G. Tagliavini, *J. Org. Chem.*, 1996, **61**, 2731.

11 (*a*) C.-J. Li, *Tetrahedron*, 1996, **52**, 5643; (*b*) T. Fukuma, S. Lock, N. Miyoshi and M. Wada, *Chem. Lett.*, 2002, **3**, 376; (*c*) D. D. Laskar, M. Gohain, D. Prajapati and J. S. Sandhu, *New. J. Chem.*, 2002, **26**, 193.

12 (*a*) B. M. Trost, *Chem. Pharm Bull.*, 2002, **50**, 1; (*b*) B. M. Trost, *Abstr. Pap. Am. Chem.*, 1999, **S217**, 340-ORGN, Part 2; (*c*) B. M. Trost, *Chem. Eur. J.*, 1998, **4**, 2405; (*d*) B. M. Trost, *Angew. Chem., Int. Ed. Engl.*, 1995, **34**, 259; (*e*) T.-H. Chan and C.-J. Li, *J. Chem. Soc., Chem. Commun.*, 1992, 747.

An eco-friendly novel separation of carrier-free thallium radionuclide from mercury and lead radionuclides using algae as bio-reagent

Dalia Nayak,[a] Susanta Lahiri,*[a] Arpita Mukhopadhyay[b] and R. Pal[b]

[a] *Chemical Sciences Division, Saha Institute of Nuclear Physics, 1/AF Bidhannagar, Kolkata 700 064, India. E-mail: slahiri@hp1.saha.ernet.in; Fax: 0091-33-337-4637*
[b] *Department of Botany, University of Calcutta, 35, Ballygunge Circular Road, Kolkata 700 019, India*

Received 23rd August 2002
First published as an Advance Article on the web 16th October 2002

Here we report a novel separation technique for the clinically important ^{199}Tl radionuclide from its precursor lead and daughter product mercury. Two algal genera, *Lyngbya major*, from cyanophyceae and *Rhizoclonium hieroglyphicum* from chlorophyceae have been used as natural bioreagents in the separation of thallium radionuclides in ultra-trace scale. 24 h algal treatment of an aqueous solution at pH 8 containing a mixture of radionuclides shows that *Rhizoclonium* accumulates 100% Hg, $>80\%$ Pb and a small fraction of thallium (15%). Thus a large fraction of thallium remains in the solution not accumulated by algae. Thus the selectivity of various algae towards different metals in sorption and desorption processes may be exploited in the separation of these metals from a mixture of them.

Introduction

^{199,201}Tl are important radionuclides in the field of nuclear medicine. Thallium-201 is used for myocardial perfusion imaging and evaluation of coronary artery disease, while occasionally also ^{199}Tl is used. The emission characteristics of ^{199}Tl for imaging are not worse than those of ^{201}Tl, but the associated equivalent dose is 10 times less per unit of activity in comparison with that of the ^{201}Tl.[1,2] Though thallium radionuclides are useful stable thallium is, however, toxic. Thus it is important to separate thallium radionuclides in carrier-free form, so that the minimum chemical toxicity of thallium is administered.

Several methodologies have been proposed for the production and separation of carrier-free thallium radionuclides.[3–6] However some of the standard methods cannot avoid small amounts of stable thallium contamination with the separated thallium radionuclides as they used thallium as a target. Recently we have proposed a new method for the production of thallium radionuclides by ^{7}Li irradiation on a gold target and developed the method of separation of carrier-free thallium radionuclides using conventional chemicals.[7] In our method as thallium is produced by heavy ion activation from a gold target, no stable thallium isotopes are present in the system. In fact, to the best of our knowledge, no other heavy ion production and separation of thallium radionuclides has been proposed so far.

In our method or the method proposed by other researchers, it is important to isolate carrier-free thallium or mercury radionuclides. The reagents which have been mainly used so far for this purpose are $Fe(OH)_3$, $PbSO_4$, hydrazine, ammonium acetate, trioctylamine (TOA), *etc.* In this correspondence we present a preliminary report on the first time use of an eco-friendly separation of carrier-free thallium from lead and mercury radionuclides using two types of algal genera as bio-reagents for separation. This method definitely reduces the requirement of chemicals, which is one of the main strategies of green chemistry. It is true that heavy metal accumulation by bio-organisms and even by algae was studied many years ago. However until now not many intentional separations have been carried out, especially by algae. Moreover, as far we are aware, separation has not been carried out with heavy metals on an ultra-trace scale, nor for radioactive materials.

Experimental

Culture of algae

Two algal genera, *Lyngbya major*, from cyanophyceae and *Rhizoclonium hieroglyphicum* from chlorophyceae were cultured in laboratory conditions. *Lyngbya*, a fresh water cyanobacteria, was cultured in cyanophycean agar containing KNO_3, K_2HPO_4, $MgSO_4$ and ferric ammonium citrate. *Rhizoclonium*, a brackish water species, was cultured in artificial sea water medium[8] at 20 °C in a 16/8 h light/dark cycle under a cool fluorescent light (light intensity 20–30 μ einstein m^{-2} s^{-1}). Both the genera were isolated locally and raised the unialgal cultures.

Green Context

Radionuclides have many important applications in medicine. These include thallium-199 which obviously presents difficulties due to its toxicity. It is particularly important to separate the nuclide in a carrier-free form and here we see described a novel and environmentally benign procedure for the separation based on algae. It is shown by using ^{199}Tl as an example that the different selectivities of various algae towards different metals may be exploited in metal separation. ***JHC***

DOI: 10.1039/b208276d

Irradiation

A pure gold foil of thickness 8.5 mg cm^{-2} was subjected to irradiation with a collimated beam of 49 MeV $^{7}Li^{3+}$ at BARC-TIFR Pelletron, Mumbai, India with an average beam current of 200 nA for 5 h.[7] The following reactions for production of carrier-free thallium radionuclides using ^{7}Li beam has been considered:

$$^{197}Au(^{7}Li, xn)^{197-200}Pb\ (EC)\ ^{197-200}Tl\ (EC)\ ^{197}Hg\ (23.8\ h)$$

After irradiation, the gold target was removed from the irradiation chamber and cooled for 1 h. The product radionuclides were detected by their corresponding γ-energy peaks. Nuclear characteristics of the radionuclides produced are presented in Table 1. An HPGe detector of 2.13 keV resolution at 1.33 MeV in conjunction with a PC based MCA, PCA2 (OXFORD) was used for γ-spectrometric studies. The radionuclides identified were ^{197}Hg, ^{197}Tl, ^{198}Tl ^{199}Tl, ^{200}Tl, ^{199}Pb and ^{200}Pb.

Chemical separation of the carrier-free radionuclides from the target was made according to the method described in ref. 7. After the separation, the aqueous phase contained only carrier-free radionuclides of mercury, thallium and lead, which were exposed subsequently to the algal system for bio-separation studies.

Exposure of algae to the radioactive solution

Healthy growing algal cultures were taken for each set of experiment. ~ 1 g of *Lyngbya* and ~ 0.4 g of *Rhizoclonium* were exposed to the 20 mL radionuclide solution of Hg, Tl and Pb. Alkaline pH levels were maintained for each set of experiments. These radionuclides were monitored by choosing a particular photopeak of ^{197}Hg, ^{200}Tl, ^{200}Pb, and the initial concentration of these radionuclides in the stock solution were ^{197}Hg = 1 kBq mL^{-1}; ^{200}Tl = 8 kBq mL^{-1}; ^{200}Pb = 29 kBq mL^{-1}. Each alga was exposed for 24 h. The mixture was stirred very gently at room temperature. Each time a fraction (2 mL) of the supernatant liquid was removed and assayed for radionuclides by means of HPGe detector and was compared to the counts of initial counts per mL of the particular algal culture solution. The results are expressed as accumulation (A) in the algal biomass (in percentage terms).

$$A = ((1 - C^{1}_{t})/C^{0}_{t}) \times 100\%$$

where, C^{1}_{t} = count mL^{-1} of a particular radionuclide of the supernatant solution after time t and C^{0}_{t} = count mL^{-1} of the particular radionuclide of the initial solution of algal culture after time t (with appropriate decay correction).

Results and discussion

The accumulation of different radionuclides by algal genera after 24 h of exposure is presented in Fig. 1. It has been found that *Rhizoclonium* accumulates 100% Hg and more than 80% Pb after 24 h treatment at pH = 8, while the accumulation of thallium radionuclide is less than 15%. In *Lyngbya* the accumulation of both mercury and lead radionuclides is around 80% while that of thallium is around 25% (Fig. 1 and Table 2). Thus after 24 h of treatment the aqueous solution will be highly enriched with thallium radionuclides and specially in case of *Rhizoclonium*, thallium will be almost free from mercury and lead contamination. However, complete decontamination from mercury is not possible as it is the daughter product of thallium. The separation factor of thallium is defined as following:

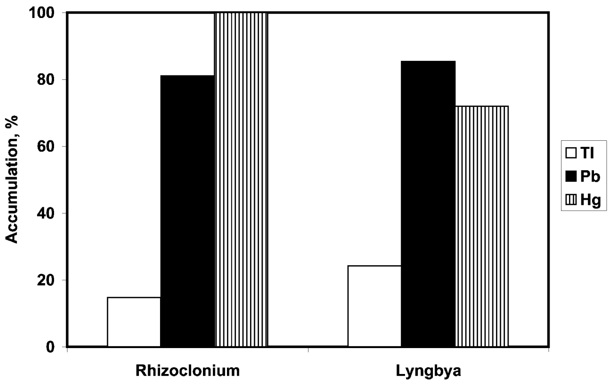

Fig. 1 Percentage of accumulation of radionuclides by *Rhizoclonium* and *Lyngbya* at pH = 8 after 24 h of exposure.

Table 2 Accumulation (%) of metals by two different algae, *Rhizoclonium* and *Lyngbya* after 24 h exposure

	Accumulation (%)	
Element	*Rhizoclonium*	*Lyngbya*
Tl	14.8 ± 0.80	24.2 ± 0.90
Pb	80.8 ± 1.50	85.4 ± 1.44
Hg	100 ± 3.40	72 ± 7.70

$$S_{Hg/Tl} = D_{Hg}/D_{Tl}$$

while,

$$D_{Hg} = \frac{\text{Accumulation of mercury in Algal biomass}}{\text{activity of mercury in solution}}$$

The separation factors in *Rhizoclonium* are $S_{Hg/Tl}$ = 5750 and that of lead to thallium is $S_{Pb/Tl}$ = 25. The separation factors in *Lyngbya* are $S_{Hg/Tl}$ = 8 and $S_{Pb/Tl}$ = 18.

In order to assess the different parameters these biomasses were removed from the solution after 24 h of treatment and subjected to recourse in gamma spectroscopy in four different ways: (a) without washing the biomass, (b) washed with distilled water, (c) washed with dilute HCl or (d) washed with ethylenediaminetetraacetic acid (EDTA) solution. In Fig. 2 the results have been expressed in terms of the percentage of

Table 1 Nuclear characteristics of the radionuclides produced by ^{7}Li irradiation of gold

Target	Nuclear reaction	Activation product (half life)	Principal γ-energies	1st Daughter product (half life)	Principal γ-energies	2nd Daughter product (half life)	Principal γ-energies
Au	^{7}Li, 4n	^{200}Pb (21.5 h)	147.6, 268.3	^{200}Tl (26.1 h)	367.9, 579.3, 1205.7		
	^{7}Li, 5n	^{199}Pb (90 m)	366.9, 1135.1	^{199}Tl (7.4 h)	158.3, 208.2, 455.5		
	^{7}Li, 6n	^{198}Pb (2.4 h)	290.3	^{198}Tl (5.3 h)	411.8		
	^{7}Li, 7n	^{197}Pb (43 min)	Not detected	^{197}Tl (2.84 h)	425.8	^{197}Hg (23.8 h)	133.9

Table 3 Accumulation (%) of metals by two different algae, *Rhizoclonium* and *Lyngbya* after 24 h exposure under four different conditions

	Accumulation (%)							
	Rhizoclonium				*Lyngbya*			
Element	Without wash	Distilled water wash	Acid wash	EDTA wash	Without wash	Distilled water wash	Acid wash	EDTA wash
Tl	14.8 ± 0.01	14.8 ± 0.09	6 ± 0.01	12.2 ± 0.02	24.2 ± 0.03	24.2 ± 0.06	5.95 ± 0.02	21 ± 0.05
Pb	80.8 ± 0.04	16.4 ± 0.03	5.5 ± 0.02	7.7 ± 0.02	85.4 ±0.07	85.2 ± 0.15	11.67 ± 0.04	11.44 ± 0.04
Hg	100 ± 0.60	37.58 ± 0.60	40.47 ± 0.64	58 ± 0.81	72 ± 0.41	65.66 ± 0.76	41 ± 0.54	60.84 ± 0.72

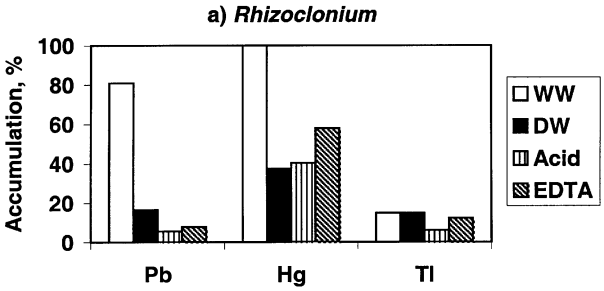

a) *Rhizoclonium*

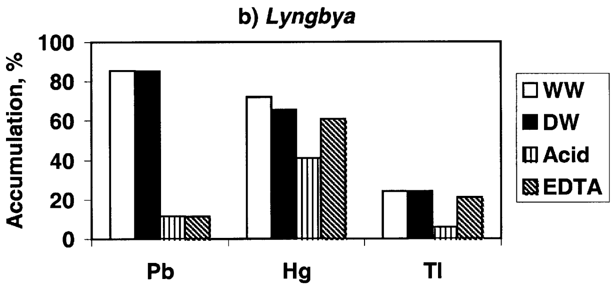

b) *Lyngbya*

Fig. 2 Percentage of accumulation of Hg, Pb and Tl after 24 h exposure to the radionuclide solution, with respect to the total accumulation without washing (WW), by (a) *Rhizoclonium* and (b) *Lyngbya* under three different conditions [washing with distilled water (DW), washing with dilute HCl (Acid), washing with EDTA (EDTA)].

retention of different radionuclides after treatment with water, acid and EDTA with respect to the total accumulation by algal biomass without washing. Table 3 shows the same set of data detailing the errors in measurements in each case.

Fig. 2(a) depicts the fact that the accumulation of Pb at basic pH by *Rhizoclonium* is due to an adsorption process, as the washing of the algal biomass with dilute acid, EDTA or even by distilled water drastically reduced its metal content. Therefore it becomes clear that *Rhizoclonium* adsorbs Pb at basic pH, *via* extracellular or cell wall ligands. Accumulated Hg was removed by 40% with EDTA, implying that a fraction of Hg was adsorbed by cell wall surface ligands and the remainder of the accumulated Hg was absorbed internally. *Rhizoclonium* accumulates only 15% Tl after 24 h treatment and a large fraction remains in the solution. Distilled water, acid or EDTA washings do not remove accumulated Tl, which implies the accumulation of thallium even in smaller amounts is due to an active absorption (accumulation inside the cell) process. Fig. 2(b) shows the results from *Lyngbya*, which are similar to those obtained from *Rhizoclonium* except for the case of distilled water washing of biomass. Thus in *Lyngbya* also Pb accumulation is explained by an adsorption process, whereas that of Hg is both adsorption as well as an absorption process. Tl mainly remains in the solution, though a small fraction is actively absorbed. For *Lyngbya* all the three metals adsorbed on the cell surface were not removed at all by distilled water washing (DW) unlike to that for *Rhizoclonium*. This indicates that there is strong bonding between the cell wall surface ligands and the metals, which can be broken only by acid and EDTA washing. This may be due to the fact that cyanophycean cell walls, especially *Lyngbya*, contains much more polysaccharides as sheath material than *Rhizoclonium*.

In both the cases a major portion of Tl remains in the solution not accumulated by *Lyngbya* and *Rhizoclonium*. Thus both *Rhizoclonium* as well as *Lyngbya* are good bioreagents for the separation of Tl radionuclides from a mixture of Pb and Hg. The advantages of this method is that thallium remains in the aqueous solution thus which can be taken in any desired medium depending upon its application. It is noteworthy to mention that an average 20–30% accumulation of lead and mercury was found for both the algae when the contact time was 10 min. This preliminary experiment suggests that optimization of the contact time and understanding on the kinetics of the accumulation is necessary as the radionuclides under discussion have shorter half-lives. Careful manipulation of different parameters such as choice of appropriate pH for separation studies, salinity of the solution, and contact time with the solution may result in excellent bio-reagents for this type of separation.

From the present study it can be concluded that the property of difference in selectivity of various algae towards different metals in sorption and desorption process may be exploited in the separation of metals from a mixture. Also algae from different taxonomic groups have different mechanisms for metal accumulation. Before using this thallium for *in vivo* uses further studies will be required to check for any biological contamination in the aqueous phase.

Acknowledgement

We gratefully acknowledge Dr S. B. Manohar, Head, Radiochemistry Division, Bhabha Atomic Research Centre and Dr A Ramaswami, Radiochemistry Division, Bhabha Atomic Research Centre, India, for providing necessary facilities at the Radiochemistry Laboratory. We also acknowledge Pelletron operation staff of BARC-TIFR Pelletron, Mumbai for their help and co-operation during this work. We also sincerely thank Mr Ajoy Das for his help in target preparation.

References

1 Y. Nagame, H. Nagahara and Y. Murakami, *Int. J. Appl. Radiat. Isot.*, 1979, **30**, 669.
2 N. V. Kurenkov, V. P. Lunev and Yu. N. Shubin, *Appl. Radiat. Isot.*, 1999, **50**, 411.
3 E. Lebowitz, M. W. Greene, R. Fairchild, R. Bradley, P. R. Moore, H. L. Atkins, A. N. Ansari, P. Richards and E. Belgrave, *J. Nucl. Med.*, 1975, **16**, 151.
4 M. C. Lagunas-Solar, J. A. Jungerman and D. W. Paulson, *Int. J. Appl. Radiat. Isot.*, 1978, **29**, 159.
5 S. M. Qaim, R. Weinreich and H. Ollig, *Int. J. Appl. Radiat. Isot.*, 1979, **30**, 85.
6 T. N. vander Walt and C. Naidoo, *Radiochim. Acta*, 2000, **88**, 185.
7 D. Nayak, S. Lahiri and A. Ramaswami, *Appl. Radiat. Isot.*, 2002, **57**, 483.
8 F. D. Ott, *Virginia J. Sci.*, 1965, **16**, 205.

Enantioselective electrophilic fluorination in ionic liquids

Christine Baudequin, Jean-Christophe Plaquevent, Christophe Audouard and Dominique Cahard*

UMR 6014 de l'IRCOF (Institut de Recherche en Chimie Organique Fine), Université de Rouen, F-76821 Mont Saint Aignan Cedex, France. E-mail: dominique.cahard@univ-rouen.fr

Received 10th September 2002
First published as an Advance Article on the web 11th October 2002

It has been demonstrated that enantioselective electrophilic fluorination performed by means of *N*-fluorocinchonium salts in ionic liquids presents substantial advantages over the use of classical solvents.

Introduction

Fluorine is perhaps the element which has experienced the greatest recent interest as pointed out by the exceptionally high percentage of fluorinated new compounds over the recent decades. The building block strategy is by far the most common approach, whereas late fluorination represents an elegant alternative. However, asymmetric synthesis of stereogenic fluorinated centers is highly challenging. Reagent-controlled enantioselective fluorination has been described by us[1] and others.[2] Our approach involves a novel class of [N–F]$^+$ reagents derived from the naturally occurring cinchona alkaloids. These fluorinating agents were successfully applied to the asymmetric fluorination of various substrates including ketone and ester enolates, β-ketoesters, silyl enol ethers and nitrile anions, with enantiomeric excesses up to 94%. In the literature, two catalytic methods for the fluorination of β-ketoesters have also been reported.[3,4] Although our chiral [N–F]$^+$ reagents are innovative and of wide scope, the recovery of the cinchona alkaloids, as well as the low-temperature reaction required to reach high enantioselection, and the poor choice of solvents (restricted to either CH_3CN or acetone), still remain as limitations.

Recently, ionic liquids (ILs) have emerged as a new class of solvents, which are often fluid at room temperature, and consist of entirely ionic species. ILs are good solvents for a wide range of organic and inorganic compounds, they have practically no vapor pressure and are presented as potential replacements for volatile solvents.[5] There are few reports of enantioselective reactions in ILs. Literature examples refer to transition metal catalyzed reactions such as hydrogenation of α,β-unsaturated acids,[6] ring opening of epoxides,[7] epoxidation,[8] allylic substitution,[9] and cyclopropanation.[10] Biocatalysis in ILs has also been the subject of recent research.[11] Since in these solvents, reagents having ionic character can be immobilized, we wondered whether the ILs might be good media for our novel class of [N–F]$^+$ fluorinating reagents. We herein report on the first enantioselective reaction, which does not involve a metal catalysis nor a biocatalysis, for the construction of carbon–fluorine bonds in ILs.

Results and discussion

In a previous structure-enantioselectivity relationship study, we found that *N*-fluoroammonium salts of cinchona alkaloid derivatives bearing a capped hydroxyl function such as a benzoyl ester, induce a higher degree of enantioselection than the free OH alkaloids.[1c] These electrophilic fluorinating agents produced high enantioselectivities in reactions run in acetonitrile at −40 °C on silyl enol ethers of tetralone and indanone derivatives. We examined the behavior of these chiral [N–F]$^+$ reagents on silyl enol ethers in the following ILs: 1-hexyl-3-methylimidazolium hexafluorophosphate [hmim][PF_6], 1-butyl-3-methylimidazolium hexafluorophosphate [bmim][PF_6] and 1-ethyl-3-methylimidazolium tetrafluoroborate [emim][BF_4]. From a wide range of ILs, we have selected these based on the presence of poorly nucleophilic PF_6^- and BF_4^- ions. The chiral [N–F]$^+$ reagents slowly dissolve in ionic liquids at room temperature (sonication helps to obtain homogeneous solutions) and then the silyl enol ether is added at 0 °C (Scheme 1). The fluorinated product is quantitatively separated from the reaction mixture by extraction with Et_2O. The results are presented in Table 1 along with comparative data obtained in acetonitrile.

The enantioselectivity is noted to be superior or identical to that measured in acetonitrile. Quinine-based [N–F]$^+$ reagents produce higher enantioselectivities and the absolute configuration of the fluorinated stereogenic center is the same in both solvents. Advantageously, the reactions are run at 0 °C in ILs whereas a temperature below −40 °C was essential to reach similar enantioselectivities in acetonitrile. The dramatic role of

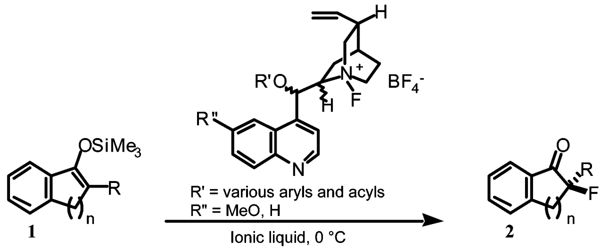

Scheme 1 Enantioselective electrophilic fluorination of silyl enol ethers in ILs.

Green Context

The selective fluorination of organic molecules has become a very important target reaction in sectors ranging from pharmaceuticals to electronics. Traditional methods can however, present considerable health and safety and environmental problems. Electrophilic fluorination long associated with dangerous F_2-based reagents can now be achieved with safer reagents such as N-fluoro compounds. Here reagents of this type are used for the first time to effect enantioselective fluorination in non-volatile ionic liquids which further add to their green chemistry credentials. *JHC*

DOI: 10.1039/b208817g

Table 1 Results of enantioselective fluorination of silyl enol ethers in ionic liquids

1	*n*	R	IL	$[N–F]^{+a}$	$\mathbf{2}^b$	Ee^c (%)	Yield (%)
1a	2	Me	[emim][BF_4]	F-pClBzQD-BF_4	**2a**	22 (22)	83
			[bmim][PF_6]	F-pClBzQD-BF_4		34 (22)	91
			[hmim][PF_6]	F-pClBzQD-BF_4		34 (22)	75
1b	1	Me	[bmim][PF_6]	F-pClBzCN-BF_4	**2b**	24 (4)	91
				F-pClBzCD-BF_4		43 (26)	99
				F-pClBzQD-BF_4		53 (37)	96
				F-pClBzQN-BF_4		64 (62)	89
				F-pNO_2BzQN-BF_4		65 (65)	94
				F-pMeOBzQN-BF_4		60 (59)	82
1c	1	Et	[hmim][PF_6]	F-pClBzQN-BF_4	**2c**	82 (82)	82
				F-2NaphtQN-BF_4		83 (80)	98
1d	1	Bn	[hmim][PF_6]	F-pClBzQN-BF_4	**2d**	86 (82)	89
				F-pClBzCD-BF_4		73 (26)	61
				F-pMeOBzQN-BF_4		84 (84)	74
				F-QNLQN-BF_4		66 (38)	65
				F-PhNQN-BF_4		74 (72)	91
				F-1NaphtQN-BF_4		86 (75)	93
				F-2NaphtQN-BF_4		84 (84)	87

[a] CD = cinchonidine, CN = cinchonine, QD = quinidine, QN = quinine, DHQN = dihydroquinine, QNL = 2-quinolyl ether, PhN = 9-phenanthryl ether, 1Napht = 1-naphthoyl ester. [b] F–QN–BF_4 and F–CD–BF_4 derivatives produce fluorinated products of *R* configuration while F–QD–BF_4 and F–CN–BF_4 derivatives give the *S* configuration. [c] In parentheses, enantiomeric excesses measured in reactions run in acetonitrile at −40 °C.

the solvent was thus convincingly demonstrated. In the optimization studies, we further restricted our choice of IL to [hmim][PF_6], which exhibits a higher fluidity, thus making the stirring easier. The trimethylsilyl enol ethers **1a–c** are liquid and smoothly react with the $[N–F]^+$ reagents in the IL (the reactions were completed after 2–6 h) while the trimethylsilyl enol ether of 2-benzyl-1-indanone **1d** is solid, thus leading to longer reaction time (48 h). The rate of the reaction was not improved by dissolving substrate **1d** in the minimun amount of either Et_2O giving a two-phase system or acetonitrile which forms a homogeneous phase with [hmim][PF_6]. The co-solvent had no significant effect on the enantioselectivity. Using wet ILs (saturated with water) or anhydrous ILs did not change the enantiomeric excesses or the yield of the reactions, showing that no special care of the ILs need be taken.

In the aim to simplify the system, the enantioselective fluorination has been performed with an *in situ* formation of the chiral $[N–F]^+$ reagent. This has been made possible thanks to a transfer-fluorination also effective in the ionic liquid. Moreover, we have evaluated NFSi (*N*-fluorobenzenesulfonimide) as an alternative achiral N–F reagent to selectfluor™ for the transfer-fluorination step. We found that the transfer-fluorination is five times quicker with NFSi (Scheme 2). The asymmetric fluorination of the silyl enol ether **1d** by means of the *in situ* generated F-pClBzQN-BF_4 or F-pClBzQN-$(PhSO_2)_2N$ produced the fluorinated compound respectively with 72 and 77% ee.

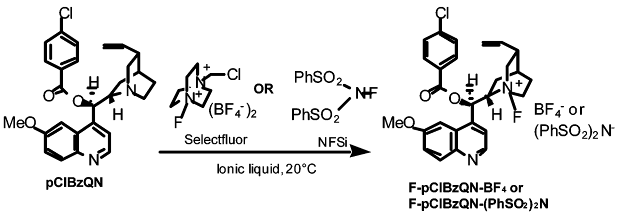

Scheme 2 Transfer-fluorination in ILs.

During the workup, Et_2O is used to extract the fluorinated products from the IL, and we observed that the amount of cinchona alkaloid dissolved in the Et_2O phase is negligible. Consequently, the fluorination was repeated in the same reaction vessel with the recovered IL containing the cinchona alkaloid by adding another equivalent of selectfluor™ (or NFSi). We have found that the IL and the cinchona alkaloid can be reused without significant alteration in the enantioselectivity. The cinchona alkaloid, the precursor of the $[N–F]^+$ reagent is thus immobilized in the IL which acts as a reservoir.

Conclusion

We have thus demonstrated that ionic liquids are excellent media for ionic reagents such as enantioselective electrophilic fluorinating agents. ILs proved to be superior to acetonitrile in terms of enantioselectivity, experimental conditions and are ideal solvents in the context of ″green″ chemistry. ILs can selectively dissolve the cinchona alkaloids in preference to Et_2O, allowing for IL and chiral agent recycling. Further studies are in progress, in particular the investigation of the organocatalyzed version of this fluorination.

Experimental

^1H, ^{13}C and ^{19}F NMR spectra were recorded on a Bruker DPX 300 spectrometer in acetone-d_6 for the $[N–F]^+$ reagents and in $CDCl_3$ for the fluorinated products. Trichlorofluoromethane served as internal standard (δ = 0) for ^{19}F NMR. High-performance liquid chromatography (HPLC) was carried out using a WATER 600 apparatus equiped with Chiracel columns.

A typical experimental procedure for the fluorination of 1d; 2-benzyl-2-fluoroindan-1-one

A fine powder of F-1NaphtQN-BF_4[1c] (388 mg, 0.7 mmol) was added slowly to a stirred solution of the ionic liquid [hmim][PF_6] (5 mL). After 2 h at room temperature, the mixture was cooled to 0 °C for the addition of the enoxytrimethylsilane of 2-benzyl-1-indanone (206.12 mg, 0.7 mmol). After 48 h at 0 °C under stirring, the fluorinated product was extracted with Et_2O (10 mL × 5) and then dried over $MgSO_4$. Concentration *in vacuo* and purification by chromatography (silica gel, heptane–diethyl ether) afforded (*R*)-2-benzyl-2-fluoroindan-1-one (93% yield, 86% ee determined by HPLC analysis using a Chiralcel OB-column (10% Pr^iOH–heptane, 1 mL min^{-1}, λ = 254 nm, retention time: *R* (major) 9.5 min, *S* [(minor) 13.4 min)]. Spectral data are in agreement with literature values.[2d]

2-Ethyl-2-fluoroindan-1-one

Using the same procedure, reaction of the enoxytrimethylsilane of 2-ethyl-1-indanone (162.7 mg, 0.7 mmol) with F-2NaphtQN-BF_4[1c] (388 mg, 0.7 mmol) gave 2-ethyl-2-fluoro-indan-1-one (98% yield, 83% ee determined by HPLC analysis using a Chiralcel OB-column (1% Pr^iOH–hexane, 1 mL min^{-1}, λ = 254 nm, retention time: *R* (major) 72 min, *S* (minor) 91 min)). Spectral data are in agreement with literature values.[2d]

2-Methyl-2-fluoro-indan-1-one

Using the same procedure, reaction of the enoxytrimethylsilane of 2-methyl-1-indanone (152.9 mg, 0.7 mmol) with F-pNO_2BzQN-BF_4[1c] (405.5 mg, 0.7 mmol) gave 2-methyl-2-fluoro-indan-1-one (94% yield, 65% ee determined by HPLC analysis using a Chiralcel OB-column (10% *i*PrOH-heptane, 1 mL/min, λ = 254 nm, retention time: *R* (major) 10.5 min, *S* [(minor) 27.1 min)]. Spectral data are in agreement with literature values.[2d]

2-Methyl-2-fluoro-1-tetralone

Using the same procedure, reaction of the enoxytrimethylsilane of 2-methyl-1-tetralone (162.7 mg, 0.7 mmol) with F-pClBzQD-BF_4[1c] (398.1 mg, 0.7 mmol) gave 2-methyl-2-fluoro-tetralone (75% yield, 34% ee determined by HPLC analysis using a Chiralcel OB-column (10% *i*PrOH-heptane, 1 mL/min, λ = 254 nm, retention time: *R* (minor) 9.9 min, *S* [(major) 14,4 min)]. Spectral data are in agreement with literature values.[2d]

A typical experimental procedure for the *in-situ* preparation of the fluorinating agent *N*-fluoro-*p*-chlorobenzoylquininium tetrafluoroborate (F-pClBzQN-BF_4) in ionic liquids

Selectfluor™ [(88.56 mg, 0.25 mmol) or NFSi (78.84 mg, 0.25 mmol)] was added to a solution of *p*-chlorobenzoylquinine (119.65 mg, 0.25 mmol) in the ionic liquid [hmim][PF_6] (1.8 mL) at room temperature. The mixture was stirred until it became homogeneous, 24 h with Selectfluor™ and 4 h with NFSi. Then, the silyl enol ether was added at 0 °C and the procedure continued as described above.

Acknowledgements

Financial support from Rhodia Organique Fine is gratefully acknowledged. We thank Jean-Marc Paris and Thierry Vidal for helpful discussion.

References

1 (*a*) D. Cahard, C. Audouard, J. C. Plaquevent and N. Roques, *Org. Lett.*, 2000, **2**, 3699; (*b*) D. Cahard, C. Audouard, J. C. Plaquevent, L. Toupet and N. Roques, *Tetrahedron Lett.*, 2001, **42**, 1867; (*c*) B. Mohar, J. Baudoux, J. C. Plaquevent and D. Cahard, *Angew. Chem., Int. Ed.*, 2001, **40**, 4214; B. Mohar, J. Baudoux, J. C. Plaquevent and D. Cahard, *Angew. Chem.*, 2001, **113**, 4339.

2 (*a*) E. Differding and R. W. Lang, *Tetrahedron Lett.*, 1988, **29**, 6087; (*b*) F. A. Davis, P. Zhou and C. K. Murphy, *Tetrahedron Lett.*, 1993, **34**, 3971; (*c*) F. A. Davis, P. Zhou, C. K. Murphy, G. Sundarababu, H. Qi, R. M. Przeslawski, B.-C. Chen and P. J. Carroll, *J. Org. Chem.*, 1998, **63**, 2273; (*d*) Y. Takeuchi, T. Suzuki, A. Satoh, T. Shiragami and N. Shibata, *J. Org. Chem.*, 1999, **64**, 5708; (*e*) Y. Takeuchi, A. Satoh, T. Suzuki, A. Kameda, M. Dohrin, T. Satoh, T. Koizumi and K. L. Kirk, *Chem. Pharm. Bull.*, 1997, **45**, 1085; (*f*) N. Shibata, E. Suzuki and Y. Takeuchi, *J. Am. Chem. Soc.*, 2000, **122**, 10728; (*g*) N. Shibata, E. Suzuki, T. Asahi and M. Shiro, *J. Am. Chem. Soc.*, 2001, **123**, 7001.

3 (*a*) L. Hintermann and A. Togni, *Angew. Chem., Int. Ed.*, 2000, **39**, 4359; (*b*) S. Piana, I. Devillers, A. Togni and U. Rothlisberger, *Angew. Chem., Int. Ed.*, 2002, **41**, 979.

4 D. Y. Kim and E. J. Park, *Org. Lett.*, 2002, **4**, 545.

5 (*a*) T. Welton, *Chem. Rev.*, 1999, **99**, 2071; (*b*) P. Wasserscheid and W. Keim, *Angew. Chem., Int. Ed.*, 2000, **39**, 3773; (*c*) M. J. Earle and K. R. Seddon, *Pure Appl. Chem.*, 2000, **72**, 1391; (*d*) R. Sheldon, *Chem. Commun.*, 2001, 2399; (*e*) R. Hagiwara and Y. Ito, *J. Fluorine Chem.*, 2000, **105**, 221.

6 (*a*) A. L. Monteiro, F. K. Zinn, R. F. de Souza and J. Dupont, *Tetrahedron: Asymmetry*, 1997, **8**, 177; (*b*) A. Berger, R. F. de Souza, M. R. Delgado and J. Dupont, *Tetrahedron: Asymmetry*, 2001, **12**, 1825; (*c*) R. A. Brown, P. Pollet, E. Mckoon, C. A. Eckert, C. L. Liotta and P. G. Jessop, *J. Am. Chem. Soc.*, 2001, **123**, 1254; (*d*) S. Guernik, A. Wolfson, M. Herskowitz, N. Greenspoon and S. Geresh, *Chem. Commun.*, 2001, 2314.

7 C. E. Song, C. R. Oh, E. J. Roh and D. J. Choo, *Chem. Commun.*, 2000, 1743.

8 C. E. Song and E. J. Roh, *Chem. Commun.*, 2000, 837.

9 S. Toma, B. Gotov, I. Kmentova and E. Solcaniova, *Green Chem.*, 2000, **2**, 149.

10 J. M. Fraile, J. I. Garcia, C. I. Herreiras, J. A. Mayoral, D. Carrié and M. Vaultier, *Tetrahedron: Asymmetry*, 2001, **12**, 1891.

11 (*a*) R. M. Lau, F. van Rantwijk, K. R. Seddon and R. A. Sheldon, *Org. Lett.*, 2000, **2**, 4189; (*b*) J. Howarth, P. James and J. Dai, *Tetrahedron Lett.*, 2001, **42**, 7517; (*c*) K.-W. Kim, B. Song, M.-Y. Choi and M.-J. Kim, *Org. Lett.*, 2001, **3**, 1507; (*d*) S. Park and R. J. Kazlauskas, *J. Org. Chem.*, 2001, **66**, 8395; (*e*) S. H. Schöfer, N. Kaftzik, P. Wasserscheid and U. Kragl, *Chem. Commun.*, 2001, 425; (*f*) P. Kielbasinski, M. Albrycht, J. Luczak and M. Mikolajczyk, *Tetrahedron Asymmetry*, 2002, **13**, 735.

Disproportionation, isomerization and de-*tert*-butylation of 2,6-di-*tert*-butylphenol catalyzed by H-MCM-41

Anil Wali, Jagannath Das, S. Muthukumaru Pillai* and M. Ravindranathan

Research Centre, Indian Petrochemicals Corporation Ltd, Baroda- 391 345, India.
E-mail: sm_pillai@yahoo.com

Received 24th July 2002
First published as an Advance Article on the web 11th October 2002

Mesoporous H-MCM-41 is an efficient catalyst for conversion of 2,6-di-*tert*-butylphenol to 2-*tert*-butylphenol, 2,4,6-tri-*tert*-butylphenol, 2,4-di-*tert*-butylphenol and 4-*tert*-butylphenol besides di- and tri-isobutylene in solvent free conditions. At low temperature (100 °C) and shorter reaction times 2-*tert*-butylphenol and 2,4,6-tri-*tert*-butylphenol are major products whereas at high temperature (180 °C) 4-*tert*-butylphenol is the most favoured product. H-MCM-41 steamed for 6 h at 520 °C was found to be the most active catalyst with maximum turnover of the products.

Introduction

Alkylphenols are an important class of compounds used extensively in the polymer industry as antioxidants, UV absorbers and heat stabilizers.[1] Alkylation of phenols by alkenes in the presence of a suitable catalyst leads to such products. Several acidic catalysts such as SAPO-11,[2] H-Beta Zeolite,[3] ZSM-12,[4] Zeolite-Y,[5] H-FeMCM-41[6] and heteropoly acids[7] are generally used in the alkylation reactions. However, the alkylates can be made by other routes also. Bigi *et al.* [8] reported that in the presence of montmorillonite KSF catalyst, an equimolecular mixture of phenol and 2,4-di-*tert*-butylphenol can be converted into 4-*tert*-butylphenol. This is quite interesting as the removal of a *tert*-butyl group from aromatic compounds requires an excess of $AlCl_3$ or similar hard Lewis acids.[9,10] Kinetic studies on the microwave activated catalytic de-*tert*-butylation of *tert*-butylphenols on KSF have also been recently reported.[11] 2,6-Di-*tert*-butylphenol undergoes complete dealkylation in presence of H_2SO_4 and HCl under severe conditions[12] and transalkylation with aromatics in presence of acid catalysts such as H_2SO_4, CF_3SO_3H, cation-exchanged resin, Nafion-H *etc.*[13,14]

Our interest in the exploitation of solid acids for synthesis of fine chemicals[15,16] has prompted us to study the reaction of 2,6-di-*tert*-butylphenol on H-MCM-41 in solvent free conditions. Reactions employing eco-friendly catalysts, *e.g.* zeolites and/or solventless media, are important characteristics of green chemistry. The results of our investigations are summarized in this work.

Experimental

Synthesis of H-MCM-41 zeolite

A solution of 6 g NaOH in 200 ml water was added to a solution of $Al_2(SO_4)_3{\cdot}xH_2O$ (5.0 g dissolved in 100 ml water) with stirring. This was followed by the addition of 14.58 g of cetylmethylammonium bromide (in 240 ml of water) with continuous stirring. Finally 41.7 g of $Si(OEt)_4$ was added dropwise to the above mixture with vigorous stirring. The resultant alkaline gel was transferred to a Teflon lined autoclave and treated hydrothermally at 100 °C for 96 h under autogenous pressure. The product was isolated by filtration, washed with hot distilled water and dried at 120 °C. XRD analysis confirmed the solid material as MCM-41. Dried MCM-41 was calcined slowly and stepwise up to 540 °C in flowing dry N_2 for 6 h followed by another calcination in air at the same temperature for the same period. The mesorporous molecular sieve in the Na^+ form was further ion-exchanged four times with a 10% NH_4NO_3 solution at 90 °C for 4 h and finally subjected to a thermal treatment at 520 °C for 8 h in the presence of dry air to remove ammonia and convert the MCM-41 into the H^+ form.

Synthesis of steamed H-MCM-41 zeolite

Steam was passed over H-MCM-41 (SiO_2/Al_2O_3 = 60) at 520 °C for 6 h in the first stage. In the second stage mesoporous material steamed as above was further steamed for another 7 h at 520 °C after a cooling period at 25 °C. This was followed by activation of the material at this temperature under dry air.

Synthesis of Al^{3+}-MCM 41 zeolite

1.5 gm of K^+-MCM 41 (SiO_2/Al_2O_3 = 15) was suspended in 50 ml of 0.05 M $Al_2(NO_3)_3{\cdot}9H_2O$ solution and heated at 90 °C with agitation for 6 h for Al^{3+} exchange reaction. The solid material was filtered off, air-dried and calcined at 550 °C in air for 5 h.

Temperature programmed desorption studies

Temperature programmed desorption (TPD) of NH_3 was carried out[15] in a TPD unit. 50 mg of H-MCM-41 sample was

Green Context

Alkylphenols are widely used in areas including UV-absorbers, heat stabilisers and antioxidants. Both alkylation and dealkylation (including transalkylation) are important processes in industry and alternatives to the traditional acid catalysts ($AlCl_3$, H_2SO_4, *etc.*) are required. Here the mesoporous solid acid H-MCM-41 is shown to be an efficient and environmentally benign catalyst for the conversion of 2,6-di-*tert*-butylphenol into mono and tri-*tert*-butylphenols under solvent free conditions. Reaction conditions can be used to help control the product selectively. *JHC*

DOI: 10.1039/b207276a

placed in a pulse reactor and calcined at 550 °C in a flow of He for 2 h. The temperature of the reactor was then brought down to 120 °C. Then a series of 0.5 ml NH_3 gas pulses were injected at 120 °C. The pulses were continued until no more uptake of NH_3 was observed. The system was flushed with He for 30 min and then the adsorbed NH_3 was desorbed at a programmed heating rate of 10 °C min^{-1}. The desorbed NH_3 was detected by a thermal conductivity detector and estimated.

Reaction of 2,6-di-*tert*-butylphenol with H-MCM-41

2,6-Di-*tert*-butylphenol (Fluka, Switzerland; ⩾ 97%(GC); 3.8 g, 18 mmol) and H-MCM-41 (200 mg) were mixed in a small round bottomed flask provided with a magnetic pellet, condenser and N_2 blanket. The flask was immersed in an oil -bath maintained at 160 °C. The reaction mixture was agitated with vigorous stirring for the specified period. Then the flask was removed from the oil-bath and the catalyst removed by filtration. The products were isolated by column chromatography, recrystallised and identified by mp, elemental analysis, GC-MS and comparison with authentic samples. Quantification was carried out on Shimadzu 15A gas chromatograph using a 5 m long 1.5 wt% OV-17 column on a FID detector.

Results and discussion

Disproportionation, isomerization and de-*tert*-butylation of 2,6-di-*tert*-butylphenol

2,6-Di-*tert*-butylphenol (2,6-DTBP) easily undergoes a disproportionation reaction (Fig. 1) to give 2-*tert*-butylphenol (2-TBP) and 2,4,6-tri-*tert*-butylphenol (2,4,6-TTBP) in the presence of an acid catalyst. The sterically hindered phenol 2,4,6-TTBP in a subsequent reaction is converted into 2,4-di-*tert*-butylphenol (2,4-DTBP) and di and triisobutylene. It is also possible that 2,6-DTBP and 2-TBP undergo isomerization to give 2,4-DTBP and 4-TBP, respectively. The dialkylated phenol 2,4-DTBP can undergo further de-*tert*-butylation to give the stable 4-*tert*-butylphenol (4-TBP) and isobutylene oligomer depending upon the acidity of catalysts.

Evaluation of catalysts

Several catalysts such as $FeCl_3$, $ZrOCl_2{\cdot}xH_2O$, H-Beta zeolite, H-ZSM5, H-Y zeolite and H-MCM-41 have been employed for the above reaction at 120–160 °C under solvent free conditions (Table 1). $FeCl_3$ is an active catalyst and 2,4,6-TTBP and 2,4-DTBP are the major products in CCl_4 medium. In solvent-free conditions 2,4-DTBP is the predominant product followed by 4-TBP as the next major product. With methanesulfonic acid (MSA) catalyst both 2,4-DTBP and 4-TBP are formed as the main products but the difference in yield of these products is much lowered. In this case 2% 2-octyl-4-*tert*-butylphenol is also formed by the alkylation of 4-*tert*-butylphenol and diisobutylene. Both microporous H-ZSM-5 (pore size = 5 Å) and H-Y zeolite exhibited no activity. Over medium pore H-Beta zeolite (pore size = 8 Å) at 29% conversion of 2,6-DTBP, 2-TBP and 4-TBP are predominantly formed. On the other hand the mesoporous material H-MCM-41 (pore size ~30 Å) is an excellent catalyst for the disproportionation followed by de-*tert*-butylation of 2,6-DTBP leading to predominant formation of 2,4-DTBP and 4-TBP. H-MCM-41 recovered at the end of the reaction by filtration, washed with acetone and dried at 270 °C in air was reused for a further two cycles and showed excellent activity and selectivity towards the products 2,4-DTBP and 4-TBP. It is interesting to note that the product profile with this material is quite similar to that produced with MSA except for 2-octyl-4-*tert*-butylphenol. Among the zeolite materials the pore size is quite critical suggesting that the reaction takes place inside the cavities of the alumino silicates.

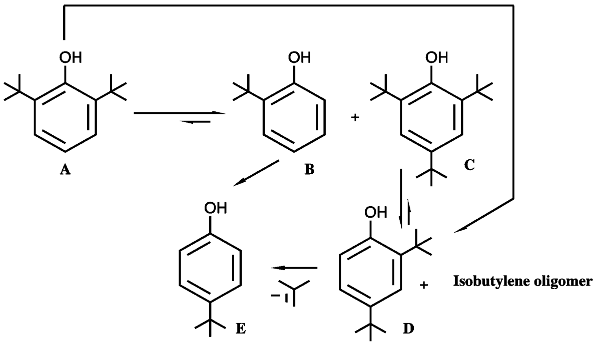

Fig. 1 Disproportionation, isomerization and de-*tert*-butylation of 2,6-DTBP.

Effect of temperature

The effect of temperature on conversion of 2,6-DTBP using H-MCM-41 was studied in the temperature range 100–180 °C and results are summarized in Fig. 2. At low temperature (100 °C), 2-TBP is the predominant product and the yield of 2,4,6-TTBP is maximum. At this temperature, formation of 2-TBP from 2,6-DTBP *via* disproportionation and direct de-*tert*-butylation, is the dominant reaction. At 180 °C, yields of both 2-TBP and 2,4,6-TTBP are minimum. 2,4,6-TTBP being sterically hin-

Table 1 Reaction of 2,6-di-*tert*-butylphenol under various reaction conditions

Entry	Catalyst	Reaction conditions [a]	Conversion of 2,6-DTBP (%)	Selectivity (%) 2-TBP	2,4,6-TTBP	2,4-DTBP	4-TBP
1	$FeCl_3$	CCl_4 = 4 ml; 85 °C; 2 h	83	8.8	14.8	65.4	11
2	$FeCl_3$	160 °C; 2 h	99.5	—	1.8	79.2	19
3	CF_3SO_3H[b]	160 °C; 2 h	99.9	2.5	1.0	56.5	38
4	H-Beta zeolite	160 °C; 3 h	29	48.4	7.0	19.7	24.9
5	H-ZSM5	160 °C; 2 h	0	—	—	—	—
6	H-Y Zeolite	120 °C; 4 h	0	—	—	—	—
7	$ZrOCl_2{\cdot}xH_2O$	160 °C; 3 h	8	94.6	—	5.4	—
8	γ-Al_2O_3	160 °C; 3 h	0	—	—	—	—
9	H-MCM-41 (SiO_2/Al_2O_3 = 30)	160 °C; 3 h	100	2.3	1.4	55.9	40.4
10	1st recycle of above catalyst	160 °C; 3 h	99.8	2.2	1.7	58.6	37.5
11	2nd recycle of above catalyst	160 °C; 3 h	99.8	2.3	1.2	53.9	42.6

2,6-DTBP = 2,6-Di-*tert*-butylphenol; 2-TBP = 2-*tert*-butylphenol; 4-TBP = 4-*tert*-butylphenol; 2,4-DTBP = 2,4-di-*tert*-butylphenol; 2,4,6-TTBP = 2,4,6-tri-*tert*-butylphenol.[a] 2,6-DTBP = 3.8 g; catalyst = 0.2 g. [b] Catalyst = 0.022 g; selectivity to 2-octyl-4-*tert*-butylphenol = 2.

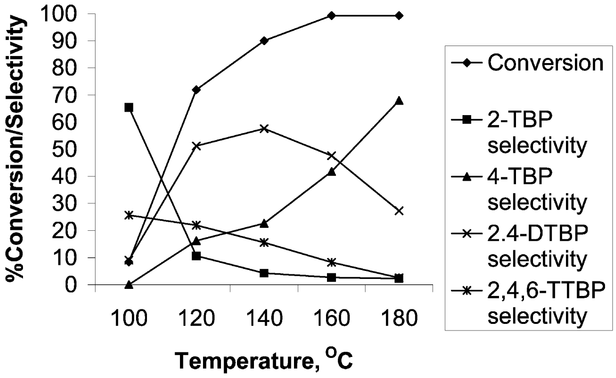

Fig. 2 Effect of temperature on conversion of 2,6-DTBP catalyzed by H-MCM-41.

dered undergoes de-*tert*-butylation quite rapidly to give 2,4-DTBP and 4-TBP as the temperature is increased. In the temperature range 120–180 °C, 2,6-DTBP may undergo direct isomerization to 2,4-DTBP with steady increase in selectivity up to 140 °C and beyond this temperature the selectivity to this phenol decreases. When the temperature is increased to 180 °C, 4-TBP becomes the dominant product possibly because of its thermal stability. The de-*tert*-butylation, disproportionation and isomerization reactions of the dialkylated and monoalkylated phenols are very sensitive to temperature and they occur on the acidic sites of H-MCM-41 within a narrow 40 °C temperature range leading to different yields of products.

The effect of temperature on the conversion of 2,6-DTBP using H-MCM-41 steamed for 6 h at 520 °C is shown in Fig. 3. It is interesting to note that formation of 4-TBP takes place above 100 °C both in presence of steamed and the original H-MCM-41 (SiO_2/Al_2O_3 = 60).

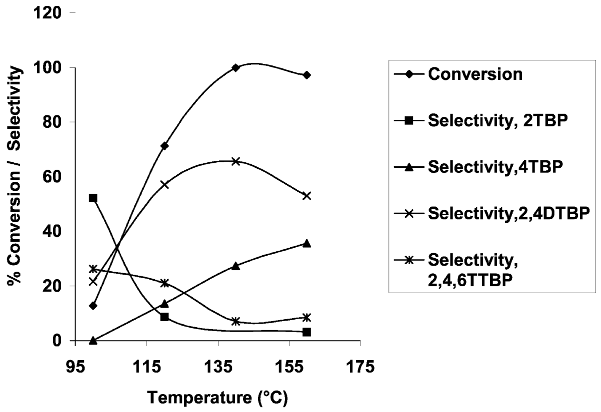

Fig. 3 Effect of temperature on conversion of 2,6-DTBP catalyzed by steamed (6 h) H-MCM-41.

Effect of reaction time

The effect of reaction time on conversion of 2,6-DTBP was studied at 160 °C and the results are given in Fig. 4. In 45 min 91.5% of 2,6-DTBP is converted into products and by 3 h the reaction is almost complete. Results given in Fig. 4 clearly suggest that over a period of time products 2-TBP, 2,4,6-TTBP and 2,4-DTBP derived from 2,6-DTBP tend to become 4-TBP.

Effect of substrate/catalyst weight ratio

To arrive at the optimum substrate/catalyst weight ratio, conversion of 2,6-DTBP was studied in the weight ratio of 19–136 at 160 °C over a period of 3 h (Table 2). As the interaction of substrate with the active sites occurs within the pores of H-MCM-41 the diffusion of the substrate into the pores is quite critical and hence the substrate/catalyst ratio becomes an important factor in this reaction. At a weight ratio of 136 only about 79% of 2,6-DTBP is converted into products over H-MCM-41 (SiO_2/Al_2O_3 = 60). The conversion, however, depends upon the acidity of the HMCM-41 employed.

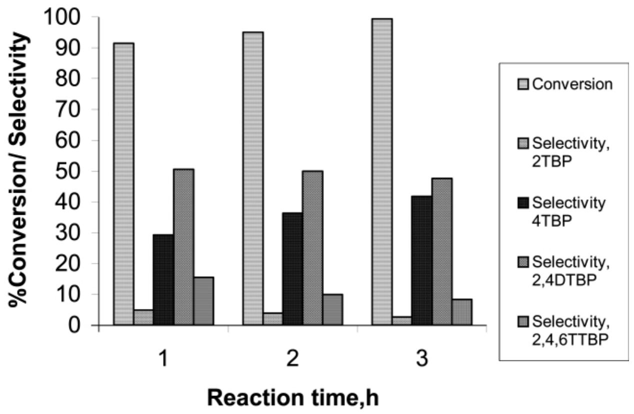

Fig. 4 Effect of reaction time on conversion of 2,6-DTBP and selectivity of products catalyzed by H-MCM-41.

Effect of acidity

As the acid sites play an important role in the conversion of 2,6-DTBP, the acidity of H-MCM-41 was varied by changing the SiO_2/Al_2O_3 ratio, steaming, and Al^{3+}cation exchange. The total acid density of the H-MCM-41 materials, measured by NH_3 adsorption followed by desorption by TPD, is given in Table 3. The effect of these solids on the reaction of 2,6-DTBP as well as the selectivity of various products formed is shown in Table 4. A cursory look at Table 2 reveals that H-MCM-41 steamed for 6 h has higher turnover than H-MCM-41 as such. H-MCM-41 steamed for 13 h has lower acidity than the aluminosilicate steamed for 6 h and other H-MCM-41 catalysts investigated in this study. Both 2-TBP and 2,4,6-TTBP are formed in equal proportions suggesting that this low acidic material is suitable for disproportionation of 2,6-DTBP. During steaming, Al^{3+} ions are lost from the aluminosilicate framework resulting in a decrease in acidity (Table 3).

It is observed that generally turnovers of products 2-TBP, 2,4,6-TTBP and 2,4-DTBP decreases whereas turnover of 4-TBP increases with increase in acidity. At high acidity, de-*tert*-butylation and isomerization dominate leading to more stable 4-TBP. In the presence of steamed H-MCM-41, the acid density is decreased and formation of 2,4-DTBP is relatively more than that formed with H-MCM-41. When Al^{3+}exchanged MCM-41 is used, formation of 2,4-DTBP is decreased and even de-*tert*-butylation of mono-*tert*-butylphenols to phenol takes place. This clearly shows Lewis acid sites on the H-MCM-41 are catalyzing the de-*tert*-butylation reaction and influence the composition of the products. On the other hand when K^+-MCM-41 is used the conversion of 2,6-DTBP is reduced. Selectivity to 2-TBP is high similar to the performance of the other low acidic materials. Selectivity of 4-TBP is moderate suggesting that Brönsted acid sites are essential for isomerization of 2-TBP to 4-TBP.

Mechanism

Disproportionation, isomerization and de-*tert*-butylation are the three main reactions taking place in the conversion of 2,6-DTBP with H-MCM-41 catalyst. All these reactions take place within the pores of aluminosilicates. Disproportionation of 2,6-DTBP

Table 2 Effect of H-MCM-41 catalyst concentration on conversion of 2,6-di-*tert*-butylphenol and turnovers of the products

				Selectivity (%)			
Entry	Catalyst	Weight of cata lyst/g	Conversion of 2,6-DTBP (%)	2-TBP	2,4,6-TTBP	2,4-DTBP	4-TBP
1	H-MCM-41 (SiO_2/Al_2O_3 = 60)	0.2	99.4 (113.6)	2.6 (3)	8.3 (9.4)	47.6 (54)	41.8 (47.2)
2	H-MCM-41 (SiO_2/Al_2O_3 = 60)	0.095	98.7 (254.9)	1.5 (3.9)	9.3 (23.7)	50 (127.6)	39.1 (99.7)
3	H-MCM-41 (SiO_2/Al_2O_3 = 60)	0.05	95.7 (471.8)	3.5 (16.6)	11 (51.9)	50 (235.9)	35.5 (167.4)
4	H-MCM-41 (SiO_2/Al_2O_3 = 60)	0.028	78.9 (697)	9.3 (64.8)	14.6 (102)	49.9 (347.6)	26.2 (182.6)
5	Steamed (6 h) H-MCM-41 (SiO_2/Al_2O_3 = 60)	0.2	97.2 (142.8)	3 (3)	8.4 (12)	52.9 (75.6)	35.6 (50.8)
6	Steamed (6 h) H-MCM-41 (SiO_2/Al_2O_3 = 60)	0.028	94.2 (939)	4.1 (34.4)	13.6 (114.2)	55.7 (467.2)	26.6 (223.2)
7	Steamed (13 h) H-MCM-41 (SiO_2/Al_2O_3 = 60)	0.025	71.9 (846)	12.2 (103)	12.8 (108)	51.6 (437)	23.4 (198)
8	H-MCM-41 (SiO_2/Al_2O_3 = 30)	0.2	100 (105.9)	2.3 (2.4)	1.4 (1.5)	55.9 (59.2)	40.4 (42.8)
9	H-MCM-41 (SiO_2/Al_2O_3 = 30)	0.028	98.4 (79.2)	2.8 (22.4)	7.9 (62.9)	55.8 (442.2)	33.4 (264.5)
10	H-MCM-41 (SiO_2/Al_2O_3 = 15)	0.2	98.6 (125.2)	3.4 (3.3)	0.7 (0.7)	45.5 (43.2)	50.4 (48)
11	H-MCM-41 (SiO_2/Al_2O_3 = 15)	0.028	99.6 (689.2)	1.1 (7.9)	0.5 (3.5)	61.8 (425.7)	36.6 (252.1)
12[a]	K^+-MCM-41 (SiO_2/Al_2O_3 = 15)	0.1	45.3 (107.2)	29.3 (31.4)	11.5 (12.4)	44.5 (47.7)	14.7 (15.7)

2,6-DTBP = 3.8 g; 160 °C; 3 h; Values in parentheses are turnover. Turnover = mol of product/mol of acid sites of MCM-41.[a] 0.1 g catalyst employed.

Table 3 MCM-41 with various SiO_2/Al_2O_3 and the acid density values

Entry	SiO_2/Al_2O_3	Type of MCM-41 zeolite	NH_3 desorbed per g/mmol
1	15	H-MCM-41	0.891
2	30	H-MCM-41	0.811
3	60	H-MCM-41	0.77
4	—	Steamed H-MCM-41 (6 h) (SiO_2/Al_2O_3 = 60)	0.688
5	—	Steamed H-MCM-41 (13 h) (SiO_2/Al_2O_3 = 60)	0.652
6	15	Al^{3+}-MCM-41	0.8615
7	15	K^+-MCM-41	0.744

Table 4 Effect of acidity of catalyst on conversion and selectivity of the products formed from 2,6-DTBP

			Selectivity (%)			
Entry	SiO_2/Al_2O_3	Conversion of 2,6-DTBP (%)	2-TBP	2,4,6-TTBP	2,4-DTBP	4-TBP
1	15	98.6	3.4	0.7	45.5	50.4
2	30	100	2.3	1.4	55.9	40.4
3	60	99.4	2.6	8.3	47.6	41.8
4	Steamed (6 h) H-MCM-41 (SiO_2/Al_2O_3 = 60)	97.2	3.0	8.4	52.9	35.6
5[a]	Steamed (13 h) H-MCM-41 (SiO_2/Al_2O_3 = 60)	71.9	12.2	12.8	51.6	23.4
6[b]	K-MCM-41 (SiO_2/Al_2O_3 = 15)	45.3	29.3	11.5	44.5	14.7
7[c]	Al-MCM-41 (SiO_2/Al_2O_3 = 30)	99.9	2.4	1.1	49.8	43.8

2,6-DTBP = 3.8 g; MCM41 = 0.2 g; 160 °C; 3 h.[a] 0.025 g catalyst. [b] 0.1 g catalyst. [c] Phenol (selectivity = 2.9) is also formed as a product.

to 2-TBP and 2,4,6-TTBP must be taking place on Bronsted acid sites whereas de-*tert*-butylation is clearly catalyzed by Lewis acid sites. Isomerization of 2-TBP to 4-TBP is facile over Bronsted acid sites. On the other hand isomerization of 2,6-DTBP to 2,4-DTBP is favoured over both Bronsted and Lewis sites.

Conclusions

We have found that mesoporous H-MCM-41 shows very good activity for disproportionation, de-*tert*-butylation and isomerization of 2,6-DTBP to give 2-TBP, 2,4,6-TTBP, 2,4-DTBP and 4-TBP in solvent free conditions. Reaction conditions control the product pattern. 2,4-DTBP and 4-TBP are the major products formed in this reaction. All products are most likely formed inside the channels and on acidic sites of the mesoporous material. The catalyst is recyclable and offers an environment-friendly route to synthesize the products from 2,6-DTBP.

Acknowledgments

The authors are grateful to the management of Indian Petrochemical Corporation Ltd., Baroda for permission to publish this work. The technical assistance of Mr K. N. Solanki is greatly acknowledged.

References

1 J. F. Lorenc, G. Lambeth and W. Scheffer, in *Encyclopedia of Chemical Technology*, ed. J. I. Kroschwitz and M. Howe-Grant, John Wiley & Sons, New York, 4th edn., 1992, vol. 2, p. 113.
2 S. Subramanian, A. Mitra, C. V. V. Suryanarayana and D. K. Chakrabarthy, *Appl. Catal. A*, 1997, **159**, 229.
3 K. Zang, D. Xu, H. Zhang, S. Lu, C. Huang, H. Xiang and H. Li, *Appl. Catal. A*, 1998, **166**, 89.
4 C. D. Chang and S. D. Hellring, *US Pat.*, 5288 927, 1994.
5 A. Corma, H. Garcia and J. Primo, *J. Chem. Res. (S)*, 1988, 40.
6 S. K. Badamali, A. Sakthivel and P. Selvam, *Chem. Lett.*, 2000, **65**, 153.
7 I. V. Kozhevnikov, A. I. Tsyganok, M. N. Timofeeva, S. M. Kulikov and U. N. Sidelnikov, *React. Kinet. Catal. Lett.*, 1992, **46**, 17.
8 F. Bigi, M. L. Conforti, R. Maggi, A. Mazzacani and G. Sartori, *Tetrahedron Lett.*, 2001, **42**, 6543.
9 M. A. Harmer, Q. Sun, A. J. Vega, W. E. Farneth, A. Heidekum and W. F. Hoelderich, *Green Chem.*, 2000, **2**, 7.
10 M. Tashiro, T. Yamato and G. Fukata, *J. Org. Chem.*, 1978, **43**, 1413.
11 M. Hajek and M. T. Radoiu, *J. Mol. Catal. A: Chem.*, 2000, **160**, 383.
12 I. V. Kozhevnikov, S. N. Kulikov, M. N. Timofeeva and T. P. Titov, *React. Kinet. Catal. Lett.*, 1991, **45**, 257.
13 G. A. Olah, G. K. S. Prakash, P. S. Iyer, M. Tashro and T. Yamato, *J. Org. Chem.*, 1987, **52**, 1881.
14 W. M. Kruse and J. F. Stephen, *US Pat.*, 4482755, 1984.
15 A. Wali, S. Muthukumaru Pillai, S. Unnikrishnan and S. Satish, *J. Mol. Catal. A: Chem.*, 1996, **109**, 149.
16 A. Wali, S. Muthukumaru Pillai and S. Satish, in *Catalysis: Present and Future (International Series on Chemical Engineering)*, ed. P. Kanta Rao and R. S Beniwal, Wiley Eastern Ltd., New Delhi, 1995, p. 167.

Amberlyst-15®: a novel and recyclable reagent for the synthesis of 1,5-benzodiazepines in ionic liquids

J. S. Yadav,* B. V. S. Reddy, B. Eshwaraiah and K. Anuradha

Division of Organic Chemistry, Indian Institute of Chemical Technology, Hyderabad-500 007, India. E-mail: yadav@iict.ap.nic.in; Fax: 91-40-7160512

Received 5th July 2002
First published as an Advance Article on the web 18th October 2002

The solid acid, Amberlyst-15® immobilized in the air- and moisture-stable ionic liquid, 1-butyl-3-methylimidazolium hexafluorophosphate is found to catalyze efficiently the condensation of *o*-phenylenediamines with ketones under mild conditions to afford the corresponding 1,5-benzodiazepine derivatives in high yields with high selectivity.

Introduction

Benzodiazepines are an important class of bioactive molecules, widely used as anticonvulsant, antianxiety and hypnotic agents.[1,2] Some benzodiazepine derivatives are used as dyes for acrylic fibers[3] in photography and also as anti-inflammatory agents.[4] Particularly, 1,5-benzodiazepines are useful precursors for the synthesis of some fused ring benzodiazepine derivatives[5] such as triazolo-, oxadiazolo-, oxazino- or furanobenzodiazepines. Despite their wide range of pharmacological activity, industrial, and synthetic applications, the synthesis of 1,5-benzodiazepines has received little attention.[6] Also, there are no reports on the use of heterogeneous solid acids such as clays, zeolites and ion exchange resins for the synthesis of 1,5-benzodiazepines of biological and synthetic importance. The use of recyclable solid acid catalysts makes the process convenient, economic and environmentally benign.

One of the prime concerns of industry and academia is the search for replacements to the environmentally damaging solvents used on a large scale, especially those that are volatile and difficult to handle. As a result, several environmentally benign procedures have successfully been developed to avoid, or at least minimize, these effects. Ionic liquids have recently gained recognition as possible environmentally benign alternative solvents in various chemical processes.[7] Room-temperature ionic liquids, especially those based on the 1-*n*-alkyl-3-methylimidazolium cation, have shown great promise as an attractive alternative to conventional solvents. They provide an eco-friendly reaction medium for a variety of organic transformations, as they are non-volatile, recyclable, non-explosive, easy to handle, thermally robust, and in addition they are compatible with various organic compounds and organometallic reagents.[8] Enhanced reaction rates and improved selectivity have been obtained in ionic liquids compared to normal solvents. Several organic reactions catalyzed by ionic liquids have been reported with high performance.[9] Because of distinct advantages of ionic liquids, they can make a great contribution to green chemistry.

Results and discussion

In view of the emerging importance of ionic liquids as novel reaction media, we wish to explore the use of ionic liquids as recyclable media for the synthesis of 1,5-benzodiazepine (Scheme 1).

Treatment of *o*-phenylenediamine with acetone in the presence of Amberlyst-15® immobilized in 1-butyl-3-methylimidazolium hexafluorophosphate ionic liquid resulted in the formation of 2,3-dihydro-2,2,4-trimethyl-1*H*-1,5-benzo[*b*]-[1,4]diazepine in 95% yield. In a similar fashion, various ketones reacted smoothly with *o*-phenylenediamines under these reaction conditions to give the corresponding 1,5-benzodiazepine derivatives in 85–95% yield. The reactions proceeded efficiently in high yields at ambient temperature under mild conditions. The crude products were purified either by recrystallization from *n*-hexane or by silica gel column chromatography. The reaction of cyclic ketones with *o*-phenylenediamine in the presence of Amberlyst-15® immobilized in 1-butyl-3-methylimidazolium hexafluorophosphate ionic liquid afforded fused ring 1,5-benzodiazepine derivatives in good yields. All the products were characterized by ^{1}H NMR, IR and mass spectral analysis and also by comparison with authentic samples.[5] The reactions of various ketones with *o*-phenylenediamines in the presence of Amberlyst-15®, were studied in hydrophilic 1-butyl-3-methylimidazolium tetrafluoroborate ([bmim]BF_4) and hydrophobic 1-butyl-3-methylimidazolium

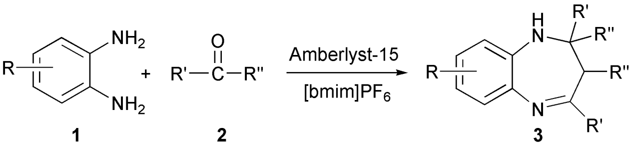

Scheme 1

Green Context

The combination of green chemical technologies will often prove to be the best way to progress the application of the principles of green chemistry to improving the environmental performance of chemical processes. Here we see this demonstrated in a new cleaner synthesis route to benzodiazepines. These are important biologically active compounds used in areas including hypnotic agents and anticonvulsants. Solid acid catalysts are found to be active in the key condensation step of reacting *o*-phenylenediamines with ketones thus easing separation and minimising salt waste. By conducting the reactions in ionic liquids, the reactions are particularly efficient and avoid VOC-related problems.

JHC

DOI: 10.1039/b206558b

hexafluorophosphate ([bmim]PF_6) ionic liquids. Among these ionic liquids, 1-Butyl-3-methylimidazolium tetrafluoroborate ([bmim]BF_4) was found to be superior in terms of yields and reaction rates and the results are presented in Table 1. The advantage of the use of ionic liquids as novel reaction media for this transformation is that ease of catalyst/substrate separation provided by a heterogeneous catalyst. Since the products were weakly soluble in the ionic phase, they were easily separated by simple extraction with diethyl ether. The rest of the viscous ionic liquid was thoroughly washed with ether and reused in subsequent reactions. While the products were obtained in the same purity as in the first run the yields were gradually decreased in runs carried out using recycled ionic liquid. For example, the reaction of *o*-phenylenediamine and acetone afforded the corresponding 2,3-dihydro-1,5-benzodiazepine in 95, 87, 85 and 81% yields over four cycles. The decrease in yield using recycled ionic liquid may be attributed to the *in situ* formation of water in the reaction. However, the activity of ionic liquid was consistent in runs and no decrease in yield was obtained when recycled ionic liquid was activated in each cycle

Table 1 Amberlyst-15® promoted synthesis of 1,5-benzodiazepine in ionic liquids

				[bmim]BF_4		[bmim]PF_6	
Entry	Diamine	Ketone	Product[a]	Time/h	Yield[b] (%)	Time/h	Yield[b] (%)
a	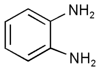	CH_3COCH_3	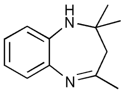	3.5	95	5.0	90
b	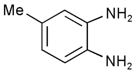	CH_3COCH_3	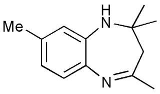	3.0	92	4.5	87
c	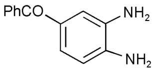	CH_3COCH_3	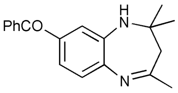	4.5	90	5.5	85
d	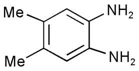	CH_3COCH_3	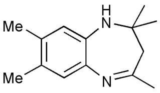	3.0	93	5.0	92
e	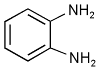	$PhCOCH_3$	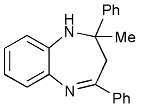	4.0	89	5.5	85
f	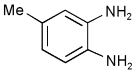	$PhCOCH_3$	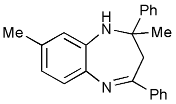	4.5	91	6.5	87
g	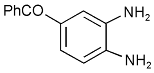	$PhCOCH_3$	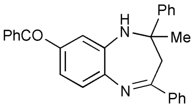	5.0	85	6.5	80
h	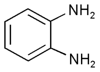	$CH_3COCH_2CH_3$	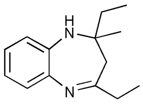	4.0	88[c]	5.0	85[c]
i	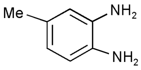	$CH_3COCH_2CH_3$	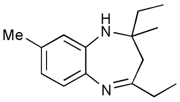	3.5	90[c]	4.5	87[c]
j	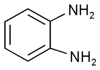	$CH_3CH_2COCH_2CH_3$	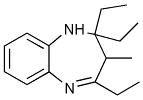	4.0	89	6.0	83
k	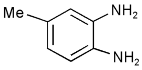	$CH_3CH_2COCH_2CH_3$	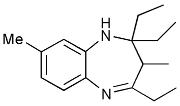	3.0	90	4.0	85
l	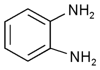	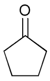	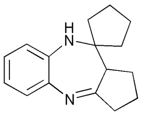	4.5	85	5.0	82
m	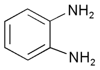	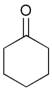	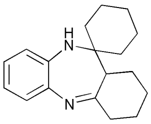	5.0	87	6.0	80

[a] All products were characterized by ^1H NMR, IR and mass spectra. [b] Isolated and unoptimized yields. [c] 5–10% of the other regioisomeric product was observed in the ^1H NMR spectrum of the crude product.

at 80 °C under vacuum. Furthermore, the products were formed in low yields (30–45%) when the reactions were carried out using acid resin in a mixture of water and [bmim]PF_6 ionic liquid (1:1). Finally, the catalytic performances of various quaternary ammonium salts were studied. The condensation of ketones with *o*-phenylenediamine was not successful when *n*-tetrabutylammonium chloride (*n*-Bu_4NCl) or 1-*n*-butyl-3-methylimidazolium chloride (BMImCl) was used as reaction media. We have also performed the reactions in polar organic solvents such as DMF and *N*-methylpyrrolidine to compare the efficiency of ionic liquids. The reactions did not proceed in these solvents even under heating (75–80 °C) in the presence of ion-exchange resin. However, the products were obtained in low to moderate yields (45–60%) when the reactions were carried out in chloroform in the presence of acid resin. Compared to conventional solvents, enhanced reaction rates, improved yields and high selectivity are the features obtained in ionic liquids. For example, the treatment of *o*-phenylenediamine with 2-butanone in the presence of acid resin in ionic liquid for 3.0–4.0 h afforded the corresponding product **3h** in 88% yield with only a trace amount of the other regioisomeric product (5%) whereas the same reaction in chloroform after 7 h gave the regioisomeric products in 60% yield in a 1:1 ratio. This clearly indicates the efficiency of ionic liquids for this transformation.

Conclusion

The paper describes a facile synthesis of 2,3-dihydro-1,5-benzodiazepines by the condensation of ketones with *o*-phenylenediamines using a heterogeneous solid acid, Amberlyst-15® in environmentally benign ionic solvents. The simple procedure combined with ease of recovery and reuse of this novel reaction media make this method economic, benign and a waste-free chemical process for the synthesis of 1,5-benzodiazepines of biological importance.

Experimental

Melting points were recorded on Buchi R-535 apparatus and are uncorrected. IR spectra were recorded on a Perkin-Elmer FT-IR 240-c spectrophotometer using KBr optics. ^1H and ^{13}C NMR spectra were recorded on Gemini-200 spectrometer in $CDCl_3$ using TMS as internal standard. Mass spectra were recorded on a Finnigan MAT 1020 mass spectrometer operating at 70 eV. 1-Butyl-3-methylimidazolium tetrafluoroborate ([bmim]BF_4) and 1-butyl-3-methylimidazolium hexafluorophosphate ([bmim]PF_6) ionic liquids were prepared according to the procedures reported in the previous literature.[10]

General procedure for the synthesis 2,3-dihydro-1,5-benzodiazepines

A mixture of *o*-phenylenediamine (1 mmol), ketone (2.5 mmol), and Amberlyst-15® (0.75 g) in 1-butyl-3-methylimidazolium hexafluorophosphate or 1-butyl-3-methylimidazolium tetrafluoroborate (2 mL) was stirred at ambient temperature for an appropriate time (Table 1). After completion of the reaction, as indicated by TLC, the reaction mixture was washed with diethyl ether (3 × 10 mL). The combined ether extracts were concentrated *in vacuo* and the resulting product was directly charged on a small silica gel column and eluted with ethyl acetate–*n*-hexane (2:8) to afford the pure diazepine. The remainder of the viscous ionic liquid was further washed with ether and recycled in subsequent reactions. Spectral data for selected products: **3a**: solid, mp 137–138 °C, ^1H NMR ($CDCl_3$): δ 1.35 (m, 6H, 2-CH_3), 2.25 (s, 2H, –CH_2–), 2.35 (s, 3H, 3-CH_3) 3.45 (br s, NH), 6.55–7.20 (m, 4H). ^{13}C NMR (Proton decoupled, $CDCl_3$): δ 29.7, 30.4, 44.9, 68.3, 121.6, 122.0, 125.4, 126.7, 137.8, 140.6, 172.3. EIMS: *m*/*z* 188 [M^+], 173, 132, 104, 77, 65. IR (KBr) ν/cm^{-1}: 3340, 1638, 1595. **3e**: Solid, mp 150–152 °C, ^1H NMR ($CDCl_3$): δ 1.80 (s, 3H), 2.95 (d, 1H, *J* = 12.8 Hz), 3.15 (d, 1H, *J* = 12.8 Hz) 3.45 (br s, NH), 6.55–7.0 (m, 3H), 7.15–7.35 (m, 7H), 7.55–7.65 (m, 4H). ^{13}C NMR (Proton decoupled, $CDCl_3$): δ 29.7, 42.9, 73.3, 121.2, 121.4, 125.2, 126.1, 126.8, 126.9, 127.8, 128.1, 128.5, 129.5, 137.9, 139.5, 139.9, 147.4, 167.3. EIMS: *m*/*z* 312 [M^+], 297, 235, 194, 103, 77, 40. IR (KBr) ν/cm^{-1}: 3320, 1631, 1597. **3j**: Solid, mp 143–145 °C, ^1H NMR ($CDCl_3$): δ 0.70–1.0 (m, 10H), 1.20–1.38 (m, 4H), 1.50–1.65 (m, 2H), 2.40–2.60 (m, 2H), 2.87 (q, 1H, *J* = 6.8 Hz), 3.65 (br s, NH), 6.58 (d, 1H, *J* = 8.0 Hz), 6.65 (t, 1H, *J* = 8.0 Hz), 6.90 (t, 1H, *J* = 8.0 Hz), 7.38 (d, 1H, *J* = 8.0 Hz). ^{13}C NMR (Proton decoupled, $CDCl_3$): δ 7.4, 7.8, 11.4, 12.1, 28.0, 28.4, 35.6, 46.2, 68.8, 117.5, 118.0, 126.7, 132.8, 13.9, 142.4, 173.8. EIMS: *m*/*z* 244 [M^+], 229, 215, 194, 103, 77, 40. IR (KBr) ν/cm^{-1}: 3320, 1631, 1597.

Acknowledgements

B. V. S. and K. A. thank CSIR, New Delhi, for the award of fellowships.

References

1 (*a*) H. Schutz, *Benzodiazepines*, Springer, Heidelberg, 1982; (*b*) J. K. Landquist, in, *Comprehensive Heterocyclic Chemistry*, ed. A. R. Katritzky and C. W. Rees, Pergamon, Oxford, 1984, vol. 1. pp. 166–170.

2 L. O. Randall and B. Kappel, *Benzodiazepines*, ed. S. Garattini, E. Mussini and L. O. Randall, Raven Press, New York, 1973, p. 27.

3 R. C. Haris and J. M. Straley, *US Pat.* 1,537,757, 1968; *Chem. Abstr.*, 1970, **73**, 100054w.

4 J. R. De Baun, F. M. Pallos and D. R. Baker, *US Pat.* 3,978,227, 1976; *Chem. Abstr.*, 1977, **86**, 5498d.

5 (*a*) M. Essaber, A. Baouid, A. Hasnaoui, A. Benharref and J. P. Lavergne, *Synth. Commun.*, 1998, **28**, 4097; (*b*) A. M. El-Sayed, H. Abdel-Ghany and A. M. M. El-Saghier, *Synth. Commun.*, 1999, **29**, 3561; (*c*) K. V. V. Reddy, P. S. Rao and D. Ashok, *Synth. Commun.*, 2000, **30**, 1825.

6 (*a*) M. S. Balakrishna and B. Kaboudin, *Tetrahedron Lett.*, 2001, **42**, 1127; (*b*) M. Curini, F. Epifano, M. C. Marcotullio and O. Rosati, *Tetrahedron Lett.*, 2001, **42**, 3193; (*c*) W. Zhong, Y. Zhang and X. Chen, *Tetrahedron Lett.*, 2001, **42**, 73.

7 (*a*) T. Welton, *Chem. Rev.*, 1999, **99**, 2071; (*b*) P. Wasserscheid and W. Keim, *Angew. Chem. Int. Ed.*, 2000, **39**, 3772.

8 (*a*) R. Sheldon, *Chem. Commun.*, 2001, 2399; (*b*) C. Wheeler, K. N. West, C. L. Liotta and C. A. Eckert, *Chem. Commun.*, 2001, 887; (*c*) J. Peng and Y. Deng, *Tetrahedron Lett.*, 2001, **42**, 5917.

9 (*a*) A. C. Cole, J. L. Jensen, I. Ntai, K. L. T. Tran, K. J. Weaver, D. C. Forbes and J. H. Jr. Davis, *J. Am. Chem. Soc.*, 2002, **124**, 5962; (*b*) C. Wheeler, K. N. West, C. L. Liotta and C. A. Eckert, *Chem. Commun.*, 2001, 887; (*c*) J. Peng and Y. Deng, *Tetrahedron Lett.*, 2001, **42**, 5917.

10 (*a*) S. Park and R. J. Kazlauskas, *J. Org. Chem.*, 2001, **66**, 8395; (*b*) P. Bonhote, A. P. Dias, N. Papageorgiou, K. Kalyanasundaram and M. Gratzel, *Inorg. Chem.*, 1996, **35**, 1168.

Clean synthesis of *F*-carboxylic esters of *sec*-alcohols and ω-haloalkyl alcohols

Takumi Taniguchi,[a] Eiji Hayashi[b] and Taizo Ono*[b]

[a] *Polymer Electrolyte Group, TOYOTA Central Research & Development Laboratories, 41-1, Yokomichi, Nagakute, Nagakute-cho, Aichi-gun 480-1192, Japan. E-mail: takumi@taniguchi.tec.toyota.co.jp*

[b] *Molecular Structure Design Group (MOSTG), Institute for Structural and Engineering Materials, National Institutes of Advanced Industrial Science and Technology (AIST), 2266-98, Anagahora, Shimoshidami, Moriyama-ku, Nagoya 463-8560, Japan. E-mail: t.ono@aist.go.jp*

Received 23rd July 2002
First published as an Advance Article on the web 21st October 2002

The addition reactions of *F*-carboxylic acids to terminal and cyclic olefins and of *F*-alkanoyl halides to cyclic ethers has been found to be useful for preparing *F*-carboxylic esters of *sec*-alcohols and ω-haloalkyl alcohols, respectively. Both types of reaction can be performed under solvent-free conditions and no accompanying by-products are formed; in some cases a 100% atom efficiency was achieved.

Introduction

So called "Green Chemistry" is being pursued in many areas of chemistry. The term, atom economy, introduced by Trost[1] is closely related to this concept. The reaction best satisfying these concepts is one in which all the starting materials are quantitatively incorporated into the products. An addition reaction could be such an example. We recently found two kinds of such addition reactions which could produce *F*-carboxylic esters. One is the addition of *F*-carboxylic acids to olefins and another is the addition of *F*-alkanoyl halides to ethers. Both reactions were conducted under solvent-free conditions and, if taking into account the recovery of the excess part of the starting materials, a 100% atom economy was attained in both reactions in some cases. The products are *F*-carboxylic esters of *sec*-alcohols and ω-haloalkyl primary alcohols which have various industrial uses such as repellents, lubricating oils, or as intermediates for further synthetic elaboration.[2] Both reactions are also interesting from a view point of recently proposed environmentally friendly techniques of fluorous synthesis[3] or of fluorous biphase strategy utilizing so called pony tails.[4] We here report on such reactions.

Results and discussion

The results of the reaction of *F*-carboxylic acids with a series of olefins are summarized in Table 1 and Scheme 1. The reaction proceeded by simply heating a mixture of the acid and excess olefin without a solvent. The conversion of **2a** to the adduct ester **3a** was as low as 41% under conditions of 2 h heating at 100 °C (entry 1), but 98% conversion was attained by 5 h heating at 150 °C (entry 3). The conversion was only 58% when heated at 150 °C for 1 h (entry 2). The products were easily purified by a simple distillation. The excess of olefin was easily recovered in a cold trap and thus are easily recyclable. The excess use of olefin is better if considering a conversion rate, but even when using stoichiometric concentrations a conversion and yield of 83 and 90%, respectively (entry 4), was achieved.[5] The reactivity of the shorter chain olefin, 1-hexene, is lower, but the use of a large excess of the olefin made it possible to attain

Green Context

Partially fluorinated organic molecules have proven to be among the most useful of functionalised compounds. Fluorocarboxylic esters for example, have numerous proven uses including lubricant oils and repellents. It is especially important that the synthesis of such expensive and often biologically active compounds is conducted under clean synthesis conditions. Here we see described highly atom efficient addition reactions to produce these compounds under solvent-free conditions. In this way we can achieve high utilisation of substrates and produce little waste. *JHC*

Table 1 Addition of *F*-carboxylic acids (*F*-3-pyrrolidino- and *F*-2-morpholino-propionic acids) to olefins

Entry	*F*-Acid	Olefin	Product	Ratio **2**:**1**	Temp./°C	Time/h	Conv. (%)	Yield[a] (%)
1	**1a**	**2a**	**3a**	6.5	100	2	41	96
2	**1a**	**2a**	**3a**	3.8	150	1	58	96
3	**1a**	**2a**	**3a**	3.8	150	5	98	96 (82)
4	**1a**	**2a**	**3a**	1.0	150	5	83	90
5	**1a**	**2b**	**3b**	5.3	150	5	92	96 (77)
6	**1a**	**2c**	**3c**	4.0	150	5	No reaction	
7	**1a**	**2d**	**3d**	4.0	150	5	79	98 (73)
8	**1b**	**2a**	**3e**	4.0	110	48	100	100

[a] The yields were calculated by ^{19}F NMR spectroscopy; isolated yields are in parentheses.

DOI: 10.1039/b207215g

almost the same levels in both conversion and yield (92 and 96%, entry 5).

The simplest olefin, ethylene, was completely inert in this reaction so that at least one alkyl substituent is necessary for this addition reaction. Cyclic olefin, **2d** is slightly less reactive than 1-octene, but again the reaction is clean with good (79% conversion and 98% yield, entry 7). Branched *F*-carboxylic acid, *F*-2-morpholinopropionic acid, **1b**, is much more reactive compared with *F*-3-pyrrolidinopropionic acid, thus 100% atom economy was obtained in this case (100% conversion and 100% yield).

We next investigated the addition of *F*-*n*-alkanoic acids (C_2, C_3, C_4, C_8) which are commercially available and have been widely used in industry. The best condition obtained in Table 1 was used as the protocol condition (Scheme 2). The results are summarized in Table 2. *F*-*n*-alkanoic acids are found to be less reactive than the *F*-carboxylic acids having *F*-heterocycle substituents (entry 1–4). However, both conversion and yield were synthetically meaningful in all the reactions investigated (71–82% conversions and more than 93% yields). The longer chain *F*-*n*-alkanoic acids (C_4, C_8) are more reactive than the shorter ones (C_2, C_3), but the reason for this difference of reactivity is not clear at the moment due to the lack of reliable acidity data for *F*-carboxylic acids. The acidity constant (K_a) of trifluoroacetic acid recently reported by Moroi *et al.*[6] is 0.32, contrasting with the long-believed value 0.58–1.8.[7] According to Moroi, K_a of *F*-*n*-butyric acid (C_4) is 0.23, thus less acidic than shorter chain acids, suggesting that there should be some factors other than the acidity on the addition rate as was seen in the case of the *F*-carboxylic acids having a *F*-heterocycle substituent. Of course, much less acidic non-fluoro carboxylic acids, for example, *n*-propionic acid did not react with 1-octene at all under the protocol condition, even for a prolonged reaction time (19 h). Certain cation-exchanged montmorillonites are reported to catalyze the direct addition of acetic acid to terminal alkenes, but high temperatures 200–220 °C are necessary and what is worse the products are a low selective mixture of 2- and 3-alkyl ester isomers.[8]

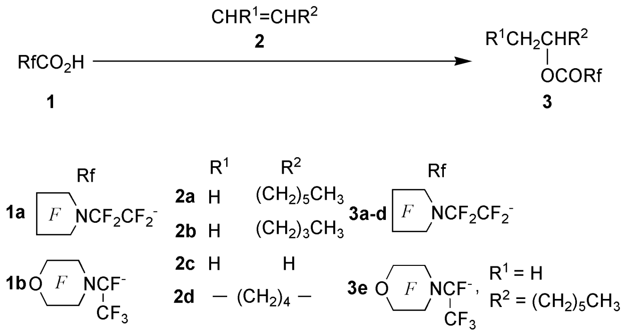

Scheme 1 *F* inside the rings denotes that all bonds are to fluorines.

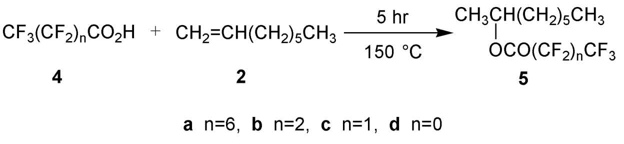

Scheme 2

Table 2 Addition of *F*-*n*-alkanoic acids to 1-octene

Entry	Reagent	Product	Ratio **2a**:**4**	Conv. (%)	Yields[a] (%)
1	**4a** (1.5 mmol)	**5a**	4.0	78.3	94.0 (66)
2	**4b** (3.0 mmol)	**5b**	4.0	81.5	94.5 (62)
3	**4c** (3.0 mmol)	**5c**	4.0	72.4	93.3 (63)
4	**4d** (3.0 mmol)	**5d**	4.0	70.8	93.2 (56)

[a] Yields were calcualted by ^{19}F NMR spectroscopy; isolated yields are in parentheses.

Another green process for preparing *F*-carboxylic esters by using *F*-alkanoyl halides is presented here (Table 3, Scheme 3). We have been interested in *F*-alkanoyl iodides as the key materials for the synthesis of fluoro organic compounds and have investigated a convenient preparative method[9] and also a new reaction *i.e.* metal catalyzed decarbonylative addition to olefins.[10] In the course of the investigation, we happened to find that *F*-octanoyl iodide **6a** added to tetrahydrofuran (THF) in a ring-opening manner to give ω-iodobutyl ester **7a** by simply mixing **6a** and THF at room temperature for 15 min. The reaction is so clean that **7a** was quantitatively obtained (entry 1). The Br-, Cl- and F-counterparts, **6b–d**, were totally inert under the same reaction condition (entries 2–4), but the reactions did proceed at a higher temperature of 100 °C to give ω-bromobutyl ester **7b** and ω-chlorobutyl ester **7c** in high yields (72.8 and 88.7%, respectively, entries 5 and 6). In contrast to **6a–c**, *F*-octanoyl fluoride **6d** did not react with THF at all (entry 7). This kind of acylative cleavage by the non-fluoro alkanoyl chloride has been known as a Stille deprotective method[11] of an ether linkage, but requires a palladium catalyst and trialkyltin chloride. Our reaction using *F*-alkanoyl iodide is very much superior to the Stille method which uses hazardous tin reagents. It is highly probable that *F*-alkanoyl iodides could be used for such a protective–deprotective method because the reaction proceeds under mild conditions and is also easily expected to be applicable to other organic functional groups.

Table 3 Addition of *F*-octanoyl halides to THF

Entry	X	Time	Temp.	Product	Yield[a] (%)
1	**6a** (X = I)	15 min	RT	**7a**	100
2	**6b** (X = Br)	48 h	RT	**7b**	0
3	**6c** (X = Cl)	48 h	RT	**7c**	0
4	**6d** (X = F)	48 h	RT	**7d**	0
5	**6b**	24 h	100 °C	**7b**	72.8
6	**6c**	72 h	100 °C	**7c**	88.7
7	**6d**	24 h	100 °C	**7d**	0

[a] NMR yield.

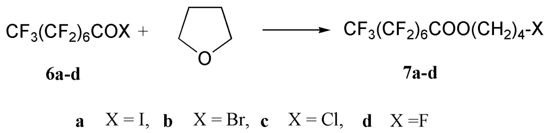

Scheme 3

Conclusions

Cleaner methods for the synthesis of *F*-carboxylic esters were realized by the addition reaction of *F*-carboxylic acids and *F*-alkanoyl halides to various olefins and ethers, respectively. By avoiding the use of hazardous reagents such as thionyl chloride and the need for organic solvents, together with the use of strongly electronegative groups in the carboxylic acids and alkanoyl halides, a number of successful reactions were accomplished.

Experimental

N-containing *F*-carboxylic acids **1a–c** were prepared according to the reported methods.[12] *F*-octanoyl halides **6a–c** were prepared by our new method.[13] *F*-Octanoyl fluoride **6d** was prepared by the reaction of *F*-octanoic acid with sulfur tetrafluoride.[14] All other reagents were used as purchased. IR spectra were measured on a JASCO IR-810 spectrometer by a capillary method using KBr disks. Mass spectra (EI, 70 eV) were run on a Shimadzu QP-5000 quadrupole mass spectrometer using a capillary column (60 m × 0.25 i.d., 1.5 mm NEUTRA BOND-1, GL Sciences Inc.). ^{1}H-, ^{19}F- and ^{13}C-NMR spectra were measured using $CDCl_3$ as solvent with a Varian Unity Inova-300 spectrometer operating at 299.95, 282.24 and 75.423 MHz, respectively. Chemical shifts of ^{1}H-, ^{19}F- and ^{13}C-NMR were reported on the δ scale. TMS was used as an internal standard for ^{1}H- and ^{13}C-NMR and $CFCl_3$ for ^{19}F-NMR. ^{13}C-NMR spectra were obtained with simultaneous decoupling of H and F nuclei.

General procedure for the addition of *F*-carboxylic acids to olefins

A typical procedure (a protocol condition) is exemplified by the reaction of *F*-(3-pyrrolidinopropionic acid) **1a** with 1-octene **2a**: compound **1a** (540 mg, 1.5 mmol) and **2a** (672 mg, 6 mmol) were placed in a 20 ml round-bottomed flask attached with a magnetic stirrer bar and a cooler. After introducing argon, the flask was heated in oil-bath maintained at 150 °C. The reagents were not miscible at room temperature, but became a clear homogenous mixture at 150 °C. After 5 h stirring, the reaction mixture was transferred into the Kugelrohr apparatus and distilled under reduced pressure (2–10 Torr). The fraction collected at 140 °C/2 Torr was the colorless liquid **3a** (546 mg, 82%); ^{19}F NMR: δ −133 (s, 4F), −119.2 (qnt, J = 10.3 Hz, 2F), −93.36 (qnt, J = 12.0 Hz, 2F), −90.62 (qnt, J = 11.1 Hz, 4F), ^{1}H NMR: δ 5.14 (sextet, J = 6.4 Hz, 1H), 1.70 (m, 1H), 1.60 (m 1H), 1.34 (t, J = 6.3 Hz, 3H), 1.28–1.35 (m, 8H), 0.89 (t, J = 7.2 Hz, 3H), ^{13}C NMR: δ 158.0, 113.4, 113.0, 107.8, 107.1, 77.24, 35.44, 31.62, 28.90, 24.98, 22.52, 19.42, 13.98, IR (KBr): 1778 ($\nu_{C=O}$), MS (EI, 70 eV): *m/z* 314 ($CF_2CF_2N(CF_2CF_2)_2$, 4.6), 43 (100). The reaction of **1a** with other olefins were conducted in the same manner to give: **3b**: (77%); ^{19}F NMR: δ −133 (s, 4F), −119.2 (qnt, J = 9.5 Hz, 2F), −93.36 (qnt, J = 12.0 Hz, 2F), −90.93 (tt, J = 12.0, 9.5 Hz, 4F), ^{1}H NMR: δ 5.14 (sextet, J = 6.5 Hz, 1H), 1.71 (m, 1H), 1.61 (m, 1H), 1.34 (d, J = 6.3 Hz, 3H), 1.29–1.37 (m, 4H), 0.91 (t, J = 6.6 Hz, 3H), ^{13}C NMR: δ 158.1, 113.4, 113.1, 107.8, 107.1, 77.30, 35.14, 27.17, 22.35, 19.42, 13.81, IR: 1778 ($\nu_{C=O}$), MS (EI, 70 eV): *m/z* 386 (1.6), 43 (100). **3d**: (73%); ^{19}F NMR: δ −133.0 (s, 4F), −119.3 (qnt, J = 9.9 Hz, 2F), −93.48 (qnt, J = 12.0 Hz, 2F), −90.63 (tt, J = 12.0, 9.9 Hz, 4F), ^{1}H NMR: δ 5.04 (tt, J = 8.7, 3.9 Hz, 1H), 1.91 (m, 2H), 1.78 (m, 2H), 1.57 (m, 3H), 1.40 (m, 3H), ^{13}C NMR: δ 157.8, 113.4, 113.1, 107.8, 107.1, 78.29, 30.95, 25.07, 23.26, IR: 1776 ($\nu_{C=O}$), MS (EI, 70 eV): *m/z* 314 (0.8), 82 (100). **3e**: (a 1:1 mixture of two inseparable diastereomers **3e-1** and **3e-2**, quantitative); ^{19}F NMR (tentatively assigned for each isomer): **3e-1** and **3e-2**: δ −140.1 (m, 1F), −88.27, −83.68 (AB quartet, J = 148 Hz, overlapped 8F), −75.87 (m, 3F); −142.5 (m, 1F), −93.47, −87.66 (AB quartet, J = 202 Hz, 4F), −93.14, −87.26 (AB quartet, J = 202 Hz, 4F), −76.71 (m, 3F), ^{1}H NMR (**3e-1** and **3e-2**): δ 5.13 (m, 1H), 1.70 (m, 1H), 1.60 (m, 1H), 1.33 (d, J = 6.3 Hz, 3H), 1.28–1.35 (m, overlapped, 8H), 0.89 (t, J = 7.2 Hz, 3H), ^{13}C NMR (overlapped except the asymmetric carbons C* and the carbons next to C*) **3e-1** and **3e-2**: δ 158.5, 158.4 (C=O), 119.1 (CF_3), 113.0, 110.7 ($O(CF_2CF_2)_2N$), 94.47, 94.40 (CF_3C^*N), 78.02, 77.91 (OC*), 35.28, 35.27 (OC^*CH_2), 31.62, 28.90, 24.79, 22.50 (CH_2), 18.97, 18.93 (CH_3C^*), 13.97 (CH_3), IR: 1778 ($\nu_{C=O}$), MS (EI, 70 eV) **3e-1** and **3e-2**: *m/z* 330 (9.6), 43 (100); 330 (7.4), 57 (100). **5a**: (66%); ^{19}F NMR: δ −126.62 (m, 2F), −123.14 (overlapped, 4F), −122.52 (br s, 2F), −122.08 (br s, 2F), −119.04 (t, J = 10.7 Hz, 2F), −81.27 (t, J = 10.3 Hz, 3F), ^{1}H NMR: δ 5.14 (sextet, J = 6.6 Hz, 1H), 1.70 (m, 1H), 1.61 (m, 1H), 1.34 (d, J = 6.3 Hz, 3H), 1.28–1.35 (overlapped, m, 8H), 0.88 (t, J = 6.4 Hz, 3H), ^{13}C NMR: δ 158.2 (C=O), 117.5, 111.14 (overlapped), 110.9 (overlapped), 108.9, 108.4, 77.29, 35.67, 31.75, 29.03, 25.06, 22.57, 19.45, 13.87, IR: 1778 ($\nu_{C=O}$), MS (EI, 70 eV): *m/z* 441 (0.6), 43 (100). **5b**: (62%); ^{19}F NMR: δ −127.5 (s, 2F), −120.0 (q, J = 8.1 Hz, 2F), −81.3 (t, J = 8.6 Hz, 3F), ^{1}H NMR: δ 5.14 (sextet, J = 6.4 Hz, 1H), 1.70 (m, 1H), 1.59 (m, 1H),1.34 (d, J = 6.4 Hz, 3H), 1.28–1.35 (overlapped, m, 8H), 0.89 (t, J = 6.3 Hz, 3H), ^{13}C NMR: δ 158.1 (C=O), 117.8 (CF_3), 108.5, 107.9, 77.23, 35.61, 31.69, 28.97, 25.01, 22.54, 19.44, 13.88, IR: 1778 ($\nu_{C=O}$), MS (EI, 70 eV): *m/z* 241 (2.2), 41 (100). **5c**: (63%); ^{19}F NMR: δ −122.32 (s, 2F), −83.35 (s, 3F), ^{1}H NMR: δ 5.14 (sextet, J = 6.4 Hz, 1H), 1.70 (m, 1H), 1.60 (m, 1H), 1.34 (d, J = 6.3 Hz, 3H), 1.28–1.35 (overlapped, m, 8H), 0.89 (t, J = 6.6 Hz, 3H), ^{13}C NMR: δ 158.2 (C=O), 118.1 (CF_3), 106.3, 77.0, 35.7, 31.7, 29.0, 25.1, 22.6, 19.5, 13.9, IR: 1778 (νC=O), MS (EI, 70 eV): *m/z* 191 (3.9), 41 (100). **5d**: (56%); ^{19}F NMR: δ −75.93, ^{1}H NMR: δ 5.10 (sextet, J = 6.4 Hz, 1H), 1.70 (m, 1H), 1.61 (m, 1H), 1.34 (d, J = 6.4 Hz, 3H), 1.28–1.35 (overlapped, m, 8H), 0.89 (t, J = 5.1 Hz, 3H), ^{13}C NMR: δ 157.4 (C=O), 114.9 (CF_3), 76.68, 35.67, 31.74, 29.02, 25.13, 22.58, 19.53, 13.91, IR: 1782 ($\nu_{C=O}$), MS (EI, 70 eV): *m/z* 141 (6.9), 41 (100).

General procedure for the addition of *F*-*n*-alkanoyl halides to the cyclic ether THF

A mixture of *F*-*n*-alkanoyl halides and 5 equivalents of THF was stirred at room temperature or 100 °C for a period of time shown in Table 3. The product was isolated by simple distillation. **7a**: (95%); ^{19}F NMR: δ −126.6 (m, 2F), −123.2 (m, 2F), −123.1 (m, 2F), −122.5 (br s, 2F), −122.1 (m, 2F), −118.8 (t, J = 12.1 Hz, 2F), 81.3 (t, J = 10.3 Hz, 3F), ^{1}H NMR: δ 4.42 (t, J = 6.0 Hz, 2H), 3.22 (t, J = 6.4Hz, 2H), 1.91 (m, 4H), ^{13}C NMR: δ 158.5 (C=O), 117.5, 111.1 (br by superposition), 110.8 (br by superposition), 108.8, 108.4, 67.4, 29.6, 29.4, 4.1. MS (EI, 70 eV): *m/z* 469 (M − I, 2.9), 55 (100). **7b**: (69%); ^{19}F NMR: δ −126.6 (m, 2F), −123.1 (m, 4F), −122.5 (br s, 2F), −122.1 (br s, 2F),−118.9 (t, J = 12.0 Hz, 2F), −81.3 (t, J = 9.5 Hz, 3F), ^{1}H NMR: δ 4.43 (t, J = 5.7 Hz, 2H), 3.44 (m, 2H), 1.97 (m, 4H), ^{13}C NMR: δ 158.4 (C=O), 117.3, 110.8 (br by superposition), 110.5 (br by superposition), 108.6, 108.2, 67.6, 32.2, 28.8, 27.0. MS (EI, 70 eV): *m/z* 55 (100). **7c**: (69%); ^{19}F NMR: δ −126.6 (m, 2F), −123.1 (m, 4F), −122.5 (br s, 2F), −122.1 (br s, 2F), −118.9 (t, J = 12.0 Hz, 2F), −81.3 (t, J = 9.5 Hz, 3F), ^{1}H NMR: δ 4.43 (t, J = 6.0 Hz, 2H), 3.58 (t, J = 6.0 Hz, 2H), 1.91 (m, 4H), ^{13}C NMR: δ 158.4 (C=O), 117.2, 110.8 (br by superposition), 110.5 (br by superposition), 108.5, 108.2, 67.8, 43.9, 28.7, 25.7, MS (EI, 70 eV): *m/z* 55 (100).

Acknowledgments

The support of AIST is gratefully acknowledged.

References

1 B. M. Trost, *Science*, 1991, **254**, 1471–1477.

2 (*a*) H. Itoh and K. Ueda, *Jpn. Pat.*, JP6–316548, 1994 (*b*) A. M. Lovelace, D. A. Rausch and W. Postelnek, *American Chemical Society Monograph Series in Aliphatic Fluorine Compounds*, Reinhold Publishing Co., 1958, p. 229.

3 A. Studer, S. Hadida, R. Ferritto, S.-Y. Kim, P. Jeger, P. Wipf and D. P. Curran, *Science*, 1997, **275**, 823–826.

4 (*a*) I. T. Horvváth and J. Rábai, *Science*, 1994, **266**, 72–75; (*b*) L. P. Barthel Rosa and J. A. Gladysz, *Coord. Chem. Rev.*, 1999, **190–192**,

587–605; (*c*) E. de Wolf, G. van Koten and B.-J. Deelman, *Chem. Soc. Rev.*, 1999, **28**, 37–41.

5 The products contained 2- and 3-octyl esters as ascertained by preparing authentic samples by condensation of 3-octanol with *F*-octanoyl chloride. A yield of 90% indicates 90% 2-octanoyl and 10% 3-octanoyl isomers.

6 Y. Moroi, H. Yano, O. Shibata and T. Yonemitsu, *Bull. Chem. Soc. Jpn.*, 2001, **74**, 667–672.

7 (*a*) R. D. Chambers, in *Fluorine in Organic Chemistry*, John Wiley & Sons, 1973, p. 65; (*b*) M. Hudlicky and A. E. Pavlath, *ACS Monograph 187, in Chemistry of Organic Fluorine Compounds II A Critical Review*, 1995, p. 988.

8 J. A. Ballantine, M. Davies, H. Purnell, M. Rayanakorn, J. M. Thomas and K. J. Williams, *J. Chem. Soc., Chem. Commun.*, 1981, 8–9.

9 H. Fukaya, T. Matsumoto, E. Hayashi, Y. Hayakawa and T. Abe, *J. Chem. Soc., Perkin Trans. 1*, 1996, **9**, 915–920.

10 T. Ono and T. Abe, *Tetrahedron Lett.*, to be submitted.

11 I. Pri-Bar and J. K. Stille, *J. Org. Chem.*, 1982, **47**, 1215–1220.

12 (*a*) T. Abe, E. Hayashi, H. Fukaya and H. Baba, *J. Fluorine Chem.*, 1990, **50**, 173–196; (*b*) T. Abe, E. Hayashi, H. Baba and H. Fukaya, *J. Fluorine Chem.*, 1990, **48**, 257–279; (*c*) T. Abe, E. Hayashi, H. Fukaya, Y. Hayakawa, H. Baba, S. Ishikawa and K. Asahino, *J. Fluorine Chem.*, 1992, **57**, 101–111; (*d*) T. Abe, H. Fukaya, E. Hayashi, Y. Hayakawa, M. Nishida and H. Baba, *J. Fluorine Chem.*, 1994, **66**, 193–202.

13 Our new preparative method of *F*-acyl halides: Y. Hayakawa, T. Taniguchi, T. Abe and T. Ono, *J. Fluorine Chem*., to be submitted.

14 W. R. Hasek, W. C. Smith and V. A. Engelhardt, *J. Am. Chem. Soc.*, 1960, **82**, 543.

Dry-media one-pot syntheses of fluorinated-2,3-dihydro-1,5-benzothiazepines under microwave activation

Anshu Dandia,*[a] Meha Sati[a] and André Loupy[b]

[a] *Department of Chemistry, University of Rajasthan, Jaipur 302 004, India.*
E-mail: dranshudandia@eth.net
[b] *Laboratoire des Réactions Sélectives Sur Supports, ICMMO, UMR 8615, Building 410,*
Université Paris-Sud, 91405 Orsay cedex, France

Received 17th July 2002
First published as an Advance Article on the web 30th October 2002

A new efficient and environmentally friendly green chemistry procedure for the syntheses of a series of 8-substituted-2-carboxy-2,3-dihydro-1,5-benzothiazepines under microwave irradiation and solvent-free conditions is described. Results were compared with those obtained following classical thermal method. A judicious choice of the reaction conditions allowed the final products **4a–f** to be generated in excellent yields in a one-step procedure, whereas experiments under thermal conditions led to benzothiazepines along with other products in lower yields with tedious work-up.

The immense chemotherapeutic applications of 1,5-benzothiazepines especially that of *diltiazem* in the treatment of ailments of the cardiovascular system such as coronary vasodilation,[1] hypertension[2] *etc.* enthused great interest in a detailed study of this class of compounds. While carrying out drug design, it was found that an important number of fluorinated 1,4- and 1,5-benzodiazepines had been introduced as pharmacological and cardiovascular agents, such as *fluorodiazepam, triflubazam, etc.* Incorporation of fluorine atoms on 1,5-benzothiazepines or analogous nucleus enhances pharmacological properties by increasing the solubility in lipid materials and fat deposits in the body when compared to their non-fluorinated analogs.[3]

It was also found that Cl,[4] Me,[5] CF_3[6] or a free COOH group[7] when present on different positions in the 1,5-benzothiazepine nucleus act as potential pharmacophores. A series of 1,5-benzothiazepines bearing fluorine and 4-fluorophenyl groups have been found to be effective for treatment of cancer metastasis[8] and recently 8-fluoro-1,5-benzothiazepine reported from our laboratory has been found to be a promising anti-AIDS agent in preliminary screening.[9] It has been extensively studied by various workers that the reaction between α,β-unsaturated carbonyl compounds with 2-aminobenzenethiols takes place in two steps[10,11] involving the previous formation of the Michael adduct as an intermediate[11,12] which readily undergoes dehydrative cyclization to give 1,5-benzothiazepines. It was observed that the formation of the intermediate and the final cyclized product is affected by the reaction conditions,[13] catalyst,[14] type of groups or substituents present[15] on the compounds (Scheme 1).

Traditional methods applied for the syntheses of 2-carboxy-2,3-dihydro-1,5-benzothiazepines involve the use of volatile organic solvents under reflux and strong acids/bases as catalyst, giving low yields due to the extended reaction time which favors the formation of the corresponding disulfides.[16,17] Microwave (MW) assisted reactions within shorter times is becoming more popular for organic chemists and have recently been reviewed.[18] Thus more interest has been focused on dry media synthesis under MW irradiation and especially by carrying out experiments with supported reagents on mineral oxides. Such procedures lead to (a) improved efficiency of impregnated reagents, (b) better conversions within shorter reaction times, (c) clean, efficient, safe and economical technology and (d) higher selectivity, yield and purity compared to conventional methods.

Hence, in an attempt towards a non-traditional approach to the experimental set up of organic reactions, and our continuing interest on the synthesis of fluorine containing biodynamic heterocycles and as an extension of our work on the reactions of 2-aminobenzenethiols with α,β-unsaturated ketones and analogous compounds[19,9] under MW irradiation, we report herein, for the first time, the synthesis of title compounds **4a–f** by varying different parameters. They include solid supports such as (i) acidic or basic aluminas, (ii) strongly acidic montmorillonite KSF, (iii) *p*-toluenesulfonic acid (PTSA) and solvents such as ethanol + HCl (conc.). For the sake of comparison, with conventional methods, the reagents were refluxed in (i) ethanol and dry HCl gas, (ii) toluene + TFA and (iii) methanol + traces of glacial AcOH.

The reaction has also been performed under neat conditions (without any solvent or support) but with a small amount (a few drops) of DMF. In order to determine the role of DMF, the same reaction was carried out without any additive. Observed yields were significantly lower than those obtained using the micro-

Green Context

Minimising the number of auxiliaries is an important green chemistry reduction in the context of clean synthesis. Solvents, acids and bases are the most common auxiliaries used in traditional organic syntheses including the preparation of the chemotherapeutically valuable 1,5-benzothiazepines. Here we see how these auxiliaries can be avoided while maintaining good product yields. This is achieved through the use of microwave activation and solid, recoverable catalysts. The authors compare their method with the traditional one and show that while the microwave route is fast, one-step and gives excellent product yields, the traditional route gives a complex product mixture and involves a tedious work-up procedure. ***JHC***

DOI: 10.1039/b207004a

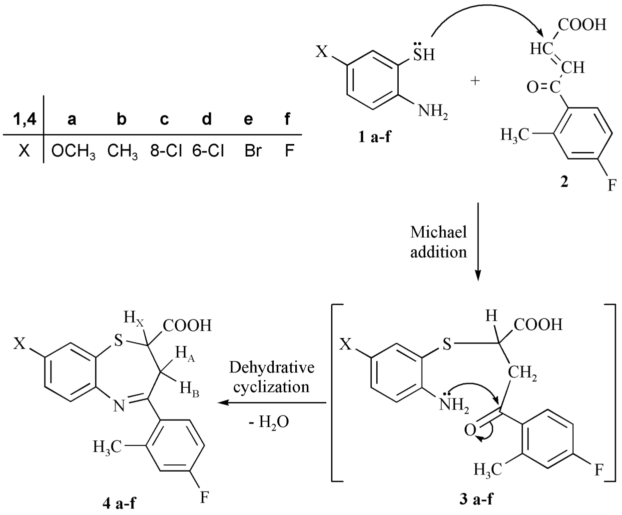

Scheme 1

wave–DMF method (Table 1). Small quantities of DMF are sufficient to increase the temperature and consequently to enhance the yield of the reaction. This ability to act as an energy transfer agent was recently advocated.[20] The presence of DMF here as an energy transfer active MW compound did not lead to side-reactions and no formation of any detectable by-products was observed.

From those results it is obvious that montmorillonite KSF is the most adaptable and simplest catalyst for the synthesis of **4a**, since comparatively higher yield is achieved in shorter reaction time by this method as also observed earlier in clay supported reactions.[21] Consequently, we have extended those conditions to synthesize a series of 2,3-dihydro-1,5-benzothiazepines **4b**–**f** (Table 2). Identity of the compounds synthesized by conventional and microwave induced method was confirmed.

Finally, in order to check the possible intervention of specific (non-thermal) microwave effects or molecular superheating, the best results obtained under microwaves were extrapolated to conventional heating. The reaction, in the case of compound **4a** has been carried out using a pre-heated oil-bath, under the same conditions as under microwaves (time, temperature, vessel), for 13 min at 138 °C in the two better cases (montmorillonite KSF and Neat + DMF). It has been found that reaction proceeds with only 22% yield under thermal conditions instead of 71% under MW activation in the former, while in the latter only traces of the product were obtained and most of the reactant remained unchanged. Lower yields were obtained under conventional heating even after 1 h of reaction (Table 1). This indicates that the effect of microwaves is not purely thermal and can be related to the effect of the support as they behave as poorly heating conductors whereas they are strongly absorbent of electromagnetic field.[22]

The specific non-thermal MW effects observed here are consistent with the consideration of mechanisms[18c] and with the assumption that MW effects are increased when the polarity of a system is enhanced.[23] The rate-determining step consists in the Michael addition of thiophenol moiety on the carbon–carbon double bond of the α,β-unsaturated carbonyl compound. One can expect an important specific microwave effect due to the evolution of polarity of the system during the reaction progress which is provided by ionic dissociation of the ion pairs from the ground state of the reaction towards the transition

Table 1 Comparative study of the synthesis of **4a** (X = OMe). (A) under microwave irradiation (B) by thermal heating

Entry	Medium	MW Power/W	Time/min	Temp.[a]/°C	Yield[b] (%)
A					
1	Montmorillonite KSF	640	**13**	**138**	**71**
2	Silica gel	640	8	110	60
3	Acidic alumina	640	16	100	63
4	Basic alumina	640	18	90	58
5	PTSA	275	10	125	56
6	Neat (without DMF)	640	13	100	58
7	Neat + DMF (2–3 drops)	640	13	140	66
8	Ethanol + HCl (conc.)	275	10	78	65
B		Time/min	Temp.[a]/°C	Yield[b] (%)	
1	Ethanol + dry HCl gas	420	Reflux	62	
2	Toluene + TFA	720	Reflux	46	
3	Methanol + gl. AcOH	420	Reflux	44	
4	Montmorillonite KSF	13	138	22	
5	Montmorillonite KSF	60	138	42	
6	Neat + DMF	13	140	Traces	
7	Neat + DMF	60	140	29	

[a] The final temperature is measured at the end of microwave irradiation by introducing a glass thermometer in the reaction [b] Yield of the isolated products.

Table 2 Physical and analytical data of 8-substituted-2-carboxy-4-(4-fluoro-2-methylphenyl)-2,3-dihydro-1,5-benzothiazepines (**4a**–**f**)

		Reaction time/min (yield %)						
Compd.	X	Classical method	Microwave method	Temp.[a]/°C	Mp/°C	R_f[b]	Formula	N (%) Found (Calc.)
4a	OCH_3	420 (62)	13 (71)	138	178	0.78	$C_{18}H_{16}O_3NSF$	3.8 (4.0)
4b	CH_3	720 (53)	11 (64)	140	157	0.69	$C_{18}H_{16}SO_2NF$	4.0 (4.3)
4c	8-Cl	600 (56)	14 (61)	135	186	0.70	$C_{17}H_{13}SO_2FCl$	4.2 (4.0)
4d	6-Cl	780 (52)	12 (59)	142	192	0.75	$C_{17}H_{13}NSO_2FCl$	3.8 (4.0)
4e	Br	600 (50)	9 (63)	140	166	0.76	$C_{17}H_{13}NSO_2BrF$	2.5 (2.6)
4f	F	840 (53)	15 (62)	139	140 (138[c])	0.79	$C_{17}H_{13}NSO_2F_2$	4.1 (4.2)

[a] Final temperature is measured at the end of microwave irradiation by introducing a glass thermometer in the reaction mixture. [b] Using solvent system benzene : ethyl acetate (8:2). [c] Ref. 25

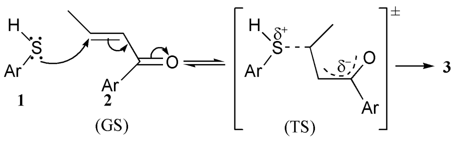

Scheme 2

state,[24] which is more polar due to the negative charge delocalization. The more important stabilization of the transition state is therefore responsible for an enhancement of reactivity by a decrease of the activation energy (Scheme 2).

This step is followed by intramolecular nucleophilic addition to the carbonyl group, which also involves the formation of a dipolar transition state, which is stabilized by microwaves (Scheme 3). Hence, formation of **4** is also expected to be substantially accelerated by MW under solvent-free conditions.

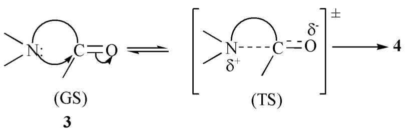

Scheme 3

IR spectra of the products **4a–f** did not reveal characteristic ketocarbonyl absorption peaks in the range 1675–1670 cm^{-1} and also, absorption of primary amino groups (two bands in the region 3450–3150 cm^{-1}) were absent. On another hand, the copresence of an absorption at around 1710–1685 cm^{-1} ν(C=O), a broad absorption in the range 3215–2550 cm^{-1} characteristic of a hydrogen bonded carboxylic group, C–O stretching, and O–H bending frequencies in the range 1380–1250 cm^{-1}, are assigned to the presence of a carboxylic function. The C–F absorption band was observed in the range 1190–1145 cm^{-1}.

In the ^{1}H NMR spectra, absorptions as three double doublets at δ 3.75–3.63 (H$_B$, dd, J_{AB} = 16–15, J_{BX} = 8.2–7.9 Hz C-3-H$_B$), 3.22–3.15 (H$_A$, dd, J_{AB} = 16–15, J_{AX} = 9–8 Hz, C-3-H$_A$), 4.20–4.17 (H$_X$, dd, J_{AX} = 9–8, J_{BX} = 8.2–7.9 Hz, C-2-H$_X$) in the ABX pattern were characterized for two methylene protons at C-3 and one methine proton at C-2 in **4a–f**.

Formation of the final compound **4a** was further confirmed on the basis of ^{13}C and ^{19}F NMR and mass spectrum. In the ^{13}C NMR spectrum of **4a**, (X = OCH$_3$) sharp signals were observed at δ 186.3 (COOH), 55.3 (OCH$_3$), 21.3 (CH$_3$), 155.3 (C=N), 42.0 (C-2–H$_X$), 36.7 (C-3–H), 112.4, 113.3, 116.9, 118.6, 120.2, 121.51, 130.1, 130.9, 131.0, 133.1, 141.8, 146.2 (for 12 aromatic ring carbons). In the mass spectrum of **4a**, the appearance of molecular ion peaks, m/z, [M]$^+$ and [M + 2]$^+$ at 345 and 347 corresponds to the molecular mass of the compound. The presence of fluorine atom in the compound **4a** has been confirmed on the basis of its ^{19}F NMR spectrum. A sharp signal at δ −108 appeared to be due to fluorine at position-4 of the phenyl ring linked to C-4 of the benzothiazepine ring.

Experimental

Melting points were determined on a Toshniwal melting point apparatus and are uncorrected. IR spectra were recorded in KBr on a Perkin-Elmer Infracord spectrophotometer model 577 (ν_{max} in cm^{-1}), ^{1}H NMR, ^{13}C NMR and ^{19}F NMR were recorded on a model Bruker-DRX-300 spectrometer using CDCl$_3$ + DMSO d$_6$ as a solvent for ^{1}H NMR and ^{13}C NMR and CDCl$_3$ for ^{19}F NMR at 300.13 MHz, 75.47 MHz and 282.37 MHz, respectively. TMS was used as an internal reference for ^{1}H NMR and TFA as an external reference for ^{19}F NMR. Mass spectrum of the representative compound **4a** was recorded on Kratos-30 spectrometer. Progress of the reaction was monitored by TLC using silica gel ′G′ coated glass plates and benzene–ethyl acetate (8 : 2) as eluent. The microwave induced reactions were carried out in a BMO-700T domestic oven manufactured by BPL multimode Sanyo utilities and appliances Ltd. operating at 700 W generating 2450 MHz frequency.

5-Substituted-2-aminobenzenethiols[25] **1a–f** and *3-(4-fluoro-2-methylbenzoyl)-2-propenoic acid*[19f] **2** were prepared by literature reported methods.

2-Carboxy-8-methoxy-4-(4-fluoro-2-methylphenyl)-2,3-dihydro-1,5-benzothiazepine **4a**: this was prepared by two different ways: (1) conventional synthesis and (2) microwave mediated synthesis.

Conventional synthesis

(a) Using ethanol + dry hydrogen chloride gas:

An equimolar mixture of **1a** (1 mmol, 155 mg) and **2** (1 mmol, 208 mg) was refluxed for 7 h with dry ethanol (25 mL) saturated with hydrogen chloride gas, whereupon the reaction mixture changed from yellow to dark green. Excess of solvent was concentrated by distillation under reduced pressure. The product so obtained was recrystallized from methanol to give light green crystals of **4a** (Tables 1 and 2).

Similarly **4a** was prepared by reflux with toluene and trifluoroacetic acid (2–3 drops)–methanol containing traces of glacial acetic acid to check the most effective method of synthesis.

Microwave assisted synthesis

(a) Using different solid supports such as montmorillonite KSF, basic alumina, acidic alumina, silica gel, *p*-toluenesulfonic acid (PTSA).

An equimolar mixture of 5-methoxy-2-aminobenzenethiol **1a** (1 mmol, 155 mg) and 3-(4-fluoro-2-methyl benzoyl)-2-propenoic acid **2** (1 mmol, 208 mg) were introduced in a beaker and dissolved in acetone (15 mL). Inorganic solid support (20% by weight of the reactants) was then added and swirled for a while followed by removal of the solvent under gentle vacuum. The dry free flowing powder thus obtained was placed into a Pyrex-glass open vessel and irradiated in the microwave oven at a power output of 90% (640 W), for the times and at the final temperature as indicated in Table 1. When the irradiation was stopped, the final temperature was measured by introducing a glass thermometer into the reaction mixture and homogenizing it, in order to obtain a temperature value representative of the whole mass. After completion of the reaction (monitored by TLC) the recyclable inorganic solid support was separated by filtration after eluting the product with methanol. The solvent was evaporated to give light green crystals of **4a** which were found to be pure by TLC and do not require further recrystallization (Tables 1 and 2).

(b) Ethanol containing catalytic amount of conc. HCl.

An equimolar mixture of **1a** and **2** in ethanol (15 mL) containing a catalytic amount of concentrated HCl (1 mL) was placed in a microwave oven (using 30% power, *i.e.* 275 W) and irradiated for 10 min. The irradiation was completed with a short interruption of 1 min after every 3 min to avoid overheating of the solvent. Progress of the reaction was monitored by TLC. The reaction mixture was cooled down and the residue was crystallized from methanol gave light green crystals of **4a** (Tables 1 and 2).

Comparison of all the methods indicated the easy work-up and better yield by the microwave assisted method using montmorillonite KSF as the energy transfer medium. Com-

Table 3 IR spectral data of **4a–f**, ν in cm^{-1}

	COOH absorption				Aliphatic	Aromatic
Compd.	ν(C=O)	ν(O–H)	ν(C=N)	ν(C–F)	ν(C–H)	ν(C–H)
4a	1685	3215–2735	1615	1145	2935	3080
4b	1710	3100–2550	1608	1150	2980	3077
4c	1695	3000–2550	1605	1185	2950	3060
4d	1708	3080–2570	1608	1170	2945	3076
4e	1698	3090–2600	1600	1190	2940	3070
4f	1708	3180–2720	1610	1150	2960	3065

Table 4 ^{1}H NMR spectral data of **4a–f** (δ values in ppm, J in Hz)

		C-3–H					
Compd.	C-2–H_X (J_{AX} = 9, J_{BX} = 8)	H_A (J_{AB} = 16, J_{AX} = 9)	H_B (J_{AB} = 16, J_{BX} = 8)	C-8 OCH_3/CH_3	CH_3	COOH	Ar–H (m, 6H)
4a	4.17	3.18	3.68	3.6	2.57	8.1	6.75–7.8
4b	4.15	3.20	3.70	2.67	2.54	8.2	6.72–7.20
4c	4.20	3.15	3.75	—	2.61	8,15	6.70–7.15
4d	4.17	3.18	3.72	—	2.59	8.17	6.72–7.18
4e	4.21	3.22	3.63	—	2.55	8.19	6.73–7.75
4f	4.19	3.16	3.73	—	2.55	8.2	6.78–7.86

pounds **4b–f** were similarly prepared by the above method and results were compared with those following conventional thermal method (ethanol + dry HCl gas). The structures of compounds **4a–f** were confirmed by IR, ^{1}H NMR spectroscopy and elemental analyses for nitrogen. (Tables 2, 3 and 4).

Acknowledgements

Financial assistance from CSIR, New Delhi is gratefully acknowledged. We are also thankful to RSIC, CDRI, Lucknow, for the elemental and spectral analyses.

References

1 K. Weiss, P. Fitscha, A. Gazso, D. Gludovacz and H. Sinzinger, *Prog. Clin. Biol. Res.*, 1989, **301**, 353; *Chem. Abstr.*, 1989, **111**, 70642v.

2 M. Takeda, A. Oishi, H. Nakajima and T. Nagao, (Tanabe Seiyaku Co. Ltd.) Jpn. *Kokai Tokyo Koho JP. 61*, 1986, **103**, 828 [86, 103 828] (Cl A61 K31/55), 1986, Appl. 84/225, 030, 1984; *Chem. Abstr.*, 1986, **105**, 183965x.

3 R. Filler, *Chem. Tech.*, 1974, **4**, 752.

4 (*a*) A. Odawara and T. Ikeo, *Jpn. Kokai. Tokkyo. Koho JP. 06*, 1994, **183**, 978 [94, 183, 978] (Cl. A 61. K 31/55), Appl. 92/341, 753; *Chem. Abstr.*, 1992, **122**, 96150c; (*b*) A. Lochead, J. C. Muller, C. Denys and H. Dumas, *Eur. Pat. Appl.* EP 1989, **338**, 892 (C 1 CO7 D 281/10), *FR Appl.*, 88/5, 131, 1988; *Chem. Abstr.*, 1990, **112**, 158278m.

5 K. S. Atwal, S. Z. Ahmed, D. M. Floyd, S. Moreland and A. Hedberg, *Biorg. Med. Chem. Lett.*, 1993, **3**, 2797.

6 D. M. Floyd, S. D. Kimball, J. Krapcho, J. Das, C. F. Turk, R. V. Mosquin, M. W. Lago, K. J. Duff, V. G. Lee and R. E. White, *J. Med. Chem.*, 1992, **35**(4), 756.

7 Y. Inada, M. Tanabe, K. Itoh, H. Sugihara and K. Nishikawa, *Jpn., J. Pharmacol.*, 1988, **48**(3), 323; *Chem. Abstr.*, 1989, **110**, 539x.

8 N. K. Ahmed, *Can. Pat. Appl.*, CA2, 030, 159 [C1. A61 K31/55], 1991; *US Appl.*, 441, 083, 1989; *Chem. Abstr.*, 1991, **115**, 198515f.

9 M. Upreti, S. Pant, A. Dandia and U. C. Pant, *Phosphorus, Sulfur Silicon*, 1996, **113**, 165.

10 W. D. Stephens and L. Field, *J. Org. Chem.*, 1959, **24**, 1576.

11 A. Levai and R. Bognar, *Acta. Chim. Acad. Sci. Hung.*, 1976, **88**, 293.

12 H. Duddeck, M. Kaiser and A. Levai, *Liebigs Ann. Chem.*, 1985, 869.

13 A. Levai and R. Bognar, *Acta. Chim. Acad. Sci. Hung.*, 1977, **92**, 415.

14 W. Reid and W. Marx, *Chem. Ber.*, 1957, **90**, 2683.

15 C. H. Hankovszky and K. Hideg, *Acta. Chim. Acad. Sci. Hung.*, 1971, **68**, 403.

16 H. Inoue, M. Konda, T. Hoshiyama, H. Otsaka, K. Takashi, M. Gaino, T. Date, K. Aoe, M. Takeda, S. Murata, H. Narita and T. Nagao, *J. Med. Chem.*, 1991, **34**, 675.

17 H. Kugita, H. Inoue, M. Ikezaki and S. Takeo, *Chem. Pharm. Bull.*, 1970, **18**, 2028.

18 (*a*) M. Jeselnik, R. S. Varma, S. Polanc and M. Kocevar, *Green Chem.*, 2002, **4**, 35; (*b*) P. Lidström, J. Tierney, B. Wathey and J. Westman, *Tetrahedron*, 2001, **57**, 9225; (*c*) A. Loupy and L. Perreux, *Tetrahedron*, 2001, **57**, 9199; (*d*) A. De. LA. Hoz, A. D-Ortis, A. Moreno and F. Langa, *Microrev., Eur. J. Org. Chem.*, 2000, 3659; (*e*) N. Elander, J. R. Jones, S.-Y. Lu and S. Stone-Elender, *Chem. Soc. Rev.*, 2000, **29**, 239; (*f*) S. Deshayes, M. Liagre, A. Loupy, J. Luche and A. Petit, *Tetrahedron*, 1999, **55**, 10851; (*g*) R. S. Varma, *Green Chem.*, 1999, **1**, 43; (*h*) A. Loupy, A. Petit, J. Hamelin, F. Texier-Boullet, P. Jacquault and D. Mathe, *Synthesis*, 1998, 1213.

19 (*a*) A. Dandia, R. Singh, H. Sachdeva and K. Arya, *J. Fluorine Chem.*, 2001, **111**, 61; (*b*) A. Dandia, H. Sachdeva and R. Singh, *J. Chem. Res. (S)*, 2000, 272; (*c*) A. Dandia, M. Upreti, B. Rani, U. C. Pant and I. J. Gupta, *J. Fluorine Chem.*, 1998, **91**, 171; (*d*) A. Dandia, M. Saha and H. Taneja, *J. Fluorine Chem.*, 1998, **90**, 17; (*e*) A. Dandia, M. Saha and B. Rani, *J. Chem. Res. (S)*, 1998, 360; (*f*) U. C. Pant, M. Upreti, S. Pant, A. Dandia, G. K. Patnaik and A. K. Goel, *Phosphorus, Sulfur Silicon*, 1997, **126**, 193; (*g*) A. Dandia, B. Rani, M. Saha and I. J. Gupta, *Phosphorus, Sulfur Silicon*, 1997, **130**, 217.

20 (*a*) H. Marquez, A. Plutin, Y. Rodriguez, E. Perez and A. Loupy, *Synth. Commun.*, 2000, **30**, 1067; (*b*) M. Suarez, A. Loupy, E. Salfran, L. Moran and E. Rolando, *Heterocycles*, 1999, **51**, 21; (*c*) R. Perez, E. Perez, M. Suarez, L. Gonzalez, A. Loupy, M. L. Jimeno and C. Ochoa, *Org. Prep. Proced. Int.*, 1997, **29**, 671; (*d*) M. Suarez, A. Loupy, E. Perez, L. Moran, G. Gerona, A. Morales and M. Autie, *Heterocycl. Commun.*, 1996, **2**, 275.

21 B. Perio, M. J. Dozias, P. Jacqualt and J. Hamelin, *Tetrahedron Lett.*, 1997, **38**, 7867; K. Toshima, Y. Ushiki, G. Matsuo and S. Matsumara, *Tetrahedron Lett.*, 1997, **38**, 7375.

22 (*a*) B. Syassi, K. Bougrin and M. Soufiaoui, *Tetrahedron Lett.*, 1997, **38**, 8855; (*b*) E. R. Perez, A. L. Marrero, R. Perez and M. A. Autie, *Tetrahedron Lett.*, 1995, **36**, 1779; (*c*) R. S. Varma, M. Varma and A. K. Chatterjee, *J. Chem. Soc., Perkin Trans 1*, 1993, 999; (*d*) A. Ben Alloum, B. Labiad and D. Villemin, *J. Chem. Soc., Chem. Commun.*, 1989, 607.

23 (*a*) R. A. Abramovitch, *Org. Prep. Proced. Int.*, 1991, **23**, 685; (*b*) R. N. Gedye, F. E. Smith and K. C. Westaway, *Can. J. Chem.*, 1988, **66**, 17.

24 A. Loupy, L. Perreux, M. Liagre, K. Burle and M. Moneuse, *Pure Appl. Chem.*, 2001, **73**, 161.

25 U. C. Pant, B. S. Gaur and M. Chugh, *Indian J. Chem., Sect. B*, 1987, **26**, 947.

Thermal degradation of ABS-Br mixed with PP and catalytic debromination by iron oxide carbon composite catalyst (Fe–C)

Thallada Bhaskar,*[a] Kazuya Murai,[a] Mihai Brebu,[b] Toshiki Matsui,[c] Md. Azhar Uddin,[d] Akinori Muto[a] and Yusaku Sakata*[a]

[a] *Department of Applied Chemistry, Faculty of Engineering, Okayama University, 3-1-1 Tsushima Naka, 700-8530 Okayama, Japan. E-mail: bhaskar@cc.okayama-u.ac.jp*
[b] *"P.Poni" Institute of Macromolecular Chemistry, 41 A Gr. Ghica Voda Alley, Ro 6600 Iasi, Romania*
[c] *Toda Kogyo Co., Ltd, Hiroshima 739-0652, Japan*
[d] *Process Safety and Environment Protection Group, School of Engineering, The University of Newcastle, Callaghan, NSW 2308, Australia*

Received 5th July 2002
First published as an Advance Article on the web 29th October 2002

The degradation of brominated (Br: 9.59 wt%) flame retardant containing acrylonitrile–butadiene–styrene (ABS) copolymer [waste from electric and electronic equipment, (WEEE)] mixed with polypropylene (PP) was performed at 450 °C using iron oxide carbon composite catalyst (Fe–C) and produced bromine-free liquid products. The majority of nitrogen present in the acrylonitrile portion of ABS-Br was converted into ammonia and also light aliphatic nitriles. The liquid products can be used as a fuel oil or feedstock in the petroleum refinery.

Introduction

Plastics are the materials of choice because they make it possible to balance modern day needs with environmental concerns. To appreciate this we must look at their total use, seeking conservation of resources in production, use and maximizing recovery at the end of a useful life. However, the disposal of waste plastics is a serious environmental problem and the development of viable recycling technologies for waste plastics is becoming increasingly important due to stringent environmental regulations to protect the environment. Feedstock recycling of waste plastics has more advantages than mechanical recycling or energy recovery, as the energy consumption of the process is very low (only about 10% of the energy content of the waste plastic are used to convert the scrap into petrochemical products).[1a]

High impact polystyrene (HIPS-Br) accounts for more than half of the plastic housing used in domestic electrical and electronic appliances, and acrylonitrile–butadiene–styrene (ABS) plastic is the next most commonly used plastic.[1b] Waste from electrical and electronic equipment (WEEE) may contain polybrominated biphenyls, polybrominated diphenyloxides or tetrabromobisphenol-A. The pyrolysis of halogenated waste plastics has several problems than non-halogenated plastics into valuable hydrocarbons. Halogenated plastics such as ABS-Br produce highly corrosive hydrobromic acid (HBr) during thermal degradation, and it may lead to formation of halogenated hydrocarbons in liquid products. The presence of such toxic and corrosive compounds in the liquid products means they cannot be used as fuel, necessitating the removal of the halogen content from the waste plastic derived oil.

In the recent past, various technologies have emerged for the treatment of halogenated (PVC and PVDC) and non-halogenated waste plastics. An excellent monograph on the feedstock recycling of plastic waste describing the economics and environmental impact of plastic waste has been published.[2] Kaminsky and Hartmann[3] have highlighted the new pathways in plastic recycling and the current status of plastics recycling. We have reported earlier on the thermal and catalytic degradation of polyethylene (PE), polypropylene (PP), PVC and their mixtures into fuel oil[4–6] and also the thermal and catalytic degradation of ABS (without brominated flame retardant).[7,8] However, no studies have been made on the feedstock recycling of ABS-Br waste from electrical and electronic equipment into halogen-free liquid products. Here we report, for the first time, the single step conversion of brominated flame retardant containing acrylonitrile–butadinene–styrene (ABS-Br) copolymer mixed with polypropylene (PP) into bromine-free liquid products using an iron oxide carbon composite catalyst (Fe–C).

Results and discussion

The degradation of ABS-Br mixed with PP was performed thermally at atmospheric pressure in a batch process at 450 °C and also using iron oxide carbon composite (Fe–C) catalyst. The products of ABS-Br/PP mixed plastic degradation were classified into three groups: gas, liquid and degradation residue. Furthermore the degradation residue was separated into two

Green Context

Giving a second useful life to a product at the end of its normal lifetime is an important method for reducing the environmental burden associated with that product. In the case of plastics their degradation to fuel oil or petroleum feedstock can provide such a lifetime extension. Safe and environmentally acceptable plastic degradation can however, be seriously hindered by the presence of additives. In the case of domestic electrical and electronic goods for example, the commonly used acrylonitrile–butadiene–styrene plastics may often contain bromo-organic flame retardants. Here we see described a new degradation process that removes all of the bromine from the derived fuel oil. Additionally, most of the nitrogen is converted into ammonia. ***JHC***

DOI: 10.1039/b206487a

portions, such as wax residue (the coated solid compounds on the top of glass reactor) and carbon residue (the remaining black material in the bottom of reactor). Table 1 shows the material balance and yield of products such as gas, liquid, residue, average carbon number, and density of liquid products obtained during thermal degradation of ABS-Br/PP and also with Fe–C. The thermal degradation process yielded about 75 wt% liquid products with an average carbon number of 9.6 and a density of 0.75 g cm^{-3}. The degradation of ABS-Br/PP in the presence of Fe–C gave about 71 wt% liquid products, with an average carbon number of 9.1 and a density of 0.74 g cm^{-3}. The small decrease in liquid product quantity with the Fe–C catalyst relative to the thermal degradation might be due to the larger amount of gaseous products in the presence of Fe–C catalyst.

The quantitative analysis of bromine content in the liquid products was done by GC–AED, as it can selectively detect bromine compounds in the liquid products. The bromine content in residue products was analyzed by combustion followed by ion chromatography and results presented in Table 2. The thermal degradation of ABS-Br mixed with PP plastics produced liquid products with 2040 ppm of bromine and 2630 ppm of nitrogen. However, the use of Fe–C (2 g) in the degradation process, led to the bromine content being completely removed from the liquid products and the nitrogen content was decreased to 210 ppm. The majority of bromine was observed in the wax and carbon residue products when Fe–C was used in the degradation process. As can be seen from Table 2 the bromine content in the carbon residue was about 7 wt% during thermal degradation and increased to 34 wt% by the use of Fe–C. The bromine content in wax residue was 61 wt% during thermal degradation and with the use of Fe–C it was decreased to 37 wt%. The nitrogen compounds during thermal degradation produced about 21.5 wt% in liquid products, 0.3 wt% as NH_3, 1.4 wt% as HCN (Table 3). However, the use of Fe–C catalyst in the degradation process, decreased the nitrogen content in liquid products (18.5 wt%). The Fe–C catalyst facilitated the formation of NH_3 and HCN during degradation. NH_3 and HCN formation was very high during degradation with Fe–C (Table 3). The Fe–C catalyst converted the nitrogen into ammonia by reacting the hydrogen produced during the degradation. We could not analyze the bromine and nitrogen compounds present in the gaseous products. Brebu *et al.* reported[9] that iron oxides such as γ-Fe_2O_3, Fe_3O_4 and α-FeOOH are catalytically active for decreasing the concentration of nitrogen in ABS degradation oil.

The liquid products were analyzed by GC–MS to identify the major hydrocarbons, and also bromine, nitrogen containing compounds. In our present study, the major hydrocarbons during thermal and degradation with Fe–C were benzene, toluene, ethyl benzene, isopropyl benzene, styrene, 1,3-diphenylpropane, α-methyl styrene *etc.*, The major aromatic nitrogen compound was found to be 4-phenyl butyronitrile and aliphatic compounds such as acetonitrile, acrylonitrile and propionitrile. The major bromine compound in the thermal degradation liquid products was found to be bromophenol. The gaseous products collected in a sealed Teflon bag was analysed by GC–TCD and the presence of hydrocarbons such as methane, ethane, propane, butane and lower unsaturated alkenes such as ethene, propene and butene was observed. The formation of $SbBr_3$ was observed in earlier studies on the thermal degradation of polyester flame-retarded with antimony oxide/brominated polycarbonate. In the present investigation we have not observed any such compounds in the liquid products. However, the presence of antimony in carbon residue was confirmed by X-ray diffraction analysis.

Richard *et al.*,[10] reported that the high temperature degradation of polybrominated flame retardant materials produced bromobenzenes, bromophenols, polybrominated dibenzodioxins (PBDD) and polybrominated dibenzofurans (PBDFs). However, they were subsequently destroyed at high temperature (800 °C). Dioxin formation (PHDD) and furan formation (PHDF) in the thermal treatment of plastics containing polybrominated diphenyl ether with several flame retardants has been reported[11] and the diantimony trioxide and decabromodiphenylene ethers (heating of HIPS for 20 min) produced dioxins at 275 °C. Former test campaigns by the Forschungszentrum Karlsruhe and the Association of Plastic

Table 3 The distribution of nitrogen content in various degradation products for ABS-Br (2 g) mixed with PP (8 g) at 450 °C

	Nitrogen in degradation products (wt%)			
		Inorg. gas[a]		
	Liquid[L]	NH_3	HCN	Others (Org. gas/catalyst)
Thermal	21.5	0.3	1.4	76.8
Fe–C	18.5	7.4	2.0	67.6

[a] n.d. not detected

Table 1 Material balance of products during degradation of ABS-Br (2 g) mixed with PP (8 g) at 450 °C

	Yield of degradation products (wt%)					
			Residue [R]			
Method	Liquid [L]	Gas[a] [G]	Carbon	Wax	Cnp[b]	Density/g cm^{-3}
Thermal	75	13	6	6	9.6	0.75
Fe–C (2 g)	71	17	9	3	9.1	0.74

[a] G = 100 – (L + R) [b] Average carbon number of liquid products

Table 2 The distribution of bromine content in various degradation products for ABS-Br (2 g) mixed with PP (8 g) at 450 °C

	Bromine in degradation products (wt%)				
			Residue [R]		
Method	Liquid [L]	Inorg. gas[a] [G]	Carbon	Wax	Others (Org. gas/catalyst)
Thermal	8.1	n.d	7	61	23.9
Fe–C	n.d.	n.d	34	37	29.0

[a] n.d. = not detected

Manufacturers in Europe, in the Karlsruhe TAMARA test facility for waste combustion, focussed on the existence, partitioning and destruction of bromine and its influence on the formation of bromine containing dibenzo-*p*-dioxins and dibenzofurans.[12,13]

X-Ray diffraction studies confirmed the presence of the Fe_3O_4 phase in the fresh Fe–C catalyst. X-Ray diffraction patterns for the used Fe–C (2 g) shows that there are few additional peaks in addition to the Fe_3O_4 peaks. We cannot rule out the formation of an $FeBr_2$ phase, which is below the detection limit (40 Å) of the powder X-ray diffraction technique even though there are no characteristic peaks due to iron bromide. The formation of $FeBr_2$ was observed in our earlier studies on HIPS-Br/PVC degradation using Fe–C at 430 °C.[14] From the above observations, we can conclude that the iron oxide based catalysts can effectively be used for debromination during recycling of halogenated plastics to produce halogen-free liquid products. The lifetime of catalyst and applicability of Fe–C catalyst for our waste plastic pyrolysis pilot plant at Mizushima, Japan is underway.

Experimental

Materials

Commercially available brominated flame retardant containing acrylonitrile–butadiene–styrene copolymer (ABS-Br) was used in the present study. The grain size of ABS-Br was 3 × 1.5 × 1 mm. The synergist Sb_2O_3 was present in ABS-Br. Polypropylene (PP) was obtained from Ube Chemical Industries Co. Ltd., Japan. The structure of the brominated flame retardant (Br: 9.59 wt%) is shown in Fig. 1.

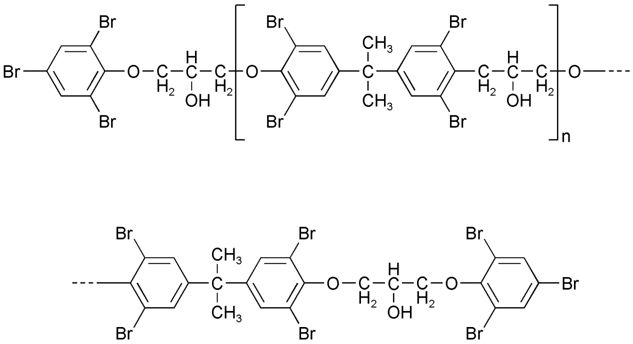

Fig. 1 The structure of the brominated flame retardant.

Preparation of Fe–C

About 90 wt% of α-FeOOH was mixed with 10 wt% phenol resin (Kanebo Corporation, Japan; BELLPEARL S890) by mechanical kneading during which 20% of water was added to the mixture and pellet formation was performed using a molding method. The prepared catalyst was calcined at 500 °C for 1 h in a nitrogen atmosphere and in the calcination process the phenol resin was converted into carbon. The addition of phenol resin and calcination imparted a good mechanical strength and loss of hygroscopic nature to the catalyst, which are important parameters for the successful use of the catalyst in a pilot plant. The finished catalyst designated as Fe–C [iron oxide carbon composite catalyst] had a surface area (BET) of 93 m^2 g^{-1}. The Fe–C pellet catalyst was crushed into 1 mm av. diameter for the degradation experiments. Powder X-ray diffraction analysis confirmed the presence of the Fe_3O_4 phase in Fe–C. The Fe–C catalyst was cooperatively developed with Toda Kogyo Co., Ltd., Hiroshima, Japan.

Degradation procedure

Thermal and catalytic degradation of ABS-Br mixed with PP was performed in a glass reactor (length: 350 mm; id: 30 mm) under atmospheric pressure by a semi-batch operation. A schematic experimental setup for the degradation is shown in Fig. 2. A special, transparent glass furnace was used for heating, and the temperature was monitored and controlled. About 10 g of ABS-Br (2 g) mixed with PP (8 g) polymer was degraded in each experiment. In a typical run, after setting the reactor, the reactor was purged with nitrogen gas at a flow rate of 50 mL min^{-1} up to 150 °C (5 °C min^{-1}) Above this temperature the nitrogen flow was removed and heating continued up to the degradation temperature (450 °C at a heating rate of 5 °C min^{-1}). Once the nitrogen was cut off from the reactor system, a Teflon bag was connected to the end of the reactor to collect the gaseous products coming out of the reactor. The temperature of the waste plastic bed is taken as the temperature of degradation. The gaseous products were condensed (using a cold water condenser) into liquid products and trapped in a measuring jar.

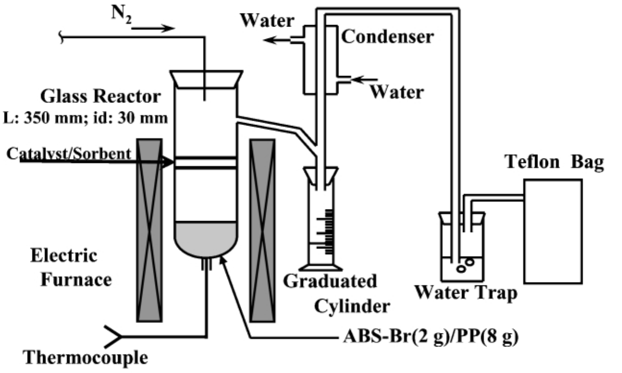

Fig. 2 Schematic experimental setup for the pyrolysis of ABS-Br mixed with PP at 450 °C.

Analysis procedure

The quantity of bromine and nitrogen content (organic) in the thermal degradation liquid products and degradation with Fe–C were analyzed by a gas chromatograph equipped with an atomic emission detector (AED; HP G2350A; column, HP-1; cross-linked methyl siloxane; 25 m × 0.32 mm × 0.17 μm). 1-Bromohexane and nitrobenzene were used as the internal standards for the quantitative determination of bromine and nitrogen, respectively in. the GC–AED analysis. The liquid products were also analyzed by gas chromatography with a mass selective detector [GC–MSD; HP 5973; column, HP-1; cross-linked methyl siloxane, 25 m × 0.32 mm × 0.17 μm; temperature program, 40 °C (hold 10 min) → 300 °C (rate 5 °C min^{-1}) hold for 10 min]. The weight of the reactor including the mixed plastics was measured before and after the degradation process. The weight difference between before and after the degradation was considered as the yield of liquid and gas products. The residue was the difference between the total feed (plastic sample) and the sum of liquid and gas products. There was a very small amount of liquid products on the reactor walls and on the side arm. Ammonia absorbed in a water trap was determined by using an ORION ammonia electrode Model 95-12 using Ionic Strength Adjuster (ISA: 5 M NaOH/0.05 M Na_2H_2EDTA/10% methanol with color indicator). Hydrogen cyanide absorbed in water was determined by means of an ion meter (WTW inoLab pH/Ion Level 2) using a cyanide ion selective electrode (ORION Model 9406 Cyanide Half-Cell and Model 90-02 double junction reference electrode). The residue (carbon residue and wax residue) was combusted in a flask and then analyzed by ion chromatography for bromine content. About 10 mg of residue sample (placed on a filter paper) was placed in a platinum combustion boat and the two arms were connected to a power source. The combustion boat with the sample was inserted into the 500 ml combustion flask, then flushed with the ultra high pure oxygen for 5 min. The residue sample was combusted with the power supply to the combustion flask. After the combustion process, the combustion flask and combustion boat were washed with ion exchanged water and analyzed by anion chromatography. However, the nitrogen content analysis in residue products is complicated, as the nitrogen content will be converted into various nitrogen oxides and acids during combustion of which the nitrogen oxides are unable to be detected using ion chromatography. The acid content, *e.g.* HNO_2 (NO_2^-) and HNO_3 (NO_3^-) can be analyzed. It is thus difficult to analyze the total nitrogen content in the residue by this method.

Conclusions

The degradation of brominated flame retardant containing acrylonitrile–butadiene–styrene (ABS-Br) mixed with polypropylene (PP) was carried at 450 °C using an iron oxide carbon composite catalyst (Fe–C) and completely removed the bromine content from the liquid products. A single step process for the degradation and debromination was performed. The majority of nitrogen content converted into ammonia. The light aliphatic nitriles present in liquid products can be separated by a distillation process. The liquid products can be used as fuel oil or feed stock in the petroleum refinery.

Acknowledgements

The authors would like to thank New Energy Development Organization (NEDO), Japan for financial support to carry out this research work under the Chugoku regional consortium project (2000–2003). We are grateful to Dr Katsuhide Murata of K. Murata Research Inc, Ichihara, Japan, for his valuable discussions.

References

1 (*a*) D. C. Saunders, *Technical workshop report, on Sustainable management for plastics with bromine in Tokyo*, 1999; (*b*) L. Tange, *Technical workshop report, on Sustainable management for plastics with bromine in Tokyo*, 1999.
2 J. Aguado and D. Serrano, *RSC Clean Technology monographs, on Feedstock Recycling of Waste Plastic*, ed. J. H. Clark, Royal Society of Chemistry, Cambridge , 1999.
3 W. Kaminsky and F. Hartmann, *Angew. Chem., Int. Ed.*, 2000, **39**, 331.
4 Y. Sakata, Md. A. Uddin and A. Muto, *J. Anal. Appl. Pyrolysis*, 1999, **51**, 135.
5 Md. A. Uddin, K. Koizumi, K. Murata and Y. Sakata, *Polym. Degrad. Stab.*, 1997, **56**, 37.
6 Y. Sakata, Md. A. Uddin, A. Muto, M. Narazaki, K. Koizumi, K. Murata and K. Mitsuo, *Ind. Eng. Chem. Res.*, 1998, **37**, 2889.
7 M. Brebu, Md. A. Uddin, A. Muto, Y. Sakata and C. Vasile, *Energy Fuels*, 2000, **14**, 920.
8 M. Brebu, Md. A. Uddin, A. Muto, Y. Sakata and C. Vasile, *J. Anal. App. Pyro.*, 2002, **63**, 43.
9 M. Brebu, Md. A. Uddin, A. Muto, Y. Sakata and C. Vasile, *Energy Fuels*, 2001, **15**, 559.
10 C. S. Richard, A. R. Wayne, A. T. Debra and B. Dellinger, *Chemosphere*, 1991, **23**, 1197.
11 H. Kaufer and O. von Quast, *Kunststoffe Plast Eur.*, 1997, 20.
12 J. Vehlow and E. E. Mark, *APME Tech. Rep.*, 1995.
13 J. Vehlow, B. Bergfeldt, K. Jay, H. Seifert, T. Wanke and E. E. Mark, *Waste Manag. Res.*, 2000, **18**, 131.
14 Md. Azhar Uddin, T. Bhaskar, J. Kaneko, A. Muto, Y. Sakata and T. Matsui, *Fuel*, 2002, **81**, 1819.

Isomerization of eugenol and safrole over MgAl hydrotalcite, a solid base catalyst†

D. Kishore and S. Kannan*

Silicates Catalysis Discipline, CSMCRI, GB Marg, Bhavnagar- 364 002, India.
E-mail: salt@csir.res.in; Fax: +91-278-566970; Tel: +91-278-567760

Received 12th August 2002
First published as an Advance Article on the web 30th October 2002

Isomerization of olefins, in particular eugenol and safrole, is an important reaction as the products, namely isoeugenol and isosafrole, find application in pharmaceuticals and fragrances. The catalyst employed to carry out this reaction is either a strong alkaline solution (KOH or KO*t*Bu) or precious metal catalysts under homogenous conditions, which pose severe environmental problems such as handling and effluent disposal as well as cost. The present paper discloses a new alternative route wherein hydrotalcite is used as a solid base catalyst, which is environmentally friendly as well as economical in obtaining good yields of the isomerized products.

Introduction

Isomerization of eugenol and safrole to the corresponding thermodynamically stable isomers namely isoeugenol and isosafrole (Scheme 1), is an important olefin isomerization reaction wherein the products find application in the fragrance and pharmaceutical industries.[1,2] Traditionally these reactions are catalyzed by alkalis such as KOH in alcoholic solutions (most often in higher alcohols) at high temperatures.[3,4] Alternatively, complexes of group VIII elements are used to catalyze these reactions.[5,6] Cerveny *et al.*[7] have studied isomerization of eugenol over both alcoholic alkali solution as well as on anhydrous $RhCl_3$. A high concentration of alkali was needed (nearly seven times the concentration of substrate) to achieve stoichiometric yield while a reduction in the concentration of alkali decreased the conversion of eugenol. Isomerization over $RhCl_3$ showed a strong negative influence when the reaction was carried out in the presence of water and the inherent activity of the catalyst decreased with time. Radhakrishna and coworkers[8,9] have carried out isomerization of eugenol and safrole on KF on neutral alumina in dry ethylene glycol and obtained around 75% yield at 150 °C. Conversion improved when they used 'dry media' without using any solvent. However, in these cases, the amount of base employed was 10–20 times (w/w ratio) more than the substrate. Very recently, Thach *et al.*[10,11] have employed a microwave batch reactor to facilitate these isomerization reactions in both dry media as well as under alkaline solutions. A conversion of 73% was obtained for eugenol and 86% was obtained for safrole at 220 °C for 15 min in the presence of NaOH. Replacement of conventional alkali based catalysts by solid base catalysts is one of the important tasks in view of easier process handling, effluent control, easy separation and in turn resulting in a cleaner environment.[12–14] Hydrotalcite-like (HT-like) compounds are one of such promising heterogeneous solid base catalysts, which have been exploited for various base catalyzed transformations such as aldol condensation,[15,16] double bond isomerization of alkenes[17] and dehydrogenation of 2-propanol.[18] They are layered materials with the general formula $[M(\textsc{ii})_{1-x}M(\textsc{iii})_x(OH)_2][A_{x/n}^{n-}]\cdot mH_2O$ where M(II) is a bivalent metal ion and M(III) is a trivalent metal ion, A is the interlayer anion and x can generally have the values between 0.2 and 0.35. Structurally, they possess a brucite-like ($Mg(OH)_2$) layered network wherein a partial substitution of bivalent ion by trivalent ion, say Al^{3+}, occurs, and the resulting excess positive charge in the layers is compensated by anions located in the interlayers.[19] Corma *et al.*[20] have explored these materials for the production of citronitril, a fine chemical used in the perfume industry through condensation of ethyl cyanoacetate and benzyl alcohol over calcined MgAl hydrotalcites and claimed highest activity for the catalyst with an Mg/Al atomic ratio of 3.0. Kaneda and coworkers[21] have exploited the basic character of hydrotalcites in the epoxidation of olefins using hydrogen peroxide in presence of nitriles. Common linear and cyclo olefins such as oct-1-ene and cyclohexene gave the corresponding epoxide as the sole product in excellent yield while for α,β-unsaturated ketones, such as cyclohex-2-en-1-one, epoxidation occurred exclusively without formation of Bayer–Villiger oxidation products. Very recently Kumbhar *et al.*[22] have carried

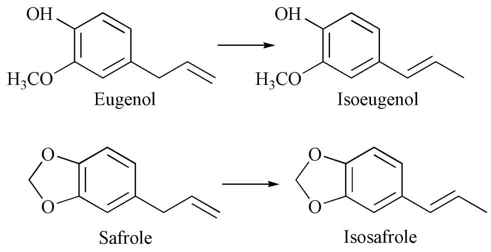

Scheme 1 Isomerization of eugenol and safrole.

Green Context

The isomerisation of olefins is an important chemical transformation used in many industrial processes. Among the most valuable of these are the isomerisation of eugenol to isoeugenol and safrole to isosafrole. Like many other olefin isomerisations these are commonly carried out using conventional bases such as KOH in alcoholic solvents. Other catalysts have been reported but common problems are caustic waste streams and the need for very large quantities of base to give good substrate conversions. Here the benign solid base hydrotalcite is shown to be very active for these isomerisations. Waste streams can thus be avoided and the catalyst which is shown to be insensitive to the atmosphere, is easy and safe to handle. *JHC*

---

† Electronic supplementary information (ESI) available: Figs. S1 and S2: PXRD patterns. See http://www.rsc.org/suppdata/gc/b2/b207865a/

DOI: 10.1039/b207865a

out cyanoethylation of methanol over rehydrated hydrotalcites and claimed a very high activity in the liquid phase under mild reaction conditions. In the present paper, we report our first results on the isomerization of safrole and eugenol over MgAl hydrotalcite-like compounds. For completeness, end members of the series, namely $Mg(OH)_2$ and $Al(OH)_3$, are also synthesized and their activities are compared.

Results and discussion

Table 1 summarizes the physicochemical properties of the compounds synthesized. Elemental analysis showed no significant deviation between the input Mg/Al atomic composition and the final solid composition, except at higher Mg/Al atomic ratios where deviations are likely due to preferential precipitation,[23] ensuring the completion of precipitation. PXRD of the samples (Fig. S1, ESI†) showed a pure hydrotalcite-like phase for Mg/Al atomic ratios up to 6.0. With a further increase in the ratio, an additional phase, namely magnesium carbonate ($5MgO{\cdot}4CO_2{\cdot}5H_2O$, JCPDS 01-0168) was observed along with the HT-like phase. It is known in the literature, that the pure HT-like phase is obtainable for M(II)/M(III) atomic ratios in the range 1.5–5.7.[19] The lattice parameters of these samples were calculated (‘c’ was calculated from the position of the first basal peak appearing around $2\theta = 11°$ as $c = 3d_{(003)}$ and ‘a’ was calculated from the position of first peak of the doublet appearing around $2\theta = 60°$ as $a = 2d_{(110)}$), and are summarized in Table 1. An increase in the ‘a’ parameter was observed with an increase in Mg/Al atomic ratio, while the ‘c’ parameter increased up to Mg/Al atomic ratio of 6.0 and then was not altered significantly with a further increase in the ratio. The increase in the ‘a’ parameter is attributed to higher ionic radius of Mg^{2+} (0.72 Å) with respect of Al^{3+} (0.53 Å) while the increase in the ‘c’ parameter is rationalized by lower electrostatic interactions between layers and interlayers due to the lower concentration of aluminum (in turn on carbonate content in the interlayers). Further, with an increase in Mg/Al atomic ratio a continuous decrease in the surface area was noted.

Table 1 Physicochemical properties of the samples synthesized

	Mg/Al atomic ratio		Lattice parameters		
Catalyst	Solution	Solid	*a*	*c*	Surface area/$m^2\ g^{-1}$
MgAl-2HT	2.0	2.0	3.04	22.85	102
MgAl-3HT	3.0	2.7	3.06	23.20	80
MgAl-4HT	4.0	3.5	3.07	24.41	83
MgAl-6HT	6.0	4.2	3.08	23.85	61
MgAl-8HT	8.0	5.8	3.09	24.12	49
MgAl-10HT	10.0	6.4	3.10	24.19	44

Table 2 Isomerization activities of eugenol and safrole over various MgAl hydrotalcites

	Eugenol			Safrole		
		Selectivity (%)			Selectivity (%)	
Catalyst	Conv. (%)	*cis*	*trans*	Conv. (%)	*cis*	*trans*
MgAl-2HT	34	29	71	2	—	100
MgAl-3HT	48	23	77	1	—	100
MgAl-4HT	73	17	83	28	11	89
MgAl-6HT	45	27	73	75	15	85
MgAl-8HT	40	30	70	33	15	85
MgAl-10HT	23		100	54	15	85
$Mg(OH)_2$	—	—	—	0.3	—	100
$Al(OH)_3$	—	—	—	0.1	—	100
Blank	—	—	—	—	—	100

Substrate: 0.5 g, solvent: DMF (20 ml), catalyst: 250 mg, reaction temp./time: 200 °C/6 h.

Table 2 summarizes the isomerization activity of various MgAl hydrotalcites towards both safrole and eugenol. End members, namely $Mg(OH)_2$ and $Al(OH)_3$, are also included for comparison. It is clear from the Table that both end members are not active for eugenol and exhibited very low activity for safrole. The mixed hydroxycarbonates of Mg and Al crystallizing in the hydrotalcite-like phase showed considerable activity, which, however, varied with the Mg/Al atomic composition. In the case of eugenol an Mg/Al atomic ratio of 4.0 (MgAl-4HT) showed maximum activity with the conversion of around 73% with a *cis*:*trans* ratio of 17:83 while the catalyst with Mg/Al atomic ratio of 6.0 (MgAl–6HT) showed maximum activity for safrole, exhibiting around 75% conversion with a *cis*:*trans* ratio of 15:85. *Trans* isomers were formed predominantly in both cases due to their better thermodynamic stability. The activity of MgAl–2HT was lower compared to the catalysts mentioned above for both transformations, despite having maximum surface area, suggesting the necessity of appropriate basicity. For both series of catalysts, an increase in the conversion was noted with an increase in Mg/Al atomic ratio, however, conversion reached a maximum and decreased with a further increase in this ratio. This could probably be due to variation in the basicity of the catalysts. Although basicity correlation with the observed activity is underway, it is known in the literature that basicity varies in a similar trend with the Mg/Al atomic composition, in line with the activity trend depicted above.[18,24] Further, the catalysts possessing maximum activity for the two different substrates were different, suggesting a difference in basicity requirements for propagating the two reactions. To compare the activity of our catalysts with conventional catalysts, we have carried out isomerization of eugenol over KOH and KO*t*Bu in excess substrate:catalyst mole ratio (1:3 for KOH and 1:1.5 for KOtBu). A conversion of 9% and 5% of eugenol to isoeugenol was observed respectively, far less compared to our hydrotalcite-based catalysts, indicating their superior behavior in addition to their environmental benefits.

From the results above, we selected MgAl–4HT for eugenol and MgAl–6HT for safrole, as they showed maximum activity for the corresponding isomerization reactions, for further study. Table 3 shows the influence of catalyst:substrate mass ratio for eugenol and safrole over these catalysts. The conversion increased with an increase in catalyst:substrate ratio for both the series of catalysts. At equivalent mass ratio (which is nearly 1:3.6 catalyst:substrate mole ratio), a conversion of 85% of eugenol with a *cis*:*trans* ratio of 15:85 was observed. To our knowledge, this is the highest conversion for eugenol reported in the literature so far under conventional conditions. In the case of safrole, 88% conversion of safrole was obtained under equivalent substrate:catalyst mass ratio. Further in both cases, the mass balance of substrates were better than 95% suggesting selective isomerization without forming any additional or

Table 3 Isomerization activities of eugenol over MgAl-4HT and safrole over MgAl-6HT

	Eugenol			Safrole		
		Selectivity (%)			Selectivity (%)	
Sub:Cat mass ratio	Conv. (%)	*cis*	*trans*	Conv. (%)	*cis*	*trans*
10:1	30		100	20	25	75
5:1	45	22	78	45	18	82
3.3:1	60	17	83	53	15	85
2.5:1	65	15	85	56	14	86
2:1	73	16	84	75	15	85
1:1	85	15	85	88	13	87

Substrate: 0.5 g, solvent: DMF (20 ml), reaction temp./time : 200 °C/6 h consecutive reaction products. High conversion with exceptionally good yields of isomerized products for both eugenol and safrole over these solid base catalysts, suggests their application for commercial exploitation.

Solvent variation studies showed that, among the various solvents screened, namely THF, DMF, DMSO, toluene, glycerol, acetonitrile and glycol, DMF was best for eugenol and DMSO was best for safrole isomerization, and hence were selected for further study. Variation in the reaction temperature for these isomerization reactions showed (Fig. 1A), in the case of eugenol, conversion was noticed above 160 °C (1.8%) and increased with an increase in the temperature. However, a sharp increase in the conversion was noticed when the temperature was raised to 200 °C (75%). However, in the case of safrole, a gradual increase was noted with an increase in reaction temperature, wherein 98% conversion was achieved at 200 °C with a *cis*:*trans* ratio of 10:90. These results show that, despite both the isomerization reactions being carried out over similar catalysts, the kinetics of the reaction varied with the nature of substrate. However, the influence of solvent in affecting the course of the reaction cannot be completely ruled out. The effect of reaction time substantiated the difference in kinetics (Fig. 1B) wherein more than 95% conversion of safrole to isosafrole was obtained in 1 h while a gradual increase in the conversion of eugenol was noticed with an increase in time, wherein more than 70% conversion was observed after 4 h. No significant change in the yield of isomeric products was noticed with a further increase in time suggesting the absence of consecutive reactions.

In an anticipation to find better catalysts, MgAl-4HT was calcined at various temperatures (200, 400, 600 and 800 °C) and tested for eugenol isomerization activity. Although recent interest has been in exploring the basic and/or redox properties of fresh hydrotalcites for various catalytic transformations, much of the earlier work involved using calcined hydrotalcites as base catalysts.[19] In our case, conversion decreased with an increase in the calcination temperature, however, reasonable conversion (~ 40% with a *cis*:*trans* ratio of 10:90) was shown at 200 and 400 °C. With a further increase in the temperature, conversion drastically decreased (3%) probably due to loss in specific surface area and phase transformation of HT-like network to mixed metal oxides (Fig. S2, ESI†). Constantino and Pinnavaia[25] have earlier observed this for the reaction of 2-methyl-3-butyn-2-ol over MgAl hydrotalcite, wherein they claimed thermal activation below the structural decomposition point (< 250 °C) resulted in higher activities compared to amorphous metal oxides formed by thermal activation at 450 °C. To determine the influence of the reaction atmosphere, eugenol isomerization was carried out over MgAl-4HT under nitrogen. The conversion decreased (44% with *cis*:*trans* ratio of 20/80) under inert conditions, suggesting the non-influence of atmosphere on the basic sites of these materials in catalyzing the reaction. This is advantageous in view of the general hurdle posed by basic catalysts prone to CO_2 and/or H_2O poisoning, forcing operation under inert conditions. Further, when the same catalyst was externally calcined at 200 °C for 5 h and tested for the reaction, the conversion of eugenol (39% conversion with *cis*:*trans* ratio of 10:90) was less than for the fresh catalyst subjected to 200 °C for the reaction, suggesting the superior nature of basic sites generated *in situ* under reaction conditions. This is our first report on the use of hydrotalcite-derived solid base catalysts for isomerization reactions. A further detailed investigation of various parameters such as influence of bivalent and trivalent metal ions, substrate concentration and basicity correlations with observed activity is underway.

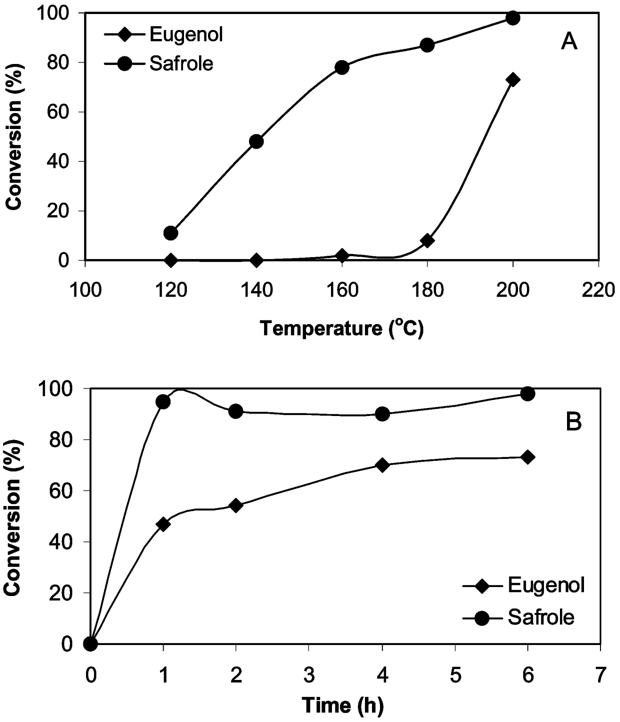

Fig. 1 A. Influence of reaction temperature (reaction time; 6 h) B. Influence of reaction time (reaction temperature; 200 °C) on the isomerization activities of eugenol and safrole over MgAl-4HT and MgAl-6HT, respectively—substrate: 0.5 g, catalyst: 250 mg, solvent: DMF, 20 ml for eugenol and DMSO, 10 ml for safrole.

Experimental

MgAl hydrotalcites with different Mg/Al atomic ratio (2.0, 3.0, 4.0, 6.0, 8.0 and 10.0) were synthesized by coprecipitation under low supersaturation.[19] A typical synthesis involves simultaneous addition of two solutions: Solution-A containing appropriate concentration of magnesium nitrate and aluminum nitrate solutions and Solution-B containing NaOH and Na_2CO_3 solutions as precipitants while maintaining the pH around 9–10 under vigorous stirring at room temperature. The precipitate was aged in the mother-liquor at 65 °C for 18 h, filtered off, washed thoroughly with distilled water (until total absence of nitrates and sodium in the filtrate) and dried at 110 °C for 12 h. The solids obtained here are referred as MgAl-*x*HT where *x* is the Mg/Al atomic ratio. Powder X-ray diffraction of the samples were recorded in a Philips Xpert MPD System using Cu-Kα radiation (λ = 1.5406 Å) with a step size of 0.02° and step time of 1 s. Specific surface area of these samples was measured by nitrogen adsorption at 77 K using a sorptometer (ASAP-2010, Micromeritics). The samples were degassed at 120 °C for 4 h prior to measurements.

Isomerization of eugenol and safrole was conducted in a batch reactor (50 ml), wherein the substrate, solvent and catalyst were charged all at once and raised to the reaction temperature, and the products were withdrawn using a syringe at definite time intervals and analyzed (using authentic samples) by gas chromatography (Shimadzu-14B, OV-17) using FID. Quantification of the products was done using isopropanol as internal standard. Identification of the products was also further verified using GC-MS (HP-5890-II GC connected to HP-5971 mass selective detector) as well as ^{1}H NMR (Bruker, Avance-200).

Acknowledgements

S. K. Thanks Indian National Science Academy, New Delhi (BS/YSP-22) and Council of Scientific and Industrial Research, New Delhi for financial assistance granted under Young

Scientist Schemes. The authors would also like to thank the referees for their constructive criticism, which has helped in improving the quality of the manuscript.

References

1 K. Bauer, D. Garbe and H. Surberg, Flavors and Fragrances, in *Ullmann Encyclopedia of Industrial Chemistry*, Electronic Release, 6th edn., 2002.
2 P. Gandilhon, *US Pat.*, 4,138,411, 1979.
3 A. J. Hubert and H. Reimlinger, *Synthesis*, 1969, 97.
4 G. V. Salmoria, E. C. Dall'Oglio and C. Zucco, *Synth. Commun.*, 1997, **27**, 4335.
5 T. Karlen and A. Ludi, *Helv. Chim. Acta*, 1982, **75**, 1604.
6 J. Andrieux, D. H. R. Barton and H. Patin, *J. Chem. Soc., Perkin Trans. 1*, 1977, 359.
7 L. Cerveny, A. Krejeikova, A. Marhoul and V. Ruzicka, *React. Kinet.-Catal. Lett.*, 1987, **33**, 471.
8 A. S. Radhakrishna, S. K. Suri, K. R. K. Prasada Rao, K. Sivaprakash and B. B. Singh, *Synth. Commun.*, 1990, **20**, 345.
9 L. N. Thach, D.-L. Hanh, N. Ba Hiep, A. S. Radhakrishna, B. B. Singh and A. Loupy, *Synth.Commun.*, 1993, **23**, 1379.
10 L. N. Thach, T. H. Anh, N. A. Kiet and T. M. Phuong, *Tap Chi Hoa Hoc*, 1999, **37**, 92.
11 L. N. Thach and C. R. Strauss, *J. Chem.*, 2000, **38**, 76.
12 Y. Ono and T. Baba, in *Catalysis*, Specialist Periodical Report, ed. J. J. Spivey, Royal Society of Chemistry, Cambridge,2000, p. 1.
13 K. Tanabe and W. F. Holderich, *Appl. Catal. A*, 1999, **161**, 399.
14 H. Hattori, *Chem. Rev.*, 1995, **95**, 527.
15 W. T. Reichle, *J. Catal.*, 1985, **94**, 547.
16 B. M. Choudary, M. Lakshmi Kantam, V. Neeraja, K. Koteswara Rao, F. Figueras and L. Delmotte, *Green Chem.*, 2001, **3**, 257.
17 H. Schaper, J. J. Berg-Slot and W. H. J. Stork, *Appl. Catal.*, 1989, **54**, 79.
18 A. L. McKenzie, C. T. Fisher and R. J. Davis, *J. Catal.*, 1992, **138**, 547.
19 F. Trifirò and A. Vaccari, in *Comprehensive Supramolecular Chemistry, Solid State Supramolecular Chemistry: Two and Three-dimensional Inorganic Networks*, ed. J. L. Atwood, J. E. D. Dasvies, D. D. MacNicol, F. Vogtle, J.-M.Lehn, G. Aberti and T. Bein, Pergamon, Oxford, 1996, vol. 7, p. 251.
20 A. Corma, S. Iborra, J. Primo and F. Rey, *Appl. Catal.*, 1994, **114**, 215.
21 S. Ueno, K. Yamaguchi, K. Yoshida, K. Ebitani and K. Kaneda, *Chem. Commun.*, 1998, 295.
22 P. S. Kumbhar, J. Sanchez-Valente and F. Figueras, *Chem. Commun.*, 1998, 1091.
23 A. De Roy, C. Forano, K. El Malki and J. P. Besse, in *Expanded Clays and Other Microporous Solids, Synthesis of Microporous Materials*, ed. M. L.Occelli and H. Robson, van Nostrand Reinhold, New York, 1992, ch. 7, p. 108.
24 C. T. Fishel and R. J. Davis, *Catal. Lett.*, 1994, **25**, 87.
25 V. R. L. Constantino and T. J. Pinnavaia, *Inorg. Chem.*, 1995, **34**, 883.

Synthesis of morpholinated and 8-hydroxyquinolinated silica gel and their application to water softening

Mohammad Ali Zolfigol,*[a] Tayyebeh Madrakian,[a] Ezat Ghaemi,[a] Abbas Afkhami,[a] Saeid Azizian[a] and Shahrara Afshar[b]

[a] *Chemistry Department, College of Science, Bu-Ali Sina University, Hamadan Zip Code 65174 Post Box No 4135, Iran. E-mail: zolfi@basu.ac.ir*
[b] *Iran University of Science and Technology (IUST), Department of Chemical Engineering, Narmak, 16844 Tehran, Iran*

Received 2nd September 2002
First published as an Advance Article on the web 1st November 2002

Morpholinated and 8-hydroxyquinolinated silica gel were obtained *via* reaction of silica chloride with morpholine and 8-hydroxyquinoline, respectively. The applicability of the synthesized reagents for softening of different water samples was studied. The quality of softened water was tested by measuring concentrations of Mg^{2+}, Ca^{2+} and HCO_3^- ions. The results show that the above reagents are suitable for water softening. The isotherms for adsorption of Ca^{2+} and Mg^{2+} were obtained.

1. Introduction

The concentration of calcium and magnesium ions in natural waters generally far exceeds that of other metal ions; thus, hardness has come to mean the total concentration of calcium and magnesium expressed in terms of the calcium carbonate equivalent. The removal of hardness is a useful process for increasing the quality of water for household and industrial uses. The importance for the latter is due to the fact that hard water, upon heating, precipitates calcium carbonate, which then clogs boilers and pipes.

Several methods have been reported for softening, desalination and preconcentration of trace metals from natural waters.[1–3] In some reported methods, several exchange materials have been prepared by loading water-insoluble inorganic ion-exchangers or chelating precipitants on silica gel or other supports.[4–6] The use of chelating functional groups attached to silica gel was also reported.[7–11] This methods requires no previous addition of chemicals, and can be used for online collection at the natural pH of the sample. Several methods based on activated carbon have also been reported. The sample is either filtered through an activated carbon layer on filter paper or is mixed with activated carbon, which is filtered off after shaking or standing for a given time.

In continuation of our studies on the application of heterogeneous systems,[12,13] we decided to synthesize the novel insoluble chelating matrices, morpholinated (**2**) and 8-hydroxyquinolinated (**3**) silica gels. The resulting silica gels were used to remove Ca^{2+} and Mg^{2+} from several water samples with excellent efficiency. We wish to report a simple method for the effective water softening under mild and heterogeneous media.

2. Experimental

2.1 Apparatus

A Shimadzu model 670 atomic absorption spectrometer was used for determination of concentration of metal ions. The following conditions were used: absorption lines: Ca: 422.7 nm, Mg: 285.2 nm; slit widths: Ca: 0.5 nm, Mg: 0.5 nm; and lamp currents: Ca: 6 mA, Mg: 4 mA. The flow rates of air and acetylene were set as recommended by the manufacturer.

2.2 Reagents

Triply distilled water was used and analytical reagent grade chemicals were purchased from Fluka, Merck, Riedel-dehaen AG and Aldrich chemical companies.

2.3. Preparation of silica chloride (1)

To an oven-dried (120 °C, vacuum) silica gel (10 g) in a round bottomed flask (250 mL) equipped with a condenser and a drying tube, was added thionyl chloride (40 mL) and the reaction mixture refluxed for 48 h. The unreacted thionyl chloride was distilled off and the resulting white-grayish powder was flame-dried and stored in a tightly capped bottle.[14] This silica chloride can be used for months without losing its activity (eqn. (1)). It should be noted that the adsorption of water

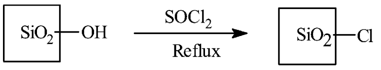

1

(1)

Green Context

Water treatment so as to improve the quality for household or industrial uses is of fundamental importance for a sustainable society. Water treatment consumes resources however, and it is very important that we minimize the environmental impact of the process through the use of the most efficient and benign procedures. This paper reports new heterogeneous water treatment agents for the removal of calcium and magnesium. The agents are based on non-hazardous and readily available silica gels. The used agents are simply regenerated and are effective without pH control.
JHC

DOI: 10.1039/b208526g

by silica chloride causes its conversion to original silica gel by generation of HCl. The percentage of chloride in the silica chloride (**1**) was determined by acid–base titration according to the following reaction (eqn. (2)). The librated HCl was titrated

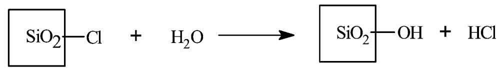

(2)

1

by standard NaOH and the amount of chloride in silica chloride (**1**) was calculated.

2.4. Synthesis of reagents

2.4.1. Preparation of morpholinated silica gel (2): a typical procedure. Morpholine (100 ml) was added to 60 g of silica chloride (**1**) and the slurry was stirred vigorously for 24 h and then the mixture was filtered. The nitrogen sites in morpholine and 8-hydroxyquinoline can act as a base. Therefore, after nucleophilic reaction on the silica chloride, the librated HCl could be adsorbed by nitrogen sites and converted the products to the corresponding morpholinum or 8-hydroxyquinolinum salts. In order to remove HCl from morpholinated silica gel (**2**) or 8-hydroxyquinolinated silica gel (**3**) 100 mL triethylamine (as a strongly organic liquid base which was completely miscible with water) was added to the residue. The slurry was stirred vigorously for 2 h, then, the residue was washed with triply distilled water (3 × 150 ml). The residue was added to 300 ml triply distilled water and stirred for 15 min and was filtered by suction. To the resulting residue was added acetonitrile (200 ml) and stirred for 30 min and filtered. The morpholinated silica gel (**1**) was then dried in an oven (60 °C). Microanalysis of **2** is in close agreement with its structure.

2.4 Water softening

0.5 g of **2** was transferred into a column of 15 cm length and 0.5 cm diameter the column having being washed with triply distilled water. Then 50 ml of a water sample was passed through the column. The concentration of Ca^{2+} and Mg^{2+} in the stripped solution was then measured by AAS at 422.7 and 285.2 nm, respectively.

The ability of **3** for adsorption of Ca^{2+} and Mg^{2+} from water samples was also studied as described for **2**.

3. Results and discussion

It is interesting that the addition of morpholine and 8-hydroxyquinoline to a reaction mixture containing silica chloride produces morpholinated and 8-hydroxyquinolinated silica gels (Scheme 1).The products were pale yellow solids. These reagents (**2**) and (**3**) are suitable for the adsorption of metal ions by complex formation.

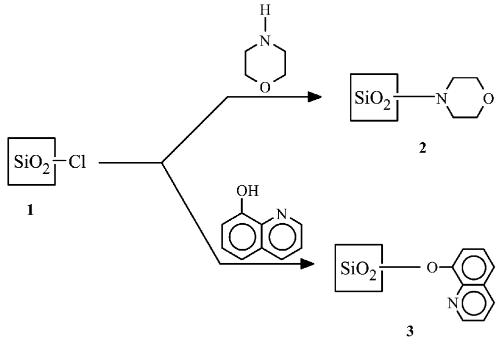

Scheme 1

3.1 Adsorption of Ca^{2+} and Mg^{2+} ions and water softening

As mentioned above, the hardness of water has come to mean the total concentration of calcium and magnesium. In order to evaluate the applicability of the reagents, their efficiency in removing Ca^{2+} and Mg^{2+} ions from standard solutions and water softening on the bench scale was studied. 0.5 g of **2** was transferred to the column and the column was washed with triply distilled water. Then 40 ml of 30 mg l^{-1} Ca^{2+} standard solution was passed through the column and then the column was washed with 10 ml of triply distilled water. The concentration of Ca^{2+} in stripped solution was then measured by AAS at 422.7 nm. The results are given in Tables 1–3.

The above procedure was also performed with a 40 ml of 20 mg l^{-1} Mg^{2+} and the concentration of Mg^{2+} in the stripped solution was measured by AAS at 285.2 nm.

The ability of **3** for adsorption of Ca^{2+} and Mg^{2+} from standard solutions was also studied as described for **2**. The results are given in Tables 1–3. As seen from these tables, the reagents are highly efficient for removing Ca^{2+} and Mg^{2+} from water samples.

Table 1 The concentration of Ca^{2+}, Mg^{2+} and HCO_3^- in feed and stripped standard and other water samples for columns packed with silica gel

	Amount of ions in feed solution			Amount of ions in stripped solution		
Sample	Ca^{2+}/mmol l^{-1}	Mg^{2+}/mmol l^{-1}	HCO_3^-/meq l^{-1}	Ca^{2+}/mmol l^{-1}	Mg^{2+}/mmol l^{-1}	HCO_3^-/meq l^{-1}
Standard 1	0.80	—	—	0.56	—	—
Standard 2	—	0.82	—	—	0.58	—
Tap water	2.31	0.72	6.80	2.21	0.47	6.11
Spring water 1	2.64	0.93	7.33	2.44	0.81	7.13
Spring water 2	3.68	1.78	12.50	3.55	1.63	10.26

Table 2 The concentration of Ca^{2+}, Mg^{2+} and HCO_3^- in feed and stripped standard and other water samples for columns packed with **2**

	Amount of ions in feed solution			Amount of ions in stripped solution		
Sample	Ca^{2+}/mmol l^{-1}	Mg^{2+}/mmol l^{-1}	HCO_3^-/mmeq l^{-1}	Ca^{2+}/mmol l^{-1}	Mg^{2+}/mmol l^{-1}	HCO_3^-/mmeq l^{-1}
Standard 1	0.80	—	—	0.00	—	—
Standard 2	—	0.82	—	—	0.00	—
Tap water	2.31	0.72	6.80	0.03	0.00	0.11
Spring water 1	2.64	0.93	7.33	0.16	0.00	0.42
Spring water 2	3.68	1.78	12.50	0.26	0.00	0.76

The quality of several water samples before and after passing through the columns was studied. The columns were prepared as described before. Then 50 ml of a water sample was passed through each column and the concentration of Ca^{2+}, Mg^{2+} and HCO_3^- in stripped and feed waters was measured by AAS and alkalimetry, respectively. Tables 1–3 show the results. These experiments were also performed by passing the standard solutions and tap water samples through a column that was packed with silica gel. The results showed that the amount of the adsorption of Ca^{2+} and Mg^{2+} by silica gel is not significant. As Tables 1–3 show, the reagents are highly efficient for water softening. Passing water through columns containing **2** or **3** did not cause any bad smell. The presence of 8-hydroxyquinoline and morpholine in softened water samples was tested by UV spectrophotometry. The results indicated that these compounds are not present in the softened water samples.

3.2. Recycling the chelating reagents

The Ca^{2+} and Mg^{2+} retained on **2** and **3** were eluted by elution of the columns with 10 ml of a 0.1 M HCl solution. The columns were then washed with triply distilled water until the pH of eluate reached to about 5.5. In order to investigate the efficiency of the recycled reagents, they were used for the removal of Ca^{2+} and Mg^{2+} from standard Ca^{2+} and Mg^{2+} solutions as described above. The results show that the efficiencies of the recycled reagents for removing Ca^{2+} and Mg^{2+} ions are nearly the same as those of the fresh ones even after four times recycling.

3.3 Adsorption isotherm

The adsorption isotherms for both cations (Ca^{2+} and Mg^{2+}) from water on **2** and **3** are shown in Figs. 1 and 2 respectively. The number of moles adsorbed per gram of adsorbent (N_f) *versus* the equilibrium concentration of cations are illustrated. For the series of isotherms the data reveal that the adsorption processes conform to the Langmuir model. Such isotherms are generally associated with monolayer adsorption. The initial slopes in Figs. 1 and 2 lie very close to the *y*-axis which shows that the affinity of both cations for **2** and **3** are strong. The Langmuir isotherm shows that the amount of cations adsorbed increases as the concentration increases, up to a saturation point. As long as there are available sites, adsorption will increase with increasing cation concentrations, but as soon as all of the sites are occupied, a further increase in concentrations of cations will not increase the amount of cations on adsorbents.

The Langmuir equation was used to calculate the maximum retention capacity (N_s) and standard Gibbs free energy of adsorption (ΔG_{ads}).[7,15,16] The general form of Langmuir isotherm is

$$Y = KC_s/(1 + KC_s) \qquad (3)$$

Where Y is the fraction of adsorbent surface covered by adsorbed species, K is a constant and C_s is the equilibrium concentration of the cation solution. In our case, $Y = N_f/N_s$, where N_f represents the number of moles of cation adsorbed per gram of adsorbent (mol g^{-1}) at equilibrium concentration, C_s, and N_s is the maximum amount of solute adsorbed per gram of surface (mol g^{-1}) which depends on the number of adsorption sites. After linearization of the Langmuir isotherm, eqn. (3), we obtain

$$C_s/N_f = (C_s/N_s) + (1/KN_s) \qquad (4)$$

All these adsorption studies were based on the linearization form of the Langmuir isotherm derived from C_s/N_f as a function of C_s. These plots for Ca^{2+} and Mg^{2+} on **2** and **3** are shown in

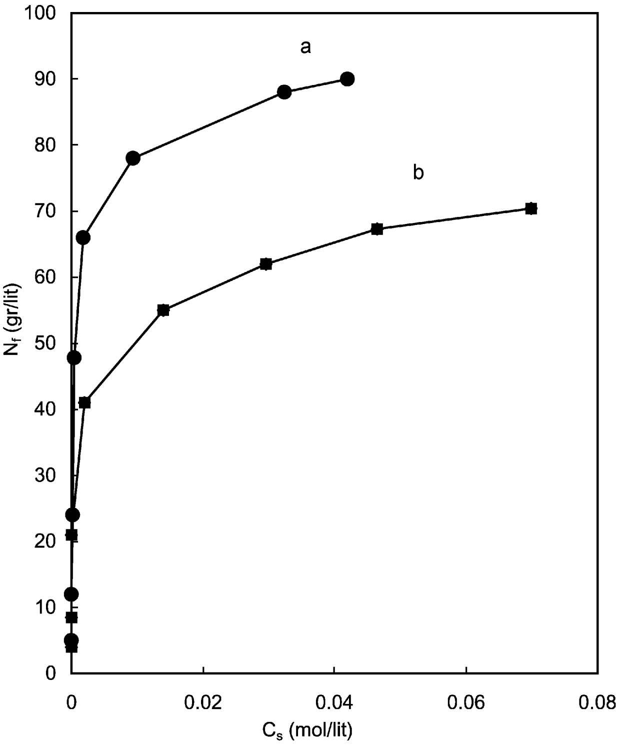

Fig. 1 Adsorption isotherm of (a) Ca^{2+} and (b) Mg^{2+} on **2**.

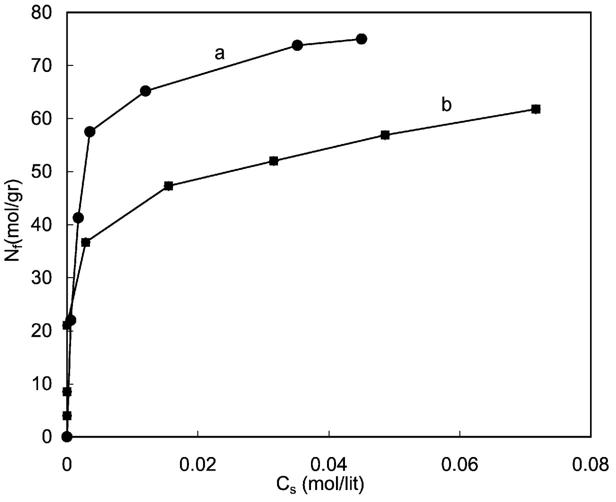

Fig. 2 Adsorption isotherm of (a) Ca^{2+} and (b) Mg^{2+} on **3**.

Table 3 The concentration of Ca^{2+}, Mg^{2+} and HCO_3^- in feed and stripped standard and other water samples for columns packed with **3**

	Amount of ions in feed solution			Amount of ions in stripped solution		
Sample	Ca^{2+}/mmol l^{-1}	Mg^{2+}/mmol l^{-1}	HCO_3^-/mmeq l^{-1}	Ca^{2+}/mmol l^{-1}	Mg^{2+}/mmol l^{-1}	HCO_3^-/mmeq l^{-1}
Standard 1	0.80	—	—	0.00	—	—
Standard 2	—	0.82	—	—	0.00	—
Tap water	2.31	0.72	6.80	0.04	0.00	0.18
Spring water 1	2.64	0.93	7.33	0.19	0.00	0.53
Spring water 2	3.68	1.78	12.50	0.31	0.20	1.05

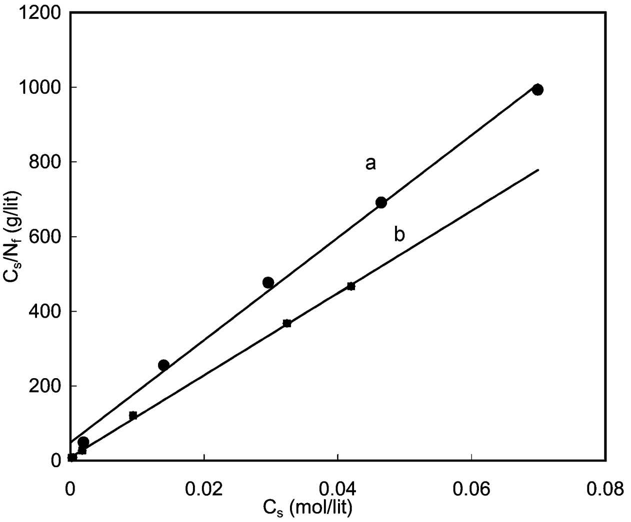

Fig. 3 Linearization of the adsorption isotherm of (a) Ca^{2+} and (b) Mg^{2+} on **2**.

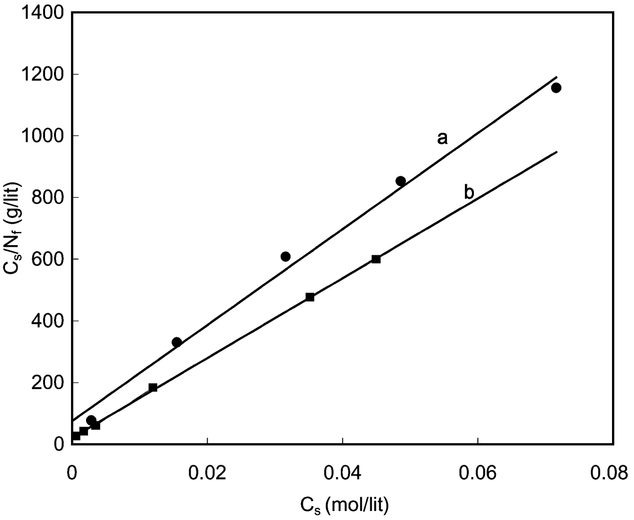

Fig. 4 Linearization of the adsorption isotherm of (a) Ca^{2+} and (b) Mg^{2+} on **3**.

Figs. 3 and 4. For all adsorption isotherms of Ca^{2+} and Mg^{2+} on **2** and **3** (Figs. 3 and 4) the plot of C_s/N_f *vs.* C_s gives a straight line with slope equal to $1/N_s$, and intercept equal to $1/KN_s$. Therefore the Langmuir isotherm is an adequate description of the adsorption of Ca^{2+} and Mg^{2+} on **2** and **3**. The maximum retention capacity (N_s) was determined for each cation–surface interaction from the slope, and the value of K from the intercept of the curve.

The N_s values obtained from Figs. 3 and 4 are listed in Table 4. This data show that the maximum retention capacity (N_s) followed the sequence $Ca^{2+} > Mg^{2+}$ on both surfaces.

Table 4 The properties of ions ($\Delta H°_{hyd}$, C_R), surfaces (N_s) and ion–surface interaction (K, $\Delta G°_{ads}$)

	Ca^{2+}/**2**	Mg^{2+}/**2**	Ca^{2+}/**3**	Mg^{2+}/**3**
N_s/μmol g^{-1}	90.77	72.87	77.28	64.26
K/l mol^{-1}	1326	284	634	20 7
$\Delta G°_{ads}$/kJ mol^{-1}	−17.8	−14.0	−16.0	−13.2
$\Delta H°_{hyd}$/kJ mol^{-1}	1650	1920	1650	1920
$10^9 C_R$/C m^{-1}	3.2	4.9	3.2	4.9

The constant K is related to the equilibrium constant, $K°$, by $K° = KC°$, where $C°$ is the standard concentration (1 mol l^{-1}),[7,15,16] while the standard Gibbs free energy of adsorption ($\Delta G°_{ads}$) is given by:

$$\Delta G°_{ads} = -RT\ln K° \qquad (5)$$

The $\Delta G°_{ads}$ values, obtained from eqn. (5) are listed in Table 4. This values show that the standard Gibbs free energy of Ca^{2+} adsorption is larger than for Mg^{2+} for both surfaces, which indicate the greater affinity of **2** and **3** for Ca^{2+} adsorption.

The sequence of adsorption of cations on both surfaces can be correlated with the hydration enthalpy, $\Delta H°_{hyd}$, or charge/radius, C_R, relationship, which are listed in Table 4. The cation acidities can be considered as a reflection of the values of the charge/radius relationship and the hydration enthalpy, whose properties are directly proportional to the acidity of the metal ion. This correlation suggests that a decrease in acidity makes the interactions of metal ion with the adsorption sites of **2** and **3** easier. This fact is in complete agreement with calculated standard Gibbs free energy of adsorption.

4. Conclusion

The application of this type of synthetic agents for water softening offers certain ecological and economic advantage compared to other methods.[1,2] The used materials are simply regenerated, and we do not need to change or control of pH, because the removal of ions occurs at nearly neutral pH.

In conclusion, a cheap and easy procedure for water softening has been achieved with one of the most interesting features of our results being the recycling ability of the softening agents. Also, in contrast to reported *N*-silyl or *O*-silyl compounds, **2** and **3** are completely stable and could be reused several times. The scope and limitation of the described methodology for other metal ions, especially transition metal ions, is under investigation in our laboratory.

Acknowledgment

Financial support for this work by the Research Affairs, Bu-Ali Sina University, Hamadan, Iran and also University of Science and Technology (IUST), Tehran, Iran (as a common project) are gratefully acknowledged.

References

1 S. P. Bindra and Walid Abosh, *Desalination*, 2001, **136**, 49.
2 D. D. Zhang, M. Peart, Y. Zhang, An Zhu and X. Cheng, *Desalination*, 2000, **29**, 247.
3 K. Terada, K. Matsumoto and H. Kimura, *Anal. Chim. Acta*, 1983, **3**, 237.
4 K. Terda, H. Hayakawa, K. Sawada and T. Kiba, *Talanta*, 1970, **17**, 955.
5 K. Terada, A. Inoue, J. Inamurs and T. Kiba, *Bull. Chem. Soc. Jpn.*, 1977, **50**, 1060.
6 K. Terada. K. Morimoto and T. Kiba, *Bull. Chem. Soc. Jpn.*, 1980, **53**, 1605; K. Terada. K. Morimoto and T. Kiba, *Anal. Chim. Acta*, 1980, **116**, 127.
7 A. G. S. Prado and C. Airoldi, *Anal. Chim. Acta*, 2001, **432**, 201.
8 P. Liu, Q. Pu and Z. Su, *Analyst*, 2000, **125**, 147.
9 O. Zaporozhets, N. Petruniock and V. Sukhan, *Talanta*, 1999, **50**, 865.
10 O. Zaporozhets, N. Petruniock, O. Bessarabova and V. Sukhan, *Talanta*, 1999, **49**, 899.
11 F. Mohanazadeh, A. R. Momeni and Y. Rangbar, *Tetrahedron Lett.*, 1994, **33**, 6127.
12 M. A. Zolfigol, M. H. Zebarjadian, G. Chehardoli, S. E. Mallakpour and M. Shamsipur, *Tetrahedron*, 2001, **57**, 1627.
13 M. A. Zolfigol, *Tetrahedron*, 2001, **57**, 9509 and our references cited therein.
14 H. Firouzabadi, N. Iranpoor, B. Karimi and H. Hazarkhani, *Synlett.*, 2000, 263.
15 G. Attord and C. Barnes, *Surfaces*, Oxford University Press Inc., New York, 1998.
16 C. Kaewprasit, E. Hequet, N. Abidi and J. P. Gourlot, *J. Cotton Sci.*, 1998, **2**, 164.

Mild, solvent-free oxidation of toluene and substituted toluenes to their benzoic acids using carboxylic acid-promoted heterogeneous catalysis

T. W. Bastock,[a] **J. H. Clark,**[b] **K. Martin***[a] **and B. W. Trenbirth**[a]

[a] *Contract Chemicals Ltd, Penrhyn Road, Knowsley Business Park, Prescot, Merseyside, UK L34 9HY. E-mail: keith.martin@contract-chemicals.com*
[b] *Clean Technology Centre, University of York, Heslington, UK YO1 5DD*

Received 29th August 2002
First published as an Advance Article on the web 30th October 2002

The commercial production of aromatic acids, in particular benzoic acid, is still performed using homogeneous cobalt acetate in acetic acid at high temperatures and pressures. Operating under these reaction conditions consumes large amounts of energy and produces large volumes of acidic toxic waste. Envirocat EPAC is a heterogeneous catalyst that can achieve the same transformation at atmospheric pressure, in the liquid phase, in the presence of a catalytic amount of carboxylic acid promoter, in the absence of a solvent. This process has eliminated the production of large amounts of toxic, acidic waste and significantly reduced the energy required to run the process as the oxidation is performed in the liquid phase at atmospheric pressure and lower temperatures, thus making the oxidation of aromatic methyls a considerably greener process.

Introduction

The commercial production of benzoic acid, from the oxidation of toluene, is achieved by heating a solution of the substrate, cobalt acetate and bromide promoter in acetic acid to 250 °C, under an atmosphere of oxygen, at several atmospheres of pressure.[1] Although complete conversion of toluene is achieved in a matter of hours, the work up procedure to recover benzoic acid results in the production of large volumes of toxic acidic waste. The system is highly corrosive and requires very expensive, specialised plant equipment, fitted with extensive safety features. Operating under such extreme reaction conditions consumes large amounts of energy.

A survey of the current patent and journal literature show that attempts are being made to make this oxidation more environmentally benign by performing the reaction in the vapour phase over solid oxidation catalysts, using ionic liquids and supercritical fluids.[2–4] However, even these methods require temperatures in excess of 200 °C, use expensive solvents or require highly specialised equipment.

We wish to report that we have developed a method that can efficiently oxidise toluene to benzoic acid in the liquid phase at atmospheric pressure using a heterogeneous supported reagent: Envirocat EPAC,[5] in the presence of a carboxylic acid promoter. The reaction is performed neat at the boiling point of toluene, using oxygen as the oxidant. Water, which is a by-product, is removed by azeotropic distillation throughout the reaction (Fig. 1). The results below also describe the experiments used to discover how the carboxylic acid promoter activates the catalyst.

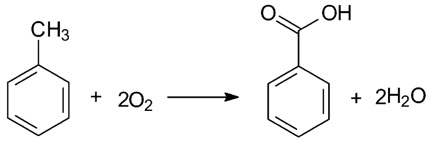

Fig. 1 Oxidation of toluene to benzoic acid.

Results and discussion

The role of the promoter

Envirocat EPAC is *not* an active catalyst in the oxidation of toluene. Previous work however, on the catalytic epoxidation of olefins, showed that a sacrificial aldehyde is required, in addition to oxygen, to effect the transformation[6] (Fig. 2). The reaction proceeds *via* the peracid, which is formed *in situ* from the oxidation of the aldehyde. This mechanism can equally be applied to the oxidation of aromatic methyls and therefore, the oxidation of toluene was repeated, doping the reaction mixture with isobutyrylaldehyde (Table 1).

The results obtained from this reaction were quite remarkable: The presence of the aldehyde promoted the oxidation of toluene to benzoic acid and the induction period, normally associated with this type of oxidation was eliminated. The

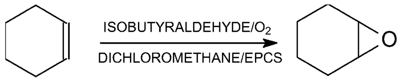

Fig. 2 Expoxidation of cyclohexene.

Green Context

The oxidation of hydrocarbon feedstocks is an area where substantial improvements need to be made. Current methods rely on harsh conditions and energy-intensive processes. Here, it is shown that the combination of a heterogeneous catalyst, a carboxylic acid promotor and air allows the oxidation of toluene and substituted toluenes to proceed under remarkably mild conditions to give the benzoic acids in high yield. The reaction appears to go *via* the formation of a peracid which oxidises the hydrocarbon, and is converted back to acid. Baeyer–Villiger reaction is also possible with this system. ***DJM***

DOI: 10.1039/b208427a

Table 1 Effect of isobutyrylaldehyde on the activity of EPAC

Initiator	None	Isobutyraldehyde
Mol of aldehyde	0	0.66
Yield of benzoic acid (%)	0	15.4 (0.31 mol)

Both reactions were performed using 5 g Envirocat EPAC in 2 mol toluene at reflux (95–115 °C) using an O_2 flow rate of ≈400 ml min^{-1} for 24 h. A Dean–Stark trap was used to continually remove water from the system. GC analysis of the reaction mixture did not detect any aldehyde at the end of the reaction. It is believed that the rapid gas flow removes it from the system.

conclusions drawn from this result was that the promotion of the oxidation was occurring *via* one of two routes:

1. The aldehyde was acting as a "co-catalyst" that was undergoing a redox cycle.
2. The aldehyde was oxidised to the carboxylic acid, which acts as a co-catalyst, undergoing a redox cycle *via* a peroxy species.

However, the reaction conditions used are highly oxidising and therefore, it is very unlikely that the carboxylic acid could be reduced to an aldehyde, as suggested in the first route. Therefore, the effect of different carboxylic acid promoters on the activity of Envirocat EPAC in the oxidation of toluene was investigated (Table 2). The results obtained were very interesting: The most effective promoter was trimethylacetic acid (pivalic acid) and surprisingly, acetic acid completely inhibited the oxidation, when not even background oxidation was observed.

The oxidation of toluene, in the presence of trimethylacetic acid, has been closely monitored by GC and the various intermediates and by-products identified by GC–MS. It appears that the oxidation proceeds *via* benzyl alcohol → benzaldehyde → benzoic acid. Other by-products, benzylbenzoate, phenylbenzoate and the benzyl acetal of benzaldehyde were detected in small concentrations (Fig. 3). Further optimisation of the reaction conditions showed that the optimum ratio of catalyst : promoter is 1 : 1 w/w and the catalyst : substrate ratio is 5 g/2 mol of substrate. Using the optimised reaction conditions increased the yield of benzoic acid to > 80% (see Experimental section).

Table 2 Effect of different carboxylic acids on the activity of EPAC

Acid	Isolated yield of benzoic acid (%)
Acetic	0
Propionic	19.2
Isobutyric	14.8
Trimethylacetic	23.2
Octanoic	12.4

All reactions were performed using 5 g Envirocat EPAC in a solution of the acid (0.66 mol) in 2 mol toluene at reflux (95–115 °C) using an O_2 flow rate of ≈400 ml min^{-1} for 24 h. A Dean–Stark trap was used to continually remove water from the system.

Baeyer–Villager oxidations are achieved by the reaction of a ketone with a stoichiometric quantity of a peracid.[7,8] Therefore, in an attempt to see if a peracid or coordinated species is continually regenerated, the oxidation of pentan-3-one was performed using the reaction conditions described above (Fig. 4). Over 18 h at 85 °C, most of the substrate has been converted to a mixture of ethyl propionate and propionic acid (7 : 3 by GC). This result clearly demonstrates that the catalyst, in the presence of O_2 is constantly generating a peroxy species and therefore, this is probably how trimethylacetic acid promotes the oxidation of toluene.

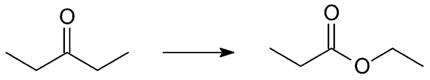

Fig. 4 BV oxidation of pentan-3-one.

Azeotropic drying of the reaction mixture

The active sites of this catalyst are highly polar and contain > 8% w/w water. Therefore, when it suspended in a non-polar environment, the water effectively stops diffusion of the substrate to the active site and no oxidation is observed. However, this water is loosely bound and can be removed from the active sites by azeotropic distillation, allowing diffusion of oxygen, substrate, promoter and products to and from the active sites, respectively. Water produced from the oxidation will preferentially partition in the active sites and if it is not continuously removed, the oxidation of the substrate will be inhibited.

Oxidation of substituted toluenes

The activity and selectivity of this catalytic system has been further evaluated by attempting to oxidise a range of substituted

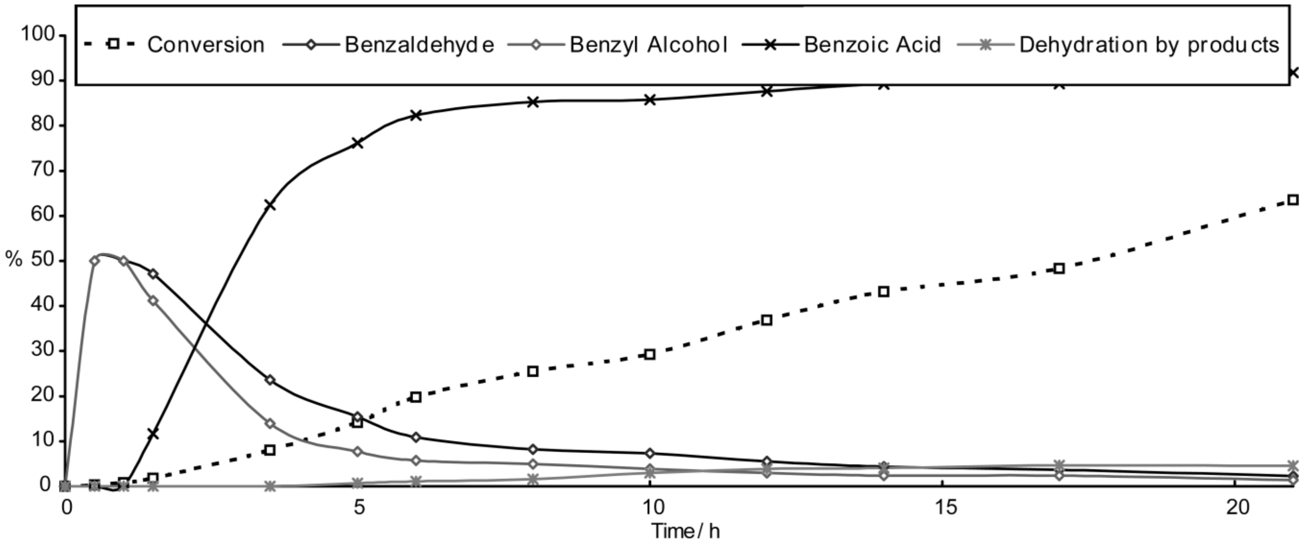

Fig. 3 Graph of reaction profile of the oxidation of toluene. The solid lines represents the normalised composition of the reaction mixture, excluding toluene, determined by GC analysis. The broken line shows the rate of reaction based on the production of water. For example, after 5 h, approximately 15% of the toluene has been converted to a mixture of 75% benzoic acid, 15% benzaldehyde, 8% benzyl alcohol and 2–3% dehydration products.

Table 3 Oxidation of substituted toluenes

Substituent	Solvent	Temperature/°C	Conversion (%)	Isolated yield (%)
H	—	110–150	106.4/22 h	85
Br	Cyclohexane	165–170	56/5 h	40
4-CH_3	Benzene	135	79/13 h	35 (37.3% Terephthalic acid)
4-OCH_3	Benzene	130–155	1.4/9.5 h	—
3,5-Dimethyl	Benzene	112–118	31/9 h	10
2-NO_2	Benzene	110–130	—	—

The conversions quoted are based on the mass of water collected in the Dean–Stark trap. Conversion of > 100% shows that a small amount of dehydration, for example esterification, acetal formation, has occurred. It should also be noted that none of the substrates or the catalyst has been dried before use. The isolated yields quoted are after purification of the isolated benzoic acid

toluenes (Table 3). Where the substrate is a solid at room temperature, an inert hydrocarbon solvent has been used to facilitate the removal of water by azeotropic distillation. The results show that the oxidation process cannot convert deactivated toluenes to their benzoic acids *e.g.* nitrotoluene to nitrobenzoic acid. However, it is possible to oxidise halogenated toluenes and xylene. It is interesting to note that the oxidation of *p*-xylene stops at *p*-toluic acid and only a small concentration of terephthalic acid is produced. This is thought to be caused by the build-up of terephthalic acid on the catalyst, which eventually blocks the active sites.

Conclusions

The above results show that aromatic side-chain oxidations can be performed under relatively mild reaction conditions using Envirocat EPAC in the presence of a catalytic amount of a carboxylic acid promoter. The advantages over the current commercial process are elimination of toxic and acidic effluents. The only by-product from the oxidation is water; unreacted substrate can be recycled and the product obtained from the oxidation is usually of a high purity (typically > 95%). Significantly less energy is required to achieve efficient oxidation as it occurs at atmospheric pressure and in the liquid phase and expensive plant equipment that needs regular rebuilding is not required.

The result from the Baeyer–Villager oxidation of pentan-3-one is potentially very exciting. This may well eliminate the need to use stoichiometric quantities of toxic and corrosive peracids, *e.g.* *m*-chloroperbenzoic acid, that are normally used in these transformations.

Overall, this work represents a major advance in the greening of oxidation technology used to oxidise toluenes and substituted toluenes to their benzoic acids.

Experimental

Oxidation of toluene

Envirocat EPAC (5 g) was suspended in a solution of trimethylacetic acid (5 g, 50 mmol) in toluene (2 mol). The reaction was performed in a 1 L baffled flask equipped with a 4-bladed, stainless steel stirrer shaft, Dean–Stark apparatus and an efficient condenser. Oxygen gas was fed down the stirrer shaft, with rapid mixing (1500–2000 rpm) at a rate of 400 ml min^{-1}. The suspension was kept at gentle reflux (110–150 °C) for 22 h. The reaction mixture was then cooled to 80–90 °C and more toluene added to dissolve the acid and then filtered to recover the catalyst. Excess toluene was recovered by distillation until a concentrated suspension was obtained. This was cooled to room temperature, filtered and washed with a little toluene and sucked dry to recover the benzoic acid. Typical yield of benzoic acid = 85%.

These reaction conditions were applied to the substrates listed in Table 3.

Oxidation of pentan-3-one

The above reaction conditions were repeated using pentan-3-one as the substrate. However, no Dean–Stark trap was used and the reaction was initially performed at 85 °C. However, as the oxidation proceeded, the temperature slowly decreased to 70 °C over 18 h. GC–MS analysis showed that all of the substrate had been converted to a mixture of ethyl propionate and propionic acid.

References

1 H. D. Holtz and L. E. Gardner (Phillips Petroleum Co.), *US Pat.*, 4088823, 1978.
2 V. Augugliaro, E. G. Lopez, V. Loddo, L. Palmisano and M. Schiavello, *Entropie*, 2002, **38**(237), 33–35.
3 M. J. Earle and S. P. Katdare, The Queen's University of Belfast, UK, World Pat., WO 2002030862, 2002.
4 A. Martin, B. Kerler and U. Armbruster, *Chem. Ing. Tech.*, 2002, **74**(5), 563.
5 www.contract-chemicals.com.
6 J. H. Clark and D. J. Macquarrie, *Handbook of Green Chemistry and Technology*, Blackwell Science Ltd., Oxford, 2002, pp. 321–337.
7 A. J. Butterworth, J. H. Clark, P. H. Walton and S. J. Barlow, *Chem. Commun.*, 1996, 1859–1860.
8 J. March, *Advanced Organic Chemistry*, Wiley-Interscience, Chichester, 4th edn., pp. 1098–1099.
9 R. C. Larock, *Comprehensive Organic Reactions*, VCH Publishers (UK) Ltd., 1989, p. 843.

Microwave-assisted conversion of oximes into nitriles in the presence of a zeolite

Adrienn Hegedüs,[a] Agnieszka Cwik,[a] Zoltán Hell,*[a] Zoltán Horváth,[b] Ágota Esek[c] and Mária Uzsoki[c]

[a] *Department of Organic Chemical Technology, Budapest University of Technology and Economics, H-1521 Budapest, Hungary. E-mail: zhell@mail.bme.hu*
[b] *Erdőkémia-ker Ltd, H-1108 Budapest, Gyömrői út 132-136, Hungary*
[c] *Chinoin Co. Ltd, Member of Sanofi-Synthélabo Group, H-1325 Budapest, P.O.Box 110, Hungary*

Received 24th July 2002
First published as an Advance Article on the web 8th November 2002

Aromatic aldoximes were converted to the corresponding nitriles in a microwave oven in the presence of a molecular sieve-type modified zeolite, Ersorb, under solvent-free conditions. The yields depended on the substituent of the oxime.

Introduction

Nitriles are important synthons in organic chemical syntheses.[1] There are two essential general methods for their preparation; (i) reaction of an alkyl or aryl halide with alkali or other metal cyanide. In this case the extremely poisonous cyanides may cause problems so the technologies obviously involve the tedious and expensive treatment of the waste water. (ii) Conversion of an aldehyde into oximes and dehydration of the latter into nitrile. Unfortunately the common dehydrating agents are insufficient for this purpose and more active reagents are required. A number of compounds have been described for this transformation, these include dicyclohexyl carbodiimide in the presence of $CuCl_2$,[2] selenium dioxide in chloroform,[3] chlorosulfonyl isocyanate,[4] triphenyl phosphine and carbon tetrachloride in acetonitrile[5] or the Burgess reagent.[6] There are also methods published for the direct conversion of aldehydes to nitriles using reagents such as hydroxylamine in toluene in the presence of pyridine,[7] or in the presence of selenium dioxide,[8] or phosphoric acid,[9] hydroxylamine hydrochloride in the presence of formic acid[10] or $MgSO_4$/*p*-toluenesulfonic acid,[11] *N*-tosylimines,[12] or trimethylsilyl azide.[13] Most of these methods, however, require corrosive, toxic, expensive or commercially unavailable reagents. Thus the development of a simpler but efficient method would be an interesting synthetic target, as well as being beneficial from an environmental point of view.

Ersorb-4 (E4) is a commercially available clinoptylolite-type zeolite material with high silicium content (Si : Al ratio = 5 : 1). The original mineral is modified with ionic exchange and with other water-phase technologies followed by a thermal treatment yielding a Ca–K mixed cation-based adsorbent with 4 Å pore size. E4 has a specific surface of 50 $m^2\ g^{-1}$ (determined by the BET-method with nitrogen at the temperature of liquid nitrogen) and has a slightly surfacial acidic character. The high silicium content leads to high stability up to 500–600 °C. E4 can adsorb small molecules such as water, hydrochloric acid, ammonia, methanol or hydrogen sulfide. The small pore size does not allow the adsorption of molecules larger than the methanol in the pores. Based upon this adsorption ability, E4 has been used as spectral drying agent in both the gas and liquid phases, suitable for the dehydration of gaseous hydrochloric acid or even liquid chlorine and sulfur dioxide. Recently we described that E4 showed good activity in different condensation reactions such as in the acylation of amino acids with aromatic acid chlorides[14] and in the cyclization of β-aminoalcohols with carboxylic acids to oxazolidine derivatives.[15]

Results and discussion

As part of the investigation of the applicability of different Ersorb types in organic syntheses we examined the reaction of aldehydes with hydroxylamine hydrochloride in the presence of E4. The aim of this examination was the development of a one-pot transformation of aldehydes into nitriles. Recently a modified montmorillonite (K10/$FeCl_3$) has already been successfully used for this transformation.[16]

Aldehydes react spontaneously with hydroxylamine hydrochloride without any catalyst. In this step E4 would serve only to bind the liberated hydrochloric acid and water. TLC examination of the reaction mixtures of different substituted aromatic aldehydes with hydroxylamine hydrochloride in the presence of E4 in boiling toluene showed that the formation of the oximes occurred but no formation of the appropriate nitrile

Green Context

Tightening and more universal legislation over the use of hazardous chemicals may indirectly hinder or prevent the manufacture of many important chemical products. Thus the manufacture of organic nitrates *via* the traditional nucleophite substitution route using highly toxic ionic cyanides may prove to be too difficult to operate. Since nitriles have so many useful applications we should seek to establish alternative, non-cyanide routes which themselves are not significantly environmentally threatening. Here we see a significant development in the cyanide-free route to nitriles starting from oximes and using a benign and reuseable zeolitic catalyst. ***JHC***

DOI: 10.1039/b207273b

Table 1 Microwave-assisted transformation of aldoximes into nitriles

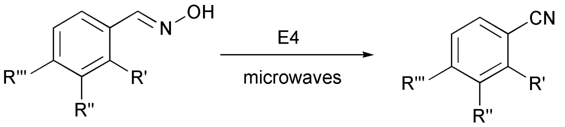

Entry	R′	R″	R‴	Reaction time/min	Microwave power/W	Yield[a] (%)	Mp/°C	lit. mp (bp)/°C
1	H	H	H	10	300	65 (82)[b]	—[c]	(40–41/1 Torr)[22]
2	H	H	$(CH_3)_2N$	10	300	32	75	75–77[23]
3	H	H	$(CH_3)_2N$	10	240	57	76–77	75–77[23]
4	H	H	$(CH_3)_2N$	10	210	95	75	75–77[23]
5	H	H	Cl	10	240	30	97–101	95–96[24]
6	H	H	Cl	10	300	30	91	95–96[24]
7	Br	H	H	5	300	90	—[c]	56[25]
8	H	H	OCH_3	10	300	83	63	62–63[26]
9	H	NO_2	H	4	300	54 (61)[b]	103	115[27]
10	H	NO_2	H	5.5	240	50 (57)[b]	101	115[27]
11	H	NO_2	H	10	150	75 (89)[b]	111	115[27]
12	Cl	H	H	10	300	37 (41)[b]	43	46–47[28]
13	OH	H	H	10	300	59 (65)[b]	95	95–96[29]
14	H	OCH_3	H	10	300	65 (71)[b]	—[c]	23[30]

[a] Preparative yield. [b] Yield estimated by GC. [c] Liquid.

was observed except in the case of 4-(dimethylamino)benzaldehyde, when 69% of 4-(dimethylamino)benzonitrile hydrochloride was isolated, and for benzaldehyde, when GC examination of the crude reaction mixture showed the formation of benzonitrile with 42% conversion.

As the one-pot reaction proved to be unsuccessful, we prepared the pure benzaldoximes by a known method,[17] and subjected these oximes to the dehydration reaction using E4 in boiling toluene or dioxane. Unfortunately TLC examination of these reactions mixtures showed only a small amount of nitrile.

There has been increasing interest in the application of microwave irradiation to chemical reactions over recent years. The publications about these experiments usually describe short reaction times (often a few minutes only), an increase in the purity of the resulting products and enhancement of chemical yield. Organic syntheses on solid or solid supported reagents coupled with microwaves, often in dry media, have particular importance from many points of view. The workup of the reaction mixture is easier, the solid reagents are often recyclable and the solvent-free technique reduces the costs of the technology and protects the environment at the same time. There are some examples for the preparation of nitriles in microwave-assisted reactions starting from aldehydes and hydroxylamine hydrochloride in the presence of alumina,[18] dibutyltin oxide supported on alumina,[19] from aldoximes in the presence of *p*-toluenesulfonyl chloride[20] or from *N*,*N*-dimethylhydrazones with oxone supported on wet alumina.[21]

In our experiments we used a Prolabo Synthewave 402 focused microwave reactor. The aldoxime and E4 were irradiated without solvent for 3–10 min with constant microwave power. The appropriate nitriles were obtained with good yield. The results are summarized in Table 1. The irradiation time and power required for good conversion depended strongly on the substituent of the aldehyde. Thus, in the reaction of 4-(dimethylamino)benzaldoxime higher microwave power resulted in the formation of resinous byproducts. The best result was obtained at 210 W (entries 2–4). 3-Nitrobenzaldoxime produced a violent reaction at higher microwave power; at 300 W in 4 min the temperature of the reaction mixture reached the maximal allowed temperature of the instrument (250 °C), so the irradiation was automatically stopped by the security system of the instrument. On the other hand, good results were obtained at 150 W irradiation power for 10 min (entries 9–11). Reaction of the 2-bromo and the 4-methoxy derivatives gave excellent yields (entries 7 and 8, respectively) but 2- and 4-chlorobenzaldoxime gave poorer results irrespective of the irradiation power (entries 5 and 6). In this case longer reaction times had no positive effect on the yield instead resulting in the formation of resinous byproducts.

Both E4 and the microwave irradiation were necessary for good conversion. The irradiation of the oximes alone or mixtures of the aldehyde and hydroxylamine hydrochloride in the absence of E4 failed to give any reaction. No solvent was required, the solid oximes melted in a few minutes which resulted in a significant acceleration of the reaction as indicated by the fast increase of the temperature of the reaction mixture. The catalyst filtered out from the reaction mixture was reusable after a simple treatment (washing with acetone and drying at 120 °C for 2 h) without significant loss of activity.

In conclusion, we have found that the simple zeolite Ersorb is a good catalyst in a new, solvent-free, microwave-assisted method for the conversion of aromatic aldoximes into nitriles. Compared with other methods a fast and environmentally-friendly synthesis of aromatic nitriles has been developed.

Experimental

Typical procedure for the reaction in microvawe oven

A mixture of the aldehyde (6 mmol) and E4 (1 g) was irradiated for 3–10 min with 150–300 W power (see Table 1). Then the mixture was diluted with acetone, the catalyst was filtered off and the filtrate was evaporated. The structures of the nitriles were confirmed by their melting point and IR spectra.

Acknowledgement

This work was supported by the Hungarian Research Fund Programs (OTKA Grant No. T-037757). The authors thank Dr Mária Balogh (Chinoin) for helpful discussion.

References

1 K. Friedrich and K. Wallenfels, *The Chemistry of Cyano Group*, ed. Z. Rappoport, Interscience, New York, 1970, pp. 92–93.
2 E. Vowinkel and J. Bartel, *Chem. Ber.*, 1974, **39**, 3424.
3 G. Sosnovsky and J. A. Krogh, *Synthesis*, 1978, 703.
4 G. A. Olah, Y. D. Vankar and A. Garcia-Luna, *Synthesis*, 1979, 227.
5 J. N. Kim, K. H. Chung and E. K. Pyn, *Synth. Commun.*, 1990, **20**, 2785.
6 J. Binoy, M. S. Sulatha, P. Madhavan Pillai and S. Prathapan, *Synth. Commun.*, 2000, **30**, 1509.
7 A. Saednya, *Synthesis*, 1982, 190.
8 G. Sosnovsky, J. A. Krogh and S. G. Umhoefer, *Synthesis*, 1979, 722.
9 I. Ganboa and C. Palomo, *Synth. Commun.*, 1983, **13**, 999.
10 G. A. Olah and T. Keumi, *Synthesis*, 1979, 1120.
11 I. Ganboa and C. Palomo, *Synth. Commun.*, 1983, **13**, 219.
12 R. S. Glass and R. C. Hoy, *Tetrahedron Lett.*, 1976, 1781.
13 K. Nishiyama, M. Oba and A. Watanabe, *Tetrahedron*, 1987, **43**, 693.
14 Z. Hell, A. Cwik, Z. Finta and Z. Horváth, *J. Mol. Catal. A: Chemical.*, 2002, **184**, 191.
15 A. Cwik, Z. Hell, A. Hegedüs, Z. Finta and Z. Horváth, *Tetrahedron Lett.*, 2002, **43**, 3985.
16 A. N. Bajpai, A. B. Deshpande and S. D. Samant, *Synth. Commun.*, 2000, **30**, 2785.
17 J. P. Dimmock, S. C. Vashishtha and J. P. Stables, *Pharmazie*, 2000, **55**, 490.
18 B. Touaux, F. Texier-Boullet and J. Hamelin, *Heteroat. Chem.*, 1998, **9**, 351.
19 J. S. Yadav, B. V. Subba Reddy and Ch. Madan, *J. Chem. Res. (S)*, 2001, 190.
20 M. Ghiaci and K. Bakhtiari, *Synth. Commun.*, 2001, **31**, 1803.
21 T. Ramalingam, B. V. Subba Reedy, R. Srinivas and J. S. Yadav, *Synth. Commun.*, 2000, **30**, 4507.
22 S. Satish and O. N. Awasthi, *Tetrahedron*, 1979, **35**, 277.
23 G. Beck, *Justus Liebigs Ann. Chem.*, 1968, **716**, 47.
24 G. G. Gallo and P. Sensi, *Ann. Chim. (Rome)*, 1956, **46**, 816.
25 H. P. Baudet, *Recl. Trav. Chim.*, 1924, **43**, 718.
26 G. Sosnovsky and H. T. Konieczny, *Z. Naturforsch. B, Anorg. Chem. Org. Chem.*, 1977, **32**, 1179.
27 T. Sandmeyer, *Chem. Ber.*, 1885, **18**, 1495.
28 A. Saednya, *Synthesis*, 1983, **9**, 748.
29 J. D. Hobson and J. R. Malpass, *J. Chem. Soc.*, 1967, 1645.
30 O. Exner and K. Bocek, *Collect. Czech. Chem. Commun.*, 1973, **38**, 50.

Trihalide-based ionic liquids. Reagent-solvents for stereoselective iodination of alkenes and alkynes

Olga Bortolini,*[a] Michele Bottai,[b] Cinzia Chiappe,*[b] Valeria Conte[c] and Daniela Pieraccini[b]

[a] *Dipartimento di Chimica, via Borsari 46, 44100 Ferrara, Italy*
[b] *Dipartimento di Chimica Bioorganica e Biofarmacia, via Bonanno 33, 56126 Pisa, Italy. E-mail: cinziac@farm.unipi.it*
[c] *Dipartimento di Scienze e Tecnologie Chimiche, via della Ricerca Scientifica, 00133 Roma, Italy*

Received 25th September 2002
First published as an Advance Article on the web 8th November 2002

A study of the preparation of trihalide-based room temperature ionic liquids (ILs) has been made and the structure of trihalide ions has been investigated by electrospray ionization mass spectroscopy and NMR. The best procedure consists of mixing equimolar amount of ICl to [hmim][Cl] and IBr to [bmim][Br] or alternatively Cl_2 or Br_2 to [emim][I]. Trihalide ILs thus generated have been tested as reagent-solvents, or as reagents carrying out the reactions in [bmim][PF_6], in iodobromination as well as iodochlorination of alkenes and alkynes. Furthermore, the addition of ICl and IBr in [bmim][PF_6] was investigated. Yields of *vic*-iodochloro or iodobromo adducts from very good to almost quantitative are observed for all the substrates examined.

Introduction

Organic salts that are liquid at conditions around room temperature, generally defined ionic liquids (ILs), are being explored as potentially environmentally benign solvents.[1,2] A major reason for this interest in ionic liquids is their negligible vapour pressure, which decreases the risk of worker exposure and the loss of solvent into the atmosphere. A large number of reactions have been performed successfully in these solvents showing great potential as reaction media able to maintain and sometimes to enhance chemical selectivity and reactivity.[3,4] Iodochlorination and iodobromination of alkenes and alkynes is an important class of industrial and pharmaceutical organic reactions because of functionalization potential by iodine atom replacement. *vic*-Halogenides may be prepared *via* Ad_E-addition processes of iodine halogenides (ICl or IBr) to olefins and acetylenes in chlorinated solvents:[5] however, these reagents often lead to by-products, due to their ability to disproportionate in these solvents, and furthermore are not easy to handle.[5] Therefore, iodochlorination reactions usually employ in situ generated iodine chloride by reaction of iodine with copper or mercury salts, or quaternary ammonium, potassium or polymeric dichloroiodate.[6–8] The reaction of $KICl_2$ in water gives[7] nevertheless generally mixtures of products. Regio- and stereospecific iodochlorination have been obtained only using ammonium or polymeric dichloroiodate in chlorinated solvents.[6,8] The use of ILs has been recently proposed as a clean, environmentally benign alternative to chlorinated solvents for the stereoselective bromination of alkenes and alkynes.[9–11] Then, following this mainstream, and stimulated by the promising result of precedent work on bromination,[10,11] we decided to extend the use of ILs to other kinds of halogenations.

Here we present our recent results on two alternative practical procedures for the stereoselective iodochlorination and iodobromination of alkenes and alkynes in several room-temperature ionic liquids using ICl, IBr or the same trihalide-base ILs as reagents.

Results and discussion

Trihalide ionic liquids

1,3-Dialkylimidazolium trihalide ionic liquids have been prepared from the corresponding 1,3-dialkylimidazolium halogenide (chloride, bromide or iodide) by reaction with ICl, IBr, Cl_2 or Br_2. The reaction of 1-hexyl-3-methylimidazolium chloride, [hmim][Cl], with 1 equivalent of ICl at 0 °C gave the water-immiscible 1-hexyl-3-methylimidazolium dichloroiodate ionic liquid, [hmim][ICl_2]. Analogously 1-butyl-3-methylimidazolium dibromoiodate, [bmim][IBr_2], was prepared by reaction of 1-butyl-3-methylimidazolium bromide, [bmim][Br], with 1 equivalent of IBr at the same temperature. These ILs were stable and can be stored in the dark at 4 °C for several months without any degradation (checked by NMR and MS) or loss of reactivity or selectivity (the same product distribution was obtained using *in situ* or pre-prepared trihalide ionic liquids). ILs having as counter-anion ICl_2^- or IBr_2^- may be obtained also by addition,

Green Context

While ionic liquids are most commonly considered as VOC solvent replacements (due to their negligible vapour pressure) they can also act as reactive solvents enabling important organic transformations to be carried out under benign conditions. Here the preparation of rather uncommon trihalide-based ionic liquids are described and more importantly, their use in organic synthesis is reported. Iodochlorination and iodobromination of alkenes and alkynes is a useful reaction for the preparation of functionalised organic compounds. Traditional methods are however associated with drawbacks involving unstable reagents and halogenated solvents. Trihalide-based ionic liquids prove to be excellent reagent-solvents for the stereoselective iodination of alkenes and alkynes. ***JHC***

DOI: 10.1039/b209436n

at 0 °C, of an equivalent of halogen (Cl_2 or Br_2) to a 1,3-dialkylimidazolium iodide. Ethyl-3-methylimidazolium iodide was used in this work. The reaction implies Cl_2 or Br_2 oxidation of iodide ion. Recent *ab initio* calculations have shown[12] the X–Y–X$^-$ anions, where Y is heavier than X, are more stable than the isomers Y–X–X$^-$ both in gas phase and solution. As a result, the Y–X–X$^-$ anions, if formed from X_2 and Y$^-$, are expected to easily isomerize to the X–Y–X$^-$ anions *via* cleavage of the X–X bond.

Trihalide-based ILs have been also prepared by addition of I_2 at [bmim][Br] or [hmim][Cl] or ICl and IBr at [emim][I]. In these cases, however, complex mixtures of trihalide anions were obtained (see below), in analogy to the behaviour in molecular solvents.[13]

In order to obtain information about these new ILs, we preliminarily analyzed our mixtures by NMR. As has been pointed out by Seddon and Bonhôte,[14,15] the chemical shift of aromatic protons in dialkylimidazolium ionic liquids is anion dependent: in particular the H(2) signal moves downfield with increasing anion basicity, and thus hydrogen-bonding capability. However, since the chemical shifts of these protons are also solvent- and concentration-dependent, and all these factors may exert opposite effects, the experiments were performed on pure ILs using DMSO-d_6 as external lock, so that the chemical shifts were only influenced by the anion capability to form hydrogen bonding. In order to avoid contamination from water, the manipulation of each sample was performed in a nitrogen-filled glove box.

Tables 1 and 2 collect the chemical shifts of proton signals of [hmim][Cl] and [bmim][Br], the former in presence of an amount of ICl and I_2 corresponding to the molarity of the solvent, the latter in presence of equimolar amount of IBr and I_2.

Table 1 Proton chemical shifts for [hmim][Cl] in the absence and in presence of equimolar amounts of ICl or I_2 at 17 °C

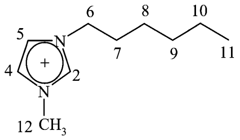

Imidazolium proton(s)	[hmim][Cl] (Pure solvent) δ	+ ICl δ	Δδ	+ I_2 δ	Δδ
2-H	9.57	7.92	1.65	7.60	1.97
4-H	7.66	6.67	0.99	6.24	1.42
5-H	7.79	6.67	1.12	6.24	1.55
6-H	3.76	3.33	0.42	2.76	1.00
12-H	3.43	3.10	0.32	2.71	0.72
7-H	1.08	1.02	0.06	0.67	0.41
8,9,10-H	0.36	0.39	0.03	0.05	0.31
11-H	−0.090	−0.084	0.006	−0.45	0.36

Table 2 Proton chemical shifts for [bmim][Br] in the absence and in presence of equimolar amounts of IBr or I_2 at 17 °C

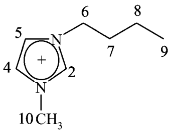

Imidazolium proton	[hmim][Br] Pure solvent δ	+ IBr δ	Δδ	+ I_2 δ	Δδ
2-H	8.70	7.54	1.16	7.12	1.58
4-H	6.99	6.16	0.83	5.83	1.16
5-H	7.09	6.16	0.93	5.85	1.24
6-H	3.23	2.70	0.53	2.55	0.68
10-H	2.93	2.46	0.47	2.31	0.62
7-H	0.57	0.31	0.26	0.20	0.37
8-H	−0.07	−0.24	0.20	−0.35	0.28
9-H	−0.51	−0.71	0.20	−0.81	0.30

Addition of higher concentrations of halogen (up to 1.5 equiv.) did not produce further modification to the spectra. The experimental data reported in Tables 1 and 2 show a decrease in anion basicity after addition of the halogen corroborating the change of the counter-anion from Cl$^-$ or Br$^-$ to trihalide species. Furthermore, the chemical shifts of the aromatic protons, and in particular that of H(2), diminish following the series Cl$^-$ > Br$^-$ > ICl–Cl$^-$ > I_2–Cl$^-$ > IBr–Br$^-$ > I_2–Br$^-$ (Table 3). This kind of analysis could not be applied to [emim][I] which is a solid at room temperature. The NMR spectra of ionic liquids pertaining to the [emim] series were therefore registered using MeCN-d_3 as the solvent and working at constant concentration (0.07 M).

Table 3 Proton chemical shift values of 1-ethyl-3-methylimidazolium salts in CD_3CN at 17 °C

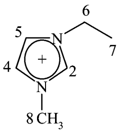

Imidazolium proton	[emim][I] δ	+ I_2 δ	+ Br_2 δ	+ IBr δ	+ Cl_2 δ	ICl δ
2-H	8.69	8.40	8.42	8.40	8.45	8.41
4-H	7.37	7.33	7.33	7.33	7.33	7.33
5-H	7.43	7.38	7.38	7.38	7.39	7.39
6-H	4.19	4.16	4.17	4.16	4.16	4.17
8-H	3.84	3.82	3.82	3.82	3.82	3.82
7-H	1.46	1.46	1.46	1.46	1.46	1.46

Also in this case the addition of ICl or IBr to [emim][I] moved the chemical shift of H(2) upfield. The same results were obtained adding Cl_2, Br_2 or I_2. Although the changes in chemical shifts in solution are significantly lower than in pure samples they are, however, in agreement with the formation of anions having a more disperse charge.

In conclusion, the NMR analysis of these ILs showed that: (i) the addition of the halogens did not determine any modification of the cationic moiety, *i.e.* no aromatic substitution reaction occurs under the reaction conditions; (2) the addition of the halogens determines a decrease in basicity of the anion, in agreement with the formation of trihalide ions. On the other hand, no information might be obtained from these experiments about the exact counter-anion identity. Furthermore, the high absorption of the imidazolium cation below 300 nm prevented the possibility to undertake an UV-Vis study to obtain more specific information about the formed anions and the equilibria involving these species.

ESI-MS experiments were therefore conducted to investigate the nature and integrity of the different ionic liquids, with particular attention to the anionic counterpart. The full scan negative ion mode spectra of CH_3CN solutions containing the IL under analysis showed the occurrence of different species identified on the basis of the observed and calculated isotopic distribution patterns. As reported in Table 4, the original counter-ion is detected in almost all cases in association with additional species likely formed by decomposition, ion-molecule reaction, exchange or aggregation, according to the general Scheme 1.

Support to the proposed reactions pathway of Scheme 1 came from MS/MS analysis of the mixed X_2Y^- species. As an example, by mass selecting the I_2Br^- anion at *m*/*z* 333, at intermediate tickling energies of *ca.* 1 V, formation of I$^-$, IBr_2^- and I_3^- is observed. On the other hand, by mass selecting the IBr_2^- ionic species at *m*/*z* 285, the occurrence of I_2Br^-, I$^-$ and I_3^- is analogously detected, although at higher energy regime (*ca.* 1.8–2 V).

Despite the non-equilibrium conditions that pertain to the analyzer used for these measurements, the relative abundances

Table 4 Full scan ESI mass spectrum of ILs in negative-ion mode using CH_3CN or CH_2Cl_2[a] as infusion solvents[b]

Entry	IL (5×10^{-3} M)	Counter-ion (*m/z*, rel. intensity %)	Additional full scan mass peaks (*m/z*, relative intensity %)				
1	[bmim][Br]	Br^- (79, 100)					
2	[bmim][Br_3]	Br_3^- (237, 35)	Br^- (79, 100)	$[C_4H_8]Br_3^-$ (293, 70)			
3	[emim][I_3]	I_3^- (381, 80)	I^- (127, 100)	[emim]$[I^-]_2$ (365, 10)			
4	[bmim][IBr_2]	IBr_2^- (285, 100)	Br^- (79, 25)	$[C_4H_8]Br_3^-$ (293, 5)			
5[a]	[bmim][IBr_2]	IBr_2^- (285, 100)	Br^- (79, 19)	$[C_4H_8]Br_3^-$ (293, 4)			
6	[emim][IBr_2]	IBr_2^- (285, 100)	Br^- (79, 35)	I^- (127, 3)	$[C_4H_8]Br_3^-$ (293, 5)		
7	[hmim][Br_2Cl]	Br_2Cl^- (193, 45)	Br^- (79, 45)	Br_3^- (237, 100)	$[C_6H_{12}]Br_3^-$ (321, 8)		
8	[bmim][I_2Br]	I_2Br^- (333, 23)	Br^- (79, 15)	I^- (127, 100)	IBr_2^- (285, 60)	$[C_4H_8]Br_3^-$ (293, 5)	I_3^- (381, 50)
9	[emim][I_2Br]	I_2Br^- (333, 20)	Br^- (79, 40)	I^- (127, 90)	IBr_2^- (285, 100)	$[C_4H_8]Br_3^-$ (293, 60)	I_3^- (381, 20)
10	[emim][I_2Cl]	I_2Cl^- (289, 5)	I^- (127, 100)	ICl_2^- (197, 40)	I_3^- (381, 50)		
11	[hmim][ICl_2]	ICl_2^- (197, 100)	I^- (127, 15)	I_2Cl^- (289, 10)	I_3^- (381, 5)		
12[a]	[hmim][ICl_2]	ICl_2^- (197, 100)	I^- (127, 22)	I_2Cl^- (289, 20)	I_3^- (381, 9)		
13	[emim][ICl_2] (5×10^{-4} M)	ICl_2^- (197, 100)	I^- (127, 13)	I_2Cl^- (289, 10)	I_3^- (381, 7)		
14	[bmim][IBr_2]	IBr_2^- (285, 50)	Br^- (79, 30)	$[C_4H_8]Br_3^-$ (293,50)	I_2Br^- (333, 45)	$[C_4H_8]Br_4^{\cdot-}$ (372, 100)	
15[a]	[bmim][IBr_2]	IBr_2^- (285, 50)	Br^- (79, 25)	$[C_4H_8]Br_3^-$ (293, 50)	I_2Br^- (333, 30)	$[C_4H_8]Br_3^{\cdot-}$ (372, 100)	

[a] CH_2Cl_2 as solvent; [b] *m/z* Values refer to ^{79}Br and ^{35}Cl.

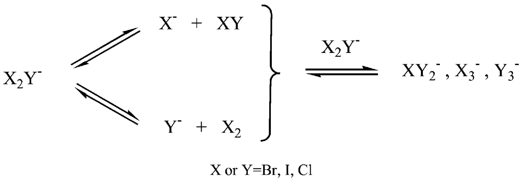

Scheme 1

of the different ionic species allow a qualitative indication of the stability of the different counter-ions (Table 4). Excluding the monomeric Br^- derivative, the various trimeric anions showed two distinct levels of stability. Derivatives like Br_3^-, I_3^-, IBr_2^- and ICl_2^- may be classified as quite stable species, whereas Br_2Cl^- I_2Br^-, I_2Cl^-, are rather unstable, in agreement with reactivity data and spectroscopic measurements.[13]

The infusion solvent appeared to have no effect on the ESI mass spectra. In fact, by replacing CH_3CN with CH_2Cl_2 for two model ionic liquids [bmim][IBr_2] and [hmim][ICl_2], in otherwise identical experimental conditions, almost matching spectra are obtained, entries 4–5, 11–12 and 14–15 of Table 4. As expected, the concentration of the analyte has a marked influence on the relative abundance and composition of the different ionic species. This is confirmed by a comparison between the mass spectrum obtained in the standard concentration (5×10^{-3} M) and a ten-fold diluted solution of [bmim][IBr_2], both in CH_3CN (entries 4 *vs* 14) and CH_2Cl_2 (entries 5 *vs* 15). Upon dilution the base peak IBr_2^- at *m/z* 285 gradually decreases in favor of other halo ions Br^-, I_2Br^- and polybromo derivatives containing an organic counterpart *i.e.* $[C_4H_8]Br_3^-$, $[C_4H_8]Br_4^{\cdot-}$.

The formation of these species, in particular of $[C_4H_8]Br_3^-$ at *m/z* 293, observed in the mass spectrum of many ILs, should necessarily involve the alkyl chain of the imidazole ring. Support to this point may be found in the ESI positive-ion full scan mass spectrum of some selected ionic liquids, described in Table 5. Together with the 1-alkyl-3-methyl imidazolium fragment, base peak in almost all cases, loss of the side chain (C_2H_4, C_4H_8, C_6H_{12}) with hydrogen shift on N-1 nitrogen is observed. The reaction with these neutral fragments or, alternatively, the loss of the alkyl chain become particularly effective in the presence of Br_3^- ions to form $[C_4H_8]Br_3^-$ and $[C_6H_{12}]Br_3^-$ species. Of note is the fact that the formation of $[C_4H_8]Br_3^-$ from [emim][IBr_2] and [emim][I_2Br] should be preceded by C_2H_4 dimerization.

As final remark, the data of Table 4 confirmed that, for identical anions, the composition and relative abundances of the different ionic species are not significantly influenced by the organic counterpart (entries 4–6, 8–9 and 11–13).

Electrophilic halogenation

Product distribution. The halogen addition to several alkyl and aryl substituted alkenes (**1**–**3**) and alkynes (**4a**–**c**) at 0 °C was therefore examined using the trihalide ILs for which ESI-MS analysis suggested the presence of an unique anion. Thus, alkenes **1**–**3** and alkynes **4** were treated with 1 or 5 equivalent of 1,3-dialkylimidazolium ICl_2^- or IBr_2^- using [hmim][Cl] or [bmim][Br] respectively, as the solvent, or alternatively [bmim][PF_6] (Scheme 2). The same reactions were also carried out using the reactants, [hmim][ICl_2] as well as [bmim][IBr_2], as reaction media. It is of note that the reactions carried out with [hmim][ICl_2] in [hmim][Cl], or with [bmim][IBr_2] in [bmim][Br], even after 24 h showed a very low, if any, conversion into the corresponding dihalo adducts (data not reported in Table). These solvents are therefore not suitable to prepare dihalo derivatives. Finally, the addition of ICl and IBr in [bmim][PF_6] was also examined.

Reactions were typically carried out by addition of the alkene or alkyne (0.3 M) under stirring, at 0 °C, to the ionic liquid (2

Table 5 Full scan ESI mass spectrum of ILs in positive-ion mode using CH_3CN as infusion solvent[a]

Entry	IL (5×10^{-3} M)	Cation (*m/z*, relative intensity %)	Additional full scan mass peaks (*m/z*, relative intensity %)	
1	[bmim][Br]	$[bmim]^+$ (139, 100)	$[bmim - C_4H_8]^+$ (83, 15)	$[(bmim)_2Br]^+$ (357, 18)
2	[bmim][IBr_2]	$[bmim]^+$ (139, 100)	$[bmim - C_4H_8]^+$ (83, 12)	$[(bmim)_2Br]^+$ (357, 48)
3	[bmim][$(PF_6)ICl$]	$[bmim]^+$ (139, 83)	$[bmim - C_4H_8]^+$ (83, 5)	$[(bmim)_2PF_6]^+$ (423, 100)
4	[bmim][$(PF_6)IBr$]	$[bmim]^+$ (139, 100)	$[bmim - C_4H_8]^+$ (83, 10)	$[(bmim)_2PF_6]^+$ (423, 100)
5	[emim][I]	$[emim]^+$ (111, 100)	$[emim - C_2H_4]^+$ (83, 15)	$[(emim)_2I]^+$ (349, 35)
6	[emim][ICl_2]	$[emim]^+$ (111, 100)	$[emim - C_2H_4]^+$ (83, 8)	$[(emim)_2Cl]^+$ (257, 37)
7	[hmim][ICl_2]	$[hmim]^+$ (167, 80)	$[hmim - C_6H_{12}]^+$ (83, 3)	$[(hmim)_2Cl]^+$ (369, 100)

[a] *m/z* Values refer to ^{79}Br and ^{35}Cl.

ml) containing the iodinating agent (1–5 equiv.) or completely transformed into the halogenating agent. In the reactions of addition of ICl and IBr in [bmim][PF$_6$] to the alkenes the complete consumption of the reagents was observed in few minutes, longer times were instead necessary for all the other reactions. The products, extracted with Et$_2$O in yields always > 85–90%, were identified on the basis of the ^{1}H and ^{13}C NMR spectra (Scheme 2; Tables 6 and 7). For the reaction carried out in [bmim][PF$_6$] the ionic liquid was recycled and reused for the same reaction at least twice. In order to establish the efficacy of the ionic liquids in the iodochlorination and iodobromination of unsatured compounds the addition in dichloromethane of tetrabutylammonium dichloroiodate (TBAICl$_2$), tetrabutylammonium dibromoiodate (TBAIBr$_2$), ICl and IBr to the same substrates was also examined.

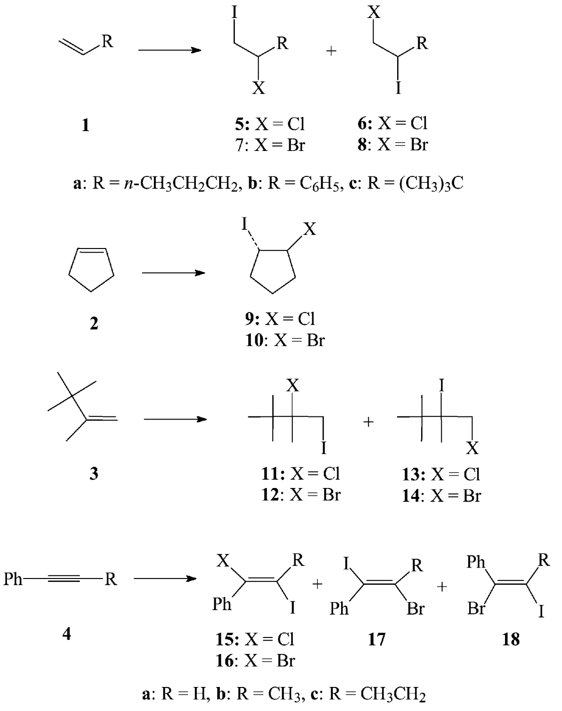

Scheme 2

The data, reported in Table 6, related to alkene **2** and alkynes **4** show that, while the reaction of ICl$_2^-$ in the ILs occurs always in an *anti*-stereospecific way, that of IBr$_2^-$ with **4b** gives also the *syn* adduct **18**.[16] Also the regioselectivity depends on the trihalide halogenating agent and is affected on the structure of alkene or alkyne. Olefin **1b** gives exclusively the Markownikoff adduct (M-adduct) **5** or **7**, with both [hmim][ICl$_2$] and [bmim][IBr$_2$], showing that these reactions are affected by electronic effects. The practically exclusive formation of the M-adduct characterizes also the reactions of the arylalkynes **4** with ICl$_2^-$ while the addition of IBr$_2^-$ can give the *anti*-Markownikoff (AM-adduct) depending on the alkyne structure. In particular **4a**, but not **4b**, gives a significant amount of the AM-adduct **17**. Finally, the reactions of **1c** with both these reactants, or of **3** with IBr$_2^-$, proceed with a complete regioselectivity to give the AM-adducts, while 1 : 1 mixtures of M and AM-adducts were obtained from **1a**. The increasing amount of the AM adduct on going from **1a** to **1c** clearly reveals that the additions of these reactants are influenced also by steric factors. Furthermore, the results related to the addition of IBr$_2^-$ and ICl$_2^-$ to **3** and **4** strongly suggest that the two reactions are differently affected by steric and electronic effects.

It is worth of note that the halogenations with TBAICl$_2$ and TBAIBr$_2$ in dichloromethane, carried out under identical

Table 6 Product distribution for ICl$_2^-$ and IBr$_2^-$ addition to **1**, **2**, **3** and **4** at 0 °C

Substrate	Reagent	Equiv.	Solvent	Time/h	Conv. (%)	Products[a]	
						5	**6**
1a	[hmim][ICl$_2$]		[hmim][ICl$_2$]	2	> 95	50	50
	[hmim][ICl$_2$]	1	[bmim][PF$_6$]	2.5	50	50	50
1b	[hmim][ICl$_2$]		[hmim][ICl$_2$]	2	> 95		[b]
	[hmim][ICl$_2$]	1	[bmim][PF$_6$]	2.5	> 95	100	
1c	[hmim][ICl$_2$]		[hmim][ICl$_2$]	2	> 95		100
	[hmim][ICl$_2$]	1	[bmim][PF$_6$]	2	> 95		100
						9	
2	[hmim][ICl$_2$]		[hmim][ICl$_2$]	2	> 95	100	
	[hmim][ICl$_2$]	1	[bmim][PF$_6$]	2	> 95	100	
						11	**13**
3	[hmim][ICl$_2$]		[hmim][ICl $_2$]	2	> 95	100	
	[hmim][ICl$_2$]	1	[bmim][PF$_6$]	2	> 95	100	
						15	
4a	[hmim][ICl$_2$]		[hmim][ICl$_2$]	2	> 95	> 95	
	[hmim][ICl$_2$]	1	[bmim][PF$_6$]		> 95	100	
4b	[hmim][ICl$_2$]		[hmim][ICl$_2$]	2	> 95	> 95	
	[hmim][ICl$_2$]	1	[bmim][PF$_6$]		50	> 95	
4c	[hmim][ICl$_2$]		[hmim][ICl$_2$]	2	> 95	> 95	
	[hmim][ICl$_2$]	1	[bmim][PF$_6$]		45	> 95	
						7	**8**
1a	[bmim][IBr$_2$]		[bmim][IBr$_2$]	2	> 95	45	55
1b	[bmim][IBr$_2$]		[bmim][IBr$_2$]	2.5	> 95	100	
1c	[bmim][IBr$_2$]		[bmim][IBr$_2$]	2	> 95		80[c]
						10	
2	[bmim][IBr$_2$]		[bmim][IBr$_2$]	2.5	> 95	100	
						12	**14**
3	[bmim][IBr$_2$]		[bmim][IBr$_2$]	2.5	> 95		100
						16	**17**
4a	[bmim][IBr$_2$]		[bmim][IBr$_2$]	24	> 95	90	10
	[bmim][IBr$_2$]	1	[bmim][PF$_6$]			66	34
						16	**18**
4b	[bmim][IBr$_2$]		[bmim][IBr$_2$]	24	> 95	66	34
4c	[bmim][IBr$_2$]		[bmim][IBr$_2$]	24	83	> 95	

[a] Yields of the isolated products > 90%. [b] Dichloro derivative. [c] The other product was identified as the corresponding dibromo adduct.

conditions (reagents concentration and temperature), showed a very similar chemo- regio- and stereoselectivity. With respect the analogous reactions in ILs these additions were however extremely slow; the addition of TBAICl$_2$ required indeed 48-72 h to obtain the complete conversion into the corresponding iodochloro derivatives, while the addition of TBAIBr$_2$ even after 72 h gave very low conversions ($<30\%$). Moreover, in both the reactions to isolate the addition products a repeated tedious aqueous work up, which drastically reduced the yields, was necessary.

vic-Iodochloro and iodobromo adduct may be obtained also by addition of ICl or IBr in [bmim][PF$_6$] to the same substrates (Table 7).

In analogy with the behaviour observed in the addition of ICl and IBr in dichloromethane (reported in Table 7), the adducts are generally formed by *anti* addition to the double and triple bonds, the sole exception being the reaction of IBr with **4b**, which gives both in dichloromethane and in [bmim][PF$_6$], the *syn*-adduct **18b**. Furthermore, also in the ionic liquid, as well as in the chlorinated solvent, the regiospecificity of the process depends on the substrate structure: aryl substituted alkenes and alkynes give exclusively the M-adducts (**1b** and **4a–b** with both ICl and IBr). Mixture of M- and AM-adducts were obtained by addition of IBr and ICl to the simple alkyl substituted alkene **1a**, while replacing the propyl group on the alkene by a *tert*-butyl group results in the exclusive formation of the AM-adducts (**1c**). Related to the product distribution in two the solvents it is finally to note that while the reaction of **3** with IBr in dichloromethane gives mainly the AM-adduct a complex mixture of products, arising from rearrangement and elimination reactions, was isolated from the reaction carried out in [bmim][PF$_6$]. However, the main difference in the product distribution characterizing in particular the electrophilic addition of IBr in [bmim][PF$_6$] with respect chlorinated solvents is the lack of dibromo adducts, whose formation in low polarity solvents has been attributed to the ability of IBr to disproportionate to I$_2$ and Br$_2$.[5]

Table 7 Product distribution for ICl and IBr addition to **1–4** in [bmim][PF$_6$] and dichloromethane (DCM) at 0 °C

Substrate	Solvent	Reagent	Time/h	Conv. (%)	Products[a]	
					5	**6**
1a	[bmim][PF$_6$]	ICl	0.5	>95	55	45
1a	DCM	ICl	3	>95	60	40
1b	[bmim][PF$_6$]	ICl	0.5	>95	100	
1b	DCM	ICl	3	>95	100	
1c	[bmim][PF$_6$]	ICl	0.5	>95		100
1c	DCM	ICl	3	>95		100
					9	
2	[bmim][PF$_6$]	ICl	0.5	>95	100	
2	DCM	ICl	3	>95	94[b]	
					11	**13**
3	[bmim][PF$_6$]	ICl	0.5	>95	80[c]	
3	DCM	ICl	3	>95	100	
					15	
4a	[bmim][PF$_6$]	ICl	2.5	65	100	
4a	DCM	ICl	3	75	100	
4b	[bmim][PF$_6$]	ICl	2.5	50	100	
4b	DCM	ICl	3	78	100	
4c	[bmim][PF$_6$]	ICl	2.5	45	100	
					7	**8**
1a	[bmim][PF$_6$]	IBr	0.5	>95	50	50
	DCM	IBr	3	>95	45	45[d]
1b	[bmim][PF$_6$]	IBr	0.5	>95	100	
	DCM	IBr	3	>95	100	
1c	[bmim][PF$_6$]	IBr	2.5	>95		100
	DCM	IBr	3	>95		>90[d]
					10	
2	[bmim][PF$_6$]	IBr	0.5	>95	100	
	DCM	IBr	3	>95	67[d]	
					12	**14**
3	[bmim][PF$_6$]	IBr	0.5	>95		[e]
	DCM	IBr	3	>95		80
					16	**17**
4a	[bmim][PF$_6$]	IBr	2.5	45	100	
	DCM	IBr	3	70	62[e]	
					16	**18**
4b	[bmim][PF$_6$]	IBr	2.5	40		100
	DCM	IBr	3	60	20	10[f]

[a] Yields of the isolated products $>90\%$. [b] The other product was identified as the corresponding dichloro adduct. [c] Adduct **11** was formed besides a complex mixture of products. [d] The other product was identified as the corresponding dibromo adduct. [e] Complex mixture of products. [f] Together with (*E*)-dibromo (59%) and (*Z*)-dibromo adduct (11%).

Finally, the formation of the *syn*-adduct **18b** in reaction of **4b** with IBr, as well as the formation of products arising from rearrangement and elimination in the reaction of **3** with both ICl and IBr, strongly suggests that the addition of these electrophiles in [bmim][PF$_6$] involves an ionic intermediate (a bridged or partially bridged iodiranium or iodirenium ion) having a sufficiently long lifetime. At variance, the exclusive formation of the addition products in the reaction of olefin **3** with both ICl$_2^-$ or IBr$_2^-$, as well as the different regio- and stereoselectivity observed in the reaction of alkynes **4**, strongly support for the halogenations with trihalide-based ILs a mechanism more similar to that proposed[11] for [bmim][Br$_3$] addition to double and triple bonds occurring through the early attack of the nucleophile (Cl$^-$ or Br$^-$) on a 1:1 unsaturated compound-halogen π-complex or, more probably in this case, on the iodiranium intermediate. The charge distribution in the transition state, or in the short lived ionic intermediate, should depend both on the substituents on the double or triple bond and on the halogenating agent. Detailed studies are now under way to further investigate the physical properties of these ILs and the mechanism of the reactions carried out with them.

Conclusions

In summary, the halogenation procedures presented above are characterized by several advantages with respect to classical methods. In particular, toxic reagents (I$_2$/CuCl$_2$, I$_2$/HgCl$_2$, ICN/AlCl$_3$) and/or chlorinated solvents, generally used for these reactions, are avoided and the applicability of a new class of 'green reagent-solvents' is presented. Furthermore, considering the stability of [hmim][ICl$_2$] and [bmim][IBr$_2$], high yield and stereoselectivity of the reactions carried out by these reagent-solvents, the facility of separation of the products from the reaction mixture by simple extraction with an immiscibile solvent, we conclude that these ILs may be surely interesting 'green' alternative media for synthesis of iodobromo- and iodochloro-derivatives, in particular when the olefin structure favour the formation of rearrangement and elimination products. It is however worth of note that a high yield and stereoselectivity may be achieved also using [bmim][PF$_6$] as the solvent and ICl or IBr as the reagent. Furthermore, in this case shorter reaction times are necessary and the IL solvent can be more easily recycled and reused. The reactions of ICl or IBr in [bmim][PF$_6$] are, at least for several substrates, the best conditions to obtain dihalo adducts.

Experimental

General remarks

^{1}H and ^{13}C NMR were recorded with a Bruker AC 200 instrument. Compound **1a** (Fluka, 99.0+ % GC), **1b** (Fluka 99.5% GC), **1c** (Aldrich, 99% GC), **2** (Aldrich, 99% GC), **3** (Aldrich, 99+ % GC), **4a–c** (Aldrich, 99% GC), bromine (1 mL in sealed ampoules, $>$99,5%), ICl, IBr, I$_2$, tetrabutylammonium bromide ([Bu_4N][Br], puriss. p.a.), tetrabutylammonium chloride ([Bu_4N][Cl], puriss. p.a.) and dichloromethane (DCM, 99,5%) were used as supplied. [hmim][Cl], [bmim][Br], [bmim][PF_6], [emim][I] were prepared following the reported procedures.[17,18] In the case of [bmim][PF_6], attention was paid to the elimination of Cl^- present in the solvent as impurities: the absence of the anion was always evaluated using Volhardt titration.

Synthesis and analysis of alogenating species

An appropriate amount of [hmim][Cl] or [bmim][Br] or [emim][I] was weighed in a calibration flask and the IL was refrigered at 0°C. An equimolar amount of halogen (ICl or IBr or Cl_2 or Br_2, respectively) was added at the same temperature and the trihalide ionic liquid was stored in the dark. Attention was paid to avoid contamination of the solutions from atmospheric by humidity. Furthermore, particular attention was also paid to avoid to add an excess of halogen. It is worth of note that the eventual presence in these trihalide based ionic liquids of small amounts of free halogenide ions does not affect the product distribution of the reactions in which they are used.

NMR Measurements

^1H NMR of [hmim][Cl], [hmim][ICl_2], [hmim][I_2Cl], [bmim][Br], [bmim][IB_2], [bmim][I_2Br] were recorded using DMSO-d_6 as external lock solvent, contained in a capillary. Spectra in solution were performed at 0.07 M concentration, as reported in Table 3. Always appropriate quantities of halogen (ICl, IBr or I_2) were weighed into known volumes of the proper ionic liquid or CD_3CN containing a proper amount of [emim][I] and were stored in the dark. Aliquotes of these solutions were analyzed by NMR.

ESI Measurements

The ESI-MS spectra, both in positive- and negative-ion mode, were obtained using a LCQ instrument (Thermoquest, San Jose, CA). The solutions are prepared by dissolving the ionic liquid under analysis (5×10^{-3} or 5×10^{-4} mol L^{-1}) in CH_3CN or CH_2Cl_2, see text. Solution flow rate 8 μl min^{-1}, capillary temperature 210 °C, spray voltage 4.0 kV, capillary voltage +5 or −15 V, tube lenses offset −15 V, nebulizing gas N_2 (40 units flow rate). The parameters related to octapoles and detector were achieved by the automatic set-up procedure. Collision induced decompositions of selected ions were obtained by applying a supplementary r.f. voltage (tickle voltage) to the end cap electrodes of the ion trap (resonance activation).

Bromination procedure and product analyses

In ionic liquids. In a standard halogenation procedure, to a round-bottom flask equipped with a magnetic stirrer flea, containing the IL (2 ml), a measured amount of halogen (ICl, IBr, Br_2) was added at 0 °C in order to obtain an halogen concentration ranging from 0.3–1.5 M or the complete conversion of the counteranion of the IL in a trihalogen species. To the solution, maintained in the dark at 0 °C, the unsaturated compound (0.3 M) was then added under stirring. A water-ice bath was used to avoid the temperature increase during the alkene or alkyne addition. Products were then extracted at the end of the reaction by three subsequent addition of Et_2O (2 ml), followed by decanting off the ethereal solution of the products. The combined extracts were concentrated on a rotary evaporator and the products were analyzed by NMR. All reactions were carried out at least in duplicate. The ratios reported in Table 6 and 7 were reproducible within 2%. The chemo-, regio- and stereochemistry of addition products was established on the basis of the NMR spectra, considering also the ^{13}C NMR spectra of the corresponding dibromo, dichloro and diiodo derivatives.

In dichloromethane. Dichloromethane solutions of ICl or IBr or $TBAICl_2$ or $TBAIBr_2$ (0.6 M) were rapidly mixed with equal volumes of solutions of substrates **1–4** (0.6 M) in the same solvent at 0 °C. The reaction mixtures were allowed to react in the dark until colorless, or for 48–72 h, and then were washed first with an aqueous $NaHSO_3$ solution, then with water and dried on $MgSO_4$. At least 7–8 washings were necessary to remove the ammonium salt in the case of the reaction carried out with $TBAICl_2$ or $TBAIBr_2$. After solvent evaporation in vacuo the reaction mixtures were analyzed by NMR. All reaction were carried out at least in duplicate.

From olefin 1a.

*1-Iodo-2-chloropentane (**5a**)*. ^1H NMR ($CDCl_3$): δ 0.93 (t, 3H, CH_3); 1.23–2.11 (br, 4H, CH_2); 3.39 (dd, 1H, HC*H*-I); 3.54 (dd, 1H, *H*CH-I); 4.19 (m, 1H, CHCl). ^{13}C NMR and DEPT-135 ($CDCl_3$): δ 10.98 (CH_2I); 13.36 (CH_3); 19.24 (CH_2); 39.27 (CH_2); 60.83 (CHCl).

*1-Chloro-2-iodopentane (**6a**)*. ^1H NMR ($CDCl_3$): δ 0.93 (t, 3H, CH_3); 1.23–2.11 (br, 4H, CH_2); 3.83 (dd, 1H, HC*H*Cl); 3.98 (m, 2H, *H*CHCl, CHI). ^{13}C NMR and DEPT-135 ($CDCl_3$): δ 13.12 (CH_3); 22.19 (CH_2); 33.12(CHI); 38.51 (CH_2); 50.00 (CH_2Cl).

*1-Iodo-2-bromopentane (**7a**)*. ^1H NMR ($CDCl_3$): δ 0.97 (t, 3H, CH3); 1.43–2.40 (br, 4H, $2CH_2$); 3.53 (dd, 1H, CH_2I); 4.05 (dd, 1H, CH_2I); 4.09–4.40 (br, CHBr). ^{13}C NMR and DEPT-135 ($CDCl_3$): δ 11.11 (CH_2I); 13.21 (CH_2); 20.18 (CH_2); 39.27 (CH_2); 53.05 (CHBr).

*1-Bromo-2-iodopentane (**8a**)*. ^1H NMR ($CDCl_3$): δ 0.97 (t, 3H, CH_3); 1.43–2.40 (br, 4H, $2CH_2$); 3.79 (m, 2H, CH_2Br); 4.09–4.40 (br, 1H, CHI). ^{13}C NMR and DEPT-135 ($CDCl_3$): δ 13.06 (CH_3); 22.16 (CH_2); 32.24 (CHI); 38.24 (CH_2); 39.57 (CH_2Br).

From olefin 1b.

*1-Chloro-2-iodo-1-phenylethane (**5b**)*. ^1H NMR ($CDCl_3$): δ 3.70 (m, 2H, CH_2I); 5.03 (dd, 1H, CHCl); 7.33 (m, 5 aromatic protons). ^{13}C NMR and DEPT-135 ($CDCl_3$): δ 9.68 (CH_2I); 61.61 (CHCl); 127.13 (2 =CH–); 128.71 (=CH–); 129.07 (=CH–); 139.01 (> C <).

*1-Bromo-2-iodo-1-phenylethane (**7b**)*. ^1H NMR ($CDCl_3$): δ 4.06 (dd, 2H, CH_2I); 5.15 (dd, 1H, CHBr); 7.39 (m, 5 aromatic protons). ^{13}C NMR and DEPT-135 ($CDCl_3$): δ 12.13 (CH_2I); 50.81 (CHBr); 127.56 (2 =CH–); 128.76 (2 =CH–); 129.08 (=CH–); 138.97 (> C <).

From olefin 1c.

*1-Chloro-2-iodo-3,3-dimethylbutane (**6c**)*. ^1H NMR ($CDCl_3$): δ 1.06 (s, 9H, $3CH_3$); 3.68 (dd, 1H, *H*CHCl, $J_{1,2}$ = 9.20 Hz, $J_{1,1'}$ = 12.20 Hz); 3.85 (dd, 1H, HC*H*Cl, $J_{1,1'}$ = 12.20 Hz, $J_{1',2}$ = 3.38 Hz); 4.07 (dd, 1H, CHI, $J_{1,2}$ = 9.20 Hz, $J_{1',2}$ = 3.38 Hz). ^{13}C NMR and DEPT-135 ($CDCl_3$): δ 28.70 ($3CH_3$); 36.24 (> C <); 49.62 (CH_2Cl); 53.23 (CHI).

*1-Bromo-2-iodo-3,3-dimethylbutane (**8c**)*. ^1H NMR ($CDCl_3$): δ 1.17 (s, 9H, 3 CH_3); 3.66 (dd, 1H, *H*CHBr, $J_{1,2}$ = 9.50 Hz,

$J_{1,1'}$ = 11.45 Hz); 3.97 (dd, 1H, HC*H*Br, $J_{1,1'}$ = 11.45 Hz, $J_{1',2}$ = 3.29 Hz); 4.22 (dd, 1H, CHI, $J_{1,2}$ = 9.50 Hz, $J_{1',2}$ = 3.29 Hz). ^{13}C NMR and DEPT.135 ($CDCl_3$): δ 28.60 ($3CH_3$); 37.12 (> C <); 38.11 (CH_2Br); 53.50 (CHI).

From olefin 2.

1-Chloro-2-iodocyclopentane (**9**). ^{1}H NMR ($CDCl_3$): δ 1.87–2.13 (br, 4H, CH_2); 2.41–2.58 (br, 2H, CH_2); 4.37 (m, 1H, CHI); 4.54 (m, 1H, CHCl). ^{13}C NMR and DEPT-135 ($CDCl_3$): δ 21.44 (CH_2); 33.22 (CHI); 33.22 (CH_2); 35.62 (CH_2); 68.02 (CHCl).

1-Bromo-2-iodocyclopentane (**10**). ^{1}H NMR ($CDCl_3$): δ 1.91–2.20 (br, 4H, CH_2); 2.52–2.75 (br, 2H, CH_2); 4.59 (m, 1H, CHI); 4.68 (m, 1H, CHBr). ^{13}C NMR and DEPT-135 ($CDCl_3$): δ 21.43 (CH_2); 34.04 (CH_2); 34.21 (CHI); 35.76 (CH_2); 59.13 (CHBr).

From olefin 3.

1-Iodo-2-chloro-2,3,3-trimethylbutane (**11**). ^{1}H NMR ($CDCl_3$): δ 1.14 (s, 9H, $3CH_3$); 1.66 (s, 3H, CH_3); 3.71 (d, 1H, HC*H*I, *J* = 10.75 Hz); 3.80 (d, 1H, *H*CHI, *J* = 10.75 Hz). ^{13}C NMR and DEPT-135 ($CDCl_3$): δ 19.59 (CH_2I); 26.78 ($3CH_3$); 27.82 (CH_3); 39.06 (> C–Cl).

1-Bromo-2-iodo-2,3,3-trimethylbutane (**14**). ^{1}H NMR ($CDCl_3$): δ 1.19 (s, 9H, 3 CH_3); 1.87 (s, 3H, CH_3); 3.84 (d, 1H, HC*H*Br, *J* = 11.0 Hz); 4.01 (d, 1H, HC*H*Br, *J* = 11.0 Hz). ^{13}C NMR and DEPT-135 ($CDCl_3$): δ 28.78 (CH_3); 27.48 ($3CH_3$); 40.45 (> C–I); 43.29 (CH_2Br).

From alkyne 4a.

trans-1-Chloro-2-iodo-1-phenylethene (**15a**). ^{1}H NMR ($CDCl_3$): δ 6.68 (s, 1H, =CHI); 7.24–7.46 (m, 5 aromatic protons). ^{13}C NMR and DEPT-135 ($CDCl_3$): δ 73.01 (=CHI); 128.13 (2 =CH–); 128.83 (2 =CH–);129.36 (=CH–); 133.94 (=C–Cl); 137.45 (> C <).

trans-1-Bromo-2-iodo-1-phenylethene (**16a**). ^{1}H NMR ($CDCl_3$): δ 6.91 (s, 1H, =CHI); 7.27–7.49 (m, 5 aromatic protons). ^{13}C NMR and DEPT-135 ($CDCl_3$): δ 75.22 (=CHI); 121.92 (> C–Br); 128.19 (2 =CH–); 128.89 (=CH–); 129.22 (=CH–); 139.17 (> C <).

trans-1-Iodo-2-bromo-1-phenylethene (**17**). ^{1}H NMR ($CDCl_3$): δ 7.07 (s, 1H, =CHBr); 7.27–7.49 (m, 5 aromatic protons). ^{13}C NMR and DEPT-135 ($CDCl_3$): δ 80.75 (=C–I); 107.14 (=CHBr); 128.19 (2 =CH); 128.72 (=CH); 128.89 (2 =CH); 139.98 (> C <).

From alkyne 4b.

trans-1-Chloro-2-iodo-1-phenyl-1-propene (**15b**). ^{1}H NMR ($CDCl_3$): δ 2.76 (s, 3H, CH_3); 7.38 (m, 5 aromatic protons). ^{13}C NMR and DEPT-135 ($CDCl_3$): δ 31.22 (CH_3); 91.94 (=C–I); 128.11 (2 =CH); 128.63 (=CH); 129.01 (2 =CH); 131.44 (=C–Cl); 141.68 (> C <).

trans-1-Bromo-2-iodo-1-phenyl-1-propene (**16b**). ^{1}H NMR ($CDCl_3$): δ 2.72 (s, 3H, CH_3); 7.22–7.42 (m, 5 aromatic protons). ^{13}C NMR and DEPT-135 ($CDCl_3$): δ 34.36 (CH_3); 93.05 (=C–I); 118.24 (=C–Br); 128.80 (=CH); 128.52 (=CH); 128.95 (=CH); 143.65 (> C <).

cis-1-Bromo-2-iodo-1-phenyl-1-propene (**18**). ^{1}H NMR ($CDCl_3$): δ 2.66 (s, 3H, CH_3); 7.19–7.30 (m, 5 aromatic protons). ^{13}C NMR and DEPT-135 ($CDCl_3$): δ 34.21 (CH_3); 92.82 (=C–I); 118.94 (=C–Br); 128.06 (2 =CH); 128.15 (2 =CH); 128.44 (=CH); 144.57 (> C <).

From alkyne 4c.

trans-1-Chloro-2-iodo-1-phenyl-1-butene (**15c**). ^{1}H NMR ($CDCl_3$): δ 1.12 (t, 3H, CH_3); 2.80 (q, 2H, CH_2); 7.28 (m, 5 aromatic protons). ^{13}C NMR and DEPT-135 ($CDCl_3$): δ 13.05 (CH_3); 36.16 (CH_2); 102.69 (=C–I); 127.54 (=C–Cl); 128.14 (2 =CH–); 128.61 (=CH); 129.05 (2 =CH); 141.65 (> C <).

trans-1-Bromo-2-iodo-1-phenyl-1-butene (**16c**). ^{1}H NMR ($CDCl_3$): δ 1.18 (t, 3H, CH_3); 2.86 (q, 2H, CH_2); 7.24–7.40 (m, 5 aromatic protons). ^{13}C NMR and DEPT-135 ($CDCl_3$): δ 12.88 (CH_3); 39.26 (CH_2); 103.5 (=C–I); 116.70 (=C–Br); 128.25 (2 =CH–); 128.50 (=CH); 129.0 (2 =CH); 143.4 (> C <).

Recycling of ionic liquids

Recycling of [bmim][PF_6] was accomplished by washing with an aqueous solution of $NaHSO_3$ and then with water. The uncoloured recovered IL was dried, analyzed by NMR and reused. Recycling of trihalide based ionic liquids was performed, after removal of the solvent used for product extraction, by addition of the consumed halogen, evaluated on the basis of the product yields.

Acknowledgment

Financial support for this research was provided by MIUR, CNR and Università di Pisa.

References

1 J. D. Holbrey and K. R. Seddon, *Clean Products Process.*, 1999, **1**, 223; M. J. Earle and K. R. Seddon, *Pure Appl. Chem.*, 2000, **72**, 1391.

2 M. J. Earle and K. R. Seddon, *Pure Appl. Chem.*, 2000, **72**, 1391.

3 T. Welton, *Chem. Rev.*, 1999, **99**, 2071.

4 P. Wasserscheid and M. Keim, *Angew. Chem., Int. Ed.*, 2000, **39**, 3773.

5 G. H. Schmid, D. G. Garrat, *The Chemistry of Double-Bonded Functional Groups*, ed. S. Patai, Wiley, New York, 1977; p. 725; Suppl. A, Vol. 2, part 1, p. 699.

6 S. Kajigaeshi, M. Moriwaki, S. Fujisaki and T. Okamoto, *Bull. Chem. Soc. Jpn.*, 1990, **63**, 3033.

7 N. S. Zefirov, G. A. Sereda, S. E. Sosonuk, N. V. Zyk and T. I. Likhomanova, *Synthesis*, 1995, 1359.

8 B. Sket, P. Zupet and M. Zupan, *Tetrahedron*, 1990, **46**, 2503.

9 N. Winterton, K. R. Seddon and Y. Patell, *PCT Int. Appl.*, WO 2000037400 A1, 29 Jun 2000.

10 C. Chiappe, D. Capraro, V. Conte and D. Pieraccini, *Org. Lett.*, 2001, **3**(7), 1061.

11 C. Chiappe, V. Conte and D. Pieraccini, *Eur. J. Org. Chem.*, 2002, 2831.

12 Y. Ogawa, O. Takanashi and O. Kikuchi, *THEOCHEM*, 1998, **429**, 187.

13 A. I. Papov and R. F. Swensen, *J. Am. Chem. Soc.*, 1955, **77**, 3724; E. Eyal and A. Treinin, *J. Am. Chem. Soc.*, 1964, **861**, 4287.

14 A. G. Avent, P. A. Chaloner, M. P. Day, K. R. Seddon and T. Welton, *J. Chem. Soc., Dalton Trans.*, 1994, 3405.

15 P. Bonĥote, A. P. Dias, N. Papageorgiou, K. Kalyanasundaram and M. Grätzel, *Inorg. Chem.*, 1996, **35**, 1168.

16 J. Barluenga, M. A. Rodriguez and P. J. Campos, *J. Org. Chem.*, 1990, **55**, 3104.

17 J. Fuller, R. T. Carlin, H. C. De Long and D. Haworth, *Chem. Commun.*, 1996, 299.

18 M. S. Selvan, M. D. McKinley, R. H. Dubois and J. L. Atwood, *J. Chem. Eng. Data*, 2000, **45**, 841.

Ultrasound-promoted N-alkylation of imidazole. Catalysis by solid-base, alkali-metal doped carbons

J. M. López-Pestaña, M. J. Ávila-Rey and R. M. Martín-Aranda*

Departamento de Química Inorgánica y Química Técnica, Universidad Nacional de Educación a Distancia (UNED), C/Senda del Rey, 9, E-28040 Madrid, Spain.
E-mail: rmartin@ccia.uned.es; Fax: +34-91-398 6697; Tel: +34-91-398-7351

Received 30th August 2002
First published as an Advance Article on the web 14th November 2002

The synthesis of N-substituted imidazoles *via* alkylation of imidazole with 1-bromobutane by sonochemical and thermally-activated reactions over two alkali-metal promoted carbons (Na^+- and Cs^+-Norit) as catalysts is reported. In this green, solvent free procedure, N-substituted imidazoles are produced exclusively in very high yields ($>80\%$) when the Cs^+-Norit carbon is employed under ultrasound activation. The basicity of the alkali metal cation increases the conversion and ultrasound activation affords a remarkable increase in the yields.

Introduction

Alkali-metal promoted carbons are highly effective for the catalytic selective N-alkylation of imidazole.[1] The yields and selectivities of the N-alkylated imidazoles (Scheme 1), which are key intermediates in the synthesis of pharmaceutically important anticonvulsants and bactericidal products, have been very high, especially when the reaction is activated by ultrasound. Recently, activated carbons have been employed to catalyse fine chemical reactions, because of their extended surface area, microporous structure, and high degree of surface reactivity.[2] Thus, this type of material is competitive with other traditionally employed catalysts for organic synthesis, such as zeolites, clays or supported oxides.[3,4] More recently, new technologies have provided innovative synthetic routes. Sonochemistry is presented as a technology in itself, and it can also be used to improve the efficiency of other methodologies.[5–14] This contribution shows the remarkable effect of ultrasonic activation for the catalytic N-alkylation of imidazole.

The sonochemical effects on the chemical reactions are attributed to the acoustic cavitation. When one of the phases is a solid, the ultrasonic irradiation has additional enhancement effects such as surface cleaning, particle size reduction, crystal defects and metal activation. This is especially useful when a solid acts as catalyst.[15,16] The reaction between a solid and a liquid (or liquid dissolved) reactant in a heterogeneous system presents some obstacles *e.g.* the small surface area of a bulk solid, the solid surface may be coated by impurities, species have to diffuse to and away from the solid surface and deposition of products may inhibit further reaction. These difficulties can be overcome by the use of ultrasound due to cavitation, as have been mentioned already: shock waves (causing plastic deformations on soft materials, break-up of coatings), microjects (causing surface erosion, defects and deformations, enhancing the surface area) and microstreaming (improving mass transfer, removing eroded particles and deposited impurities or products).

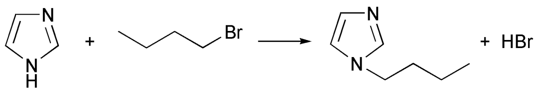

Scheme 1 N-Alkylation of imidazole with 1-bromobutane.

Experimental

An activated carbon RX-1 EXTRA Norit has been employed as the pristine carbon. The basic catalysts were prepared by ionic exchange using a corresponding solution (2 M) of the alkali-metal chlorides for about 60 h at 353 K. In all cases the liquid-to-solid ratio was 10 : 1 by weight. The samples were filtered off and washed with water until no chloride anions could be detected. After drying for 16 h at 383 K, the carbons were pelletized, crushed and sieved to a particle size <0.140 mm.[17]

Thermally activated experiments were performed using a batch reactor system under stirring. A mixture of the two reactants, imidazole (5 mmol) and 1-bromobutane (15 mmol) without any solvent, was kept in a Pyrex flask under stirring while heating to the reaction temperature (293 or 313 K). Then, the catalyst was added at which the reaction time was set to zero. Samples are taken periodically between 15 and 120 min.

The ultrasonic activated reactions were carried out in a flask, suspended into the ultrasonic bath (Selecta Ultrasound-H, 40 kHz frequency, 550 W power) with a heating system at the reaction temperature (293 and 313 K). Dry media, atmospheric pressure, 0.025 g of the corresponding catalyst (Na- or Cs-Norit) and an excess of alkyl halide were employed (imidazole, 5 mmol; 1-bromobutane, 15 mmol) for either reaction temperature. The excess of alkyl halide was recycled after the reaction.

The products were isolated by standard procedures and characterized by IR, ^{1}H NMR and GC–MS. Previously to any

Green Context

The alkylation of imidazole leads to a group of compounds with important applications as intermediates for pharmaceuticals (and also for the synthesis of ionic liquids). Here, a solvent-free unltrasound promoted approach is reported, in which imidazole and an alkyl halide are reacted together over a basic carbon. Ultrasound leads to substantially better conversions and yields over basic solids, but has little effect over untreated carbons. Thus the combination of ultrasound and 'dry' conditions leads to an effieicnt procedure. *DJM*

DOI: 10.1039/b208479c

experiment blank runs were carried out, which showed that the reaction, in the absence of the catalyst, was negligible.

Results and discussion

Undoped-Norit catalyst affords conversion values of 11.2 and 13.6% under thermal and ultrasonic activation, respectively, at 293 K after 120 min (Table 1).

Conversion on undoped Norit catalyst increases moderately with temperature and is higher under ultrasound activation. Nevertheless, when the reaction is carried out on Na- and Cs-promoted carbons, these values are considerably higher, reaching values of conversion around 60% and selectivity of 100% when Na-Norit is employed as catalyst and a selectivity of 85% when Cs-Norit is the catalyst under ultrasound activation (Fig. 1).

Fig. 1 shows the effect of the type of alkali-metal promoter on the activity of the catalysts during thermally and ultrasonically activated reactions at 293 K. The conversion is greater for the Cs-Norit carbon, which affords the highest yields to N-alkylated imidazole (80.4% at 120 min). This is mainly due to the significant increase of the number of basic sites on the surface of the catalyst.[18] The basicity of alkali-doped Norit carbons increases with the size of the alkali-metal cation, with the the order of activity Na-Norit < Cs-Norit, which parallels the order of activity under thermal and ultrasound activation at the studied temperatures (293 and 313 K).

Fig. 2 displays the catalytic results measured at 313 K on the most active catalyst, Cs-Norit. For comparative purposes, the results obtained at 293 K are also shown. Ultrasonic activation leads to much better results than thermal activation since Cs-Norit affords 90% conversion with 100% selectivity under ultrasound activation and 53.4% conversion with 100% selectivity under thermal activation (120 min and 313 K).

Table 1 Thermally and ultrasonically activated alkylation of imidazole with 1-bromobutane on undoped Norit carbon

	Thermal conversion (%)		Ultrasound conversion (%)	
Time/min	293 K	313 K	293 K	313 K
60	5.0	9.0	9.6	14.5
120	11.2	14.0	13.6	16.4

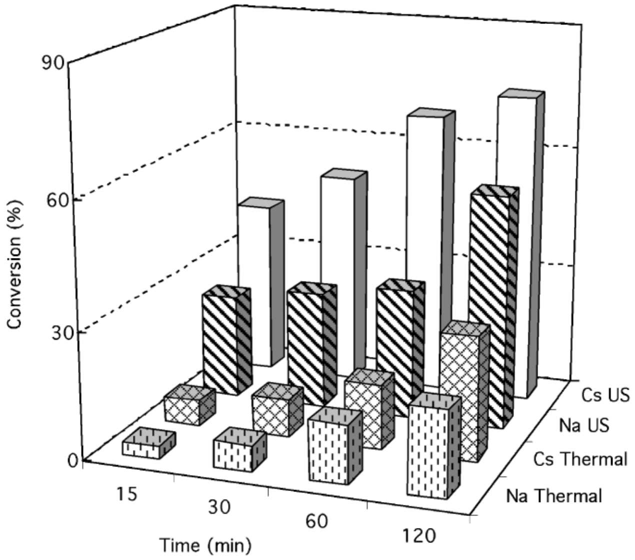

Fig. 1 Alkylation of imidazole with 1-bromobutane under thermal and ultrasonic activation. Catalysts: Na- and Cs-Norit. Reaction temperature: 293 K.

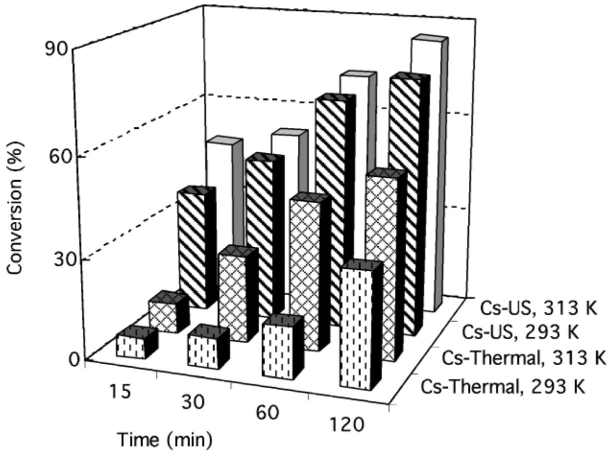

Fig. 2 Influence of the temperature on the thermal and ultrasonic activation of imidazole alkylation with 1-bromobutane. Catalyst: Cs-Norit.

Table 2 Yields of isolated pure *N*-alkylimidazoles obtained on alkali-metal doped carbons under thermal and ultrasonic activation

		Yield (%)[a]	
Catalyst	*T*/K	Thermal	Ultrasound
Na-Norit	293	16	50
	313	23	65
Cs-Norit	293	25	71
	313	45	80

[a] Reaction rate: 120 min.

The outstanding advantage of ultrasound activation becomes more evident at lower reaction temperatures (293 *vs.* 313 K). This may be understood considering that an increase of the temperature increases the vapour pressure of the liquid medium in the ultrasonic bath, leading to an easier cavitation, but to a less violent collapse, which makes cavitation less efficient.[19] The main noticeable effect was a marked increase of *N*-alkylimidazole production with the Cs-doped carbon under ultrasonic activation while a high selectivity is maintained. Table 2 shows the yields of isolated pure products obtained under thermal and ultrasonic activation after 2 h of reaction. It can be observed that a yield of *ca.* 80% is attained when the Cs-doped catalyst is used under ultrasonic activation. Finally, it is important to remark that the enhancing effects on the reaction rate by combining the basicity of the alkali-metal doped carbon with ultrasonic waves is presented as an alternative method for the production of N-substituted imidazoles. In general the use of ultrasonic waves can be extended to enhance the activity of other types of heterogeneous catalysts for industrial reactions, which demand very mild reaction conditions.

Conclusions

The results demonstrate that N-alkylation of imidazole with suitable activated carbons, under ultrasound activation, results in the efficient, mild and effective synthesis of N-substituted imidazole with nearly 100% selectivity. This method thus offers a practical alternative to conventional heating and traditional base catalysts and the process itself is environmentally friendly with minimal waste.

Acknowledgements

The authors thank the Spanish CICYT for financial support (Project MAT2001-0319).

References

1 R. M. Martín-Aranda, M. L. Rojas-Cervantes, A. J. López-Peinado and J. de D. López-González, *J. Mol. Catal.*, 1993, **85**, 253.
2 L. R. Radovic and F. Rodríguez-Reinoso, in *Chemistry and Physics of Carbon*, ed. P. A. Thrower, Marcel Dekker, New York, 1997, pp. 243, 25.
3 J. Weitkamp, M. Hunger and U. Rymsa, *Microporous Mesoporous Mater.*, 2001, **48**, 255.
4 B. F. Sels, D. E. De Vos and P. A. Jacobs, *Catal. Rev.*, 2001, **43**, 443.
5 P. Cintas and J. L. Luche, *Green Chem.*, 1999, **1**, 115.
6 J. L. Luche, *Ultrason. Sonochem.*, 1997, **4**, 211.
7 T. J. Mason and J. P. Lorimer, in, *Sonochemistry, Theory, Applications and Uses of Ultrasound in Chemistry*, Ellis Horwood, Chichester, 1988.
8 K. S. Suslick, in *Ultrasound, its physical, biological and chemical effects*, ed. K. S. Suslick, VCH, Weinheim, 1988.
9 K. S. Suslick, *Science*, 1990, **247**, 1439.
10 M. A. Margulis, *Ultrasonics*, 1992, **30**, 152.
11 D. Bremer, *Adv. Sonochem.*, 1990, **1**, 1.
12 G. Cum, G. Galli, R. Gallo and A. Spardo, *Ultrasonics*, 1991, **30**, 267.
13 R. S. Varma, K. P. Naicker and D. Kumar, *J. Mol. Catal. A., Chem.*, 1999, **149**, 153.
14 L. H. Thompson and L. K. Doraiswamy, *Ind. Eng. Chem Res.*, 1999, **38**, 1215.
15 K. S. Suslick, D. J. Casadonte, M. L. H. Green and M. E. Thompson, *Ultrasonics*, 1987, **25**, 56.
16 D. Peters, *J. Mater. Chem.*, 1996, **6**, 1605.
17 J. Rubio-Gómez, R. M. Martín-Aranda, M. L. Rojas-Cervantes, J. de D. López-González and J. L. G. Fierro, *Carbon*, 1999, **37**, 213.
18 J. de D. López-González, A. J. López-Peinado, R. M. Martín-Aranda and M. L. Rojas-Cervantes, *Carbon*, 1993, **31**, 1231.
19 T. J. Mason, *Practical Sonochemistry*, Ellis Horwood, New York, 1991.